



# **E-Beam Microcharacterization Centers & Nanoscale Science Research Centers 2011 Contractors' Meeting**

May 31 – June 2, 2011  
Annapolis, Maryland

---

**Sponsored by the  
U.S. Department of Energy, Office of Basic Energy Sciences and  
Scientific User Facilities Division**

**NOTE:** The printed version of this abstract book is provided in black-and-white; the accompanying CD contains full color versions of all the abstracts.

This document was produced under contract number DE-AC05-06OR23100 between the U.S. Department of Energy and Oak Ridge Associated Universities.

## Foreword

This volume comprises the scientific content of the 2011 Electron Beam Microcharacterization Centers (EBMCs) and Nanoscale Science Research Centers (NSRCs) Contractors' Meeting sponsored by the Scientific User Facilities Division (SUFD) in the Office of Basic Energy Sciences (BES) of the U.S. Department of Energy (DOE). The meeting held on May 31 - June 2, 2011 at The Westin, Annapolis, Maryland, is the first combined EBMC & NSRC Contractors' Meeting and only the second such meeting of the NSRCs. The meeting highlights the highly interdisciplinary and synergistic research conducted by facility scientific staff and facility users across the centers.

The EBMC activity supports three centers that operate as user facilities, work to develop next-generation electron-beam instrumentation, and conduct corresponding research. Advanced instrumentation supported at these centers includes scanning, transmission, and scanning transmission electron microscopes (TEM), including the recently developed highest resolution spherical and chromatic aberration-corrected TEM; atom probes and related field ion instruments; related surface characterization apparatus and scanning probe microscopes; and/or ancillary tools such as spectrometers, detectors, and advanced sample preparation equipment.

- Electron Microscopy Center for Materials Research (EMC), Argonne National Laboratory
- National Center for Electron Microscopy (NCEM), Lawrence Berkeley National Laboratory
- Shared Research Equipment program (SHaRE), Oak Ridge National Laboratory

The NSRC are DOE's premier user facilities for interdisciplinary research at the nanoscale, serving as the basis for a national program that encompasses new science, new tools, and new computing capabilities. Each center has particular expertise and capabilities in selected theme areas, such as synthesis and characterization of nanomaterials; nanoscale materials for energy conversion, electronics, photonics, phononics, and catalysis; soft and biological nanomaterials; imaging and spectroscopy; and nanoscale integration; theory, modeling and simulation. The centers provide cleanrooms, nanofabrication resources, one-of-a-kind signature instruments, and other instruments not generally available except at major user facilities, leveraging co-located EBMCs and other major BES facilities for X-ray and neutron scattering.

- Center for Functional Nanomaterials (CFN), Brookhaven National Laboratory
- Center for Integrated Nanotechnologies (CINT), Sandia and Los Alamos National Laboratories
- Center for Nanophase Materials Sciences (CNMS), Oak Ridge National Laboratory
- Center for Nanoscale Materials (CNM), Argonne National Laboratory
- Molecular Foundry (MF), Lawrence Berkeley National Laboratory

The purpose of the Contractors' Meeting is to bring together researchers—facility scientists and facility users of the BES EBMC and NSRC facilities and leading experts across the multi-disciplinary spectrum served by these facilities—to foster discussion of the latest research results, catalyze collaborations, and stimulate ideas for promising new directions of exploration. Dynamic exploration of research ideas and capability needs will also help DOE in assessing the needs of the research community in charting future program directions.

I wish to thank all the meeting participants for their investment of time and their willingness to share their ideas and latest research results. The efforts of the EBMC and NSRC Directors, Ulrich

Dahmen (NCEM), Dean Miller (EMC), Karren More (SHaRE), Jim DeYoreo (MF), Tony Haynes (CNMS), Emilio Mendez (CFN), David Morris (CINT), and Amanda Petford-Long (CNM), in assembling the exceptional roster of presenters representing the full spectrum of staff and user research is gratefully acknowledged. A special thanks to Linda Cerrone (BES SUFD) and to Jeannie Robinson and Deneise Terry (Oak Ridge Institute for Science and Education) for their seamless handling of all the logistical aspects of the meeting.

Mihal E. Gross  
Program Manager, NSRCs and EBMCs  
Scientific User Facilities Division  
Office of Basic Energy Sciences  
Office of Science  
U.S. Department of Energy

## E-Beam Microcharacterization Centers and Nanoscale Science Research Centers 2011 Contractors' Meeting

The Westin Annapolis  
100 Westgate Circle  
Annapolis, MD 21401  
Phone: 410-972-4300; Fax: 410-295-7420  
Meeting in Capitol D  
Poster Boards in Senate A/B

### AGENDA

#### Tuesday, May 31, 2011

- 12:00 p.m. Registration & poster set-up
- 1:30 p.m. BES Welcome and Introductory Remarks  
**Harriet Kung and Mihal Gross**, DOE Basic Energy Sciences
- 1:45 p.m. Update on overall EBMC and NSRC status, progress, and user programs  
**Mihal Gross**, DOE Basic Energy Sciences
- 2:00 p.m. **Invited Plenary Presentation:** Industrial Nanoscience: From Discovery to Product Maturity  
**Ernest Hall**, GE Global Research
- 2:45 p.m. In-Situ TEM Electrochemistry of Li-Ion Battery Materials  
**Jianyu Huang**, Center for Integrated Nanotechnologies (CINT)
- 3:10 p.m. Interfaces in Bulk Heterojunction Photovoltaics  
**Michael Chabinyk**, University of California–Santa Barbara
- 3:35 p.m. Break
- 3:50 p.m. Ultra-High-Resolution Atomic Imaging of Surfaces and the Bulk  
**Yimei Zhu**, Brookhaven National Laboratory
- 4:15 p.m. Developments in XEDS and EELS Spectroscopy for the Characterization of Nanomaterials  
**Nestor Zaluzec**, Electron Microscopy Center (EMC)
- 4:40 p.m. Probing the Microstructural Evolution of Oxide Cathode Materials Under Electrochemical Cycling for Li-Ion Batteries using Advanced Analytical Electron Microscopy  
**Miaofang Chi**, SHared Research Equipment (SHaRE)
- 5:05 – 5:25 p.m. 1-minute/1-slide Poster Previews – Poster Group D
- 5:30 – 6:30 p.m. Poster Session with refreshments (cash bar)
- 6:30 p.m. Adjourn for dinner (on your own)
- 8:30 – 9:30 p.m. Brainstorming discussions (cash bar)

### Wednesday, June 1, 2011

- 7:00 – 8:00 a.m. Continental breakfast
- 8:00 a.m. **Invited Plenary Presentation:** Imagine Electron Microscopy 2030  
**J. Murray Gibson**, *Northeastern University*
- 8:45 a.m. Charge Illuminates, Spin Interrogates: Microscopy with a Spin-Polarized Electron Beam  
**Andreas Schmid**, *National Center for Electron Microscopy (NCEM)*
- 9:10 a.m. Thermal Ground-State Ordering and Elementary Excitations in Artificial Magnetic Square Ice  
**Christopher Marrows**, *University of Leeds*
- 9:35 a.m. What Speckle Tells Us About Amorphous Materials  
**Mike Treacy**, *Arizona State University*
- 10:00 a.m. Break
- 10:20 a.m. Mesoscopic Amorphization of Supported Pt Nanoparticles: Dependency on Size, Support and Adsorbates  
**Judith Yang**, *University of Pittsburgh*
- 10:45 a.m. Exit Wave Reconstruction of Nanocrystalline Catalysts and Radiation Sensitive Materials  
**Angus Kirkland**, *University of Oxford*
- 11:10 a.m. Quantitative In-Situ Mechanical Testing of Nanowires  
**Dan Gianola**, *University of Pennsylvania*
- 11:35 a.m. The Mechanical Behavior of Nanostructures Investigated by In-Situ TEM  
**Andy Minor**, *National Center for Electron Microscopy (NCEM)*
- 12:00 – 1:15 p.m. *Buffet lunch*
- 1:15 p.m. Graphene: Synthesis, Processing and Characterization at the Atomic-Scale  
**Nathan Guisinger**, *Center for Nanoscale Materials (CNM)*
- 1:40 p.m. Atomic Structure and Properties of  $sp^2$ -bonded Materials  
**Alex Zettl**, *University of California–Berkeley*
- 2:05 p.m. From Mapping Energy Flow and Dissipation to Local Thermal and Bias Induced Transformations by SPM  
**Roger Proksch**, *Asylum Research*
- 2:30 p.m. Cryo-Electron Tomography for Protein Dynamic Structure  
**Gary Ren**, *Molecular Foundry (MF)*
- 2:55 p.m. 1-minute/1-slide Poster Previews – Poster Group A
- 3:10 Break
- 3:20 p.m. 1-minute/1-slide Poster Previews – Poster Groups B and C
- 4:00 – 6:00 p.m. Poster Session with refreshments (cash bar)
- 6:00 p.m. Adjourn for dinner (on your own)
- 7:30 – 9:00 p.m. Brainstorming discussions (cash bar)

## Thursday, June 2, 2011

- 7:00 – 8:00 a.m. Continental breakfast
- 8:00 a.m. **Invited Plenary Presentation:** A Review of the TEAM Project and its Scientific Impact  
**Ulrich Dahmen**, *TEAM I Project Team Lead, National Center for Electron Microscopy (NCEM)*
- 8:45 a.m. Probing the Structural and Chemical Information by Scanning Transmission Electron Microscopy  
**Dong Su**, *Center for Functional Nanomaterials (CFN)*
- 9:10 a.m. Discovery of Dislocation Interactions with Irradiation Defects Through In Situ TEM Deformation Experiments  
**Ian Robertson**, *University of Illinois–Urbana-Champaign*
- 9:35 a.m. Nanoscale Imaging and Analysis with Ion Beams  
**David Joy**, *Center for Nanophase Materials Sciences (CNMS)*
- 10:00 a.m. Break
- 10:20 a.m. Hydrothermal Processing of Quantum Dots and Alloy Nanoparticles  
**Mathew Maye**, *Syracuse University*
- 10:45 a.m. Characterization and Control of Monodisperse Core/Shell Nanophases in Solids  
**Velimir Radmilovic**, *National Center for Electron Microscopy (NCEM)*
- 11:10 a.m. Nitrogen-Incorporated Ultrananocrystalline Diamond as a Robust Cold Cathode Material for Advanced Spaceflight Instruments  
**Stephanie Getty**, *NASA Goddard Space Flight Center*
- 11:35 a.m. Spectroscopic and Microscopic Investigations of Model CO<sub>2</sub> Capture and Utilization Materials  
**David Starr**, *Center for Functional Nanomaterials (CFN)*
- 12:00 – 1:00 p.m. *Buffet lunch*
- 1:00 p.m. Self-Healing Radiation-Tolerant Nanostructural Steels for Advanced Nuclear Applications  
**Michael Miller**, *SHared Research Equipment (SHaRE)*
- 1:25 p.m. Defect Evolution Under Ion Irradiation Coordinated with Modeling  
**Marquis Kirk**, *Electron Microscopy Center (EMC)*
- 1:50 p.m. Tracking Solute Atom Additions during Phase Transformations in a Nanocrystalline Steel  
**Francisca Caballero**, *CENIM, Madrid*
- 2:15 p.m. Complementary Use of APT and TEM in the Study of Nanoscale Phase Separation in solids  
**Emmanuelle Marquis**, *University of Michigan*
- 2:40 p.m. Phase Evolution and Structure-Property Correlations in a New Pb-free Morphotropic Phase Boundary  
**Nagarajan Valanoor**, *University of New South Wales*
- 3:15 p.m. Closing Remarks  
**Harriet Kung and Mihai Gross**, *DOE Basic Energy Sciences*
- 3:30 p.m. Adjourn meeting



## Table of Contents

Foreword .....	i
Agenda .....	iii
Table of Contents .....	vii
 <b>Speaker Extended Abstracts</b>	
<b>Invited Plenary Presentation: Industrial Nanoscience: From Discovery to Product Maturity</b>	
<b>Ernest Hall, GE Global Research</b> .....	1
In-Situ TEM Electrochemistry of Li-Ion Battery Materials	
<b>Jianyu Huang, Center for Integrated Nanotechnologies (CINT)</b> .....	3
Interfaces in Bulk Heterojunction Photovoltaics	
<b>Michael Chabinyo, University of California–Santa Barbara</b> .....	5
Ultra-High-Resolution Atomic Imaging of Surfaces and Bulk with an Aberration Corrected Electron Microscope	
<b>Yimei Zhu, Brookhaven National Laboratory</b> .....	7
Developments in Electron-Column Based Spectroscopy for the Characterization of Nanomaterials	
<b>Nestor Zaluzec, Electron Microscopy Center (EMC)</b> .....	9
Probing the Microstructural Evolution of High Energy Density Cathode Oxides for Li-Ion Batteries using Advanced Analytical Electron Microscopy	
<b>Miaofang Chi, SHared Research Equipment (SHaRE)</b> .....	11
<b>Invited Plenary Presentation: Imagine Electron Microscopy 2030</b>	
<b>J. Murray Gibson, Northeastern University</b> .....	13
Charge Illuminates, Spin Interrogates: Microscopy with a Spin-Polarized Electron Beam	
<b>Andreas Schmid, National Center for Electron Microscopy (NCEM)</b> .....	15
Real and Effective Thermodynamics in Artificial Spin Ice	
<b>Christopher Marrows, University of Leeds</b> .....	17
What Speckle Tells Us about Amorphous Materials	
<b>Mike Treacy, Arizona State University</b> .....	19
Mesoscopic Amorphization of Supported Pt Nanoparticles: Dependency on Size, Support and Adsorbates	
<b>Judith Yang, University of Pittsburgh</b> .....	21
Exit Wave Reconstruction of Nanocrystalline Catalysts and Radiation Sensitive Materials	
<b>Angus Kirkland, University of Oxford</b> .....	23
Quantitative In-Situ Mechanical Testing of Nanowires	
<b>Dan Gianola, University of Pennsylvania</b> .....	25
In-Situ TEM Nanomechanical Testing	
<b>Andy Minor, National Center for Electron Microscopy (NCEM)</b> .....	27
Graphene: Synthesis, Processing and Characterization at the Atomic-Scale	
<b>Nathan Guisinger, Center for Nanoscale Materials (CNM)</b> .....	29

Atomic Structure and Properties of $sp^2$ -bonded Materials <b>Alex Zettl</b> , Lawrence Berkeley National Laboratory/University of California–Berkeley .....	31
From Mapping Energy Flow and Dissipation to Local Thermal and Bias Induced Transformations by SPM <b>Roger Proksch</b> , Asylum Research .....	33
Cryo-Electron Tomography for Protein Dynamic Structure <b>Gary Ren</b> , Molecular Foundry (MF).....	35
<b>Invited Plenary Presentation: A Review of the TEAM Project and its Scientific Impact</b> <b>Ulrich Dahmen</b> , TEAM I Project Team Lead, National Center for Electron Microscopy (NCEM) .....	37
Probing the Structural and Chemical Information by Scanning Transmission Electron Microscopy <b>Dong Su</b> , Center for Functional Nanomaterials (CFN) .....	39
Discovery of Dislocation Interactions with Irradiation Defects through In Situ TEM Deformation Experiments <b>Ian Robertson</b> , University of Illinois–Urbana-Champaign .....	41
Nanoscale Imaging and Analysis with Ion Beams <b>David Joy</b> , Center for Nanophase Materials Sciences (CNMS) .....	43
Hydrothermal Processing of Quantum Dots and Alloy Nanoparticles <b>Mathew Maye</b> , Syracuse University .....	45
Characterization and Control of Monodisperse Core/Shell Nanophases in Solids <b>Velimir Radmilovic</b> , National Center for Electron Microscopy (NCEM).....	47
Nitrogen-Incorporated Ultrananocrystalline Diamond as a Robust Cold Cathode Material for Advanced Spaceflight Instruments <b>Stephanie Getty</b> , NASA Goddard Space Flight Center.....	49
Spectroscopic and Microscopic Investigations of Model CO <sub>2</sub> Capture and Utilization Materials <b>David Starr</b> , Center for Functional Nanomaterials (CFN) .....	51
Self-Healing Radiation-Tolerant Nanostructural Steels for Advanced Nuclear Applications <b>Michael Miller</b> , SHared Research Equipment (SHaRE).....	53
Defect Evolution under Ion Irradiation with Coordinated Modeling <b>Marquis Kirk</b> , Electron Microscopy Center (EMC).....	55
Tracking Solute Atom Additions during Phase Transformations in a Nanocrystalline Steel <b>Francisca Caballero</b> , CENIM, Madrid .....	57
Complementary Use of APT and TEM in the Study of Radiation Damage in Alloys <b>Emmanuelle Marquis</b> , University of Michigan.....	59
Atomic-Scale Z-Contrast STEM and EELS Investigation of New Lead-Free Morphotropic Phase Boundary BiSmFeO <sub>3</sub> Thin Films <b>Nagarajan Valanoor</b> , University of New South Wales.....	61

## Poster Extended Abstracts

### Poster Group A

1. Nanoparticle Composites: From Catalysis to Engineering Biology <b>Tijana Rajh</b> , Center for Nanoscale Materials (CNM) .....	63
2. Membrane-Based Nanocomposites <b>Matt Goertz</b> , Center for Integrated Nanotechnologies (CINT).....	65
3. Interfacing Living Cells and Inorganic Materials on the Nanoscale <b>Caroline Ajo-Franklin</b> , Molecular Foundry (MF).....	67
4. A Novel Adenoviral Vector Labeled with Superparamagnetic Iron Oxide Nanoparticles for Real-Time Tracking of Viral Delivery <b>Jonathan Yun</b> , Columbia University Medical Center .....	69
5. Mimicking Biological Membrane Function: Lipid Membrane Architectures Supported on Nanoporous Metal Films <b>Gautam Gupta</b> , Center for Integrated Nanotechnologies (CINT).....	71
6. Tip Functionalization of Silicon Probes to Study Inner Ear Mechanics <b>Domenica Karavitaki</b> , Harvard Medical School.....	73
7. Effects of Aggregation on the Properties of Oligomers Used for Organic LEDs <b>Linda Peteanu</b> , Carnegie Mellon University.....	75
8. The Hard X-ray Nanoprobe: Seeing Advanced Nanomaterials <b>Robert Winarski</b> , Center for Nanoscale Materials (CNM) .....	77
9. X-ray Spectral Fingerprints of Aqueous Chemical Processes from First-Principles Simulations <b>David Prendergast</b> , Molecular Foundry (MF) .....	79
10. Manipulating Nanophase Separation in P3HT/PCBM System with a P3HT- <i>b</i> -PEO Block Copolymer Compatibilizer <b>Jihua Chen</b> , Center for Nanophase Materials Sciences (CNMS) .....	81
11. Phonon, Exciton, and Light Interactions in Semiconducting Single Walled Carbon Nanotubes <b>Anna Swan</b> , Boston University .....	83
12. LT-STM Investigations of Self-Assembled 1D Molecular Chains: Aromatic Diisocyanides on Au(111) <b>Michael White</b> , Stony Brook University/Brookhaven National Laboratory .....	85
13. Self-Assembly of Soft Materials Driven by Competing Specific and Nonspecific Interactions <b>Stephen Whitelam</b> , Molecular Foundry (MF).....	87
14. Surface-Enhanced Raman Spectroelectrochemistry of TTF-Modified Self-Assembled Monolayers <b>Wally Paxton</b> , Center for Integrated Nanotechnologies (CINT) .....	89
15. Direct Surface Imaging of Model Oxide Catalytic Supports <b>Jim Ciston</b> , National Center for Electron Microscopy (NCEM) .....	91
16. Nanofabrication Research Laboratory: Development of Unique Functionality at the Nanoscale <b>Pat Collier</b> , Center for Nanophase Materials Sciences (CNMS).....	93
17. Toward Capturing Membrane Protein Dynamics with the Fiber Force Probe <b>Paul Ashby</b> , Molecular Foundry (MF).....	95

## **Poster Group B**

18. Correlating Microstructure and Current Transport in High Temperature Superconductor Wires <b>Dean Miller</b> , <i>Electron Microscopy Center (EMC)</i> .....	97
19. Hybridization and Kondo Hole Effects in Hidden Order Phase of URu <sub>2</sub> Si <sub>2</sub> <b>Alexander (Sasha) Balatsky</b> , <i>Center for Integrated Nanotechnologies (CINT)</i> .....	99
20. Transition Metal Catalyzed Graphene: Growth, Interface Chemistry, Catalysis <b>Peter Sutter</b> , <i>Center for Functional Nanomaterials (CFN)</i> .....	101
21. Electronic Transport in Graphene and Graphene Nanoribbons <b>Yuegang Zhang</b> , <i>Molecular Foundry (MF)</i> .....	103
22. Nanostructured Graphene for Applications in Optoelectronics <b>Stefan Strauf</b> , <i>Stevens Institute of Technology</i> .....	105
23. Revealing the Electronic Structure of Complex Materials at the Atomic Scale with Single Atom Sensitivity <b>Juan Carlos Idrobo</b> , <i>SHared Research Equipment (SHaRE)</i> .....	107
24. Chemical Imaging of Functional Nanostructures Fabricated by Thermochemical Nanolithography <b>Debin Wang</b> , <i>Lawrence Berkeley National Laboratory</i> .....	109
25. Characterizing a Novel Form of Carbon with Advanced Electron Microscopy Techniques <b>Eric Stach</b> , <i>Center for Functional Nanomaterials (CFN)</i> .....	111
26. Carbon-Based Nanomaterials: Spectroscopic Studies on Single-Walled Carbon Nanotubes and Graphene <b>Andrew Dattelbaum</b> , <i>Center for Integrated Nanotechnologies (CINT)</i> .....	113
27. Combinatorial Discovery and Characterization of Upconverting Nanocrystal Probes <b>Emory Chan</b> , <i>Molecular Foundry (MF)</i> .....	115
28. Advanced Materials Science: Scanning Tunneling Microscopy of Complex Oxides and Chiral Molecular Superstructures <b>Nathan Guisinger</b> , <i>Center for Nanoscale Materials (CNM)</i> .....	117
29. Novel Approaches to Size Control in the Synthesis of Magnetic Nanoparticles <b>Dale Huber</b> , <i>Center for Integrated Nanotechnologies (CINT)</i> .....	119
30. Vortex Behavior in Patterned Magnetic Heterostructures with Circular Exchange-Bias <b>Mihaela Tanase</b> , <i>NIST</i> .....	121
31. Colloidal GeTe Nanoparticles as a Solution Processable Route to Phase Change Materials <b>Marissa Caldwell</b> , <i>Stanford University</i> .....	123
32. Synthesis, Local Structure and Size-Dependent Crystallization of Colloidal Germanium Telluride Nanoparticles <b>Indika Arachchige</b> , <i>Center for Integrated Nanotechnologies (CINT)</i> .....	125
33. Structure and Properties of Thermoelectrics from Computation and Neutron Scattering <b>Paul Kent</b> , <i>Center for Nanophase Materials Sciences (CNMS)</i> .....	127
34. New Tools to Exploit Density Functional Theory for Large-Scale Simulations of Nanomaterials <b>Qin Wu</b> , <i>Center for Functional Nanomaterials (CFN)</i> .....	129
35. Growth Mode and Electronic Structure of Nb Nano-islands on Cu <b>Cesar Clavero</b> , <b>Ale Lukaszew</b> , <i>College of William &amp; Mary</i> .....	131

### **Poster Group C**

36. Elucidating the Atomic-Scale Corrosion Mechanisms of Catalysts, Supports, and Polymers in Proton Exchange Membrane (PEM) Fuel Cell Cathodes <b>Karren More, SHared Research Equipment (SHaRE)</b> .....	133
37. Novel Nanomaterials as Anodes for Li-Ion Batteries <b>Weiqiang Han, Center for Functional Nanomaterials (CFN)</b> .....	135
38. Silicon Nanowires for Novel Thermal Battery Anode <b>Vojtech Svoboda, CFD Research Corp.</b> .....	137
39. Transient Reflectivity and Ion Production from Silicon Nanopost Arrays <b>Akos Vertes, George Washington University</b> .....	139
40. Core-Protected Platinum Monolayer Shell High-Stability Electrocatalysts for Fuel-Cell Cathode <b>Kotaro Sasaki, Brookhaven National Laboratory</b> .....	141
41. Investigating Active Sites on Carbon Based Catalysts <b>Chengdu Liang, Center for Nanophase Materials Sciences (CNMS)</b> .....	143
42. Nanocatalysis from First Principles <b>Manos Mavrikakis, University of Wisconsin–Madison</b> .....	145
43. Anisotropic Volume Expansion and Ultrafast Lithiation of Si Nanowires Revealed by In-Situ Transmission Electron Microscopy <b>Xiaohua Liu, Center for Integrated Nanotechnologies (CINT)</b> .....	147
44. In-Situ LEEM Study of Ceria-Copper Based Water-Gas Shift Catalysts <b>Jurek Sadowski, Center for Functional Nanomaterials (CFN)</b> .....	149
45. Ion Irradiation of Complex Perovskite Systems <b>Greg Lumpkin, Australian Nuclear Science &amp; Technology Organisation (ANSTO)</b> .....	151
46. High-Resolution Characterization of Oxide Scale Grain Boundaries <b>Kinga Unocic, SHared Research Equipment (SHaRE)</b> .....	153
47. Imaging Bi <sub>2</sub> O <sub>3</sub> Nanostructures with the X-ray Nanoprobe <b>Dillon Fong, Argonne National Laboratory</b> .....	155
48. Quantitative STEM: Mapping Order Parameter Fields and Phase Separation on a Single Unit Cell Level <b>Albina Borisevich, SHared Research Equipment (SHaRE)</b> .....	157
49. Radiation Tolerance of Ceramics in Extreme Environments <b>Katherine Smith, Australian Nuclear Science &amp; Technology Organisation (ANSTO)</b> .....	159
50. A Multi-technique Approach to Understand and Develop Radiation-Tolerant Nanostructures <b>Chad Parish, SHared Research Equipment (SHaRE)</b> .....	161

### **Poster Group D**

51. Manipulating Light-Matter Interactions in Nanostructures <b>Daniel López, Center for Nanoscale Materials (CNM)</b> .....	163
52. Synthesis of Abrupt Interfaces without Kinking in VLS-Growth of Si-Ge Axial Nanowire Heterostructures by Novel In Situ Catalyst Alloying <b>Daniel Perea, Center for Integrated Nanotechnologies (CINT)</b> .....	165
53. Mechanism of Plasmonic Response of Noble Metal Nanoparticles Actuated by Responsive Polymer Brush <b>Ihor Tokarev, Clarkson University</b> .....	167

54. Imaging Shape Dependent Surface Plasmon Resonances using Monochromated Electron Beams <b>Shaul Aloni</b> , <i>Molecular Foundry (MF)</i> .....	169
55. Theoretical Studies of Quantum Dot - Plasmon Interactions <b>Stephen Gray</b> , <i>Center for Nanoscale Materials (CNM)</i> .....	171
56. Photon Localization and Sub-diffusive Light Transport in Aperiodic Nanostructures <b>Luca Dal Negro</b> , <i>Boston University</i> .....	173
57. Hybrid Nanophotonic Structures for Energy Conversion <b>Gary Wiederrecht</b> , <i>Center for Nanoscale Materials (CNM)</i> .....	175
58. From Atomic-Resolution Imaging towards Nano-thermodynamics by Enabling Dynamic Experiments for Electron Microscopy with Single Atom Sensitivity at Controlled Temperature and Pressure <b>Christian Kisielowski</b> , <i>National Center for Electron Microscopy (NCEM)</i> .....	177
59. Nanomanipulation for Precise Placement of Individual Nanowires for Thermoelectric Characterization <b>Julio Martinez</b> , <i>Center for Integrated Nanotechnologies (CINT)</i> .....	179
60. Understanding the Low Contact Resistance for Direct Au-C Links to Electrodes in Single Molecule Junctions <b>Hector Vazquez</b> , <i>Columbia University</i> .....	181
61. Correlation between Electron Transport and Local Structures at the Nanoscale Revealed by Four-Probe Scanning Tunneling Microscopy <b>An-Ping Li</b> , <i>Center for Nanophase Materials Sciences (CNMS)</i> .....	183
62. Single-Molecule Spectroscopy Study of Interfacial Charge Separation in Quantum Dot Based Hybrid Systems <b>Mircea Cotlet</b> , <i>Center for Functional Nanomaterials (CFN)</i> .....	185
63. Functional Organic Materials and Their Application in Solar Cells <b>Biwu Ma</b> , <i>Molecular Foundry (MF)</i> .....	187
64. Tailored Assemblies of PS- <i>b</i> -P3HT Diblock Copolymers: Adaptable Building Blocks for High-Performance Organic Transistors and Solar Cells <b>Kai Xiao</b> , <i>Center for Nanophase Materials Sciences (CNMS)</i> .....	189
65. Directed Self-Assembly of Organic Nanostructures from Tailor-Made Electron Donors and Acceptors <b>Yi Liu</b> , <i>Molecular Foundry (MF)</i> .....	191
66. Synthesis and Characterization of Multifunctional Nanocomposite Materials <b>Quanxi Jia</b> , <i>Center for Integrated Nanotechnologies (CINT)</i> .....	193
<b>Presenter Index</b> .....	195
<b>Participant List</b> .....	197

# Speaker Extended Abstracts



**Invited Plenary Presentation**

**Industrial Nanoscience: From Discovery to Product Maturity**

**Ernest Hall**

Chief Scientist, Materials Characterization  
GE Global Research  
Niskayuna, NY 12309



## In-Situ TEM Electrochemistry of Li-Ion Battery Materials

Jian Yu Huang,<sup>1</sup> Xiao Hua Liu,<sup>1</sup> John P. Sullivan,<sup>1</sup> Li Zhong,<sup>2</sup> Li Qiang Zhang,<sup>2</sup> Scott X. Mao,<sup>2</sup> Chong Min Wang,<sup>3</sup> Wu Xu,<sup>3</sup> Nicholas S. Hudak,<sup>1</sup> Arunkumar Subramanian,<sup>1</sup> Hong You Fan,<sup>1</sup> Liang Qi,<sup>4</sup> Akihiro Kushima<sup>4</sup>, Ju Li<sup>4</sup>

<sup>1</sup> CINT, Sandia National Laboratories, Albuquerque, New Mexico 87185, USA

<sup>2</sup> University of Pittsburgh, Pittsburgh, Pennsylvania 15261, USA

<sup>3</sup> Pacific Northwest National Laboratory, Richland, Washington 99354, USA

<sup>4</sup> Department of Materials Science and Engineering, University of Pennsylvania, Philadelphia, Pennsylvania 19104, USA

**Scientific Thrust Area:** *Nanoscale Electronics and Mechanics*

**Related User Proposal:** *In-situ electron microscopy and spectroscopy studies of interfaces in advanced Li-ion batteries under dynamic operation conditions*

**Abstract:** Lithiation/delithiation of the electrode materials in Li-ion batteries (LIBs) induces large strains in the host material leading to plasticity and fracture. Lithiation is also often accompanied by phase transformations, such as electrochemically-driven solid-state amorphization (ESA). These electrochemical reaction-induced microstructural events limit the energy capacity and cycle lifetime of LIBs. However, the detailed mechanisms of strain-induced plasticity and strain accommodation in LIB materials during electrochemical charging are largely unknown.

We created the first electrochemical device inside a transmission electron microscope – consisting of a single SnO<sub>2</sub> nanowire anode, an ionic liquid electrolyte and a bulk LiCoO<sub>2</sub> cathode – and conducted the first in-situ observation of the lithiation of the SnO<sub>2</sub> nanowire during electrochemical charging [1]. Upon charging, a reaction front propagated progressively along the nanowire, causing the nanowire to swell, elongate, and spiral (Fig. 1). The reaction front is a “Medusa zone” containing a high density of mobile dislocations, which are continuously nucleated and absorbed at the moving front (Fig. 2). This dislocation cloud indicates large in-plane misfit stresses and is a structural precursor to electrochemically-driven solid-state amorphization. Because lithiation-induced volume expansion, plasticity and pulverization of electrode materials are the major mechanical effects that plague the performance and lifetime of high capacity anodes in lithium-ion batteries, our observations provide important mechanistic insight for the design of advanced batteries.

We are using our in-situ nano battery setup to study the charging and discharging processes of many battery materials, such as carbon nanotubes, graphene, Si, Ge, Sn nanowires, and some exciting results are forthcoming. It is expected that our in-situ studies can address some major issues in LIBs, such as what is the solid-electrolyte interface (SEI) and how does it affect the battery cycle lifetime; what causes the lithiation induced strain and how can we mitigate the strain? Our studies provide the fundamental science to guide the development of high energy density and high power density LIBs for electrical vehicle and portable electronics applications.

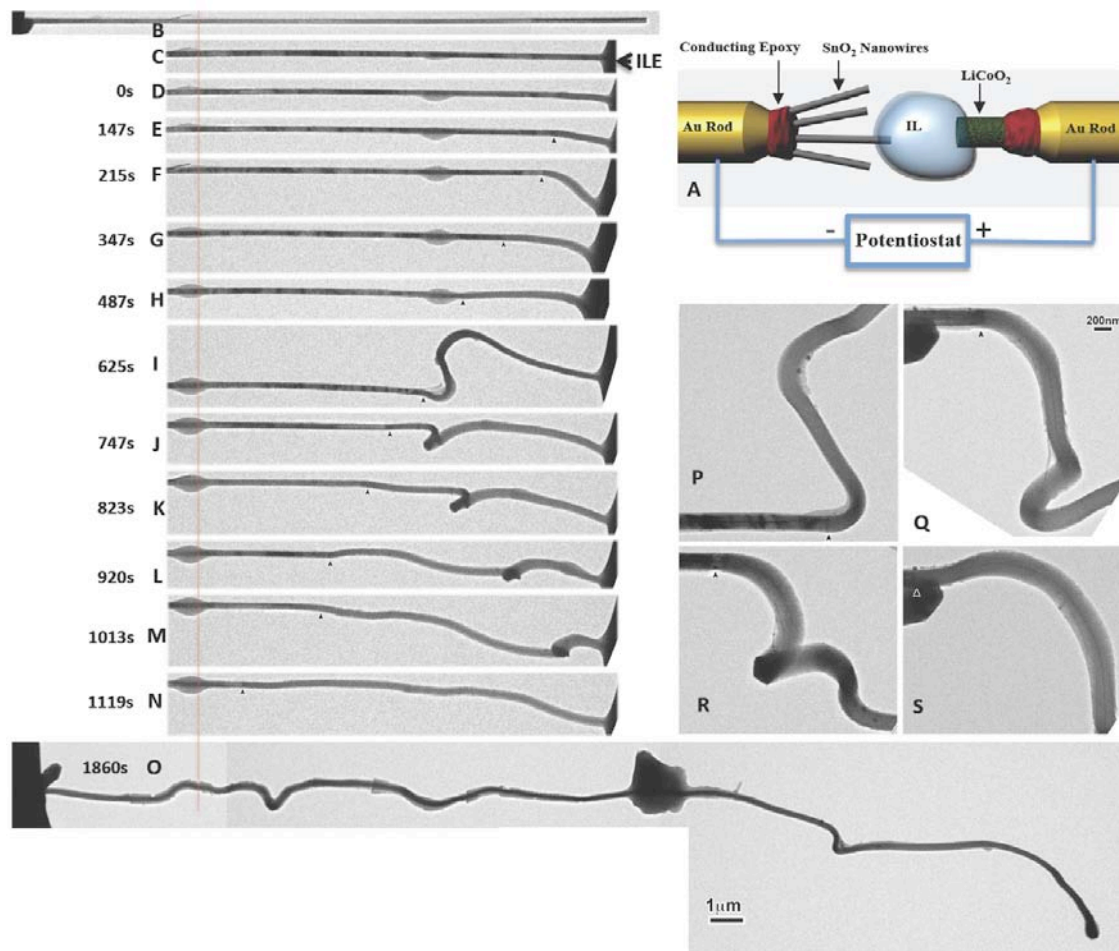


**Fig. 1** Time-lapse structure evolution of a  $\text{SnO}_2$  nanowire anode during charging at  $-3.5$  V against a  $\text{LiCoO}_2$  cathode. The single crystal nanowire was elongated 60% and the diameter increased 45% (resulting in a 240% volume expansion) following charging for 1860s. (A) Schematic of the experimental setup. The initially straight nanowire (B and C) became significantly twisted and bent after charging (D to S). The electrochemical reaction front progressed along the nanowire's longitudinal direction, as pointed out by arrowheads in (E) to (S). (P) to (S) are sequential high magnification images showing the progressive migration of the reaction front, swelling, and the twisted morphology of the nanowire after the reaction front passed by.

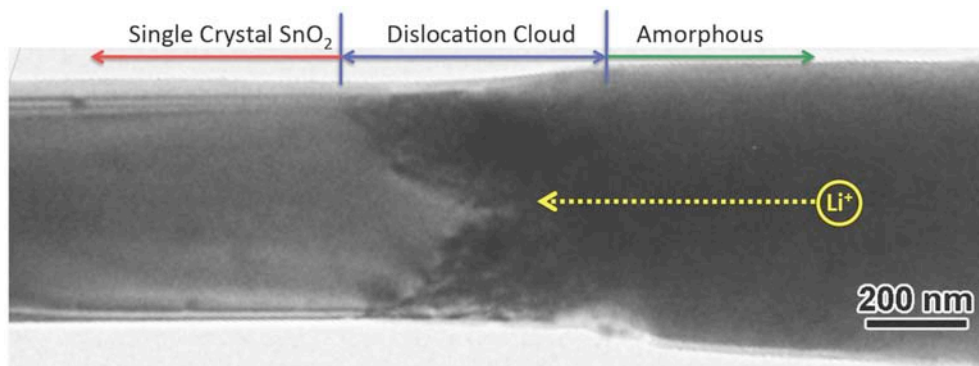


**Fig. 2** The reaction front contains high density of dislocations.

**Publications:** J.Y. Huang *et al.*, *Science* 330, 1515-1520 (2010); Y. M. Chiang, *Science* 330, 1485 (2010)

**Acknowledgement:** This work was performed, in part, at the Center for Integrated Nanotechnologies, a U.S. Department of Energy, Office of Basic Energy Sciences user facility. Sandia National Laboratories is a multi-program laboratory operated by Sandia Corporation, a Lockheed-Martin Company, for the U. S. Department of Energy under Contract No. DE-AC04-94AL85000. Portions of this work was supported by the Science of Precision Multifunctional Nanostructures for Electrical Energy Storage (NEES), an Energy Frontier Research Center funded by the U.S. Department of Energy, Office of Science, Office of Basic Energy Sciences under Award Number DESC0001160. The NEES center supported the development of TEM techniques, and some of the platform development, and fabrication and materials characterization. CINT supported the TEM capability and the fabrication capabilities that were used for the TEM characterization, in addition, this work represents the efforts of several CINT users, primarily those with affiliation external to Sandia National Labs.

## Interfaces in Bulk Heterojunction Photovoltaics

Michael Chabynec

Materials Department

University of California Santa Barbara

**Proposal Title:** Fabrication of Nanostructured Solar Cells Using Soft Imprint Lithography

**Scientific Challenge and Research Achievements.** Organic bulk heterojunction (BHJ) photovoltaics have achieved efficiencies of ~8% in laboratory cells. A BHJ is a blend of an electron donating and electron accepting material where the two components form a bicontinuous network with a high interfacial area. The further improvement of the power conversion efficiency in these devices depends on an improved understanding of charge generation at separation at the interface between donor and acceptor domains. Transparent metal oxide cathodes have received significant attention as electrodes due to their potential for improved lifetime and performance relative to reactive metallic electrodes. We have used soft nanoimprint lithography to pattern solution-processable amorphous titanium sub-oxide ( $a\text{-TiO}_x$ ) and examined the effect of increasing the electrode surface area and the processing procedures on performance of poly(3-hexylthiophene):PCBM BHJs. Increasing the electrode surface area noticeably improved the charge injection, but had little effect on the charge extraction. The open circuit voltage,  $V_{oc}$ , was sensitive to both the electrode geometry and processing method. We suggest that differential infiltration of the polymer and fullerene into the nanopores is the dominant mechanism for these changes. Recent results probing the diffusion of fullerenes in poly(3-hexyl)thiophene will also be described.

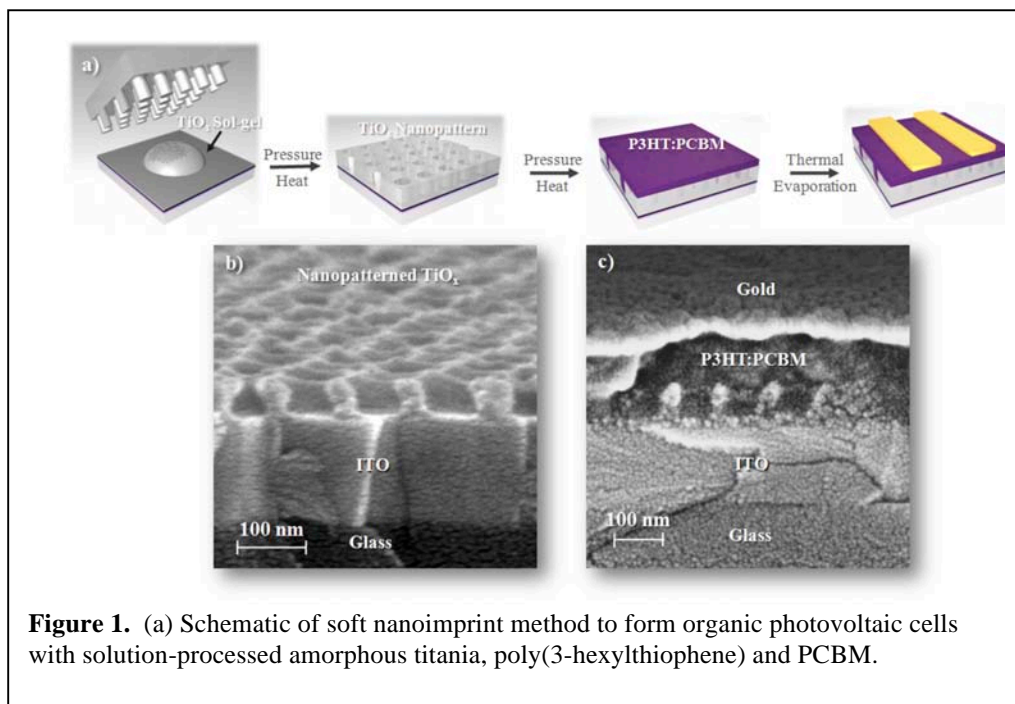


**Figure 1.** (a) Schematic of soft nanoimprint method to form organic photovoltaic cells with solution-processed amorphous titania, poly(3-hexylthiophene) and PCBM.

**Future Work**

The direct nanoimprinting of semiconducting polymers to form BHJ nanostructure is being examined. Synthesis of novel low-band gap polymers is underway to develop appropriate systems compatible with nanoimprint methods.

**Publications**

N. D. Treat, L. M. Campos, M. D. Dimitrou, B. W. Ma, M. L. Chabinye and C. J. Hawker "Nanostructured Hybrid Solar Cells: Dependence of the Open Circuit Voltage on the Interfacial Composition." *Adv. Mater.* **22** 4982-4986 (2010)

# Ultra-High-Resolution Atomic Imaging of Surfaces and Bulk with an Aberration Corrected Electron Microscope

Y. Zhu,<sup>1,2</sup> D. Su,<sup>2</sup> J. Ciston,<sup>2</sup> J. Wall,<sup>3</sup> H. Inada,<sup>4</sup> and R.F. Egerton<sup>5</sup>

<sup>1</sup> Department of Condensed Matter Physics and Materials Science, <sup>2</sup> Center for Functional Nanomaterials, <sup>3</sup> Biology Department, Brookhaven National Laboratory, Upton, NY 11973, USA

<sup>4</sup> Hitachi High Technologies Corp., Ibaraki, Japan

<sup>5</sup> Department of Physics, University of Alberta, Edmonton, Canada

## Scientific Thrust Area : Electron Microscopy

The development of aberration correction has pushed the spatial resolution of electron microscopes below the one angstrom mark. However, the advancement so far has been limited to the use of transmitted electrons, both in scanning (STEM) and stationary (TEM) mode with an improvement of 20-40%. In contrast, the improvement of the spatial resolution using secondary electrons in SEM has been stagnant, although several attempts have been made in recent years. Since the mechanism for the generation of secondary electrons (SE) is traditionally believed through the decay of collective electronic excitations generated by inelastic scattering of the incident high-energy electrons, thus, even for thin samples, the resolution is limited by delocalization to about 1nm scale.

We prove this is not the case. We demonstrate using the newly developed Hitachi HD2700C aberration corrected electron microscope at the Center for Functional Nanomaterials, BNL, it is possible to achieve one angstrom resolution in SE imaging, which represents a fourfold improvement over the best-reported resolution in any SEM. The accomplishment is attributed to better design of electro-optics (including ultra-high electric and mechanical stabilities) and more efficient detectors (Fig.1) [1]. Furthermore, the instrument allows us to probe the same sample area using simultaneously secondary electrons emerging from the surface and the transmitted electrons passing through the bulk (Fig.1, 2). The capability of selective visualization of bulk as well as surface atoms is significant [2]. It opens a door to a wide range of applications, such as observation of dopant atoms in electronic devices and study of the active sites and role of individual atoms and their bonding state during a catalytic chemical reaction, especially when combined with synchronized nanoprobe spectroscopy. Quantitative SE image analyses using the corresponding ADF-STEM image as the reference, including measurement of image intensity as a function of applied bias, sample thickness, crystal tilt and defocus will be presented. Possible scattering mechanisms [3] to achieve such astonishing resolution will also be discussed [4].

## References

[1] Y. Zhu, H. Inada, K. Nakamura, and J. Wall, "Imaging single atoms using secondary electrons with an aberration-corrected electron microscope", *Nature Materials*, **8** 808 (2009).

[2] D.C. Joy, "Second best no more", a commentary article highlights the work reported in [1], *Nature Materials*, **8** 776 (2009).

[3] Inada, H., Su, D., Egerton, R.F., Konno, M., Wu, L., Ciston, J., Wall, J., and Zhu, Y., "Atomic Imaging Using Secondary Electrons in a Scanning Transmission Electron Microscope : Experimental Observations and Possible Mechanisms", invited articles for the special issue in honor of John Spence, *Ultramicroscopy*, in press

[4] Work supported by the U.S. DOE, Office of Basic Energy Science, under Contracts No. DE-AC02-98CH10886.

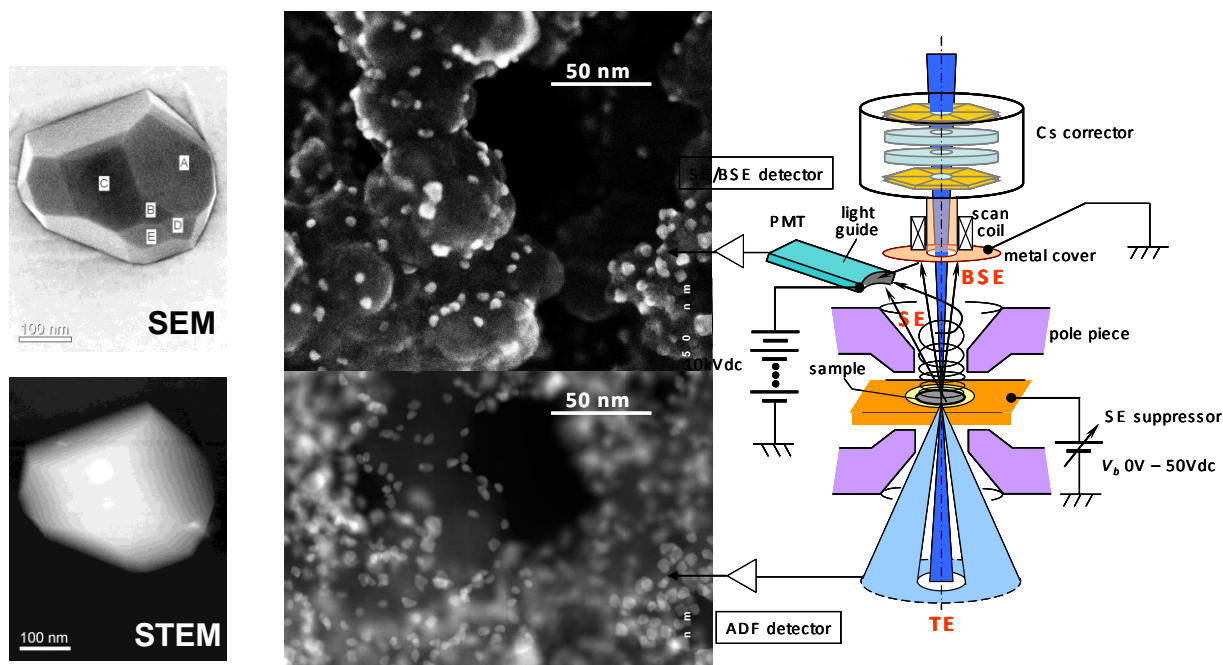


Fig.1 Simultaneous acquisition of SEM images (top left) using secondary electrons (SE), and ADF-STEM images (bottom left) using transmitted electrons (TE). The right panel shows a schematic of the instrument with an in-lens-design pole-piece. The image pairs show Pd nanoparticles on a carbon support (middle column) as well CaO particles on a MgO support. We note that the SEM image offers a much better three-dimensional view of the area.

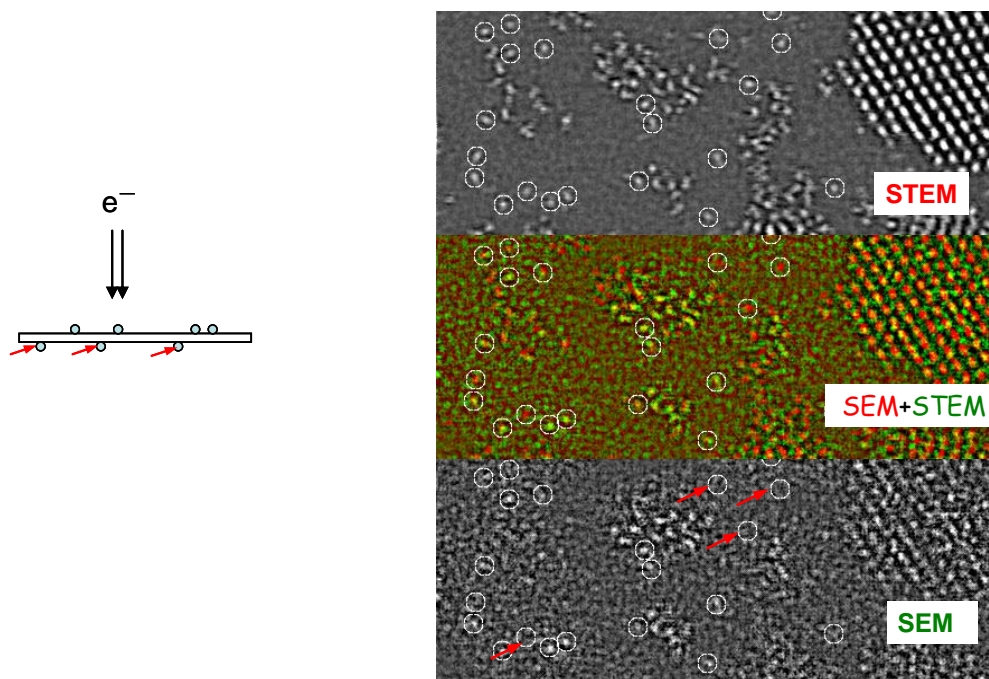


Fig.2 Simultaneous acquisition of the atomically resolved SE image (bottom-right), the ADF-STEM image (top-right), and the superposition of the two (middle), of uranium oxide nanocrystals and individual uranium atoms. Bias experiment reveals that 85-90% of SE image intensities result from secondary electrons with an energy below 20eV. Quantized intensity analysis in the ADF image suggests the areas marked by small circles are individual isolated uranium atoms. The ones pointed by the arrow are at the bottom of the C-support, as schematically shown on the left. Line profile of average intensity distribution of 354 individual atoms shows FWHM of 0.1nm (standard deviation of 20% with a mean of 14.4).

## Developments in Electron-Column Based Spectroscopy for the Characterization of Nanomaterials.

Nestor J. Zaluzec  
Electron Microscopy Center  
Argonne National Laboratory

### Scientific Thrust Area:

Instrument/Technique Development

### Scientific Challenge and Research Achievement:

When studying the new generation of nano-materials our ability to not only detect, but also to do so with high collection efficiency and to ultimately quantitatively analyze smaller and smaller volumes of material has become an increasingly important part of our repertoire of characterization methods. In nano-materials research, one of the ubiquitous instruments we employ for characterization is the electron microscope. After electrons, the signal most often measured in these instruments is the emission of characteristic x-rays. During the last 40 years, either the solid state Si(Li) or more recently the SDD Energy Dispersive Spectrometer (EDS)<sup>1,2</sup> have been the detector most often used for this task. On one hand these detectors are remarkably, simple and efficient devices, but on the other there nearly always remains opportunities for improvement. One of the factors which governs the ability to measure an x-ray signal is the detector geometrical collection efficiency and is typically defined in terms of the collection solid angle ( $\Omega$ )<sup>3</sup>. Typical solid angles for commercial systems range from 0.01-0.3 sr. We have designed and tested a new geometry of x-ray detector which provides an improvement of up to 500x the collection efficiency of commercial systems and currently reaches a solid angle of  $\pi$  sr<sup>4</sup>. These improvements allow detection and EDS analysis of individual nanoparticles and in principle single atoms under conditions of high resolution imaging<sup>5</sup>.

In a parallel research effort, we are also studying electronic excitations in plasmonic, excitonic and hybrid systems<sup>6</sup>. Conventional optical studies of such engineered nanostructures have been performed on nanoparticle ensembles using ultrafast lasers and optical spectroscopy, but only in dilute solutions. As a result, optical techniques are not able to probe the local electromagnetic environment of arrays of interacting quantum dots or molecular interactions in dense systems. In particular they lack the ability to probe electromagnetic coupling between nanoparticle systems. Preliminary results in this area as well as the potentials afforded by interfacing dedicated electron and optical spectrometers to the column of a transmission electron microscope will be presented. This technology will enable us to measure electronic dynamics in a range of nanomaterials systems with single-nm spatial resolution. Such

capabilities promise to open up the emerging frontier between traditional optical and electron energy loss spectroscopy approaches to the study of electronic excitations in densely packed nanostructures at the sub-eV energy scale.

### **Future Work:**

The current generation of detector has been fabricated to operate in a STEM/SEM mode, designs suitable for STEM/TEM application have been proposed but not yet constructed. An electron optical test bed suitable for STEM/TEM R&D work has been established, and interfaces to advanced optical and electron spectrometers are being constructed.

### **References:**

- 1.) Fitzgerald R. , Keil, K., Heinrich KFJ. (1968).Solid-state energy-dispersion spectrometer for electron-microprobe x-ray analysis. Science Vol 159, p 528
- 2.) Bertuccio G, Castoldi A, Longoni A, Sampietro M, Gauthier C (1992). New Electrode Geometry And Potential Distribution For Soft-X-Ray Drift Detectors. Nucl. Instr. Meth., Phys. Res. A312, 613
- 3.) Zaluzec, N.J. (2009) Detector Solid Angle Formulae for Use in X-ray Energy Dispersive Spectrometry, Micros & Microanaly, Vol 15, #2, p 93-98
- 4.) R&D 100 Award – 2010 & US patent Application Serial No. 13/041,265.
- 5.) Zaluzec, N.J. Single Atom Detection by XEDS in the Aberration Corrected AEM: Is it Feasible? Microscopy & Microanalysis, 15, sup 2 , 458-459, doi: 10.1017/S1431927609095646
- 6.) N’Gom M etal, Single Particle Plasmon Spectroscopy of Silver Nanowires and Gold Nanorods Nano Letters 8, #10 3200-3204 (2008)
- 7.) This work was supported by the US DoE, the Office of Science, at Argonne National Laboratory under Contract DE-AC02-06CH11357.

## Probing the microstructural evolution of high energy density cathode oxides for Li-ion batteries using advanced analytical electron microscopy

Miaofang Chi,<sup>1</sup> Christopher Fell,<sup>2</sup> Bo Xu,<sup>3</sup> and Y. Shirley Meng<sup>2,3</sup>

<sup>1</sup>Materials Science & Technology Division, Oak Ridge National Laboratory

<sup>2</sup>Department of Materials Science and Engineering, University of Florida

<sup>3</sup>Department of NanoEngineering, University of California - San Diego

**Proposal:** “Combing Analytical Electron Microscopy with First Principles Computation for Investigating the Cation Rearrangement and Surface Changes in High Energy Density Nanocomposite Oxides.” SHaRE Proposal ID 2011\_Meng\_84

**Scientific Challenge and Research Achievement:** Many complex oxides, such as lithium manganese oxides ( $\text{Li}_x(\text{TM}_y\text{Mn}_{1-y})\text{O}_2$  where TM=transition metal), are electrochemically active materials that can store and convert energy.<sup>1-3</sup> These oxides have intriguing and complex features, including nm-scale phase separation upon cycling and dynamic cation redistribution at various states of charge, that significantly affect Li mobility in Li-ion batteries. The reduction-oxidation processes that occur upon battery cycling, not only may alter the cation distributions, but can also modify the solid-solid interfaces within the material, which are critical to the transport properties as well as the structural stability of the electrodes. The objective of this work is to evaluate the cation rearrangement, vacancy evolution, defect generation, and electrode surface stability at the atomic scale for a class of lithium manganese-TM oxides that are capable of storing energy reversibly. The experimental results from analytical electron microscopy are combined with computation and electrochemical performance to draw a full picture of the compositional and structural evolution of cathodes and the cathode-electrolyte interface upon cycling. The insights gained in this study will guide the compositional and morphological design of new advanced materials for energy storage.

$\text{Li}[\text{Li}_{0.2}\text{Ni}_{0.2}\text{Mn}_{0.6}]\text{O}_2$  (LMNO) was chosen as a model compound in the present work because of its relatively high capacity. STEM was used to study the atomic structure of individual LMNO grain surfaces prepared using different synthesis methods. It was found that surface atomic structure and grain morphology significantly affected the electrochemical performance of the LMNO. The microstructure and composition of as-prepared samples were compared with samples cycled in a coin cell between 2.5 and 5.0V for one, ten, and twenty cycles. Although bulk crystalline structure and composition remains the same, surface structure modifications for the LMNO particles were observed by high angle annular dark field (HAADF) STEM imaging before and after electrochemical cycling, Fig. 1a and 1b, respectively. After 10 cycles, it was found that most of the original Li sites occupied by TM atoms (Ni in this case) at the outermost 4-5 atomic layers of the surface, which could significantly block the Li transport pathway and thus degrading battery performance. The oxidation state of Mn in this surface region was  $\sim 3^+$  instead of  $4^+$ , as in the bulk or in the as-prepared samples based on EELS analysis, while that of Ni remained  $2^+$ , as shown in Figure 2. Interestingly, this surface structural modification was observed on the oxide surface after only one cycle and the thickness of the surface region did not change with the number of electrochemical cycles. A detailed lithium de-intercalation mechanism was proposed by combining these experimental observations with first principles calculations. Such a surface phase transformation is one of the factors contributing to the first-cycle irreversible capacity loss and is the main

reason for the intrinsic poor rate capacity of these materials. Further understanding of the irreversible capacity loss within the first cycle was investigated by studying materials that were charged and discharged at different stages. The evolution of defect density, surface atomic structure, oxygen vacancies, and TM dissolution, were intensively investigated by atomic-scale STEM imaging and EELS analysis.

**Future work:** Research includes two main components: (1) in-situ observation of atomic and electronic structural evolution in cathode oxides and cathode-electrolyte solid-solid interfaces upon electrochemical cycling; (2) understand how cathode coatings work, mainly the interactions between coating materials, cathode layers, and the electrolyte, and further explore new coating materials. Future characterization via TEM, X-ray diffraction, XPS, and APT, will be correlated with electrochemical performance and theoretical calculations, to improve and design novel complex oxides for Li-ion batteries.

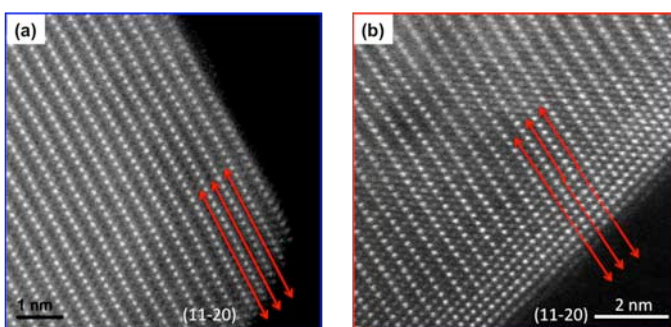


**Figure 1.** Comparison of the atomic surface structure of (a) pristine and (b) 10X cycled  $\text{Li}_{1.2}\text{Mn}_{0.6}\text{Ni}_{0.2}\text{O}_2$ . Arrowed lines show the Li diffusion pathway.

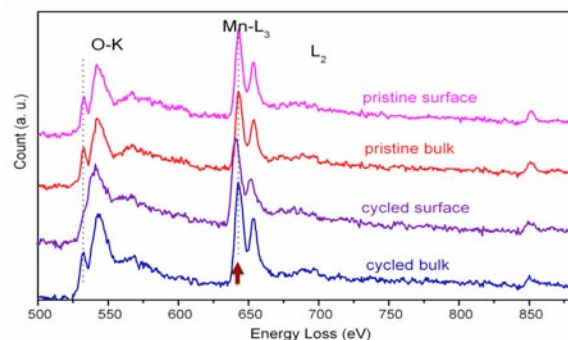


**Figure 2.** Electron energy loss spectra (EELS) from surface and bulk region of pristine and 10X cycled  $\text{Li}_{1.2}\text{Mn}_{0.6}\text{Ni}_{0.2}\text{O}_2$  respectively, which clearly reveals the modification of the electronic structure on grain surfaces after electrochemical cycling.

**Support:** Research supported by the SHaRE User Facility, Office of Basic Energy Sciences, U.S. Department of Energy.

#### References:

1. Z. Lu, D. D. MacNeil, and J. R. Dahn, *Electrochem. Solid-State Letters* **4** A191 (2001).
2. M. M. Thackeray, S.-H. Kang, C. S. Johnson, J. T. Vaughey, R. Benedek, and S. A. Hackney, *Journal of Materials Chemistry* **17** 3112 (2007).
3. B. Jiang, B. Key, Y. S. Meng, and C. P. Grey, *Chemistry of Materials* **21** 2733 (2009).

#### Publications:

1. C. R. Fell, K. J. Carroll, M. Chi, and Y. S. Meng, *Journal of the Electrochemical Society* **157**[11] A1202 (2010).
2. B. Xu, C.R. Fell, M. Chi, and Y.S. Meng, *Energy and Environmental Science* in print (2011).

**Invited Plenary Presentation**

Imagine Electron Microscopy 2030

**Murray Gibson**

Dean, College of Science  
Northeastern University  
Boston, MA 02115



## **Charge Illuminates, Spin Interrogates: Microscopy With a Spin-Polarized Electron Beam**

Andreas Schmid

National Center for Electron Microscopy, Materials Sciences Division, LBNL, Berkeley, CA 94720

### **Scientific Thrust Area**

Electron spin is a crucial quantum number even in the most basic questions of solid state physics and chemistry (such as how many electrons will occupy which orbitals in an atom, molecule or particle). Yet, control of the spin quantum number is uncommon in electron microscopy.

By illuminating surfaces with a spin-polarized electron beam, the NCEM SPLEEM (spin-polarized low-energy electron microscope) provides unique opportunities, particularly with regard to magnetic phenomena. On the nanoscale, materials properties such as magnetic transition temperatures, the easy-axis of magnetization, etc., are strongly size-dependent and are a sensitive function of contact with other materials, such as substrates or adsorbates, even when the contacting materials are not magnetic. The SPLEEM permits in-situ measurements under well-controlled experimental conditions. Simultaneously imaging a sample's magnetic structure while observing MBE-growth of film structures or the formation and properties of adsorbate layers, in controlled environments and under dynamic conditions, helps us understand proximity and confinement phenomena in films and multilayers.

### **Scientific Challenge and Research Achievement**

The Co/Ru(0001) model system is interesting because even pristine films exhibit an unusual double spin reorientation transition: one-monolayer and three or more monolayer thick films are magnetized within the film plane, while two-monolayer films are magnetized perpendicular. Capping Co/Ru(0001) films with noble metal elements modifies the spin-reorientation transitions depending on the Co and overlayer thicknesses. The resulting expanded range of structures with high perpendicular magnetic anisotropy can be explained in terms of ab-initio calculations of the layer-resolved contributions to the magnetic anisotropy energy [1].

Recent work extends the results on metal overlayers by illustrating the delicate sensitivity of the magnetism in these structures to the adsorption of gases such as hydrogen. These results may prove useful in device applications [2].

### **Future work**

At this time experimental research with spin-polarized electron beams remains limited by the small number of available instruments, and many materials and questions remain to be explored. We are continuing to expand MBE growth capabilities to enable in-situ growth of a broader range of materials, including oxides and alloys. Adapting combinatorial chemistry techniques [3], we have demonstrated parallel synthesis of spatially addressable libraries of binary alloy films with systematic variation of composition and film thickness. These samples are prepared in-situ by simultaneous evaporation high-purity constituents from separate electron-beam evaporation sources, while shadow masks intersect the vapor beams in a geometry that leads to the growth of films with crossed double-wedge concentration profiles. Among the topics we plan to study with this method is the composition and temperature dependence of the manetocaloric phase transition in FeRh alloys.

Chirality is another curious topic we may try and explore. All life on earth shares the same molecular chirality – what is the origin of this bias, and what are the consequences? Earlier this year, Goehler

et al. reported their discovery of an enormous spin-filtering effect in layers of pure DNA on gold substrates [4]. Four orders of magnitude greater than expected [5], the effect is both surprising and suggests a need to add a new tool to the molecular biology suite of instrumentation: spin-polarized electron scattering.

## **Publications**

[1] El Gabaly F, McCarty KF, Schmid AK, de la Figuera J, Munoz MC, Szunyogh L, Weinberger P, Gallego S, *New Journal of Physics* 10, 073024 (2008)

[2] “Hydrogen Sensitive Magnetic Structure” U.S. Patent Application Ser. No: 61/175,367

## **References**

[3] X. -D. Xiang et al., *Science* 268, 1738 (1995)

[4] “Spin Selectivity in Electron Transmission Through Self-Assembled Monolayers of Double-Stranded DNA”, B. Goehler et al., *Science* 331, 894 (2011)

[5] R. A. Rosenberg, *Top Curr Chem* 298, 279–306 (2011)

## Real and Effective Thermodynamics in Artificial Spin Ice

J. P. Morgan<sup>1</sup>, A. Stein<sup>2</sup>, J. Akerman<sup>1,3</sup>, S. Langridge<sup>4</sup>, & C. H. Marrows<sup>1</sup>

<sup>1</sup> School of Physics & Astronomy, University of Leeds, Leeds LS2 9JT, United Kingdom

<sup>2</sup> Center for Functional Nanomaterials, Brookhaven National Laboratory, Upton, NY 11973 USA

<sup>3</sup> Instituto de Sistemas Optoelectrónicos y Microtecnología (ISOM), Universidad Politécnica de Madrid, Avda. Complutense s/n, 28040 Madrid, Spain

<sup>4</sup> ISIS, STFC Rutherford Appleton Laboratory, Harwell Science and Innovation Campus, Didcot, Oxon. OX11 0QX, United Kingdom

### Proposal Title

Large scale arrays of frustrated nanomagnets

### Scientific Challenge and Research Achievement

Spin ices are rare earth pyrochlores where the crystal geometry leads to frustration of the rare earth moments [1], which meet at tetrahedra in the lattice. Like water ice, they violate the third law of thermodynamics, as the frustration prevents the formation of a unique ground state. Recently it has been realised that excitations of this system can be described as deconfined emergent monopoles and associated Dirac strings [2]. Nanotechnology allows many of the essential features of this physical system can be reproduced in arrays of patterned nanomagnets where moments meet at the vertices of a square grid [3]. This approach offers the opportunity to continuously tune the various parameters controlling the magnetic microstate, and also to inspect that microstate using advanced magnetic microscopy [4,5]. A significant difference with the naturally occurring spin-ices is that the change in symmetry gives rise to a true long-range ordered ground state, although the frustrated interactions in these athermal systems mean that its observation is extremely difficult [6]. Most attempts to achieve it rely on a rotating field demagnetisation protocol that produces states that show reasonably good ice rule fidelity but only short range correlations [3,6].

Here I will describe our recent work on such a system, an array of 250 nm × 80 nm Permalloy islands in the square ice geometry (shown in Figure 1), including the achievement of a thermalised ground state during fabrication and the observation of the effects of fractionalised monopoles on excitations out of it (shown in Figure 2) [7], and athermal achievement of the ground state using a suitable field protocol, both observed using magnetic force microscopy. I will also describe the application of an effective temperature formalism [8] to the frozen thermal microstates we observe and their statistical comparison with the effectively thermal states formed by the rotating field method.

This work was supported financially by EPSRC and the STFC Centre for Materials Physics and Chemistry. Parts of this research were carried out at the Center for Functional Nanomaterials, Brookhaven National Laboratory, which are supported by the U.S. Department of Energy, Office of Basic Energy Sciences, under Contract No. DE-AC02-98CH10886.

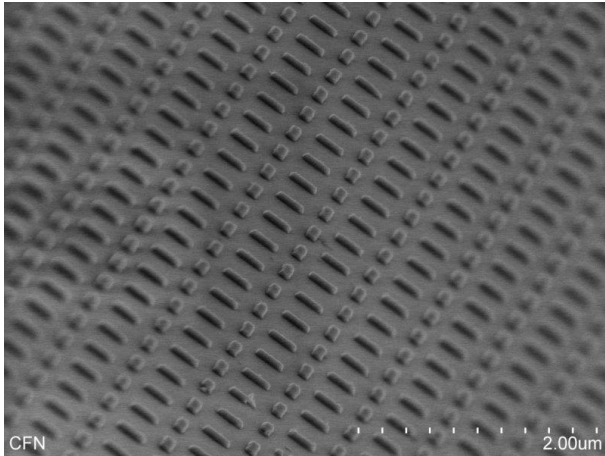


Figure 1: Scanning electron micrograph of a array of Permalloy nanomagnets, prepared using electron beam lithography, that form a frustrated square ice lattice.

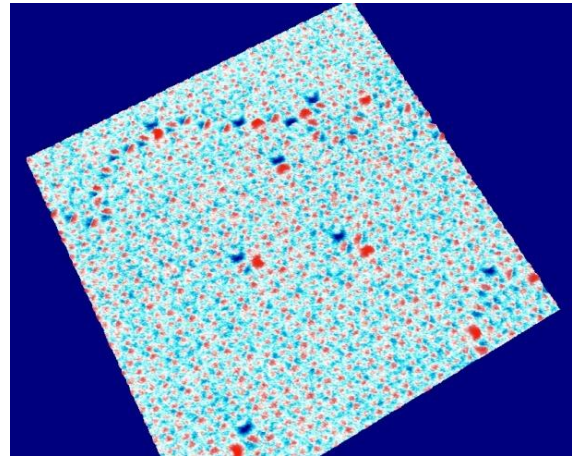


Figure 2: Rendering of a magnetic force micrograph showing the smeared magnetic charge density: monopole defects in the periodic ground state are clearly visible.

## Future Work

This experiment has given rise to many opportunities for further work. We plan to explore other array geometries, materials other than Permalloy, the effects of deliberately introducing defects in the lattice, and also making smaller elements to try to observe the onset of thermally driven magnetic dynamics.

## References

- [1] S. T. Bramwell and M. J. P. Gingras, *Science* 294, 1495 (2001).
- [2] C. Castelnovo, R. Moessner, and S. L. Sondhi, *Nature* 451, 42 (2008).
- [3] R. F. Wang et al., *Nature* 439, 303 (2006).
- [4] S. Ladak et al., *Nature Physics* 6, 359 (2010).
- [5] E. Mengotti et al., *Nature Physics* 7, 69 (2011).
- [6] X. Ke et al., *Phys. Rev. Lett.* 101, 037205 (2008).
- [7] J. P. Morgan, A. Stein, S. Langridge, and C. H. Marrows, *Nature Physics* 7, 75 (2011).
- [8] C. Nisoli et al., *Phys. Rev. Lett.* 105, 047205 (2010).

## Publications

J. P. Morgan, A. Stein, S. Langridge, and C. H. Marrows, *Nature Physics* 7, 75 (2011).

## What Speckle tells us about Amorphous Materials

M.M.J. Treacy<sup>1</sup>, J.M. Gibson<sup>2</sup>, T. Sun<sup>3</sup>, N.J. Zaluzec<sup>4</sup>

<sup>1</sup> Department of Physics, Arizona State University, Tempe, AZ 85287-1504, USA

<sup>2</sup> College of Science, Northeastern University, Boston, MA 02115, USA

<sup>3</sup> Advanced Photon Source, Argonne National Laboratory, Argonne, IL 60439, USA

<sup>4</sup> Electron Microscopy Center, Argonne National Laboratory, Argonne, IL 60439, USA

**Proposal title:** Exploration of Medium-Range Order

### Scientific Challenge and Research Achievement:

Ideal amorphous materials are a near-random assembly of atoms. They possess strong short-range order, in the sense that the centers of nearest-neighbor atoms cannot get closer to each other than their nominal atomic diameter. However, those structural correlations fade away rapidly with increasing neighbor distance. Few amorphous materials are ideally disordered; there tend to be subtle structural correlations that persist out to the so-called "medium-range"  $\sim 3.0$  nm.

Although experimental techniques such as x-ray diffraction and transmission electron microscopy (TEM) are powerful tools for studying crystalline materials, surprisingly the ability of these techniques to discern structural details are limited when studying amorphous materials. This limitation arises because the averaged background scattering strongly masks any structural ordering that may be present. Nevertheless, diffraction allows the pair distribution function to be obtained, which can reveal subtle details about differences in short-range order, and TEM can disclose the presence of medium-range inhomogeneities in the materials.

Fluctuation Electron Microscopy (FEM) is a hybrid imaging-diffraction technique that examines the variations in nanodiffraction between small volumes of amorphous materials. Such nanodiffraction patterns tend to be speckled because so few atoms are contributing to the pattern. The variation between nanodiffraction patterns tells us about the variability of the structure. In particular, it tells us if certain scattering vectors  $Q$  are more speckled than others. A measure of this speckliness is provided by the normalized variance of the set of nanodiffraction patterns,

$$V(Q; R) = \frac{\langle I^2(Q, r; R) \rangle_r}{\langle I(Q, r; R) \rangle_r^2} - 1.$$

$I(Q, r; R)$  is the nanodiffraction pattern as a function of scattering vector  $Q$ , when a probe of resolution (width)  $R$  is centered at position  $r$  on the sample. The angular brackets represent averaging over all of the patterns from each position  $r$ .

When there is medium-range order that is comparable to the resolution  $R$ , strong peaks appear in the variance plots as a function of  $Q$ . This means that some  $Q$  vectors tend to be more speckled than others, which is a strong signature of medium-range order. A truly random structure should exhibit no preference for any  $Q$  vector.

FEM has successfully shown that most forms of amorphous silicon have a paracrystalline medium-range order where some remnant of the cubic-diamond topology is still present. These samples exhibit pair distribution functions that are essentially indistinguishable from the continuous random network, illustrating the relative insensitivity of pure diffraction alone to such medium-range order. However, because the variance is actually a measure of the four-body correlations in the sample, it is notoriously difficult to invert the variance data to obtain a model. Fits to the data are made by trial-and-error simulation of plausible models.

At the Electron Microscopy Center at Argonne, we developed a variant of the FEM technique where we examine the angular correlations within the nanodiffraction patterns, which we refer to as correlographs. Howie et al. (1985) had proposed this method originally [1], but it was not appreciated that low resolution  $R$ , comparable to the MRO length scale, is needed.

We used the Argonne Tecnai F20 ST field emission scanning/transmission electron microscope (TEM/STEM) to obtain a series of nanodiffraction patterns using a highly coherent, focused probe with variable resolution ranging from 0.35 nm – 3.0 nm from an amorphous silicon sample prepared by sputtering onto amorphous carbon. The carbon was removed by plasma etching to produce a freestanding amorphous silicon film. Individual nanodiffraction patterns were processed by auto-correlating intensities around each ring of constant scattering vector  $Q$ , and then averaging over the sample. We found that there was a significant amount of correlation at  $Q$ -vectors corresponding to 111, 200, 220, 222 etc cubic silicon reflections. Modelling, assuming kinematic scattering, allows us to estimate that for this sample, about 50% of the material is in the paracrystalline state. Also, the presence of a persistent Friedel peak in the autocorrelations indicates that these correlations are not accidental long-range correlations, which will not have a significant Friedel reflection, but are indeed structurally correlated effects. A series of experimental correlographs are shown in the Figure.

### Future Work

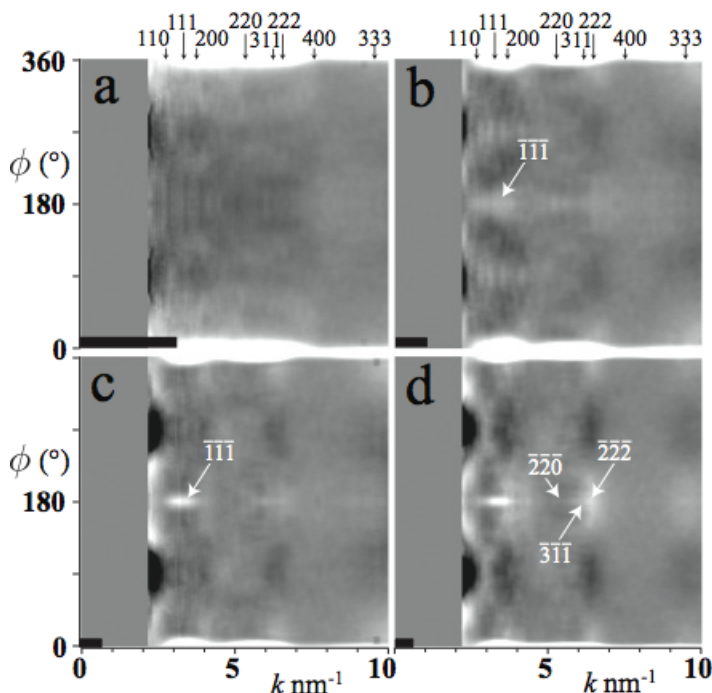
FEM is much more sensitive to decoherence and multiple scattering than is diffraction. We will conduct experiments to quantify these effects and to model them. This will allow us to invert FEM data to obtain structural models.

### Reference

[1] A. Howie, C. A. McGill and J. M. Rodenburg, *J. Phys.-Paris, C-9*, 59--62, **46**, 1985.

### Publication

[2] J. M. Gibson, M. M. J. Treacy, T. Sun and N. J. Zaluzec, Substantial crystalline topology in amorphous silicon, *Physical Review Letters* **105** 125504 (2010).



Mean correlographs, averaged over 200 probed positions, for four different probe resolutions,  $R$ . (a)  $R = 0.3$  nm. (b)  $R = 1.0$  nm. (c)  $R = 1.5$  nm. (d)  $R = 2.3$  nm. The semi-angle of the illumination disk is indicated by the black bar.

## Mesoscopic Amorphization of Supported Pt Nanoparticles: Dependency on Size, Support and Adsorbates

Long Li,<sup>1</sup> Zhongfan Zhang,<sup>2</sup> James Ciston,<sup>3</sup> Eric A. Stach,<sup>3</sup> Lin-lin Wang,<sup>4</sup> Duane D. Johnson,<sup>4</sup> Qi Wang,<sup>5</sup> Anatoly I. Frenkel,<sup>5</sup> Sergio I. Sanchez,<sup>6</sup> Matthew W. Small,<sup>6</sup> Ralph G. Nuzzo,<sup>6</sup> Judith C. Yang<sup>1</sup>

1 Department of Chemical and Petroleum Eng., University of Pittsburgh, Pittsburgh, PA 15261

2 Department of Mechanical Eng. and Materials Science, University of Pittsburgh, Pittsburgh, PA 15261

3 Center for Functional Nanomaterials, Brookhaven National Laboratory, Upton, NY 11973

4 Division of Materials Science and Eng., Ames Laboratory, Department of Materials Science and Engineering, Iowa State University, Ames, IA 50011

5 Department of Physics, Yeshiva University, New York, NY 10016

6 Department of Chemistry, University of Illinois at Urbana-Champaign, Urbana, IL 61801

Proposal Title: Dynamical studies on the size-dependent crystallinity of supported Pt nanoparticles in gas atmosphere with ETEM

Heterogeneous catalysis, which impacts the worldwide economy and sustainability due to its ubiquitous role in energy production, depends sensitively on the nano-sized 3-dimensional structural habits of nanoparticles (NPs) and their physicochemical structural sensitivity to the environment. Here, we focus on a fundamental materials' characteristic — crystalline order— and reveal a size-dependent amorphization of Pt NPs by using complimentary methods of high-resolution transmission electron microscopy (HRTEM), including aberration-corrected environmental HRTEM, extended X-ray absorption fine-structure spectroscopy (EXAFS) and first-principles theoretical calculations.

While bulk amorphous Pt is unstable, its existence in NPs is a manifestation of their mesoscopic nature. First-principles calculations predicted that the energetically preferred structure of a 1.1 nm NP in an inert atmosphere on C or  $\gamma$ -Al<sub>2</sub>O<sub>3</sub> lacks crystalline order while adsorbates stabilize a truncated fcc structure, which is more pronounced on C supports. In contrast to previous theoretical reports on free-standing NPs, icosahedral (I<sub>h</sub>) particles are not stable on supports, the support material stabilizes this amorphous phase, and hydrogen adsorbates cause a crystalline fcc transition.

To confirm the theoretical predications, we synthesized Pt/ $\gamma$ -Al<sub>2</sub>O<sub>3</sub> or Pt/C clusters by using the incipient wetness method to impregnate Pt(NH<sub>3</sub>)<sub>4</sub>(OH)<sub>2</sub>·H<sub>2</sub>O (Strem Chemicals, Inc.) onto the  $\gamma$ -Al<sub>2</sub>O<sub>3</sub> support (Aldrich, surface area 220 m<sup>2</sup>/g) or carbon black (Cabot, Vulcan XC72, surface area 250 m<sup>2</sup>/g). To ensure statistically significant results, we examined by focal-series reconstruction (FS) HRTEM over 3000 Pt NPs individually on both  $\gamma$ -Al<sub>2</sub>O<sub>3</sub> and C supports. HRTEM observation shows that NPs < 1.1 nm are disordered, and that a non-abrupt amorphous-to-ordered transition zone exists, with a narrower transition zone for Pt/ $\gamma$ -Al<sub>2</sub>O<sub>3</sub> (1.2 - 2.5 nm) than that of Pt/C (1.2 – 5 nm). Figure 1 summarizes the data for Pt/ $\gamma$ -Al<sub>2</sub>O<sub>3</sub>. Furthermore, to verify experimentally the predictions of the adsorbate effect, we performed careful structural characterization of the Pt NPs under different environmental conditions using aberration-corrected ETEM (see figure 1h) and *in situ* EXAFS.

The Pt NPs on  $\gamma$ -Al<sub>2</sub>O<sub>3</sub> were exposed in the ETEM or EXAFS environmental chamber to 1 torr H<sub>2</sub>(g) at a temperature of 385 °C and then cooled down to room temperature. We measured

the crystallinity of several NPs through FS-HRTEM to determine the crystallinity fraction within the transition zone which revealed that the H<sub>2</sub> treatments led to more Pt NPs to be more ordered. The *in situ* EXAFS measurements on the static disorder of the Pt NPs before and after H<sub>2</sub> anneal also showed that the static disorder decreased with H<sub>2</sub> exposure. Both the ETEM and *in situ* EXAFS are in agreement with the theoretical predictions of the significant impact of adsorbates.

Hence, combined HRTEM (including ETEM) and EXAFS are in excellent agreement with the theoretical predictions, but also revealed that the NPs structural behavior is more diverse than implied from theory using a limited sampling of NP sizes. Complementary methods are needed to examine the mesoscopic structural behaviors of supported catalysts, one where a statistical, not deterministic, approach is necessary to describe this regime. The results and methods presented here should also be applicable to other catalytic materials/systems and provide critical understandings on nanostructure-mesoscopic properties for a wide range of nanotechnologies.

Acknowledgements: We gratefully acknowledge DOE-BES funding: DE-FG02-03ER15476 and DE-AC02-98CH10886. The structural characterizations were performed at the CFN and NSLS at Brookhaven National Laboratory and the NCFE at the University of Pittsburgh.

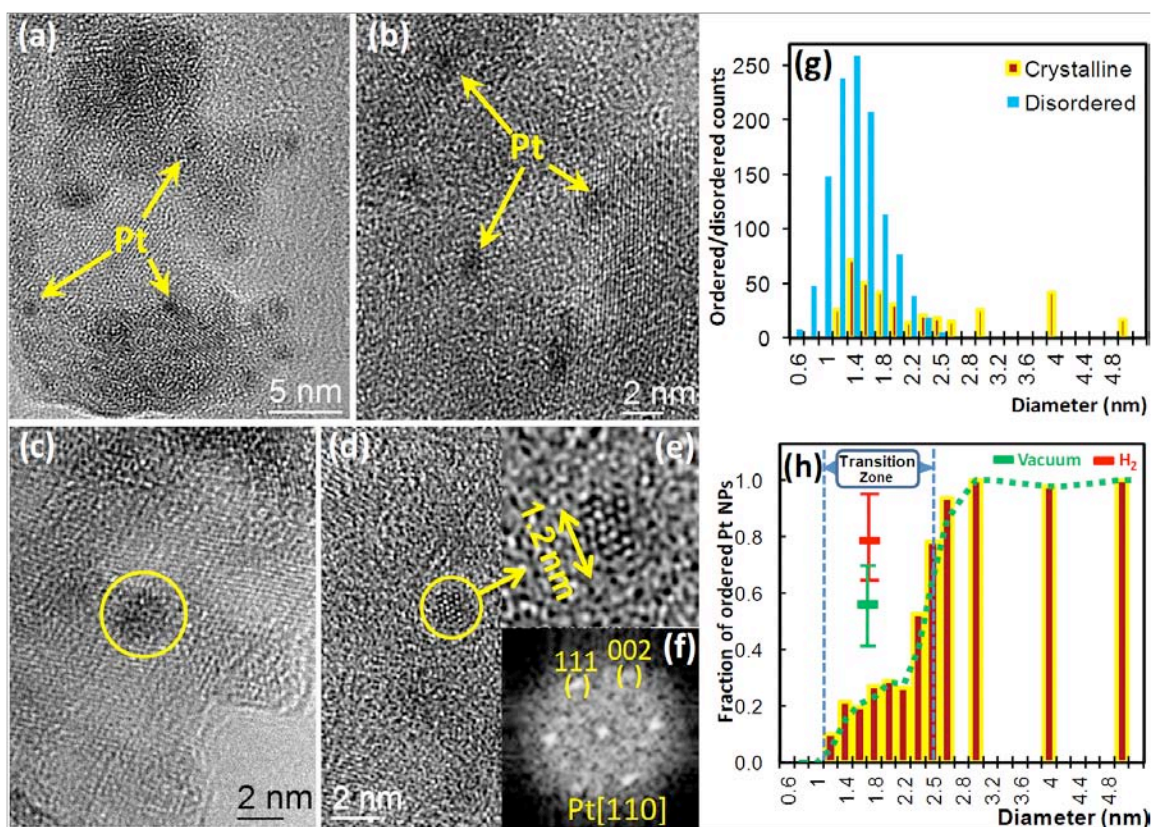


**Figure 1.** Histograms of crystalline/ disordered NPs on  $\gamma$ -Al<sub>2</sub>O<sub>3</sub> at stages of (a) as-prepared, (b) 1 torr H<sub>2</sub> in the ETEM column heated at 385 °C for 30 minutes and then cooled to RT, (c) pumped out H<sub>2</sub> in the ETEM vacuum, and (d) exposed to air for ~10 minutes and then observed in ETEM; (e-h) are distributions of fraction of ordered NPs corresponding to each stages above, respectively.

## Exit wave reconstruction of nanocrystalline catalysts and radiation sensitive materials

A Kirkland<sup>1</sup>, N P Young<sup>1</sup>, S Haigh<sup>2</sup> and C. Kisielowski<sup>3</sup>

<sup>1</sup> Department of Materials, Oxford University, Parks Road, Oxford, OX13PH, UK.

<sup>2</sup> School of Materials, University of Manchester, Grosvenor Street, Manchester M1 7HS UK.

<sup>3</sup> National Center for Electron Microscopy, Lawrence Berkeley National Laboratory, One Cyclotron Rd., Berkeley CA 94720, USA.

### NCEM User Proposal Title: Technique Development for Aberration Corrected Imaging

Morphology and surface structure in nanocrystalline metals and metal oxides is a key feature in determining their fundamental properties and in particular their catalytic activity and selectivity. In parallel quantitative structure determination of “soft” materials systems and soft / hard interfaces is a key technological challenge.

This paper will firstly discuss the characterisation of metal and metal oxide nanoparticles using aberration corrected electron microscopy and exit wavefunction reconstruction. The correlation of this data with thermodynamic models of morphology and surface structure to produce quantitative phase diagrams that predict stable forms as a function of particle size and temperature for nanoscale systems will also be described.

Nanocrystalline gold has also been demonstrated to show highly specific catalytic activity at small particle size. In situ imaging experiments at elevated and depressed temperatures provide direct evidence for morphological changes that can be correlated with theoretical models to construct the first quantitative nanoscale phase diagram relating local structure and morphology to temperature and particle size in this system.

Cerium dioxide nanocrystals, have attracted considerable interest due to their properties that lead to applications as efficient oxygen buffers in three-way automotive catalysts. These buffers are essential in stabilizing the air-to-fuel ratio necessary to achieve simultaneous conversion of NO, CO, and hydrocarbons during both the fuel-lean and fuel-rich stages of the combustion cycles. Aggregation behaviour in this system is driven by the compatibility of the shape of individual nanoparticles (characterized by the relative fractions of different crystallographic facets and their surface terminations) and can be substantially reduced by control of the shape of individual nanoparticles during synthesis. Experimental and theoretical data has been used to characterise the surface structure and chemistry within this system, which has led to a detailed understanding of the factors controlling morphology and the frequently observed oxygenated surface termination which is driven by migration of oxygen defects from the bulk of the particle.

In the second part of the talk the challenges of imaging large spatial frequencies in soft materials will be addressed. An aberration corrected transmission electron microscope images a region routinely able to recover high spatial frequency information at resolutions better than 0.1 nm. However, low spatial frequencies are absent from these high-resolution images due to the intrinsic properties of the phase Contrast Transfer Function (CTF). Where low spatial frequency information is important images are often acquired at a large defocus but this compromises high spatial frequency information transfer. I will discuss computational approaches whereby the spatial frequency bandwidth of an exit wave restoration can be increased so as to mimic the effect of a physical phase plate using images recorded with a non-uniform focal steps to optimally span the range of spatial frequencies without requiring a larger number of images.



## Quantitative *in situ* mechanical testing of nanowires

D.S. Gianola<sup>1</sup>, K. Murphy<sup>1</sup>, L. Chen<sup>1</sup>, J.P. Sullivan<sup>2</sup>

<sup>1</sup> Department of Materials Science and Engineering, University of Pennsylvania, Philadelphia, PA 19104

<sup>2</sup> CINT Science Department, Sandia National Laboratories, Albuquerque, NM 87185

### Proposal Title

*CINT User Proposal*: In situ Nanomechanical Testing of Phase Change Nanowires using the CINT Discovery Platform

### Scientific Challenge and Research Achievement

Experimentally approaching the theoretical strength of materials has been a long-term goal of structural materials research and development. However, most engineering materials fail before reaching even a small fraction of this upper limit. This talk will present experiments on a class of materials, the *ultra-strength*, which have the capability of withstanding specimen-wide mechanical stresses that approach the theoretical limit – the maximum achievable stress in crystalline materials – and represent a new frontier of materials design. Nanoscale “bottom-up” synthesis creates small volumes of materials and provides the high crystalline quality that allow for these mechanically extreme environments. However, the mechanisms that accommodate plastic deformation are not known, limiting our ability to tailor the properties of nanostructured materials in next generation technological devices that are subject to extreme mechanical and thermal duress.

Recent progress in the area of *in situ* electron microscopy (scanning and transmission) has allowed for quantitative interrogations of the deformation of nanoscale materials [1-3]. Here we describe quantitative *in situ* approaches for mechanical testing of individual nanowires in electron microscopes. In particular, the use of microelectromechanical systems-based testing devices fabricated at CINT will be highlighted. Selected experiments will be presented to illustrate how these techniques can directly correlate underlying physical phenomena with measured properties.

### Future Work

Current areas of development include couple electromechanical measurements of individual nanowires, including phase change chalcogenide materials and doped semiconductors, and elevated temperature measurements on metallic and semiconducting nanostructures.

### References

- [1] D.S. Gianola, C. Eberl, *JOM* 61 (2009) 24.
- [2] M. Legros, D.S. Gianola, C. Motz, *MRS Bull.* 35 (2010) 354.
- [3] G. Richter *et al.*, *Nano Lett.* 9 (2009) 3048.



# In situ TEM Nanomechanical Testing

Andrew M. Minor

National Center for Electron Microscopy, Lawrence Berkeley National Laboratory & Department of Materials Science & Engineering, University of California, Berkeley, CA

## Scientific Thrust Area

*In situ* transmission electron microscopy (TEM) provides dynamic observations of the physical behavior of materials in response to external stimuli such as temperature, environment, stress, and applied fields. Since the basic mechanisms that determine a materials deformation behavior occur at nanometer length scales, the development of mechanical testing methods for the electron microscope was one of the first *in situ* methods to be developed [1,2]. Starting as early as the 1950s *in situ* straining stages were developed that could lead to dynamic observations of dislocation motion in metals [3]. Throughout the last 50 years there has been great development in the field of *in situ* TEM mechanical testing [4], including the evolution of quantitative mechanical probing techniques such as *in situ* nanoindentation [5] and more recently *in situ* nanocompression, and nanotension testing (see Figure 1).

## Scientific Challenge and Research Achievement

Recent progress in both *ex situ* [6] and *in situ* [7] small-scale mechanical testing methods has greatly improved our understanding of mechanical size effects in volumes from a few nanometers to a few microns. Besides the important results related to the effect of size on the strength of small structures, the ability to systematically measure the mechanical properties of small volumes through mechanical probing allows us to test samples that cannot easily be processed in bulk form, such as a specific grain boundary or a single crystal. In the case of individual nanostructures, the need for robust small-scale testing methods is even more acute, and *in situ* TEM in many cases makes this possible [8]. We have used *in situ* TEM techniques to study mechanical size effects in metals such as Al alloys [9], NiTi shape memory alloys [10], Au bicrystals [11], Ti alloys [12], Mg alloys [13] and Cu single crystals [14]. More recently, we have developed the ability to use electromechanical *in situ* probing to directly record both mechanical and

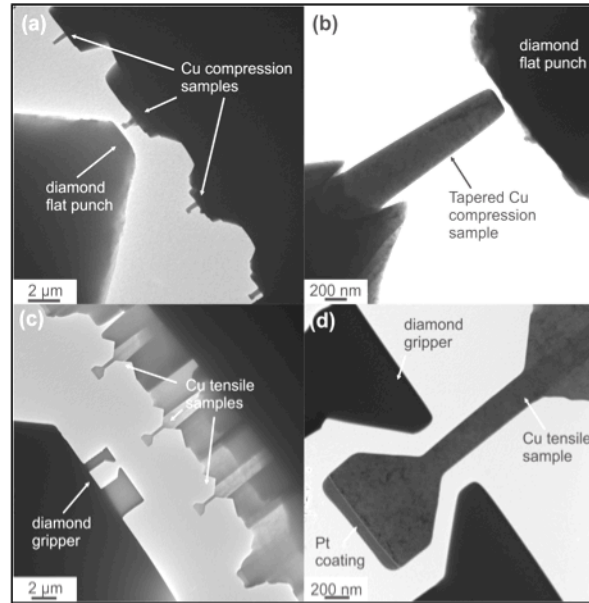


**Figure 1 - Uniaxial *in situ* TEM mechanical testing techniques.** (a) Low magnification image showing compression samples (some after testing) and (b) higher magnification of a Cu micropillar before compression. (c) Image showing several tensile samples and the structured conductive diamond tip to act as gripper. (d) Higher magnification image depicting a Cu sample and the diamond gripper aligned before testing.

electrical data to uncover the origins of piezoelectric BFO thin films [15]. This talk will describe our most recent results from in situ compression and tensile testing of metals with varying initial defect densities to illuminate the origin of size-dependent yield strength behavior and fundamental deformation structures in nanoscale samples. In addition, comparing in situ compression and tensile testing has led to some interesting observations regarding the evolution of flow strength in nanoscale samples during testing.

### Future Work

The concept that the strength of a material changes with sample size is a well established [16], but not a well understood concept in small-scale plasticity. To date, there does not exist a general theoretical description of the origin of size effects applicable to all materials so that macroscopic mechanical properties can be determined accurately through small-scale testing. We hope to address this lack of connection between small-scale mechanical testing and macroscopic properties through systematic in situ and ex situ nanomechanical testing and complementary computational modeling of important structural materials.

### Acknowledgements

This work was supported by the Center for Defect Physics, an Energy Frontier Research Center funded by the U.S. Department of Energy, Office of Science, Office of Basic Energy Sciences, and by General Motors Research and Development. The authors also acknowledge support of the National Center for Electron Microscopy and Advanced Light Source, Lawrence Berkeley National Laboratory, which is supported by the U.S. Department of Energy under Contract # DE-AC02-05CH11231.

### References

- 
- [1] P. Hirsch, A. Howie, R.B. Nicholson, D.W. Pashley, M.J. Whelan, Electron Microscopy of Thin Crystals, Krieger Publishing Co., NY, NY (1965)
  - [2] E.P. Butler, *Reports Prog. Phys.* 42, 833 (1979)
  - [3] H.G.F. Wilsdorf, *Rev. Sci. Inst.*, 29, 323 (1958)
  - [4] I. Robertson, P. Ferreira, G. Dehm, R. Hull, E.A. Stach, “Visualizing the Behavior of Dislocations-Seeing is Believing”, *MRS Bulletin*, 33, 122-131, (2008)
  - [5] A.M. Minor, S.A. Syed Asif, Z.W. Shan, E.A. Stach, E. Cyrankowski, T.J. Wyrobek, and O.L. Warren, *Nature Materials*, 5, 697-702, (2006)
  - [6] Uchic, M.D., D.M. Dimiduk, J.N. Florando, and W.D. Nix, *Science*, 305, 986-989 (2004)
  - [7] Z.W. Shan, R.K. Mishra, S.A. Syed Asif, O.L. Warren and A.M. Minor, *Nature Materials*, 7, 115-119 (2008)
  - [8] Z.W. Shan, G. Adesso, A. Cabot, M.P. Sherburne, S.A. Syed Asif, O.L. Warren, D.C. Chrzan, A.M. Minor and A.P. Alivisatos, *Nature Materials*, 7, 947-952 (2008)
  - [9] J. Ye, R.K. Mishra and A.M. Minor, *Scripta Materialia*, 59, 951-954 (2008)
  - [10] J. Ye, R.K. Mishra, A. Pelton, A.M. Minor, *Acta Materialia*, 58, 490-498 (2010)
  - [11] F. Lancon, J. Ye, D. Caliste, T. Radetic, A.M. Minor, and U. Dahmen, *Nano Letters*, 10, 695-700 (2010)
  - [12] E.A. Withey, A.M. Minor, D.C. Chrzan, J.W. Morris, Jr. and S. Kuramoto, *Acta Materialia*, 58, 2652-2665 (2010)
  - [13] J. Ye, R.K. Mishra, A.K. Sachdev, and A.M. Minor, *Scripta Materialia*, 64, 292-295 (2010)
  - [14] D. Kiener and A.M. Minor, *Acta Materialia*, 59, 1328-1337 (2011)
  - [15] J.X. Zhang, B. Xiang, Q. He, J. Seidel, R.J. Zeches, P.Yu, S.Y. Yang, C.H. Wang, Y.H. Chu, L.W. Martin, A.M. Minor and R. Ramesh, *Nature Nanotechnology*, 6, 98-102 (2011)
  - [16] Zhu, T. and J. Li, *Progress in Materials Science*, 55, 710-757 (2010)

## Graphene: synthesis, processing and characterization at the atomic-scale

Nathan P. Guisinger

Center for Nanoscale Materials, Argonne National Laboratory

### Scientific Thrust Area

Graphene is a nearly ideal two-dimensional conductor that is comprised of a single sheet of hexagonally packed carbon atoms.<sup>1</sup> Since the first electrical measurements made on graphene, researchers have been trying to exploit the unique properties of this material for a variety of applications that span numerous scientific and engineering disciplines. In order fully realize the potential of graphene for novel electronic applications, large-scale synthesis of high quality graphene and the ability to control the electronic properties of this material on a nanometer length scale are key challenges.

### Scientific Challenge and Research Achievement

We have demonstrated the reversible and local modification of the electronic properties of graphene by hydrogen passivation and subsequent electron-stimulated hydrogen desorption with a scanning tunneling microscope tip, as illustrated in Fig. 1.<sup>2,3</sup> In addition to changing the morphology, we show that the hydrogen passivation is stable at room temperature and modifies the electronic properties of graphene, opening a gap in the local density of states. This insulating state is reversed by local desorption of the hydrogen, and the unaltered electronic properties of graphene are recovered. Using this mechanism, we have “written” graphene patterns on nanometer length scales. For patterned regions that are roughly 20 nm or greater, the inherent electronic properties of graphene are completely recovered. Below 20 nm we observe dramatic variations in the electronic properties of the graphene as a function of pattern size.

Large-area synthesis of high-quality graphene is one of the main obstacles towards fabricating graphene devices. Recently, large area graphene with high electrical quality has been realized on copper foils. Copper has demonstrated its advantage in fabricating high-quality uniform graphene monolayer. In this talk, we will present our studies of graphene on single crystal Cu(111) surfaces and Cu foil by variable temperature scanning tunneling microscopy and spectroscopy.<sup>4-6</sup> We studied the bonding configurations between copper and carbon, as well as the atomic-scale electronic structure of the graphene on the copper surface. Our results provide valuable information for understanding the growth mechanism and the electronic quality of graphene on copper.

### Future Work

Future work includes optimized synthesis for large-scale “low-defect” graphene and advanced functionalization and modification.

### References

1. G. M. Rutter, J. N. Crain, N. P. Guisinger, T. Li, P. N. First, and J. A. Stroscio, “Interference and localization in epitaxial graphene,” *Science*, 317, 219 (2007).
2. N. P. Guisinger, G. M. Rutter, J. N. Crain, P. N. First, and J. A. Stroscio, “Exposure of epitaxial graphene grown on 6H-SiC(0001) to atomic hydrogen,” *Nano Lett.*, 9, 1462 (2009).
3. P. Sessi, J. R. Guest, M. Bode, and N. P. Guisinger: Patterning Graphene at the Nanometer Scale via Hydrogen Desorption, *Nano Lett.* 9, 4343 (2009).
4. L. Gao, J. R. Guest, and N. P. Guisinger: Epitaxial Graphene on Cu(111), *Nano Lett.* 10, 3512 (2010).
5. Q. Yu, *et al.*: Control and characterization of individual grains and grain boundaries in graphene grown by chemical vapour deposition, accepted *Nature Materials* (2011).

6. J. Cho, *et al.*: Atomic-scale investigation of graphene grown on Cu foil and the effects of thermal annealing, under review *ACS Nano* (2011).

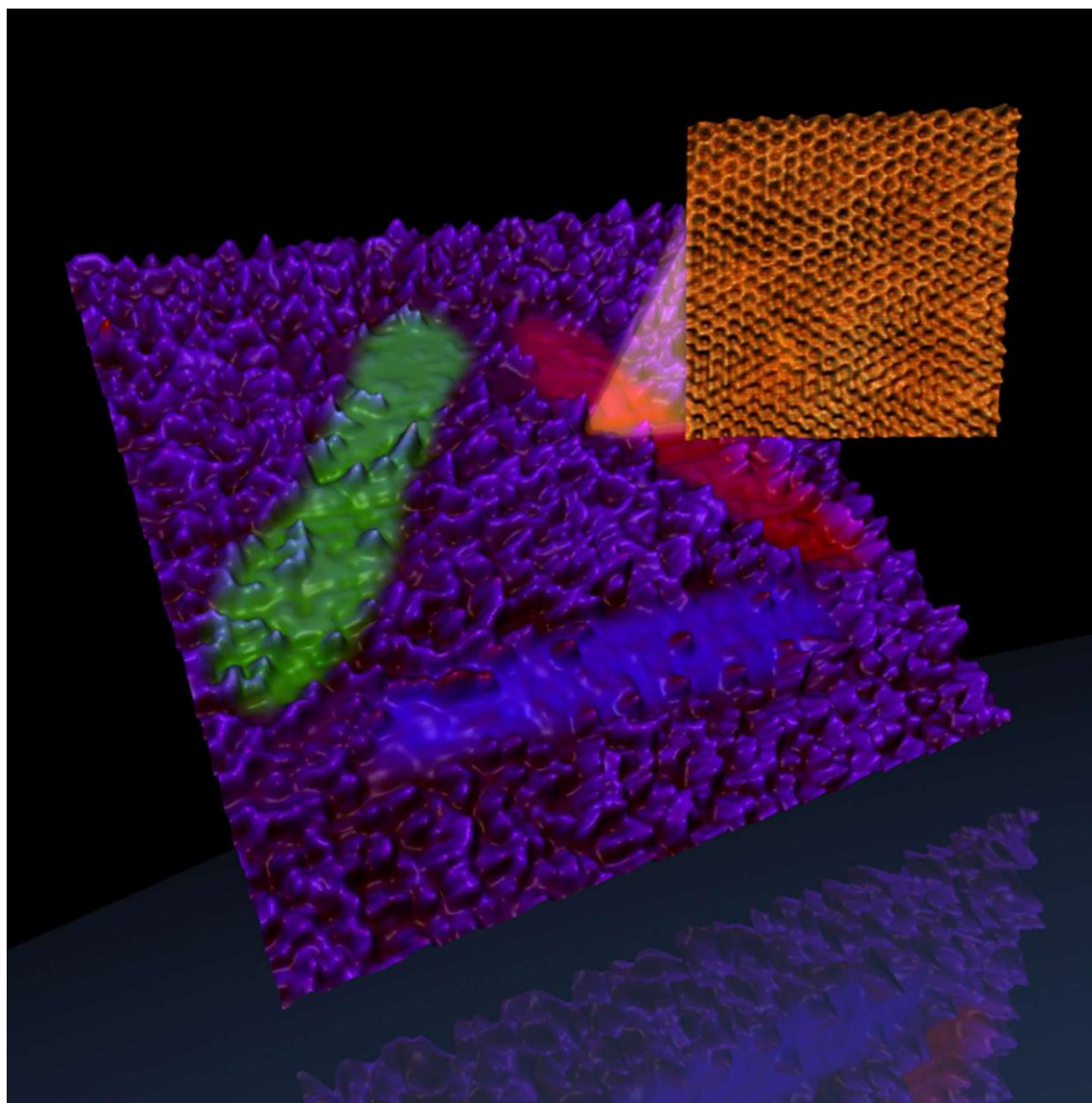


Figure 1: Argonne National Laboratory logo patterned at the atomic-scale (STM image rendered with false coloring added). Hydrogen saturated graphene was controllably patterned via STM induced electron stimulated desorption. The inset shows an atomic-scale image of the patterned graphene, which is structurally preserved and demonstrates the reversible nature of this process.

# Atomic Structure and Properties of $sp^2$ -bonded Materials

A. Zettl<sup>1,2</sup>, K. Kim<sup>1,2</sup>

<sup>1</sup>Materials Sciences Division, Lawrence Berkeley National Laboratory, Berkeley, CA

<sup>2</sup>Dept. of Physics & Center of Integrated Nanomechanical Systems, University of California at Berkeley, CA

Z. Lee<sup>3,4</sup>, W. Regan<sup>1,2</sup>, C. Kisielowski<sup>3</sup>

<sup>3</sup>National Center Electron Microscopy, Lawrence Berkeley National Laboratory, Berkeley, CA

<sup>4</sup>Ulsan National Institute of Science & Technology, Ulsan, So. Korea

NCEM Proposal # 1469 - Investigation of CVD graphene interface with metal nanoparticles

We report direct mapping of the grains and grain boundaries (GBs) of large-area monolayer polycrystalline graphene sheets, at large (several micrometer) and single-atom length scales. Global grain and GB mapping is performed using electron diffraction in scanning transmission electron microscopy (STEM) or using dark-field imaging in conventional TEM. Additionally, we employ aberration-corrected TEM to extract direct images of the local atomic arrangements of graphene GBs, which reveal the alternating pentagon-heptagon structure along high-angle GBs. Our findings provide a readily adaptable tool for graphene GB studies.

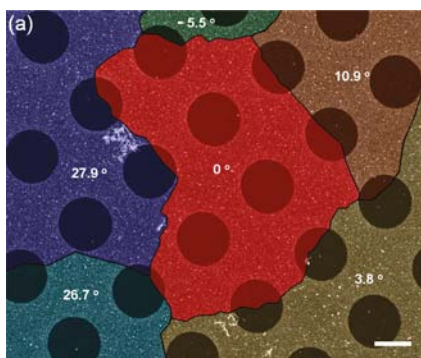


Figure 1. Grain boundary map with relative orientations. The scale bar is 1  $\mu\text{m}$ .

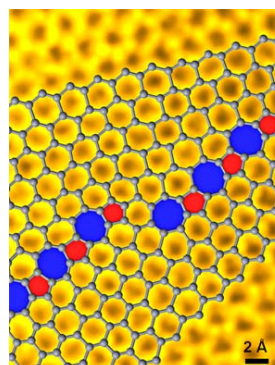


Figure 2. Atomic resolution image (TEAM microscope) of grain boundary, with superposed ball and stick model. Note the heptagons and pentagons.

## References

K. Kim, Z. Lee, W. Regan, C. Kisielowski, M.F. Crommie, and A. Zettl. Grain boundary mapping in polycrystalline graphene. *ACS Nano* **5** (3), 2142-46 (2011).



## **From Mapping Energy Flow and Dissipation to Local Thermal and Bias Induced Transformations by SPM**

Roger Proksch, Asylum Research

### **User Proposals:**

CNMS2010-095: Local Thermal Analysis of the Bacteriorhodopsin Membranes (Maxim Nikiforov, Roger Proksch, Sergei Kalinin)

CNMS2007-066: Development of Band Excitation Piezo Force Microscopy for Atomic Force Microscopy (Keith Jones, Anil Gannepalli)

**User Facility:** Center for Nanophase Materials Sciences, Origins of Functionality at the Nanoscale

Scanning Probe Microscopy techniques have now emerged as a primary tool for imaging and controlling structure and functionality of materials on mesoscopic and atomic scales. This rapid development of SPM platforms and probes is belied by the fact that single-frequency dynamic methods, the bedrock of 20,000+ SPMs worldwide, are fundamentally flawed in the amount of information they provide. Simply speaking, the number of measured variables is smaller than the minimal number of parameters defining the system, leading to spurious responses and well-recognized problems in dissipation imaging, phase imaging, topographic cross-talk, and quantitative property measurements. With the goal of improving Contact Resonance methods to allow high sensitivity and crosstalk-free imaging of domains in nanostructured ferroelectric materials, two techniques have been co-developed with researchers at the Center for Nanophase Materials Sciences: DART (Dual AC Resonance Tracking) and BE (Band Excitation). Both of these approaches allow the improved SNR of the cantilever contact resonance while avoiding issues with crosstalk between the response and the sample topography. The development of BE/DART has enabled high sensitivity studies of ferroelectric defects, switching distributions, relaxation studies and more.

One serendipitous result of the BE/DART method was the realization that the new measurement parameters also provided information about the contact stiffness and dissipation. Since the original work on ferroelectrics, this method has been used on a variety of polymeric systems to evaluate high resolution variations in the surface stiffness and dissipation, with much of the effort being focused on polyolefin materials. In particular, we have been working on relating the nanoscale mechanical properties of these polymer materials to bulk dynamic mechanical analysis data.

Extending BE/DART contact resonance measurements to locally heated probes allows observation of phase transitions in remarkably tiny volumes (~zeptoliter, or  $10^{-21}$  liters). We have measured insulin fibers, dna molecules, polyethylene surfaces and native biological membrane (purple membranes from the extremophile *Halobacterium salinarum*). Phase transitions detected by change in contact resonance are commonly measured for volumes from less than 100 molecules to perhaps the single molecule level.

Finally, in Electrochemical Strain Microscopy (ESM), the SPM tip concentrates a periodic electric field in a nanoscale volume of material, resulting in Li-ion redistribution (tip-ESM). Alternatively, the tip can detect the surface strains generated in the top electrode of a full battery stack (device ESM). Induced changes in molar volume cause local surface expansion or contraction (strain) that is transferred to the SPM probe and detected by microscope electronics. Hence, this strain-based detection allows high-resolution nanoscale mapping of Li-ion dynamics, providing never-before observed details of ionic concentration changes and flows in complex electrical storage materials.

### **Related publications from work at the CNMS**

Nikiforov, M. P.; Hohlbauch, S.; King, W. P.; Voitchovsky, K.; Contera, S. A.; Jesse, S.; Kalinin, S. V.; Proksch, R., "Temperature-Dependent Phase Transitions in Zeptoliter Volumes of a Complex Biological Membrane," *Nanotechnology* **22** (5), 055709 (2011).

Jesse, S.; Guo, S.; Kumar, A.; Rodriguez, B. J.; Proksch, R.; Kalinin, S. V., "Resolution Theory, and Static and Frequency-Dependent Cross-Talk in Piezoresponse Force Microscopy," *Nanotechnology* **21** (40), 405703 (2010).

Tselev, A.; Meunier, V.; Strelcov, E.; Shelton, W. A.; Luk'yanchuk, I. A.; Jones, K.; Proksch, R.; Kolmakov, A.; Kalinin, S. V., "Mesoscopic Metal-Insulator Transition at Ferroelastic Domain Walls in VO<sub>2</sub>," *ACS Nano* **4** (8), 4412 (2010).

Tselev, A.; Strelcov, E.; Luk'yanchuk, I. A.; Budai, J. D.; Tischler, J. Z.; Ivanov, I. N.; Jones, K.; Proksch, R.; Kalinin, S. V.; Kolmakov, A., "Interplay Between Ferroelastic and Metal-Insulator Phase Transition in Strained Quasi-Two-Dimensional VO<sub>2</sub> Nanoplatelets," *Nano Lett.* **19**(6), 2003-2011 (2010).

## Cryo-Electron Tomography for Protein Dynamic Structure

Gang (Gary) Ren

Molecular Foundry, Lawrence Berkeley National Laboratory, Berkeley, CA 94720, [gren@lbl.gov](mailto:gren@lbl.gov)

**Scientific Thrust Area:** Developing the transmission electron microscopy (TEM) technology for high-resolution structural study of high-dynamic and heterogeneous soft materials and biological macromolecules.

**Scientific Challenge:** TEM carries the capability for user to exam the hard material structure at atomic resolution level [1]. However, this capability is significantly limited in examining the soft materials and biological macromolecule due to electron radiation damage. Cryo-electron microscopy (cryoEM) associated with image processing technique is a solution for determining the structure of biological molecule at atomic resolution level, such as aquaporin 1 water channel and virus [2, 3]. In this process, the proteins are flash-froze into thin film of vitreous ice, the proteins' images were acquired under low-electron dose condition ( $< \sim 30$  electron/ $\text{\AA}^2$ ) at liquid nitrogen temperature. By averaged hundreds to thousands of proteins that contain a homogenous structural conformation and determined the Euler angles of each averages, the 3-dimensional (3D) density map of the protein was reconstructed via a back-projection algorithm. This approach requires the protein either can be crystallized into a thin layer of an extended ordered lattice or has a high-symmetry of structure with rigid body. Unfortunately, most proteins have neither high symmetry nor rigid body. It is because the dynamic nature and structural heterogeneity of proteins is essential for their functions. The heterogeneity of dynamic nature frustrates structure determination by X-ray and conventional cryoEM.

**Research Achievement:** We used the cryo-electron tomography (cryoET) technique to study dynamic and heterogeneous proteins [4], such as human IgG antibody [5] and high-density lipoprotein (HDL) [6]. The targeted proteins were imaged for a hundred times under extremely low-dose condition ( $\sim 1-3$  electron/ $\text{\AA}^2$ ) from a series of tilted viewing angles [7]; tilted viewing images of a targeted single protein was selected and windowed from the tilt series of micrographs; then the protein's center in each image is precisely aligned to each other and back-projected into a 3D density map after an iterative refinement computational process. We call this reconstruction method the focused electron tomography reconstruction (FETR) and the approach for determining the single-protein structure the individual-particle electron tomography (IPET) [4]. In FETR, we reduced the image size, so containing only one single-protein for reducing the effects from the undetectable or immeasurable tilt-angle errors prior to 3D reconstruction. During iteration, we introduced a series of automatically generated dynamic Gaussian low-pass filters and masks to enhance the searching power and precision in defining the translational parameters.

It has been shown that cryoET images acquired from a targeted single-protein can be successfully aligned and reconstructed into a 3D density map at 10-20  $\text{\AA}$  resolution, in which the small domains ( $\sim 50$ kDa molecular mass) of protein, such as Fab domains of IgG antibody and apolipoprotein portion of HDL (Fig. 1), can be visualized [4-6, 8]. The 3D density map reconstructed from single-protein that is conformation-free, dynamics-free and heterogeneity-free. Thus, this approach does not require any class averaging of multiple molecules, does not require an extended ordered lattice, and can tolerate inaccurate determination of geometric angles, high-noise, and missing-wedge. Moreover, each 3D structure can be used as a "snapshot" of protein dynamical structure. By comparing these "snapshot" structures, we studied the structural dynamics of protein. Thus, this approach provides a completely new opportunity for single-protein structure determination, and therefore could be used as a new approach for the study of protein dynamics.

**Future Work:** We believe that the TEM instrument and the dose limitation are important parameters, but not critical for obtaining subnanometer-resolution structure determination of biological macromolecule by cryoET. In contrast, we believe the image acquisition techniques and

image processing software algorithm play the keys that limited the subnanometer-resolution 3D reconstruction achievement by cryoET. Thus, we plan to continually optimize the experimental image acquisition conditions and improve our software capability for structure determination of single-protein and soft material at subnanometer-resolution.

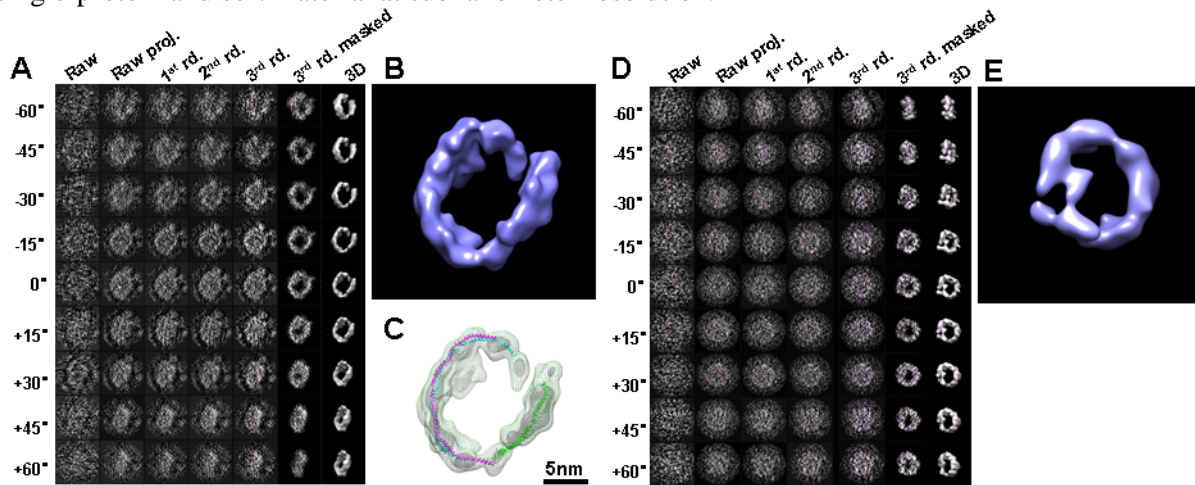


**Fig. 1 3D reconstruction of targeted single-protein particle by cryo-electron tomography.** A) A targeted 17nm low-density lipoprotein (HDL) particle was embedded in the vitreous ice and imaged by cryo-electron tomography (cryoET). The CTF corrected particle images were aligned to each other, and B) reconstructed into 3D density map by our focused electron tomography reconstruction (FETR) method. C) The map revealed a ring shape structural model for the HDL containing proteins, apolipoprotein A-I (apoA-I). The size suggested three apoA-I molecules within a 17nm rHDL particle. D) Another targeted 17nm HDL particle was also imaged by cryoET, and reconstructed by FETR. E) The 3D density map also displayed a ring-shaped structural model for containing apoA-Is.

#### References:

1. Girit, C.O., et al., *Graphene at the edge: stability and dynamics*. Science, 2009. **323**(5922): p. 1705-8.
2. Ren, G., et al., *Visualization of a water-selective pore by electron crystallography in vitreous ice*. Proc Natl Acad Sci U S A, 2001. **98**(4): p. 1398-403.
3. Zhang, X., et al., *3.3 Å cryo-EM structure of a nonenveloped virus reveals a priming mechanism for cell entry*. Cell, 2010. **141**(3): p. 472-82.
4. Zhang, L. and G. Ren, *Structural Determination of Heterogeneous Protein by Individual-Particle Electron Tomography - Combination of Electron Tomography and Local Refinement Reconstruction Method for High-Resolution Structural Determination of Each Individual Protein Particle* Biophysical Journal, 2010. **98**(3): p. 441a.
5. Zhang, L. and G. Ren, *Determining the Dynamic Protein Structure by Individual-Particle Electron Tomography: An Individual Antibody Structure at a Nanometer Resolution* Biophysical Journal, 2010. **98**(3): p. 2.
6. Zhang, L., et al., *Structure of 9.6nm Discoidal High-Density Lipoprotein Revealed by Individual-Particle Electron Tomography*. Biophysical Journal, 2010. **98**(3): p. 440a.
7. Jones, M.K., et al., *Assessment of the validity of the double superhelix model for reconstituted high density lipoproteins: a combined computational-experimental approach*. J Biol Chem, 2010. **285**(52): p. 41161-71.
8. Zhang, L., et al., *Monitoring the Structural Changes of Conjugated Antibodies by High-Resolution Electron Microscopy and Individual-Particle Electron Tomography*. Biophysical Journal, 2010. **98**(3): p. 440a-441a.

#### Publications:

1. Jones, M.K., et al., *Assessment of the validity of the double superhelix model for reconstituted high density lipoproteins: a combined computational-experimental approach*. J Biol Chem, 2010. **285**(52): p. 41161-71.
2. Zhang, L. and G. Ren, *Structural Determination of Heterogeneous Protein by Individual-Particle Electron Tomography - Combination of Electron Tomography and Local Refinement Reconstruction Method for High-Resolution Structural Determination of Each Individual Protein Particle* Biophysical Journal, 2010. **98**(3): p. 441a.
3. Zhang, L. and G. Ren, *Determining the Dynamic Protein Structure by Individual-Particle Electron Tomography: An Individual Antibody Structure at a Nanometer Resolution* Biophysical Journal, 2010. **98**(3): p. 2.
4. Zhang, L., et al., *Structure of 9.6nm Discoidal High-Density Lipoprotein Revealed by Individual-Particle Electron Tomography*. Biophysical Journal, 2010. **98**(3): p. 440a.
5. Zhang, L., et al., *Monitoring the Structural Changes of Conjugated Antibodies by High-Resolution Electron Microscopy and Individual-Particle Electron Tomography*. Biophysical Journal, 2010. **98**(3): p. 440a-441a.

## **A review of the TEAM project and its scientific impact**

U. Dahmen, P. Denes, T. Duden, R. Erni, C. Kisielowski, A. Minor, A. Schmid, V. Radmilovic, Q. Ramasse, M. Watanabe, E. Stach<sup>+</sup>, N. Browning<sup>#</sup>, D. Miller<sup>Δ</sup>, B. Kabius<sup>Δ</sup>, N. Zaluzec<sup>Δ</sup>, I. Petrov<sup>\*</sup>, I. Robertson<sup>\*</sup>, R. Twosten<sup>\*</sup>, J. Zuo<sup>\*</sup>, E. Olson<sup>\*</sup>, T. Donchev<sup>\*</sup>, I.M. Anderson<sup>°</sup>, S. Pennycook<sup>°</sup>, A. Lupini<sup>°</sup>, J. Bentley<sup>°</sup>, E. Kenik<sup>°</sup>, Y. Zhu<sup>+</sup>, J. Wall<sup>+</sup>

National Center for Electron Microscopy, Materials Sciences Division, LBNL, Berkeley, CA 94720  
<sup>+</sup>BNL, <sup>#</sup>LLNL, <sup>Δ</sup>ANL, <sup>°</sup>ORNL, <sup>\*</sup>FS-MRL

### **Scientific Thrust Area**

The atom-by-atom analysis of individual nanostructures is an important goal in nanoscience that was first formulated by Richard Feynman in his famous 1959 lecture, “There’s Plenty of Room at the Bottom”. Feynman proposed that one could analyze any substance simply by looking to see where the atoms are. Despite major progress, Feynman’s challenge to electron microscopy has been out of reach. The fundamental barrier to improving the electron microscope has been the presence of unavoidable aberrations in rotationally symmetric electromagnetic lenses. The Transmission Electron Aberration-corrected Microscope (TEAM) project was initiated as a collaborative effort between several DOE laboratories (LBNL, ANL, ORNL, FS-MRL) and two commercial manufacturers (FEI, CEOS) to redesign the electron microscope around aberration-corrected optics in order to extend the spatial resolution to 50 pm, enhance contrast and increase energy resolution.

### **Scientific Challenge and Research Achievement**

The vision for the TEAM project was the idea of providing a sample space for electron scattering experiments in a tunable electron optical environment by removing some of the constraints that have limited electron microscopy. It was envisaged that the resulting improvements in spatial, spectral and temporal resolution, the increased space around the sample, and the possibility of exotic electron-optical settings would enable new types of experiments. The TEAM project was successfully concluded in the fall of 2009 with an instrument that features unique corrector elements for spherical and chromatic aberrations, a novel AFM-inspired specimen stage, a high-brightness gun, a new direct electron detector and numerous other innovations that extend resolution down to the half-Angstrom level. The improvement in sensitivity, brightness, signal to noise and stability make it possible to address major challenges such as single atom spectroscopy, atomic resolution tomography and high resolution imaging at low voltage and low dose.

This talk will review the origin, structure and organization of the TEAM project, summarize its numerous technical advances and highlight its scientific impact with representative examples of some of the many scientific results that have resulted from the TEAM microscope [see publications].

### **Future work**

The many technological and scientific advances made under the TEAM project have opened new opportunities for experiments and instrumentation. From the start, TEAM was envisioned as a platform for the development of a new generation of instruments built around aberration correction. This presentation will give a summary of the scientific needs and opportunities for instruments built on this platform, with special emphasis on the cross-disciplinary needs of DOE user facilities for nanoscience research and electron scattering.

## Publications

- Probing the out-of-plane distortion of single point defects in atomically thin hexagonal boron nitride at the picometer scale, N. Alem et al., *PRL* **106**, 126102 (2011)
- Grain boundary mapping in polycrystalline graphene K. Kim et al., *ACS Nano* **5** 2142–2146 (2011)
- Three-dimensional atomic imaging of crystalline nanoparticles, S. Van Aert et al., *Nature* **470** 374-377 (2011)
- Spontaneous vortex nanodomain arrays at ferroelectric heterointerfaces, C.T. Nelson et al., *Nano Letters* **11** 828–834 (2011)
- Air-stable magnesium nanocomposites provide rapid and high-capacity hydrogen storage without using heavy-metal catalysts K. Jeon et al., *Nature Materials* **10** 286-290 (2011)
- Stability and dynamics of small molecules trapped on graphene R. Erni et al., *PRB* **82**, 165443 (2010)
- Twin boundary structure in Bi<sub>2</sub>Te<sub>3</sub>: experiment and theory, D.L. Medlin et al., *JAP* **108** 043517 (2010)
- Free-floating ultrathin two-dimensional crystals from sequence-specific peptoid polymers, K. T. Nam et al., *Nature Materials* **9** 454-460 (2010)
- Clean and highly ordered graphene synthesized in the gas phase, A. Dato et al., *Chem.Comm.* **40** 6095 (2009)
- Direct imaging of soft-hard interfaces enabled by graphene, Z. Lee et al., *Nano Letters* **9** 3365-3369 (2009)
- Cluster imaging with a direct detection CMOS pixel sensor in transmission electron microscopy, M. Battaglia et al., *Nucl. Inst. Meth. A* **608** 363-365 (2009)
- Direct fabrication of zero- and one-dimensional metal nanocrystals by thermally assisted electromigration J. M. Yuk et al., *ACS Nano* **4** 2999-3004 (2010)
- Optimization of exit-plane waves restored from HRTEM through-focal series, R. Erni et al., *Ultramicrosc.* **110** 151-61 (2010)
- A strain-driven morphotropic phase boundary in BiFeO<sub>3</sub>, R. J. Zeches et al., *Science* **326** 977 (2009)
- Electron beam mapping of plasmon resonances in electromagnetically interacting gold nanorods, M. N’Gom et al., *PRB* **80** 113411 (2009)
- DNA-templated synthesis of Pt nanoparticles on single-walled carbon nanotubes, L. Dong, *Nanotechnology* **20** 465602 (2009)
- Aberration-corrected electron microscopy imaging for nanoelectronics applications, C. Kisielowski et al., *AIP Conf. Proc.* **1173** 231 – 241 (2009)
- Atomically thin hexagonal boron nitride probed by ultrahigh-resolution transmission electron microscopy N. Alem et al., *PRB* **80** 155425 (2009)
- Background, status and future of the transmission electron aberration-corrected microscope project U. Dahmen et al., *Phil. Trans. Roy. Soc. A* **367** 3795-3808 (2009)
- Atomic-resolution three-dimensional imaging of germanium self-interstitials near a surface: aberration-corrected transmission electron microscopy, D. Alloyeau et al., *PRB* **80** 014114 (2009)
- Atomic-resolution imaging of lithium in Al<sub>3</sub>Li precipitates, M. D. Rossell et al., *PRB* **80** 024110 (2009)
- First application of Cc-corrected imaging for high-resolution and energy-filtered TEM, B. Kabius et al., *Journal of Electron Microscopy* **58** 147–155 (2009)
- Graphene at the edge: stability and dynamics, Ç. Ö. Girit et al., *Science* **323** 1705 (2009)
- Atomic-resolution imaging with a sub-50-pm electron probe, R. Erni et al., *PRL* **102** 096101 (2009)
- K-space navigation for accurate high-angle tilting and control of the TEAM sample stage, T. Duden et al., *Microscopy and Microanalysis* **15** 1228 (2009)
- Direct imaging of lattice atoms and topological defects in graphene membranes, J. C. Meyer et al., *Nano Letters* **8** 3582–3586 (2008)
- Detection of single atoms and buried defects in three dimensions by aberration-corrected electron microscopy with 0.5 Å information limit, C. Kisielowski et al., *Microscopy and Microanalysis* **14** 454-462 (2008)
- Direct measurement of charge transfer in thermoelectric Ca<sub>3</sub>Co<sub>4</sub>O<sub>9</sub>G. G. Yang et al. *PRB* **78** 153109 (2008)
- Prerequisites for a Cc/Cs-corrected ultrahigh-resolution TEM, M. Haider et al., *Ultramicrosc.* **108** 167 (2008)
- Active Pixel Sensors for electron microscopy, P. Denes et al., *Nucl. Inst. Meth. A* **579** 891-894 (2007)
- A status report on the TEAM project, U. Dahmen, *Microscopy and Microanalysis* **13** 1150 (2007)

# Probing the Structural and Chemical Information by Scanning Transmission Electron Microscopy

Dong Su

Center for Functional Nanomaterials, Brookhaven National Lab

## Scientific Thrust Area

Electron Microscopy

## Scientific Challenge and Research Achievement

In the past ten years, aberration-corrected electron microscopy demonstrated the ability to retrieve structural information at the atomic scale. By combining imaging with spectroscopy methods (energy dispersive x-ray spectroscopy (EDX) and electron energy-loss spectroscopy (EELS)), it is possible to use scanning transmission electron microscopy (STEM) to map the elemental distribution and probe the local electronic property of materials at resolutions within one nanometer. Application of Cs-corrected techniques has benefited various areas of research, from catalytic materials to functional oxides to carbon nanomaterials. In this talk, I will present our work of solving different scientific problems using analytical STEM at the CFN. For example, we have used this technique to resolve the atomic and electronic structure of interfaces between ferroelectric oxides and traditional semiconductors [1,2] (Figure 1) and study metallic interfaces between single rare-earth (R) -oxygen layers embedded in perovskite oxides [3] (Figure 2). I will also present our results in collaboration with CFN users on Pt based core-shell catalysts for Proton exchange membrane fuel cells (PEMFCs) and other nanomaterials for energy applications.[4] The structural and chemical information obtained from this technique can be very helpful to understand material properties, but extreme care is needed in both performing experiments and interpreting the results.

## Future Work

We will expand our work on probing of interfaces to look at dynamic responses of materials. Specifically, we will be exploiting the local electrical biasing holders to probe the dynamics of electronic structure at complex oxide interfaces. Additionally, we will be working to understand surface reconstruction and modification of catalyst nanoparticles in gaseous environments by combining the STEM-EELS method with the environmental TEM(FEI-Titan) at the CFN.

## References and Publications

- 1 A. M. Kolpak, F. J. Walker, J.W. Reiner, Y. Segal, D. Su, M. S. Sawicki, C. C. Broadbridge, Z. Zhang, Y. Zhu, C. H. Ahn, and S. Ismail-Beig, *Physical Review Letters*, 105, 217601 (2010).
- 2 D. Su, B. Yang, N. Jiang, M. Sawicki, C. Broadbridge, M. Couillard, J. W. Reiner, F. J. Walker, C. H. Ahn, and Y. Zhu, *Applied Physical Letters*, 96, 121914 (2010).
- 3 H. W. Jang, D. A. Felker, C. W. Bark, Y. Wang, M. K. Niranjana, C. T. Nelson, Y. Zhang, D. Su, C. M. Folkman, S. H. Baek, S. Lee, K. Janicka, Y. Zhu, X. Q. Pan, D. D. Fong, E. Y. Tsybmal, M. S. Rzechowski, C. B. Eom, *Science*, 331, 886 (2011).
- 4 Kuanping Gong, Dong Su, Radoslav R. Adzic, *J. Am. Chem. Soc.*, 132, 14364 (2010).

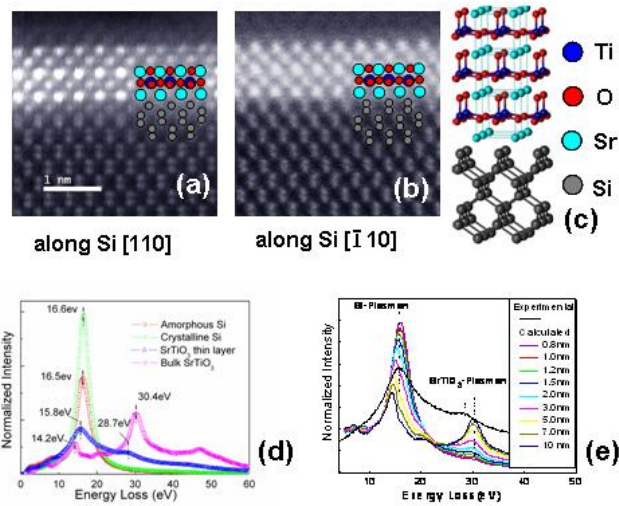


**Figure 1** (a) and (b) High angle annular dark field (HAADF) images on SrTiO<sub>3</sub>/Si interface. (c) The structure model from *a b* initio calculation confirmed the atomic structure at the interface showing in (a) and (b). (d) Valence electron energy-loss spectroscopy (VEELS) taken from sandwiched structure and bulk SrTiO<sub>3</sub>. (e) Comparison of the calculated spectra and experimental spectrum at STO layer.

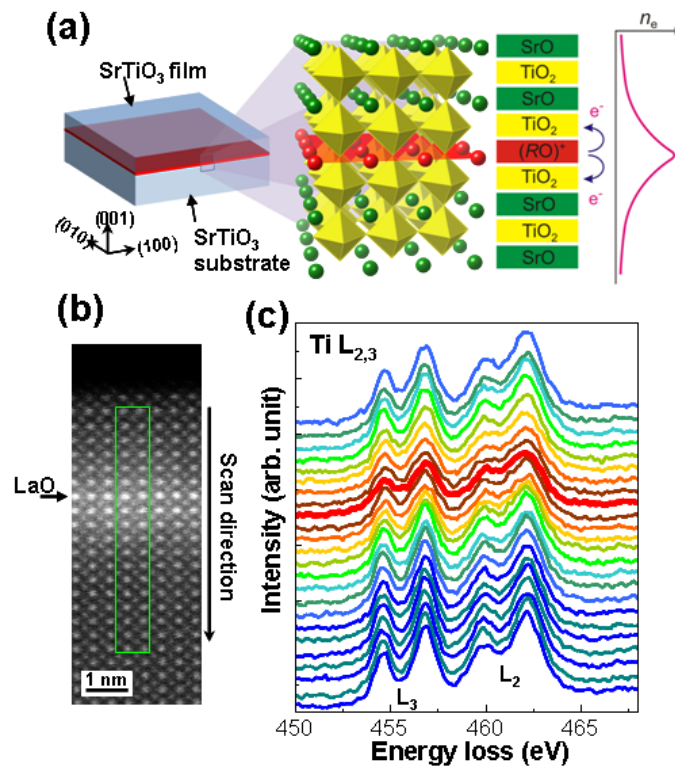


**Figure 2** (a) Schematic drawing and growth of SrTiO<sub>3</sub>/1ML RO/SrTiO<sub>3</sub> heterostructures. The +1 valent RO layer donates electrons to neighboring TiO<sub>2</sub> planes, leading to the larger electron density near the interface. (b) High angle annular dark field (HAADF) image of a 10 uc SrTiO<sub>3</sub>/1ML LaO film grown on SrTiO<sub>3</sub>. The rectangular box represents the region of EELS line scans. (c) EELS spectra of T-L<sub>2,3</sub> edges obtained from 2D line scans across the interface shown in (b).

## **Discovery of dislocation interactions with irradiation defects through *in situ* TEM deformation experiments**

I.M. Robertson, J. Kacher and G.S. Liu

University of Illinois at Urbana-Champaign, Materials Science and Engineering Department,  
Urbana, IL, 61801

**Proposal title:** Determining if a hardened matrix alters the slip transfer mechanism through grain boundaries.

### **Scientific Challenge and Research Achievement:**

The mechanical properties of irradiated materials show a decrease in ductility, an increase in tensile strength, and an increase in yield strength even to the point of creating an apparent upper and lower yield point in face-centered cubic materials [1]. The microstructure in deformed irradiated metals is characterized by the irradiation-produced defects and distinct channels that appear to have been cleared of these defects by the motion of dislocations. Identifying the source of these dislocations and discovering the mechanisms by which they annihilate the defects is essential to understanding and modeling the mechanical response. Further impetus for understanding the formation of these channels is that channel-clearing dislocations are associated with the initiation of grain boundary cracking that leads to irradiation-assisted stress corrosion cracking. To study the dislocation processes directly requires conducting either computer simulations or *in situ* experiments in the transmission electron microscope. Here the results of *in situ* TEM ion-irradiation and straining experiments on a series of austenitic stainless steels performed in the IVEM-accelerator facility at Argonne National Laboratory are reported.

To address the question of the role, if any, of the pre-existing mobile dislocations on channel formation, an unirradiated sample was deformed until a dislocation source was activated and several dislocations were ejected from it [2]. After the dislocations came to rest, the sample was irradiated with 1 MeV Kr ions to a dose on the order of  $10^{17}$  ions  $m^{-2}$ ; these conditions were selected to produce a high density of small defects, presumably vacancy in nature, throughout the electron transparent foil. The sample was further deformed but the previously mobile dislocations remained stationary even though the dislocation source continued to generate dislocations. An example of this “locking” of pre-existing mobile dislocations is presented in Figure 1 in the form of a difference image in which a negative image of the dislocation positions after irradiation and further deformation is superimposed on a positive image of the initial position [3]. The lack of contrast in this image comes from the cancellation between superimposed images, indicating that no dislocation motion has occurred. Therefore, a key conclusion is that the dislocations which created the channels were generated post-irradiation and were not pre-existing ones. A second is that the dislocation source at a grain boundary or a stress concentrator such as a crack tip is unaffected by the irradiation, which suggests that the mechanical property changes result from the difficulty of dislocation propagation and not from nucleation. Consequences of this include: a dislocation pile-up can form at any location within a grain if the propagation stress on the leading dislocation does not exceed the combined obstacle field barrier strength; and the formation of a dislocation pile-up at a grain boundary differs in terms of the rate of formation and inter-dislocation spacing from an unirradiated material. The former effect can create a dislocation pile-up at a grain boundary source, which could shut down the source and increase the back-stress on the grain boundary. The latter influences how the

local stress evolves due to the formation of a dislocation pile-up. A comparison of these structures is presented in Figure 2. Both structures could influence how the grain boundary responds during deformation, perhaps establishing the conditions for cracking.

The movement of these new dislocations through the obstacle field was observed to be jerky and erratic, with segments of individual dislocations jumping forward in a discontinuous manner. The activity was also sporadic, occurring for a period of time then stopping and initiating elsewhere along the same slip band [2]. Perfect dislocations were preferred initially to partial dislocations even in steels with low stacking-fault energy. That is, the source ejected perfect dislocations first and these initiated channel clearing before any partial dislocations were released. It remains to be determined if this is a source effect or reflects a difference in the efficiency of perfect and partial dislocations for annihilating the defects.

Lastly, two mechanisms for channel widening were observed: double cross-slip to avoid dislocation-defect interactions [3] and the nucleation of parallel dislocation sources at grain boundaries [4]. In order to clarify the spatial configuration associated with the double cross-slip mechanism, a sample for electron tomography was extracted from the electron transparent region of the straining bar by using focused ion beam machining; the results of this analysis will be presented and discussed.

The effects of this altered dislocation mobility and the resultant evolution of the microstructure will be discussed in terms of the local shear stresses on grain boundaries and slip systems. Implications of these results on the degradation of mechanical properties and intergranular crack initiation will be presented [5].

## References

- [1] Foreman AJE, Sharp JV. *Phil. Mag.* 1969;19:931.
- [2] Briceño M, Fenske J, Dadfarnia M, Sofronis P, Robertson IM. *J. Nucl. Mater.* 2011;409:18.
- [3] Kacher J, Liu GS, Robertson IM. *Microscopy and Microanalysis* 2011;accepted.
- [4] Kacher J, Liu GS, Robertson IM. in preparation Spring MRS meeting, 2011.
- [5] This work was supported by the US Department of Energy, Offices of Basic Energy Sciences under contract DE-FG02-07ER46443 (electron tomography) and DE-FG02-08ER46525 (effects of ion irradiation).

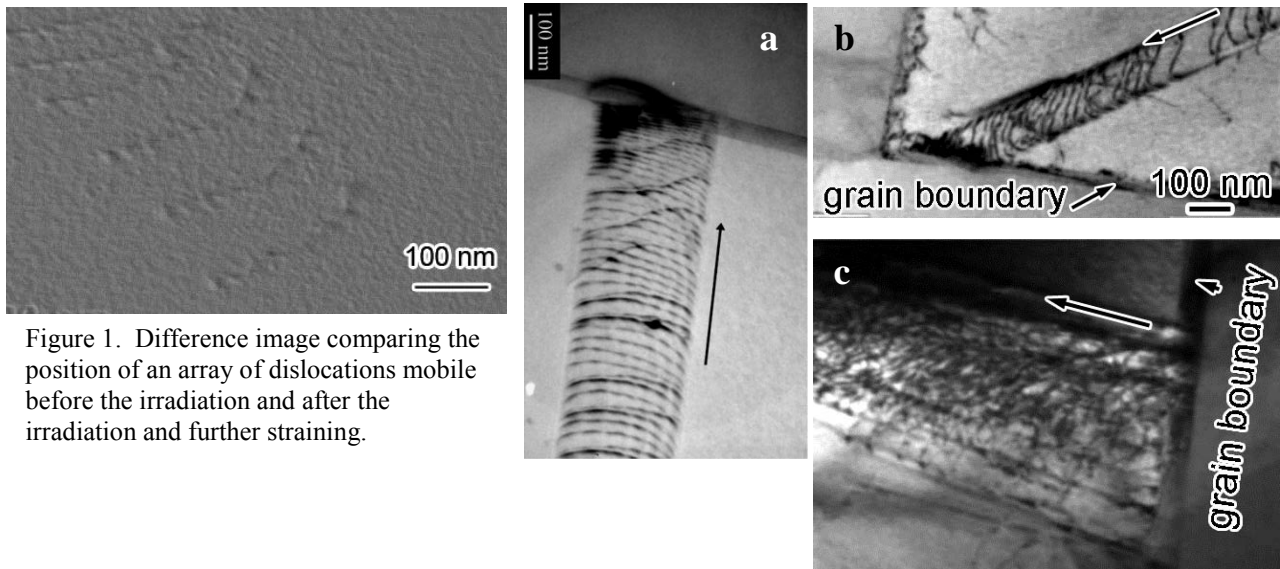


Figure 1. Difference image comparing the position of an array of dislocations mobile before the irradiation and after the irradiation and further straining.

Figure 2. Comparison of the dislocation structures at grain boundaries in *a* unirradiated, and *b* and *c* irradiated. *b* and *c* compare the incoming and outgoing dislocation structures at two different boundaries.

# Nanoscale Imaging and Analysis with Ion Beams

David C Joy

Center for Nanophase Materials Science, Oak Ridge National Laboratory

and

The University of Tennessee, Knoxville, TN

## Scientific Thrust Area

Investigating imaging with helium ion beams in reflection and transmission modes, developing theoretical models for signal generation and image interpretation, and developing techniques for chemical analysis at the nanoscale using ion beams.

## Scientific Challenge and Research Achievement

Diffraction sets a limit to imaging at the nanoscale when using electron beams. Lens aberration correctors can reduce this effect, but only at the expense of considerable complexity and a major reduction of depth of field in the image. He<sup>+</sup> ion beams have a wavelength two orders of magnitude smaller than that of electrons of the same energy so diffraction limiting is absent. This permits convergence angles  $\alpha$  of 0.1mrad or less to be used for the focused probe so eliminating both chromatic (varies as  $\alpha$ ) and spherical (varies as  $\alpha^3$ ) aberrations. Contrast transfer function measurements presently show a resolution limit of 0.6nm, at an energy of 40keV, probably limited by mechanical and power supply instability (figure 1). For a given material the stopping power of He<sup>+</sup> ions is 10 to 20 times higher than that of an electrons of the same energy so the ion beam range is significantly reduced, thus both maximizing the visibility of surface detail and improving signal yields. The ion induced secondary electron (iSE) signal displays a strong variation with the atomic number of the sample, and the variation of the iSE signal with sample topography resembles that of the electron generated (eSE) signal but varies with both the sample chemistry and the beam energy. The relative absence of SE generated by backscattered ions and the limited beam range results in excellent sensitivity to surface details, and produces high contrast even from a single layer of graphene. Because the stopping power increases with energy the iSE yield and the resolution of the instrument can both be enhanced by raising the accelerating voltage, potentially permitting sub-angstrom imaging in iSE mode, potentially even from the top atomic layers of bulk samples. We have developed a detailed Monte Carlo model (“IONiSE”) of the He<sup>+</sup> ion interaction with solids and of the production of iSE incorporating SRIM cross-sections<sup>(1)</sup> permitting detailed simulations of the iSE yield and the interpretation of ion images over a wide energy range from 10keV to 10MeV.

Ions, unlike electrons, channel strongly in crystals allowing lattice defects, grains, and grain boundary, contrast effects to readily be observed in both the iSE and backscattered ion signals. It is also possible to image crystals in ion scanning transmission mode. Although penetration by the 40keV ion beam is limited to only about 100nm in typical metals and semiconductors excellent images of nanocrystals - showing contrast features such as thickness fringes, bend contours, and dislocations – and of soft or biological materials are obtained<sup>(2)</sup>.

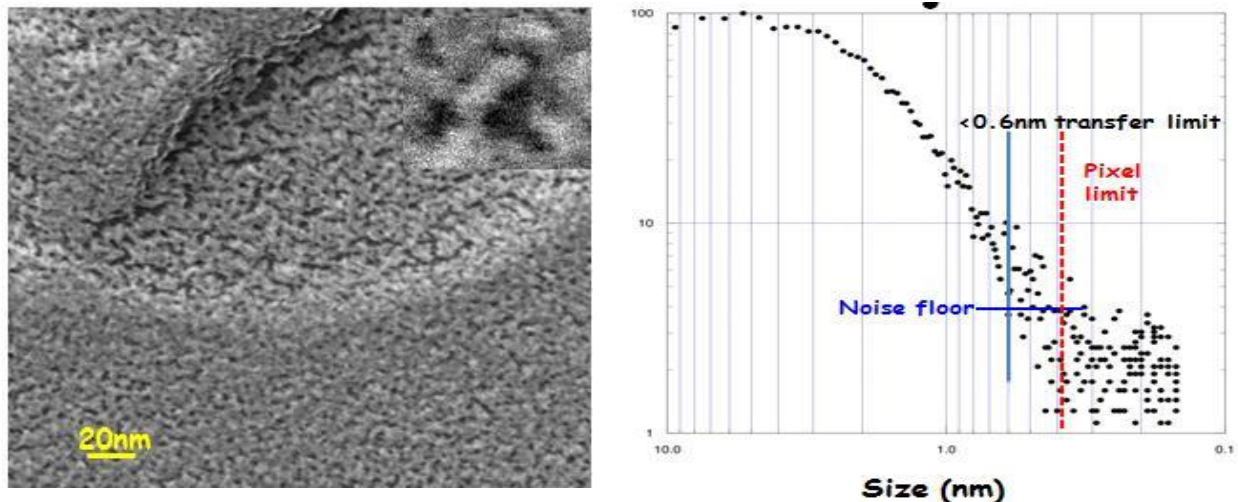


**Figure 1. (Left) iSE image of Pt on silicon imaged with He<sup>+</sup> beam at 40keV and (right) contrast transfer function derived from the image showing noise limited resolution down to about 0.6nm**

An essential requirement is to provide some form of micro-analytical capability for the HIM. Because no fluorescent X-rays are generated other options must be considered. The yield of both secondary electrons and Rutherford back scattered ions increases with the atomic number of the sample, but the signal variation with atomic number is not monotonic and so unique elemental determination is not possible. The most promising approach is Secondary Ion Mass Spectrometry (SIMS) which would permit nanometer spatial resolution and high surface sensitivity. However, the sputter yield from He<sup>+</sup> is small at beam energies above 20keV and careful optimization of the spectrometer will be required to provide adequate sensitivity.

### Future Work

Key goals are to use the unique imaging potential to visualize single atoms on a bulk substrate, and to devise and demonstrate a viable microanalytical capability at the nanoscale.

### References

- (1) Ziegler J F, (1999), "Stopping of Energetic Light Ion in Elemental Matter", *J.Appl.Phys.* **85**, 1249-1272
- (2) Notte, J; Hill, R; McVey, S; Ramachandra, R; Griffin B; Joy, D; (2010) "Diffraction Imaging in a He<sup>+</sup> Ion Beam Scanning Transmission Microscope", *Microscopy and Microanalysis* **16**, 1 – 5

### Publications

- Ramachandra R, Griffin B, Joy DC, (2009), 'A model of secondary electron imaging in the Helium Ion scanning microscope', *Ultramicroscopy* **109**, 748-757
- Joy DC, and Rack P D, (2010) "Monte Carlo Simulation of Helium Ion Beam Induced Deposition", *Nanotechnology*, **21**, 175302
- Trager-Cowan C, Sweeney F, Edwards P R, Dynowski F L, Wilkinson A J, Winkle, Day A P, Wang T, Parbrook P J, Watson I M, and Joy D C, (2008), 'Electron channeling and Ion Channeling Contrast Imaging of Dislocations in Nitride Thin Films', *Microscopy and Microanalysis* **14**, 1194-5

## **Proposal Title: Hydrothermal Processing of Quantum Dots and Alloy Nanoparticles**

Mathew M. Maye

Department of Chemistry, Syracuse University, Syracuse New York 13244. *mmmaye@syr.edu*

**Scientific Challenge and Research Achievement:** In our research we are exploring the synthesis and processing of core/shell nanomaterials via a novel hydrothermal approach.<sup>1-5</sup> Using this approach, we aim to prepare nanomaterials with a highly accessible interface, which may facilitate energy and charge transport with an assortment of dyes, polymers, or small molecules. In our design, hydrothermal conditions are achieved using automated microwave irradiation (MWI), which allows for fine control of heating and cooling rates, tunable hydrothermal temperatures, increased throughput, and the possibility of local heating at the nanoscale interface. This presentation will showcase our recent and future work characterizing these materials while working as Users of the Center for Functional Nanomaterials at Brookhaven National Laboratory. Using the ultrafast and single molecule capabilities of the CFN, we have been able to show the improved photophysical properties of CdSe/ZnS quantum dots prepared at hydrothermal temperatures.<sup>1-2</sup> The observed increase in lifetime, and single quantum dot brightness, as measured via TCSPC and FCS respectively, indicates the highly crystalline nature of the dots at increasing hydrothermal temperatures. A typical set of TCSPC results are shown in Figure 1. At increased hydrothermal temperatures, particularly at  $T > 160$  °C, the CdSe quantum dots show fluorescent lifetimes of  $t \approx 17$  ns, making them comparable to more conventional organically synthesized CdSe quantum dots. Because these quantum dots are prepared at hydrothermal conditions, they lack the typical organic capping, such as TOPO. Thus, the quantum dot interface is highly accessible to both energy and electron transfer. To demonstrate this, we combined the synthesized quantum dots with nanocrystalline TiO<sub>2</sub>, preparing a model dye sensitize photovoltaic materials. Due to the strong interfacial contact, charge transport was observed via the quenching of quantum dot fluorescence. Similar results are shown for modification of the qdot with fullerene derivatives.

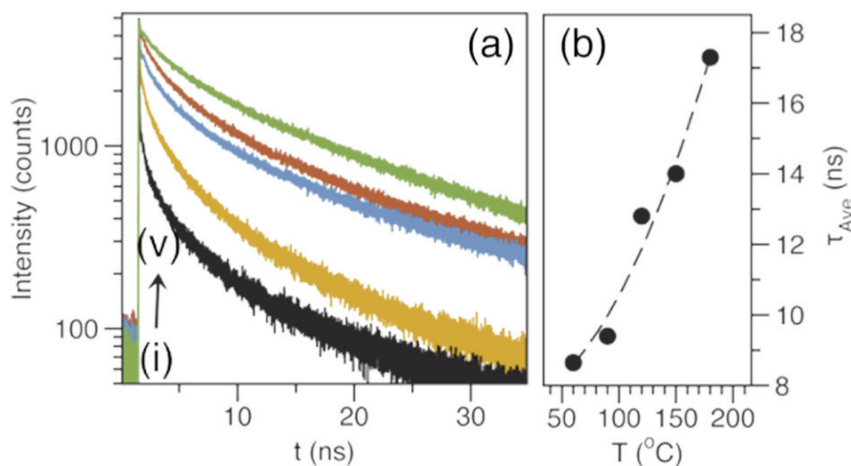


**Figure 1:** (a) TCSPC measurements collected at CFN Advanced Optics Facility for CdSe qdots prepared at 60 (i), 90 (ii), 120 (iii), 150 (iv), and 180 °C (v). An excitation of 420 nm was provided by a Ti:sapphire laser system with a 60 fs pulse, and a 45 ps instrument response function. (b) A corresponding plot of calculated  $\tau_{Ave}$  from TCSPC measurements indicating a systematic increase in  $\tau_{Ave}$  with increased hydrothermal temperature.<sup>1</sup>

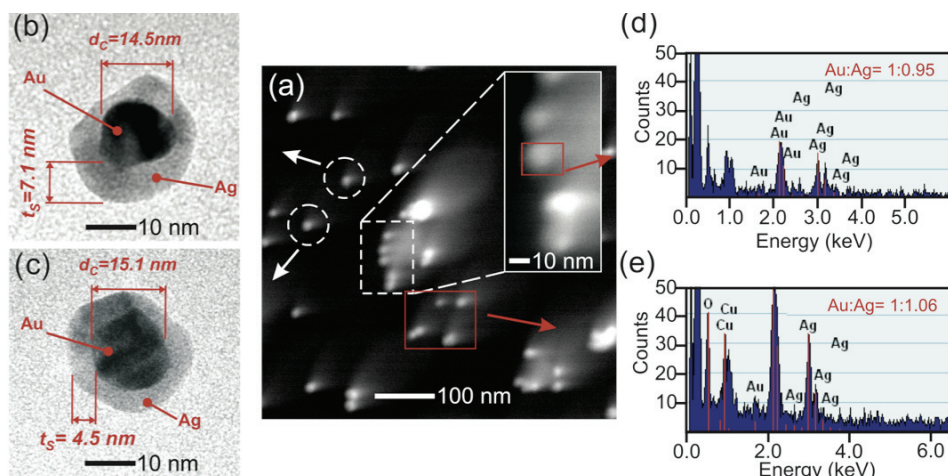


**Figure 2.** (a) A representative STEM micrograph of a Au/Ag NP prepared at  $T_H=120$  °C. (b-c) HRTEM micrographs of individual Au/Ag NPs. (d-e) Corresponding selected area EDX spectra for the regions outlined for a single NP, and group of 5 NPs.<sup>5</sup>

We also present our further exploration of this synthetic approach for the synthesis and processing of metallic core/alloy nanostructures with tunable optical properties and phase behavior.<sup>3-5</sup> The post-synthetic processing of nanomaterials may allow researchers to reach specific properties, morphologies, or phase regimes that are not accessible by simple synthesis alone. Here, we take advantage of atomic interdiffusion at nanoparticle interfaces to fabricate core/alloy nanoparticles. Modest temperature changes were found to have profound effects for the interfacial alloying of the confined nanosystem. As a proof-of-principle system, we employed  $Au/Au_xAg_{1-x}$  and  $Au/Au_yPd_{1-y}$  binary nanosystems, due in large part to its miscible phase diagram and rich plasmonic behavior. Nanostructure morphology was characterized by TEM and STEM, and composition analysis was performed via selective area EDX, and XPS (Figure 2). The resulting surface plasmon resonance signatures were observed by both UV-vis and Dark Field Microscopy at the CFN, and modeled as a function of alloy shell dimensions, and composition, using the discrete dipole approximation (DDA) method.

**Future Work:** Our future work will explore in detail the energy transfer capability of our quantum dots at the single molecule level at the CFN. We are also very interested in investigating the growth mechanism of our core/alloy metal particles, in particular the novel control of interfacial alloying. Using the phase behavior of the alloy, we believe we will be able to control morphology, growth, stability, and catalytic activity at an unprecedented level. Moreover, this approach may provide a useful platform on which to study nanoscale-alloying effects and nano-phase behavior, which have been proposed theoretically. Furthermore, with the help of the CFN, the particles will be tested for potential utility as plasmonic antenna, metamaterials, optical probes, and surface enhanced Raman substrates.

**Publications:**

1. Han, H.; Di Francesco, G.; Maye, M. M. *J. Phys. Chem. C* **2010**, *114*, 19270-19277.
2. Han, H.; Di Francesco, G.; Sexton, A.; Tretiak, A.; Maye, M. M. *Mater. Res. Soc. Symp. Proc. Vol. 1220*, **2010**, 12220-BB03-02.
3. Njoki, P. N.; Wu, W.; Zhao, H.; Hutter, L.; Schiff, E. A.; Maye, M. M. *J. Am. Chem. Soc.* **2011**, *133*, 5224 - 5227
4. Wu, W.; Njoki, P. N.; Han, H.; Zhao, H.; Schiff, E. A. Lutz, P. S.; Solomon, L.; Matthews, S.; Maye, M. M. *J. Phys. Chem. C* **2011** (In-Press)
5. Njoki, P. N.; Wu, W.; Han, H.; Solomon, L.; Maye, M. M. **2011** (In-Review)

## Characterization and control of monodisperse core/shell nanophases in solids

V Radmilovic\*, C Ophus, A. Gautam, M Asta\*\* and U Dahmen

National Center for Electron Microscopy, Materials Sciences Division, LBNL, Berkeley, CA 94720

\*Nanotechnology and Functional Materials Center, Faculty of Technology and Metallurgy, University of Belgrade, Belgrade, Serbia

\*\*Department of Materials Science and Engineering, University of California, Berkeley, CA

### Scientific Thrust Area

The properties of precipitation-strengthened alloys can be fully controlled only if we understand the factors that determine solute partitioning, precipitate size, shape and thermal stability. It is also essential to understand the fundamental features that underlie the behavior of nanoscale phases embedded in a solid matrix and their role in the evolution of microstructure in materials. Because of the scale and nature of such microstructures, electron microscopy is an essential tool in their characterization.

### Scientific Challenge and Research Achievement

Until recently, experimental studies of second-phase precipitates embedded in a solid matrix were limited by the nanometer-scale dimensions of the particles, making measurements of their composition and structure rather complicated and not fully reliable. Due to major advances in electron microscopy coupled with the development of predictive atomic-scale modeling techniques we have developed procedures to analyze local structure and composition down to the level of individual atomic columns. In recent years, by studying Al based alloy model systems we have gained an understanding of the factors that control the formation of core-shell precipitates [1,2]. We demonstrated that in AlLiSc alloys, by manipulating thermodynamic and kinetic parameters, monodisperse  $\text{Al}_3(\text{ScLi})$  core/shell ordered precipitates with a Sc and Li-rich core surrounded by a Li-rich shell can be created via a three-stage heat treatment. Conventional high-resolution phase contrast imaging reveals the fully ordered  $\text{L1}_2$  structure of the shell. EELS and EFTEM spectrum imaging indicate that Sc is present in the core while Li is present in both, the core and the shell. Aberration corrected transmission electron microscopy was employed to image Li using exit wave reconstruction. The phase of the exit wave clearly distinguished Al columns from Li columns in the Li rich  $\text{L1}_2$  shell. Using first-principles thermodynamic calculations in tandem with continuum models for precipitation kinetics, we demonstrate that incorporation of Li in the  $\text{Al}_3\text{Sc}$  core leads to a significant enhancement in nucleation rate, causing a pronounced narrowing of the experimentally observed precipitate size distribution.

### Future work

By careful selection of thermodynamic and kinetic parameters during nucleation and growth we can control precipitate size and move the size distribution into the so-called “size focusing regime”, analogous to the strategy commonly used in colloidal chemistry [3]. This approach to controlling precipitate size in core-shell structures can be used as a template and applied in other alloy system to enhance the nucleation rate, modify growth kinetics, and generate monodisperse distributions of precipitates.

### References

- [1] A. Tolley et al., *Scripta Mat.*, 52 (2005) 621.
- [2] E. Clouet et al., *Nature Mat.*, 5 (2006) 482.
- [3] Y. Yin, A.P. Alivisatos, *Nature*, 437 (2005) 664.

### Publications

- [4] V. Radmilovic, et al., *Scripta Mat.*, 58 (2008) 529.
- [5] M.D. Rossell, et al., *Phys. Rev. B* 80 (2009) 024110.



## Nitrogen-Incorporated Ultrananocrystalline Diamond as a Robust Cold Cathode Material for Advanced Spaceflight Instruments

Stephanie A. Getty<sup>1</sup>, Orlando Auciello<sup>2,3</sup>, Anirudha Sumant<sup>3</sup>, Xinpeng Wang<sup>3</sup>, Adrian Southard<sup>1</sup>, and Daniel P. Glavin<sup>1</sup>, <sup>1</sup>NASA Goddard Space Flight Center, <sup>2</sup>Materials Science Division and <sup>3</sup>Center for Nanoscale Materials, Argonne National Laboratory

**CNM User Proposal Title:** Fabrication of Nitrogen-Doped UNCD Field Emitters and Characterization of Emission Performance

### Scientific Challenge and Research Achievement

We report on the work carried out under CNM proposal (#933) for the development of a new electron field emission source based on novel nitrogen-incorporated ultrananocrystalline diamond (N-UNCD) synthesized by members of our team at the Center for Nanoscale Materials (CNM). The goal is to produce a robust, long-lived field emission cathode for the electron impact ionization source of a miniaturized time-of-flight mass spectrometer<sup>1</sup> (ToF-MS). The Volatile Analysis by Pyrolysis of Regolith (VAPoR) instrument is shown in Fig. 1. Members of our team are developing such instruments for *in situ* chemical analysis of the atmospheric and soil constituents that may be present on Solar System planetary targets, e.g., Earth's Moon, Mars, comets, asteroids, and the Outer Planets.

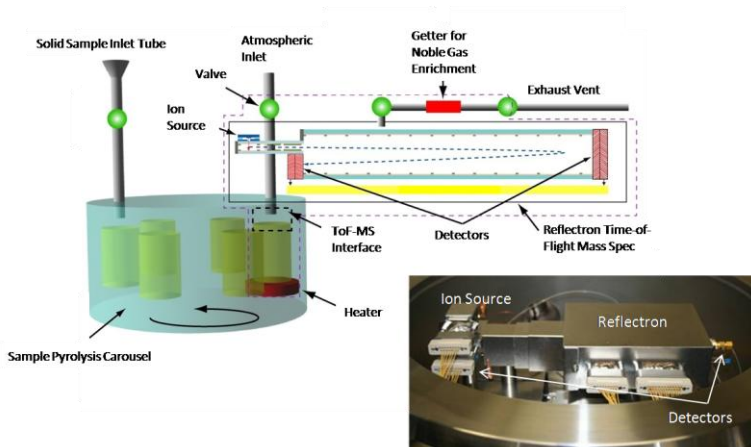


**Figure 1.** VAPoR will interface a carousel of pyrolysis ovens to a miniature ToF-MS analyzer. The prototype ToF-MS (right) features a field emission cathode in its electron impact ionization source.

For this purpose, the low power consumption of field emission technology is desirable for use in resource-constrained environments. In contrast to a thermionic filament, which uses thermal energy to release electrons from a material, field emitters operate at ambient temperatures, which make them more efficient. Although carbon nanotubes (CNTs) exhibit low threshold fields for electron emission ( $\sim 1\text{-}3\text{ V}/\mu\text{m}$ ) and provide field emission of electrons for several hundred hours, improved lifetime is desirable for long-duration spaceflight applications. Research performed in the recent past<sup>2,3</sup> demonstrated that films of UNCD, and specifically films with nitrogen atoms incorporated into the grain boundaries, exhibit low field emission thresholds ( $\sim 2\text{-}4\text{ V}/\mu\text{m}$ ), with the additional advantages of inherent field enhancement at the nanoscale grain boundaries<sup>3</sup> and low threshold field, even in the presence of residual gases such as  $\text{O}_2$ .<sup>4,5</sup> N-UNCD films may therefore provide a route to long-lived field emitters for NASA applications. We have leveraged this previous design work, first demonstrated with CNT field emitters, towards enhancing the robustness of the ToF-MS using N-UNCD films synthesized at CNM as the field emitting

cathode. Preliminary N-UNCD testing (Fig.2) reveals current densities that compare favorably with CNTs and lifetime (> 1000 hours) that surpasses that of CNTs.

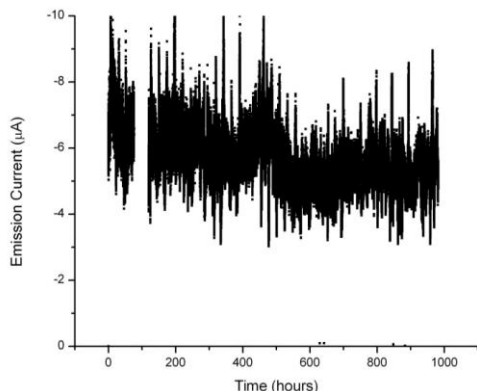


**Figure 2.** Preliminary life-time test results of electron field emission from N-UNCD films indicate that N-UNCD can provide electron currents from field emission, in high vacuum, for over 1000 hours with minimal degradation.

### Future Work

Our team is presently fabricating a scaled-up N-UNCD cathode for integration into the electron gun of the VAPoR ToF-MS. This component promises to improve the instrument's sensitivity by at least 1000x. Investments in collaborative work between the field emission developers at NASA GSFC and the UNCD thin film expertise available at the CNM could lead us to identify dual-use technologies that could also benefit NASA. For example, in addition to planetary science applications, UNCD-based field emitters exhibit low sputtering effects when impacted by ions from plasma generated in ion thrusters, owing to the low sputtering yield of carbon. Therefore, N-UNCD could provide a robust cold cathode to enable ion thrusters for resource-constrained, long-duration spaceflight missions. Another candidate for future development can be found in high-frequency UNCD resonators that are under development for DOE and DOD applications, including highly sensitive magnetometers that could find use in weapons screening applications, oil prospecting, and in medical imaging and for NASA as part of particles and fields instrument packages. Continued collaboration between CNM at Argonne National Laboratory and NASA's Goddard Space Flight Center on the development of UNCD thin film technology could enable the types of dual-use devices described above.

### References

1. S. A. Getty *et al.*, "Development of an evolved gas-time-of-flight mass spectrometer for the Volatile Analysis by Pyrolysis of Regolith (VAPoR) instrument," *International Journal of Mass Spectrometry* **295**, 124-132 (2010).
2. O. Auciello and A. V. Sumant, "Status Review of the Science and Technology of Ultrananocrystalline Diamond (UNCD<sup>TM</sup>) Films and Application to Multifunctional Devices", *Diamond and Related Materials*, **19** (2010) 699–718.
3. A. R. Krauss, O. Auciello *et al.*, "Electron Field Emission for Ultrananocrystalline Diamond Films", *J. Appl. Phys.* **89** (2001) 2958-2967.
4. M. Hajra *et al.*, "Effect of Gases on the Field Emission Properties of Ultrananocrystalline Diamond-Coated Silicon Field Emitter Arrays", *J. Appl. Phys.* vol. 94, No. 6 (2003) pp. 4079-4083.
5. M. Q. Ding, O. Auciello *et al.*, "Effect of Oxygen on Field Emission Properties of Ultrananocrystalline Diamond-Coated Ungated Si Tip Arrays", *J. Vac. Sci. & Tech.* **B 21(4)** (2003) 1644-1647.

### Publications

1. S.A. Getty, O. Auciello, A.V. Sumant, X. Wang, D. Glavin, and P.R. Mahaffy, *Proc. SPIE* **7679**, 76791N (2010).
2. Use of the Center for Nanoscale Materials was supported by the U. S. Department of Energy, Office of Science, Office of Basic Energy Sciences, under Contract No. DE-AC02-06CH11357, CNM User proposal #933, the 2010 NASA Innovation Fund, and the NASA Astrobiology Science Technology for Instrument Development Program, under Grant No. 07-ASTID07-0020.

# Spectroscopic and Microscopic Investigations of Model CO<sub>2</sub> Capture and Utilization Materials

David Starr

Center for Functional Nanomaterials, Brookhaven National Laboratory, Upton, NY 11973

## Scientific Thrust

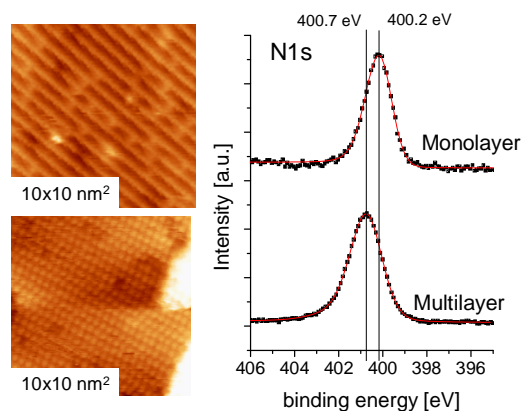
This work was conducted within the *Interface Science and Catalysis* research theme of the Center for Functional Nanomaterials at Brookhaven National Laboratory in collaboration with staff in the Chemical Sciences Division at Lawrence Berkeley National Laboratory and Chemistry Department at Brookhaven National Laboratory.

## Research Achievement

Fossil-fuel power plants are among the largest CO<sub>2</sub> emitters accounting for approximately one-third of anthropogenic CO<sub>2</sub> emissions. Due to increasing energy demands and slow deployment of clean energy alternatives, a practical near term route to CO<sub>2</sub> mitigation is through CO<sub>2</sub> capture and utilization from power plants. This presentation will focus on our efforts in developing model materials that can be used for a molecular level understanding of CO<sub>2</sub> capture processes and the catalytic conversion of CO<sub>2</sub> into commodity chemicals.

### *Model Solid Supported CO<sub>2</sub> Capture Materials*

Today, CO<sub>2</sub> capture from power plants is typically done using aqueous solutions of monoethanolamine (MEA). Disadvantages of this method include: high costs for regenerating the MEA solution after CO<sub>2</sub> capture, solution degradation by flue gases, such as NO<sub>x</sub> and SO<sub>x</sub>, and equipment corrosion by the MEA solution. As a result, solid supported capture materials are currently being investigated as alternatives to aqueous MEA solutions for CO<sub>2</sub> capture. To develop a model system for molecular-level investigations of solid supported CO<sub>2</sub> capture materials, we have studied the adsorption of MEA on rutile TiO<sub>2</sub>(100) surfaces with complementary surface science methods, including; synchrotron based X-ray photoelectron spectroscopy (XPS), Near Edge X-ray Adsorption Fine Structure (NEXAFS) and Scanning Tunneling Microscopy (STM), and Density Functional Theory (DFT) calculations. Additionally, we investigated its potential for CO<sub>2</sub> capture with ambient-pressure XPS (AP-XPS). Understanding the bonding of this simple CO<sub>2</sub> capture molecule to a solid support on a molecular level can explain why this model system lacks the ability for CO<sub>2</sub> capture.

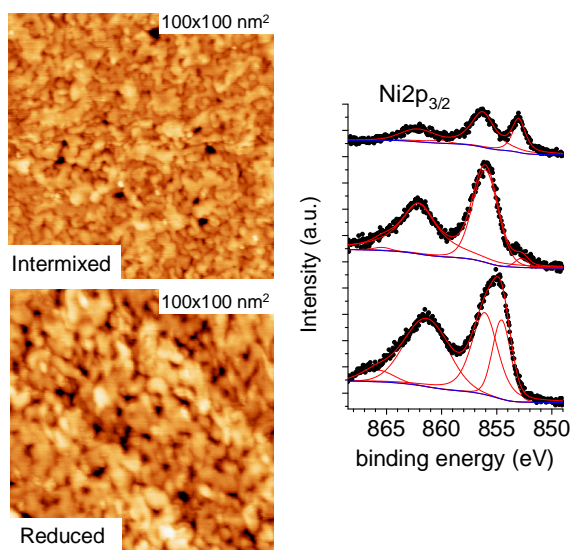


Left: STM images of TiO<sub>2</sub>(110) before and after MEA adsorption. Right: N 1s XPS spectra of MEA adsorbed on TiO<sub>2</sub>(110) as a multilayer film and monolayer.

### Model NiO-MgO Mixed Oxide Catalysts for Methane Reforming Using CO<sub>2</sub>

Dry-reforming of methane (CH<sub>4</sub>) is a potential route to produce syn-gas – a mixture of H<sub>2</sub> and CO used for Fischer-Tropsch and methanol synthesis – from two greenhouse gases, CO<sub>2</sub> and CH<sub>4</sub>. Ni-based catalysts are commonly used for methane reforming reactions. A general problem with Ni catalysts, however, is carbon deposition which leads to deactivation. Reduced mixed oxide catalysts composed of NiO and MgO have demonstrated long term stability as well as high yield for dry reforming of methane. The long term stability for the reduced mixed oxide catalyst, compared to Ni catalysts synthesized by more traditional methods, is explained by smaller Ni particles which are less susceptible to coking. Additionally, oxidation-reduction cycling of Ni in the mixed oxide during the reaction may lead to continuous re-dispersion of the catalyst therefore improving its long-term stability.

In order to explore the favorable properties of these mixed-oxide catalysts we have taken a model catalyst approach using MgO and NiO thin films deposited onto Mo(100). We have investigated the intermixing of these two oxides followed by reduction of the mixed oxide using XPS with normal and grazing emission as well as with STM. By heating the thin films the two oxides intermix forming a solid solution. Heating in hydrogen leads to partial reduction of the mixed-oxides to form metallic Ni. However, the reduced Ni diffuses to the interface between the Mo(100) and oxide thin film. Additionally, we have taken a first step towards understanding the oxidation-reduction cycling of Ni by investigating the reduction of c(2x2)-O/Ni(100) by H<sub>2</sub>(g) using AP-XPS. The presence of NiO islands located predominantly at the step edges lead to significant changes in kinetics of reduction of the c(2x2)-O on the Ni(100) surface.



Left: STM images of a NiO-MgO mixed oxide thin film before and after reduction with H<sub>2</sub>(g). Right: Ni 2p XPS spectra of the mixed oxide thin film before intermixing, after intermixing and after reduction (bottom to top).

### Future Work

We will continue our work on model CO<sub>2</sub> capture materials by investigating the bonding and geometry of secondary and tertiary amines (specifically di-ethanolamine and tri-ethanolamine) on rutile TiO<sub>2</sub>(110) and using AP-XPS to understand their CO<sub>2</sub> capture capabilities. This will allow us to directly correlate CO<sub>2</sub> capture properties to amine type and therefore aid the search for new molecule-substrate combinations and the development of future solid CO<sub>2</sub> capture materials. We are at the initial stages of investigating the use of Au(100) as a substrate for the NiO-MgO mixed-oxide thin films. The inertness of Au may allow for the reduced Ni to be located on the oxide surface following reduction of the mixed-oxide films as opposed to the substrate/oxide thin film interface. In addition we will continue investigating the oxidation and reduction of Ni single crystals using AP-XPS to provide detailed kinetics of NiO reduction and re-oxidation.

## Self-healing radiation-tolerant nanostructural steels for advanced nuclear applications

M. K. Miller, C. L. Fu, C. M. Parish, P. E. Edmondson, Y. Zhang

Materials Science and Technology Division,

Oak Ridge National Laboratory, Oak Ridge, TN 37831-6136

**Scientific Thrust Area:** Materials under extreme environments (Materials Science and Engineering Division)

**Scientific Challenge and Research Achievement:** The radiation tolerance of nanostructured ferritic alloys (NFAs) to high dose irradiation is a key requirement for their use in advanced nuclear reactors, particularly as first wall and divertor components. The properties are controlled by high number densities of nanoclusters and solute segregation to, and precipitation on, the grain boundaries. Atom probe tomography (APT) has demonstrated that the microstructures of these NFAs exhibit excellent response to high temperature creep [1], and to isothermal annealing up to 92% of the melting temperature, and have a high tolerance to neutron irradiation up to 3 displacements per atom (dpa) [2].

The aim of the study was to experimentally determine the response of NFAs to high dose ion irradiation. After ion irradiations at  $-100\text{ }^{\circ}\text{C}$  to doses between  $\sim 1$  and  $\sim 300$  dpa, no indications of 1-2 nm diameter Ti-Y-O-enriched nanoclusters or grain boundary segregation were evident. After irradiation at  $350\text{ }^{\circ}\text{C}$ , the nanoclusters were a similar size to those in the unirradiated condition. After irradiation at  $750\text{ }^{\circ}\text{C}$ , the nanoclusters were larger than those in the unirradiated condition. Grain boundary segregation of Cr and W was removed by low temperature irradiation, but was observed after high temperature irradiation. These results indicate that the solutes in the nanoclusters were driven into solid solution as a result of the ballistic cascade. At low temperatures, there was insufficient diffusion for the nanoclusters to reform despite the vacancies introduced by the cascades. At the higher temperatures, the nanoclusters quickly reformed and coarsened by a self-healing process due to the additional vacancies produced during the cascade and the higher temperature. The microstructure of these NFAs was found to have a remarkable tolerance to high dose (up to  $\sim 460$  dpa) irradiation at elevated temperatures.

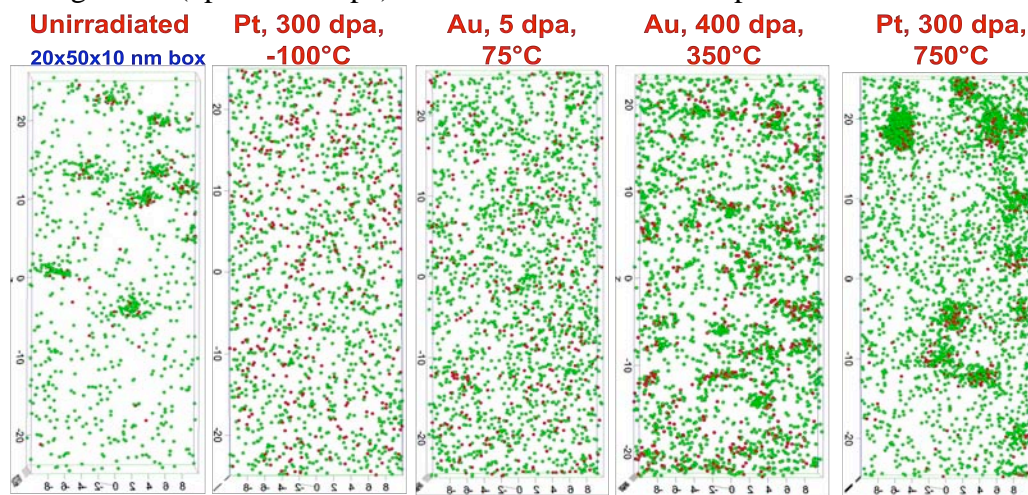


**Figure 1.** Atom maps revealing the Ti and Y distributions and the presence of nanoclusters

**Future Work:** The dynamic behavior of solutes during the early stages of nanocluster growth will be investigated through a combination of first-principles theory and atomic level microstructural characterization with APT, scanning transmission electron microscopy (STEM), and neutron scattering. APT experiments will be continued to establish and confirm the importance of vacancies during the formation of the nanoclusters through a comparison of the size, number density, and composition of nanoclusters in unirradiated and ion-irradiated NFA and a non-mechanically-alloyed F82H alloy with approximately the same composition as the NFA. The physical mechanisms responsible for the stability and self-healing of the nanoclusters under displacement cascade irradiation conditions will continue to be investigated by a synergistic approach of atomic level characterization of irradiated NFAs and computer simulation and modeling. Additional sets of ion irradiations are planned, with a range of different mass ions (He, Si, Fe, Pt) at different temperatures, doses, and dose rates in order to gain a fundamental insight into the interaction of cascades with the microstructural features, including nanoclusters, precipitates, and grain boundaries. The formation and stability of He bubbles, produced by the n, $\alpha$  reaction under neutron irradiation, is important for alloys designed for use in advanced energy production and conversion systems under extreme conditions due to the possibility of He embrittlement. Preliminary characterizations of an NFA implanted with high dose He ions have been performed with a combination of APT, EFTEM, and TEM, and indicate that the nanoclusters are efficient sinks for He-vacancy complexes, and that He bubbles are formed on their surfaces, as well as on grain boundaries and dislocations. Additional He irradiations are planned at different temperatures, doses and dose rates, and post-irradiation thermal treatments to establish the interaction of the He atoms with the microstructural features.

**Support:** Research supported by the Materials Science and Engineering Division and the SHaRE User Facility, both sponsored by the Office of Basic Energy Sciences, U.S. Dept. of Energy.

### References

1. J. H. Schneibel, C. T. Liu, M. K. Miller, M. J. Mills, P. Sarosi, M. Heilmaier, and D. Sturm, Ultrafine-grained nanocluster-strengthened alloys with unusually high creep strength, *Scripta Mater.*, 61 (2009) 793–796.
2. M. K. Miller, D. T. Hoelzer and K. F. Russell, Radiation Response of a 12YWT Nanostructured Ferritic Steel, in Proc. MRS 2009 Fall Meeting, Materials Research Needs to Advance Nuclear Energy, Boston, MA, Nov. 30-Dec. 3, 2009, eds., G. Baldinozzi, K.L. Smith, K. Yasuda, and Y. Zhang, vol. 1215-V06-02.

### Publications

- M. K. Miller, L. Spoor and K. F. Kelton, Detecting Density Variations and Nanovoids, *Ultramicroscopy*, (2011); doi:10.1016/j.ultramic.2011.01.027.
- M. K. Miller and Y. Zhang, Fabrication and Characterization of APT Specimens from High Dose Heavy Ion Irradiated Materials, *Ultramicroscopy*; (2011); doi: 10.1016/j.ultramic.2010.12.036.
- M.K. Miller and C. M. Parish, The Role of Alloying Elements in Nanostructured Ferritic Steels, *Mater. Sci. Tech.*, 27(4) (2011) 729-734.
- M. K. Miller, D. T. Hoelzer and K. F. Russell, Towards Radiation Tolerant Nanostructured Ferritic Alloys, invited, *Mater. Sci. For.*, 654-656 (2010) 23-28.
- A. Certain, K. Field, T. R. Allen, K. Sridharan, M. K. Miller, J. Bentley, J. T. Busby, Response of nanoclusters in a 9Cr ODS steel to 1 dpa, 525 °C proton irradiation, *J. Nucl. Mater.*, 407 (2010) 2-9.
- J. Xu, C. T. Liu, M. K. Miller and H. Chen, Nanocluster-associated Vacancies in Nanocluster-strengthened Ferritic Steel as Seen Via Positron-lifetime Spectroscopy, *Phys. Rev. B*, 79 (2009) 020204-1-4.
- M. K. Miller, C. L. Fu, M. Krmar, D. T. Hoelzer, and C. T. Liu, Vacancies as a Constitutive Element for the Design of Nanocluster-strengthened Ferritic Steels, *Frontiers of Materials Science in China*, 3(1) (2009) 9-14.

## Defect Evolution under Ion Irradiation with Coordinated Modeling

M. A. Kirk<sup>1</sup>, Meimei Li<sup>2</sup>, P. M. Baldo<sup>1</sup>, Donghua Xu<sup>3</sup>, and B. D. Wirth<sup>4</sup>

<sup>1</sup>EMC, Materials Science Division, Argonne National Laboratory, Argonne, IL, USA

<sup>2</sup>Nuclear Engineering Division, Argonne National Laboratory, Argonne, IL, USA

<sup>3</sup>Department of Nuclear Engineering, University of California, Berkeley, CA, USA

<sup>4</sup>Department of Nuclear Engineering, University of Tennessee, Knoxville, TN, USA

### Proposal Title

Radiation Tolerance in Advanced Structural Alloys for Next-generation Nuclear Energy Systems.

### Scientific Challenge and Research Achievement.

It has long been hoped that computer modeling can accurately predict responses in materials over many years of neutron irradiation at elevated temperatures. Although much progress has been achieved in the development of the modeling techniques, experiments involving neutron irradiation to confirm model predictions are relatively few and usually quite difficult with a long turnaround time. To solve this experimental difficulty, we are pursuing a new direction to utilize the IVEM-Tandem Facility at ANL to benchmark computer models for irradiation of materials.

TEM thin foils of molybdenum were irradiated in situ by 1 MeV Kr ions up to ~0.045 dpa at 80°C at three dose rates  $5 \times 10^{-6}$ ,  $5 \times 10^{-5}$ ,  $5 \times 10^{-4}$  dpa/s at the Argonne IVEM-Tandem Facility. The choice of an irradiation temperature of 80°C allowed a direct comparison with existing neutron irradiation data, and allows mobility of interstitial atoms but not vacancies. The low-dose experiments produced visible defect structure in dislocation loops, allowing accurate, quantitative measurements of defect number density and size distribution. Weak beam dark-field plane-view images were used to obtain defect density and size distribution as functions of foil thickness, dose, and dose rate. Diffraction contrast electron tomography was performed to image defect clusters through the foil thickness (Figure 1) and measure their depth distribution [2].

A spatially-dependent cluster dynamic model was developed to explicitly model the damage by 1 MeV Kr ion irradiation in a Mo thin foil with temporal and spatial dependence of defect distribution. The set of quantitative data of visible defects were used to improve and validate the computer model. It was shown that the thin foil thickness is an important variable in determining the defect distribution. This additional spatial dimension allowed direct comparison between the model and experiments of defect structures. The defect loss to the surfaces in an irradiated thin foil was modeled successfully (Figure 2). TEM with in situ ion irradiation of Mo thin foils was also explicitly designed to compare with neutron irradiation data of the identical material that will be used to validate the model developed for thin foils [3].

### Future Work.

New experimental data will be discussed, including the observed sink strength of dislocations, considerably higher fluences of ion irradiation at 80°C, and a unusual defect distribution from ion irradiation of thin foil at 300°C, where both interstitial and vacancies are mobile. Future modeling efforts will be challenged by this new data.

Figure 1. Cross-section view of reconstructed 3D volume showing defect clusters in Mo irradiated at 80°C to  $5 \times 10^{12}$  ions/cm<sup>2</sup> ( $\sim 0.015$  dpa) at an ion flux of  $1.6 \times 10^{11}$  ions/cm<sup>2</sup>/s ( $\sim 5 \times 10^{-4}$  dpa/s) with 1 MeV Kr ions.

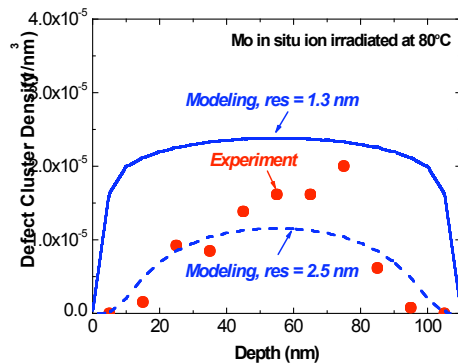
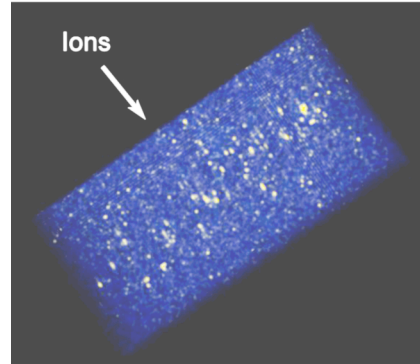


Figure 2. Comparison between *in situ* ion irradiation experiments and the model calculations with two different resolution (“res”) limits, 1.3 nm and 2.5 nm, respectively, of the spatial distribution through the foil thickness of visible defect clusters in Mo irradiated to 0.015 dpa at 80°C. The experimental data include the defects with the size of 2.5 nm and above only.

### Publications

- [1] Meimei Li, M. A. Kirk, P. M. Baldo, Donghua Xu, and B. D. Wirth, submitted to *Philos. Mag.*, 2011.
- [2] M.A. Kirk, M. Li, and P. Baldo, *Microsc. Microanal.* 16 (Supp 2) (2010) 1608.
- [3] The research was sponsored by the U.S. Department of Energy, Office of Nuclear Energy and Office of Sciences, under Contract DE-AC02-06CH11357 with Argonne National Laboratory, operated by UChicago Argonne, LLC. DX and BDW acknowledge support by the U.S. Department of Energy, Office of Fusion Energy Sciences under grant DE-FG02-04GR54750 and the U.S. Department of Energy, Office of Nuclear Engineering under the Nuclear Engineering Research Initiative Consortium Program (NERI-C) Award Number DE-FG07-07ID14894.

## Tracking solute atom additions during phase transformations in a nanocrystalline steel

F.G. Caballero<sup>1</sup> and M.K. Miller<sup>2</sup>

<sup>1</sup> Centro Nacional de Investigaciones Metalúrgicas (CENIM-CSIC), Madrid, Spain

<sup>2</sup> Materials Science and Technology Division, Oak Ridge National Laboratory

**Proposal Title:** “Complementary use of transmission electron microscopy (TEM) and atom probe tomography (APT) for carbide characterization in a nanocrystalline bainitic steels at the early stage of tempering.” SHaRE Project ID: 2011\_CaballeroFG\_45

**Scientific Challenge and Research Achievement:** A novel method for making extremely strong and inexpensive nanocrystalline steel without using severe deformation, rapid heat-treatment, or mechanical processing is under investigation. Furthermore, the material can be produced in a form that is large in all its three dimensions, and has a plethora of other properties useful in engineering design. This new generation of ultrahigh-strength steels with desirable levels of toughness has awakened great interest in the technical and scientific community. For example, with the new generation of nanocrystalline steels, automakers can slash the weight of a vehicle's body structure by as much as 35%. The excellent properties achieved are mainly a consequence of the formation of nano-scale ferrite plates at very low temperatures, temperatures at which iron diffusion during transformation were once inconceivable. In that sense, the microstructure and its characterization at an atomic level represent a scientific milestone.

The purpose of this work is to track atom distributions during phase transformation at low temperatures (200-350°C) in a nanocrystalline steel (Fe-1C-1.5Si-1.9Mn-1.3Cr-0.3Mo (in wt.%); Fe-4.3C-2.8Si-1.8Mn-1.3Cr-0.1Mo in at.%) using atom probe tomography (APT). The characterization of this novel steel at the atomic scale revealed extremely important details of the mechanisms of phase transformation, which have been controversial for the last sixty years in the field of physical metallurgy. Results have demonstrated, for the first time, the carbon supersaturation of the bainitic ferrite at the earlier stage of transformation, providing strong evidence that this transformation is essentially displacive in nature. A carbon atom map with superimposed isoconcentration surfaces obtained from a nanocrystalline steel transformed at 200 °C for 240 h is shown in Fig. 1. The analysis volume in Fig. 1a encompasses a central carbon-enriched ( $10.4 \pm 0.6$  at. % C) austenite film bounded by two ferrite plates ( $<1$  at. % C) and dislocation tangles in the vicinity of a ferrite–austenite interface (at the left of the volume), and a carbon-enriched cluster (at the right of the volume). The proximity histogram across the bainitic ferrite-austenite interface in Fig. 1b demonstrates that none of the substitutional atoms, Si, Cr, and Mn, partitions during transformation, but the partitioning of carbon into the residual austenite occurs immediately after formation.

In addition to carbon partitioning from supersaturated ferrite to austenite, other competing reactions, such as carbon segregation to dislocations and carbon clustering, were activated during ferrite transformation at low temperature. It is evident from the proximity histograms across the dislocations in ferrite, Fig. 1c, that dislocations only trap the carbon atoms ( $13.4 \pm 0.8$  at. % C). The lateral extent of the Cottrell atmosphere was estimated to be  $\sim 5$  nm. Finally, the proximity histogram across the  $\sim 3$ -nm-thick cluster, Fig. 1d, shows a maximum carbon content of  $\sim 15$  at.%, which is higher than that associated with dislocations, but with chromium and manganese contents too low (less than 2 at.%) to be identified as a carbide.

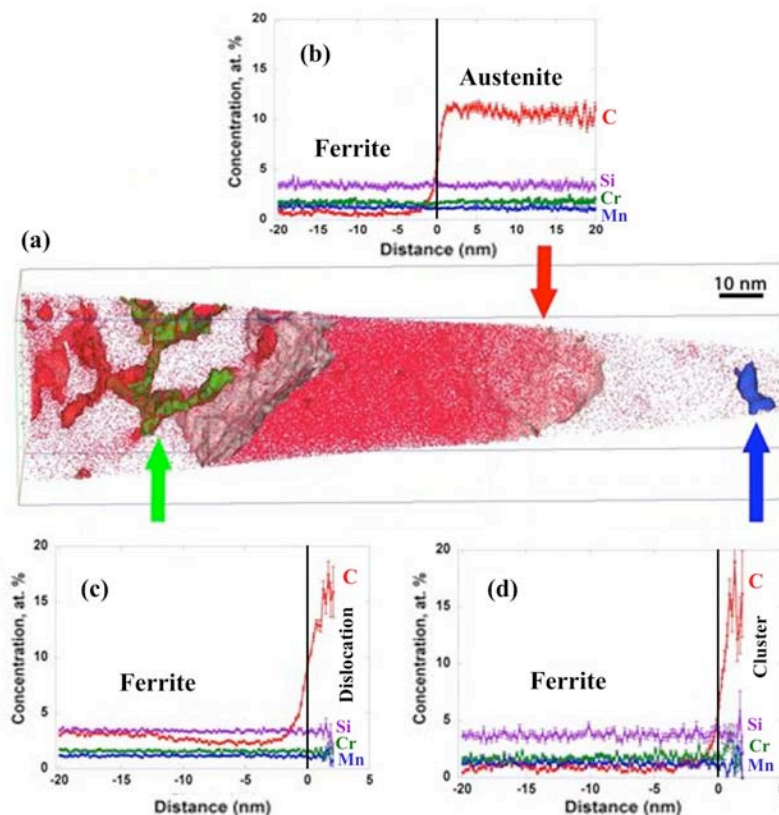


**Figure 1.** (a) Carbon iso-concentration surfaces at 8 at. % C superimposed with the carbon atom map, and proximity histograms across (b) a ferrite/austenite interface, (c) a dislocation network in the vicinity of the ferrite/austenite interface, and (d) a carbon cluster in bainitic ferrite after transformation at 200°C in Fe-1C-1.5Si-1.9Mn-1.3Cr (in wt.%), (Fe-4.3C-2.8Si-1.8Mn-1.3Cr (in at.%)), steel.

**Future Work:** Complementary characterization by TEM and APT will be used to identify the composition and structure of clusters/carbides observed at a stage of tempering prior to precipitation of  $\epsilon$ -carbide in this nanocrystalline steel. Effective complimentary applications of both techniques will provide critical information regarding the formation mechanism of the carbon-rich regions observed during low-temperature tempering (300 and 400°C). Results will confirm whether there is a stage of tempering prior to precipitation of  $\epsilon$ -carbide, in which carbon atoms cluster within the ferrite matrix.

**Support:** Research supported by the SHaRE User Facility, which is sponsored by the Office of Basic Energy Sciences, U.S. Department of Energy.

**Publications:**

F.G. Caballero, M.K. Miller, S.S. Babu, and C. Garcia-Mateo, *Acta Materialia*, Vol. 55, No. 1, 2007, pp 381-390.  
 F.G. Caballero and M. K. Miller, *Microscopy and Microanalysis*, 13 (Suppl 2), 2007, 1640-1641.  
 F.G. Caballero, M.K. Miller, C. Garcia-Mateo, C. Capdevila and S.S. Babu, *Acta Materialia*, vol. 56, No. 2, 2008, 188-199.  
 F.G. Caballero, M.K. Miller and C. Garcia-Mateo, *Journal of Materials Science*, vol. 43, No. 11, 2008, 3769 - 3774.  
 F.G. Caballero, M.K. Miller, C. Garcia-Mateo, C. Capdevila and C. Garcia de Andrés, *JOM*, 2008, Vol. 60, No 12, 16-21.  
 F.G. Caballero, C. Garcia-Mateo, M.J. Santofimia, M.K. Miller and C. García de Andrés, *Acta Materialia*, 2009, vol. 57, No. 1, 2009, 8-17. *Top 25 Hottest Articles for Oct. – Dec. 2008*.  
 F.G. Caballero, M.K. Miller and C. Garcia-Mateo, *Top 25 Hottest Articles for Jan-Mar 2010*.  
 F.G. Caballero, M.K. Miller, A.J. Clarke and C. Garcia-Mateo, *Scripta Materialia*, 2010, Vol. 63, 442-445.  
 F.G. Caballero, M.K. Miller and C. Garcia-Mateo, *Materials Science and Technology*, 2010, Vol. 26, No. 8, 889-898. *Invited Article-MST 25 year perspective*.  
 F.G. Caballero, M.K. Miller and C. Garcia-Mateo, *Metallurgical and Materials Transactions A*, 2011, DOI 10.1007/s11661-011-0699-7.

## **Complementary use of APT and TEM in the study of radiation damage in alloys**

Emmanuelle A. Marquis

Department of Materials Science and Engineering, University of Michigan, Ann Arbor MI

Proposal: Complementary use of APT and TEM for the study of alloy systems

The development of next-generation fission and fusion reactors requires new and improved materials, which will withstand extreme combinations of temperature, stress and irradiation. In order to develop these materials, fundamental understanding is required of the atomic-scale behaviour of candidate alloys subjected to extreme treatment. The combined use of atom probe tomography and transmission electron microscopy provides unique insights into the atomic processes occurring during irradiation. We report progress in the study of microstructural evolution in alloy systems after thermal and heavy ion irradiation treatments. In each case, the materials exhibit highly complex patterns of behaviour on the nanometre scale, including solute clustering, segregation to dislocations, grain boundaries and interphase interfaces, and the formation of second phase particles.

### Grain boundary segregation in ferritic Fe-Cr steels

Ferritic Fe-Cr alloys are the base for structural steels currently considered for Gen IV nuclear plants and future fusion reactors. Among the outstanding issues related to the use of these alloys under irradiation are  $\alpha'$  precipitation (and the uncertainty of the position of the solvus line at low temperatures) and radiation induced segregation (RIS) or depletion (RID) of grain boundaries. These phenomena could indeed significantly affect the properties of these alloys. Past observations have reported grain boundary Cr depletion or segregation without any clear correlation to irradiation conditions (Lu et al. Scripta Mater. 2008). Moreover, common impurities such as carbon are expected to affect the integrity of grain boundaries and modify the extent of radiation induced segregation phenomena. The experimental approach using atomic scale characterization techniques will be described and the effect of irradiation discussed.

Future work includes the direct correlation of APT and TEM concentration profiles obtained from the same grain boundaries as well as high resolution observations of grain boundary structures and defect distribution resulting from irradiation.

### **Publications**

1. A systematic approach for the study of radiation induced segregation/depletion at grain boundaries in steels, E.A. Marquis, R. Hu, T. Rousseau, J. Nuclear Materials (2011)
2. Effects of heavy-ion irradiation on solute segregation to dislocations in oxide-dispersion-strengthened Eurofer 97 steel, C.A. Williams, J. Hyde, G.D.W. Smith, E.A. Marquis J. Nuclear Materials (2011)



## Atomic -scale Z-contrast STEM and EELS investigation of new Lead-free morphotropic phase boundary BiSmFeO<sub>3</sub> thin films.

Ching-Jung Cheng,<sup>1</sup> Albina Y. Borisevich,<sup>2</sup> Daisuke Kan,<sup>3</sup> Ichiro Takeuchi,<sup>3</sup> and Valanoor Nagarajan<sup>1</sup>

<sup>1</sup>School of Materials Science and Engineering, University of New South Wales, New South Wales 2052, Australia

<sup>2</sup>Materials Science and Technology Division, Oak Ridge National Laboratory

<sup>3</sup>Department of Materials Science and Engineering, University of Maryland

**Proposal Title:** “Atomic Scale Z-contrast STEM and EELS Investigation of New Lead-free Morphotropic Phase Boundary BiSmFeO<sub>3</sub> Thin Films.” SHaRE Project ID: 2009\_ValanoorN\_01

**Scientific Challenge and Research Achievement:** Bismuth ferrite or BiFeO<sub>3</sub> (BFO) is one of the most extensively studied multiferroic materials with two robust ferroic phase transitions well above room temperature, i.e. 370°C for the anti-ferromagnetic Neel temperature and 830°C for the ferroelectric (FE) Curie temperature. BFO has a rhombohedral distorted ABO<sub>3</sub> perovskite-type oxide structure (where A and B are cations), with space group R3c, which allows anti-phase oxygen octahedral tilts and cation displacements from the centro-symmetric positions along the [111] pseudo-cubic direction. We previously reported that the A-site substitution of the perovskite BFO with Rare Earth (RE<sup>3+</sup>) ions results in a structural transition from the rhombohedral to an orthorhombic phase, where double hysteresis loops (in polarization-electric field loops) are observed, accompanied by a substantial enhancement of the electromechanical properties at the phase boundary. It was shown that the structural transition and enhanced properties can occur independent of the RE dopant species, and furthermore it can be universally achieved by controlling the average ionic radius of the A-site cation.

RE<sup>3+</sup> doping of the BFO within a critical composition range affects short-range anti-parallel (sideways) interactions between the cations, leading to formation of anti-polar PbZrO<sub>3</sub> (PZO)-like clusters (evidenced by observation of local commensurate  $\frac{1}{4}$  {011} reflections). It has been demonstrated that these anti-polar clusters then grow within a FE matrix with increasing RE<sup>3+</sup> content and at a critical concentration where FE regions are so frustrated by the surrounding anti-polar matrix, it results in an incommensuration phenomenon, where the system adopts a complex nanoscale mixture bridging between Bi-rich rhombohedral and RE-rich orthorhombic phases.

While such studies have helped to delineate the main features of structural evolution in RE-doped BFO, to date there is very little information on the atomic-level (i.e. local) chemical origins of the nascent anti-polar cluster states. Understanding the origins of these clusters is critical as it is these local clusters that are the first visible signatures of order frustration, which ultimately leads to the structural phase transition. Further information on the precise chemical environments of these clusters can help identify solid-state chemistry routes to artificially induced phase transformations potentially common to a wide range of ferroelectric piezoelectric materials.

The focus of this study is thus to elucidate the important features of the anti-polar clusters at the atomic scale and link their local chemical and structural properties to the observed functional properties. We examined 10% Sm-doped BFO (a composition known to display anti-polar clusters) with an array of transmission electron microscopy (TEM) techniques, namely high-resolution transmission electron microscopy (HRTEM) coupled with selected-area electron diffraction (SAED) analysis, aberration-corrected scanning transmission electron microscopy (STEM), and spatially resolved electron energy-loss spectroscopy (EELS), to determine the underpinning structural features of the anti-polar clusters. The structural origins are ultimately linked to the observed ferroelectric properties characterized via polarization-electric field (P-E) hysteresis loops, dielectric constant-electric field ( $\epsilon_{33}$ -E) hysteresis loops, and dielectric loss ( $\tan \delta$ ) measured as a function of temperature. We demonstrate that the anti-polar clusters in the Sm-doped BFO system are a consequence of a destabilized zone center FE polar state. Aberration-corrected STEM images

show direct evidence of the anti-polar displacement order and EELS data reveal significant changes in the Sm chemistry for the clusters in contrast to the surrounding FE matrix. Displacement maps of the cations suggest that the apparent anti-polar order in this system is actually a lamellar array of highly dense ferroelectric domains with alternating polarizations (see Figure 1). Diffraction studies reveal that the anti-polar clusters may have different orientational displacement variants (i.e. structural twins) coupled with in-phase oxygen octahedral tilts. At higher temperatures, cation interactions become much weaker and in favor of unit cell-doubled orthorhombic phase, a similar analogy to the observed room temperature structural transitions for higher  $\text{Sm}^{3+}$  content.

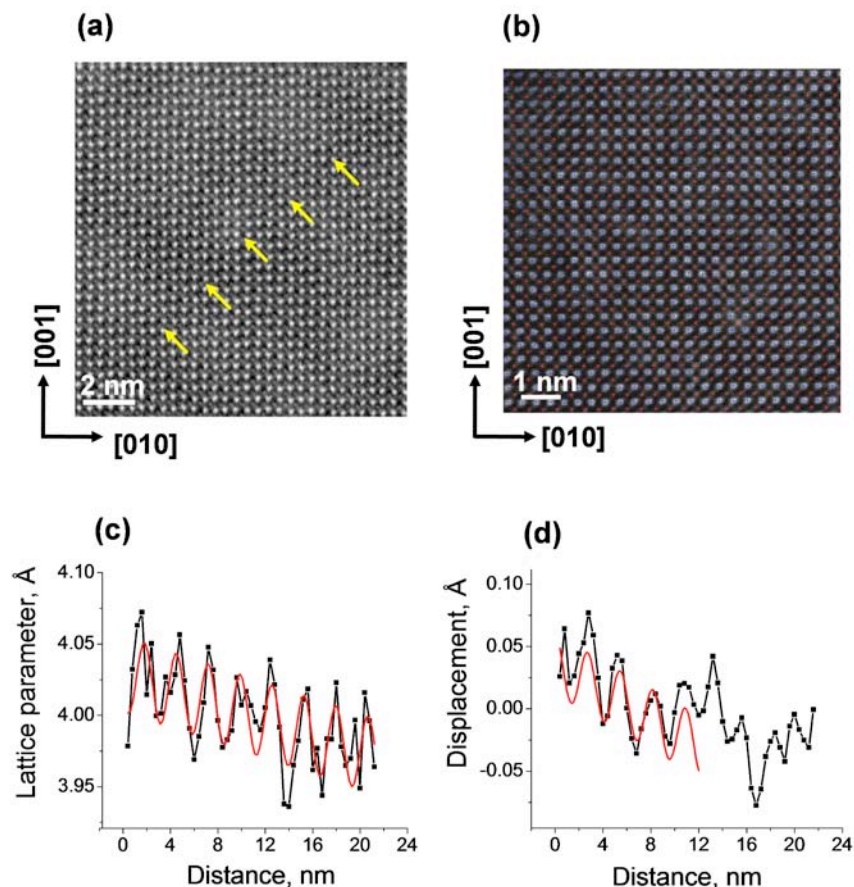


**Figure 1.** [100] zone axis BF-STEM image. The  $\frac{1}{4}$ -related superstructure domain boundaries are marked by arrows; (b) aberration-corrected Z-contrast image of the anti-polar cluster signifying A-site chemical ordering is not taking place. Image used to obtain atomic displacements of Bi (marked with blue plus markers) and Fe (marked with red plus markers) columns; (c) quantified displacements of Bi atoms along the superstructure and (d) quantified displacements of Fe atoms along the superstructure.

**Future Work:** We are developing direct atomically-resolved mapping of structural transformations at the FE-AFE boundary. Particular emphasis is placed on understanding the structural make-up at a phase boundary where competing order parameters exist such that a universal fingerprint composed of bridging phases for other morphotropic FE-FE and AFE-FE systems exist and hence mechanisms driven by competition between the structural and polarization order parameters can be active.

**Support:** Research supported by the SHaRE User Facility, Office of Basic Energy Sciences, U.S. Department of Energy.

#### Publications

C.J. Cheng, A.Y. Borisevich, D. Kan, I. Takeuchi, and V. Nagarajan *Chemistry of Materials* 22 2588-2596 (2010).

# Poster Extended Abstracts



# Poster Group A



## Nanoparticle Composites: From Catalysis to Engineering Biology

T. Rajh, E. Shevchenko, E. Rozhkova, C Fry, P. Podsiadlo, and G. Krylova

Center for Nanoscale Materials, Argonne National Laboratory, 9700 S Cass Ave, Argonne, IL

**Scientific Thrust Area:** Nanoparticle Architectures for Energy and Information Transduction

**Scientific Challenge and Research Achievement:** Important elementary steps in energy relevant processes such as energy conversion, electronics and catalysis, as well as in their biological analogs, require electron exchange within energy gradient structures. The energy and electron flow in these multiphase systems, designed and arranged to direct a specific process, delineates the desired function. In this work we try to understand how deliberate tailoring and assembling of materials on the nanoscale can lead to enhanced functionalities. Our approach to solve this key challenge involves directed synthesis and investigation of hierarchical multicomponent systems composed of nanoparticles.

Nanocrystalline structures offer unique opportunities for tailoring the electronic, mechanical and chemical properties of materials. Mixing of two noble metals or noble metals and metal oxides in a form of dumbbell or core/hollow shell nanoparticles are of a great interest for the application in catalysis. The exchange interaction between two materials in close proximity affects electron density and is dependent on the individual size and mutual geometry of the constituents. We developed a systematic approach to synthesize noble metal dumbbells in controllable way. We found that control over the concentration and oxidation states of ions located within (case of alloyed nanoparticles) or chemisorbed at the surface as seeds determines the efficiency and reproducibility of the formation of dumbbells.

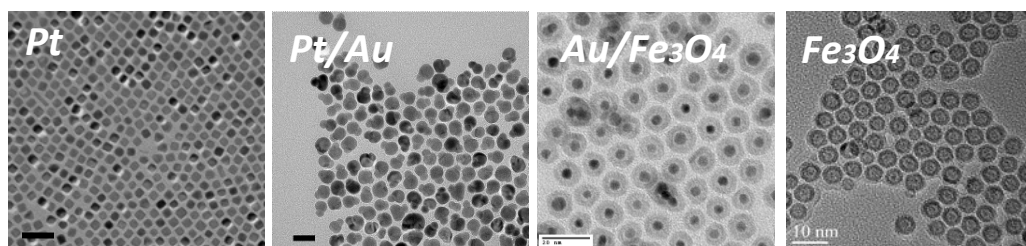


**Figure 1** TEM images of Pt, Pt/Au and Au/hollow  $\text{Fe}_3\text{O}_4$  and hollow  $\text{Fe}_3\text{O}_4$  nanoparticles (from left to right).

In the case of core/hollow shell NPs the oxide shell is expected to be transparent for the gaseous reactants participating in catalytic reaction. Despite the several studies on hollow nanoparticles the content of the hollow shell and the mechanical stability of hollow shells are not well understood. In order to address these questions we performed systematic study using small angle X-Ray scattering and X-ray diffraction techniques on hollow iron oxide and gold/hollow iron oxide nanoparticles of different sizes (Fig. 1). We have found that electron density of the inner cavity in 6 nm hollow NP is negligible, while in the case of larger hollow (~12 nm) and Au/hollow  $\text{Fe}_3\text{O}_4$  NPs the inner cavities are not empty and most likely filled with organic species. These organic “fillers” give opportunity for the development of preferred adsorption therefore fostering selective catalysis.

Catalysis and charge transfer can also be modified by incorporating peptide motifs that can bind to/interact with the surface of metal and/or metal oxide nanoparticles creating nano-bio hybrids capable of biorecognition. Proteins utilize multidomain, hierarchical self-assembly principles to engineer and tune functional systems from a limited number of building blocks, the amino acids. The redox cofactors are often incorporated to activate exogenous substrates (i.e.  $\text{O}_2$ ,  $\text{CO}_2$ ,  $\text{NO}_x$ , etc.) as well as facilitate charge and electron transport. We have designed peptides using well established principles/rules/methods to self assemble into predictable structures such as a multidomain bola-amphiphile or a vesicle-like structure. These structures are also engineered such that a multitude of redox cofactors can be incorporated in order to generate electronic properties and catalytic active sites. Nano-bio hybrids can be successfully interfaced with biological systems, such as a cell, for direct triggering of biochemical pathways via energy or information transduction. Living cells interact with

an environment through complex network of chemical signals. Nano-bio hybrids capable of spatially-controlled application can respond to external stimuli at cell membrane and alter intracellular signaling. For example, ferromagnetic disks can serve as mediators of calcium cell homeostasis and signaling under application of extremely low frequency ac fields (Fig. 2, left). These systems are appealing for wide range of application in life sciences, including gene sequencing and silencing, cell sorting and separation, and advanced medical technologies. Moreover, once these materials are incorporated into engineered artificial systems for example, self-assembled bola-amphiphile peptide vesicles (Fig. 2, right) they can serve as switches or actuators within an entirely artificial membrane system. These synthetic cells can be used to incorporate controlled transmembrane electrochemical gradients, reactants (e.g. mediators, photosynthesizers, cofactors) for stimuli initiated storage and release.

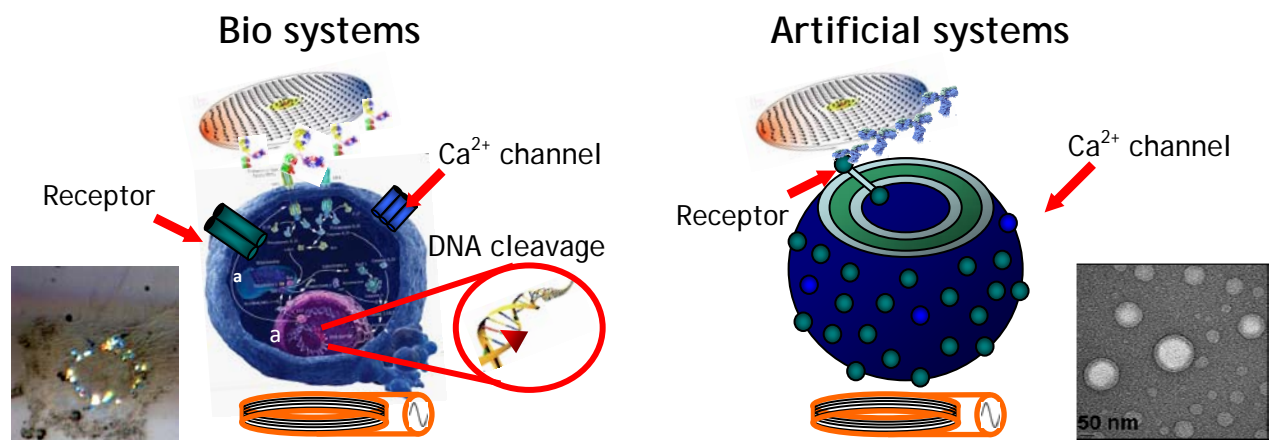


Figure 2. Bio-nano composites within cellular and artificial membrane systems. *Left* : Ferromagnetic disks are capable of signal transduction within cellular machinery upon application of low frequency ac magnetic field. *Right*: De-novo designed synthetic amphiphile peptides self-assemble into a vesicle. Incorporated membrane channel protein for controlling transmembrane electrochemical gradient in an entirely artificial system.

**Future Work:** We will continue to study electronic properties of multicomponent and self assembled hybrid systems and their behavior under external stimuli (electronic, optical and magnetic). The ultimate objective of this work is perfecting charge (energy) conversion and storage concepts in the form of nanoarchitectures that are designed and built-up from the molecular level. The nanoscale architectures will enable: 1) detailed control over morphology that allows for energy gradient optimization, 2) small diffusion lengths of charges, and 3) improved conductivity by bridging different parts of the architectures through conductive bridges designed and built-up from the molecular level.

#### **Related Publications:**

1. Podsiadlo, P. et al., High-Pressure Structural Stability and Elasticity of Supercrystals Self-Assembled from Nanocrystals. *Nano Letters* **2011**, 11, (2), 579-588.
2. Hurst, S. J.; Fry, H. C.; Gosztola, D. J.; Rajh, T., Utilizing Chemical Raman Enhancement: A Route for Metal Oxide Support-Based Biodetection. *J. Phys. Chem. C* **2011**, 115, (3), 620-630.
3. Kim, D. H. et al., Biofunctionalized Magnetic-Vortex Microdiscs for Targeted Cancer-Cell Destruction. *Nature Materials* **2010**, 9, (2), 165-171.
4. Talapin, D. V.; Lee, J. S.; Kovalenko, M. V.; Shevchenko, E. V., Prospects of Colloidal Nanocrystals for Electronic and Optoelectronic Applications. *Chem. Reviews* **2010**, 110, (1), 389-458.
5. Krylova, G.; et al., Probing the Surface of Transition-Metal Nanocrystals by Chemiluminescence. *J. Am. Chem. Soc.* **2010**, 132, (26), 9102-9110.
6. Talapin, D. V.; Shevchenko, E. V.; Bodnarchuk, M. I.; Ye, X. C.; Chen, J.; Murray, C. B., Quasicrystalline Order in Self-Assembled Binary Nanoparticle Superlattices. *Nature* **2009**, 461, (7266), 964-967.
7. Rozhkova, E. A.; Ulasov, I.; Lai, B.; Dimitrijevic, N. M.; Lesniak, M. S.; Rajh, T., A High-Performance Nanobio Photocatalyst for Targeted Brain Cancer Therapy. *Nano Letters* **2009**, 9, (9), 3337-3342.
8. Dimitrijevic, N. M.; Rozhkova, E.; Rajh, T., Dynamics of Localized Charges in Dopamine-Modified TiO<sub>2</sub> and their Effect on the Formation of Reactive Oxygen Species. *J. Am. Chem. Soc.* **2009**, 131, (8), 2893-2899.

# Membrane-based Nanocomposites

**Matt Goertz<sup>\*</sup>, Bruce Bunker<sup>\*</sup>, Gabe Montaña<sup>†</sup>,  
Nikita Goyal<sup>†</sup>, Lauryn Marks<sup>†</sup>**

*Center for Integrated Nanotechnologies*

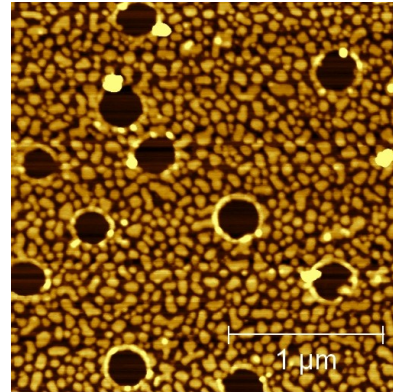
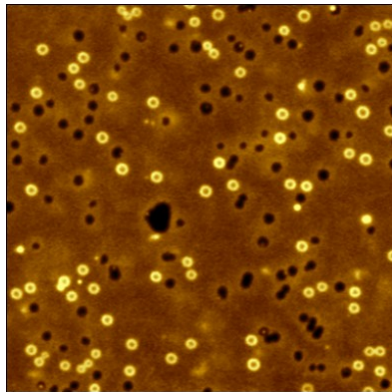
*<sup>\*</sup>Sandia National Laboratories*

*<sup>†</sup>Los Alamos National Laboratories*

*[mgoertz@sandia.gov](mailto:mgoertz@sandia.gov)*

*(505) 844-4785*

*Soft Biological & Composite Nanomaterials Thrust  
Membrane-based Nanocomposite Integrated Focus Area*



Much of the exquisite functionality and emergent behavior that we associate with living systems is derived from the behavior of nanomaterials inserted into the lipid bilayers that comprise cellular membranes. We are interested in understanding how to replicate the assembly and functionality of such membranes within artificial composites involving nanoparticles and supermolecular assemblies. In this poster, I will present recent work exploring the fundamental interactions between nanoparticles and solid-supported membranes with the goal of creating responsive nanocomposite films. Using a combination of optical microscopy methods, the atomic force microscope, and the interfacial force microscope, we attempt to develop a set of design rules to predict the behavior of such nanocomposites based on manipulations of intermolecular forces. Conditions leading to adsorption, insertion, aggregation, and the formation of macroscopic assemblies of nanoparticles within lipid/polymer bilayer hosts will be described.

In a concerted effort, we are also interested in using amphiphilic block copolymers as synthetic analogues of lipids to create membrane-based nanocomposite materials. While there is a wealth of knowledge available on vesicles made from amphiphilic polymers, very little is known about supported thin films made from the same materials. Through an exhaustive microscopy effort we have characterized topography, lateral diffusivity, thickness, and mechanical properties of membranes made by fusion of polymer vesicles to solid supports. Initial results show significant differences in membrane properties of bilayer vesicles versus solid-supported films.

Images depict pH induced manipulation of a lipid bilayer (left) and membrane bound nanoparticles (right).

Related Publications:

Goertz, M.P.; Goyal, N.; Bunker, B.C.; Montano, G.A. **Substrate Effects on Electrostatic Binding of Nanoparticles to Lipid Bilayers.** *J. Colloid & Interf. Sci. B* (2011) doi:10.1016/j.jcis.2011.02.063

Goertz, M.P.; Goyal, N.; Bunker, B.C.; Montano, G.A. **Lipid Bilayer Reorganization Under Extreme pH Conditions.** *Langmuir* (2011) DOI: 10.1021/la2001305

Goertz, M.P.; Stottrup, B.L.; Houston, J. E.; Zhu, X.-Y. **Nanomechanical Contrasts of Gel and Fluid Phase Supported Lipid Bilayers.** *J. Phys. Chem. B* (2009), 113 (27), 9335–9339.

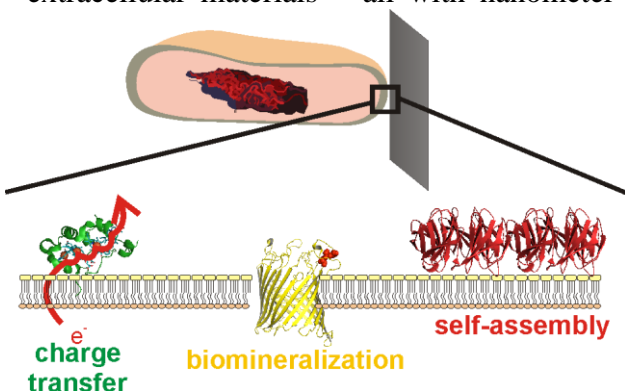
## Interfacing Living Cells and Inorganic Materials on the Nanoscale

Heather Jensen<sup>2,4</sup>, Jenny Cappuccio<sup>3</sup>, Behzad Rad<sup>1</sup>, Cheryl Goldbeck<sup>1</sup>, Mark Kokish<sup>2</sup>, Eldon Chou<sup>1</sup>, and Caroline M. Ajo-Franklin<sup>1,2</sup>

<sup>1</sup>The Molecular Foundry, Materials Sciences Division, <sup>2</sup>Physical Biosciences Division, and <sup>3</sup>Earth Sciences Division, Lawrence Berkeley National Laboratory and <sup>4</sup>Department of Chemistry, University of California, Berkeley

**Scientific Thrust Areas:** Nanointerfaces

**Scientific Challenge and Research Achievement:** The research mission of my laboratory is to explore and engineer functional interfaces between living cells and synthetic materials at the nanoscale (Fig. 1). By directly interfacing living organisms with synthetic materials, we can harness the vast capabilities of life in photo- and chemical energy conversion, chemical and material synthesis, and self-assembly and repair. Yet to accomplish this, we must control the arrangement of biomolecules at the cell's exterior and their interactions with extracellular materials – all with nanometer precision. Recognizing that many organisms have evolved to



interact with the hard materials that are part of their environment, my research group has chosen a unique approach to control this interface. We identify strategies organisms use to interact with inorganic materials and then co-opt these strategies in cells of our choosing using genetic engineering. By using this method, we ultimately seek to exert such control over processes at the cellular-inorganic surface that our engineered cells become self-replicating ‘living materials’ that are programmable at the nanoscale.

**Figure 1.** My research focuses on understanding and manipulating processes that occur at the nanointerface between living cells and inorganic materials.

### *Electronic Communication between Living Cells & Inorganic Materials:*

One of our long-term goals is to develop general methods to permit bi-directional electron flow between biological cells and inorganic materials. Creating an interface that permits electronic communication between living and non-living systems would enable new opportunities in fields such as biosensing, bioenergy, and cellular engineering. While existing technologies can transfer electrons from a cell to an electrode, no single approach has achieved what the next generation applications require: molecularly-defined electron flow across a variety of cell types.

Our work explores a radically different, biological-focused approach: to genetically introduce a new electron transfer pathway which routes electrons along a well-defined path from the cell interior to an extracellular inorganic material (Fig. 2A). This strategy specifically takes advantage of the natural electron pathway of *Shewanella oneidensis* MR-1, which has evolved to interact with and reduce a variety of solid metal oxides. As a first test of our genetic approach, we transferred three genes from the electron transfer pathway of *S. oneidensis* MR-1 into the model microbe *Escherichia coli*. These proteins are functionally expressed, are redox active, and accelerate reduction of soluble Fe(III) species in *E. coli*. Most importantly, we have shown that these genes ‘wire up’ *E. coli* to inorganic solids, i.e. they confer the ability to reduce solid  $\alpha$ -Fe<sub>2</sub>O<sub>3</sub> (Fig. 2B, C). Thus, this work provides the first example of a predetermined, molecularly-defined route for electronic communication between living cells to inorganic materials<sup>1</sup>. An additional unique advantage of our system is the ease of forming the bioelectronic connections; the living bacteria make the electron conduit and pass electrons to inorganic materials without any human intervention.

### Assembly of Inorganic Materials by Microbial Surfaces:

A second long-term goal in my group is to develop general methods to enable cells to create and assemble nanopatterned inorganic materials. Organisms in every domain of life assemble, re-model, and etch away inorganic materials with control over multiple length scales. The ability to harness this control over mineral growth would be a tremendous boost for carbon sequestration, materials synthesis and engineering applications.

To better understand how naturally-occurring microbial communities in the environment may affect mineralization of  $\text{CO}_3$  into carbonates, we exposed several different bacterial species to solutions that would favor a gradual precipitation of  $\text{CaCO}_3(\text{s})$  and used optical microscopy to monitor the presence of different phases of  $\text{CaCO}_3$  in these solutions. We find that microbes from a variety of environments all accelerate the rate at which calcite forms. Interestingly, this increase in mineralization occurs whether the microbes are living or dead. We propose that the rate increase stems from the ability of microbial surfaces enhance the nucleation of  $\text{CaCO}_3$  by binding  $\text{Ca}^{2+}$  at their cell surface. The passive nature of this mechanism means that microbes, whether living or dead, will have a profound impact on the rate at which carbonate minerals form in sequestration environments, and provides a deeper understanding of the multi-faceted ways in which microbes affect global carbon cycling.

### Future Work:

*Electronic Communication between Living Cells & Inorganic Materials:* Our short term goals in the project are: i) to demonstrate current flow from our engineered *E. coli* to an electrode and ii) to improve electron transfer by improving the design of our synthetic gene. If successful, this work will establish the first ever self-replicating, self-healing electronic connection between cells and technological devices and begin to make this process efficient enough to enable robust current flow.

*Assembly of Inorganic Materials by Microbial Surfaces:* On-going work is focused on investigating the molecular mechanisms underlying this increase in nucleation rate through a series of mutants which have well-defined changes in surface chemistry. This future research will provide one of the first quantitative and systematic studies identifying how nanoscale features on microbial surfaces affect mineralization rates and the underlying mechanisms behind these changes.

### Publications:

“Engineering of a synthetic electron conduit in living cells.” H. M. Jensen, A. E. Albers, K. Malley, Y. Y. Londer, B. E. Cohen, B. A. Helms, P. Weigele, J. T. Groves, C. M. Ajo-Franklin, *Proc. Natl. Acad. Sci. USA*, (2010).

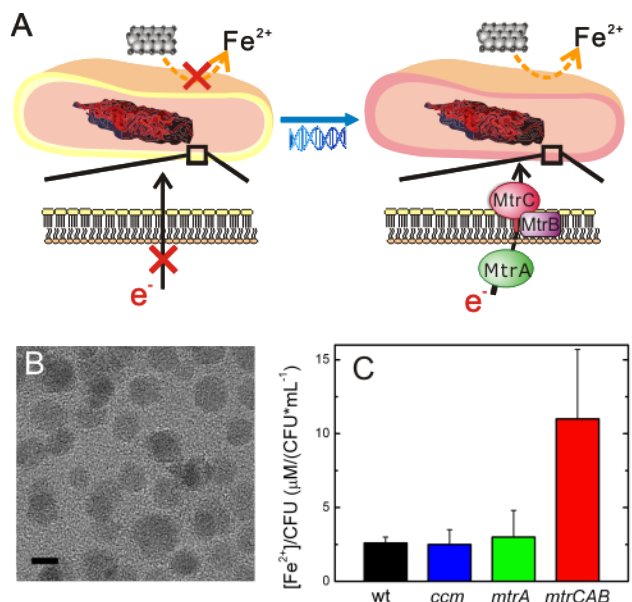


Figure 2. Engineering an electron conduit in living cells. A) Schematic of our genetic approach to create an electron pathway across cell membranes. B) Transmission electron micrograph of synthesized  $\text{Fe}_2\text{O}_3$  nanoparticles. C) Reduction of nanocrystalline  $\text{Fe}_2\text{O}_3$  by engineered *E. coli*.

**A novel adenoviral vector labeled with superparamagnetic iron oxide nanoparticles for real-time tracking of viral delivery**

Jonathan Yun<sup>1</sup>, Adam M Sonabend<sup>1</sup>, Ilya V Ulasov<sup>2</sup>, Dong-Hyun Kim<sup>3</sup>, , Valenty Novosad<sup>3</sup>, Stephen Dashnaw<sup>1</sup>, Truman Brown<sup>1</sup>, Peter Canoll<sup>1</sup>, Jeffrey Bruce<sup>1</sup>, Elena A. Rozhkova<sup>4</sup> and Maciej S. Lesniak<sup>2</sup>.

<sup>1</sup>Gabriele Bartoli Brain Tumor Laboratory, Departments of Neurosurgery, Pathology and Cell Biology, Irving Research Cancer Center, Columbia University Medical Center; <sup>2</sup>Brain Tumor Center, Division of Neurosurgery, the University of Chicago; <sup>3</sup>Argonne National Laboratory, Materials Science Division; <sup>4</sup>Argonne National Laboratory, Center for Nanoscale Materials.

**Scientific Thrust Area:**

Viral-mediated gene therapy for glioblastoma (GBM) has been limited by the inability to monitor intracranial biodistribution. Capsid modifications exist that can target tumor-specific receptors, Ad5/3 cRGD being one of such vectors. We assessed the infectivity of Ad5/3 cRGD-GFP in human glioma cell lines, and have labeled this virus with a Fe<sub>3</sub>O<sub>4</sub> super paramagnetic nanoparticle to track its distribution by MRI.

**Scientific Challenge and Research Achievement:**

*Introduction:*

Although the selectivity of adenoviral-based gene therapy for malignant gliomas can be enhanced by capsid modifications, its clinical application has been limited by the inability to monitor its biodistribution. We assessed the infectivity of Ad5/3 cRGD-GFP in human glioma and normal cell lines and have labeled the virus with a Fe<sub>3</sub>O<sub>4</sub> superparamagnetic iron oxide nanoparticle (SPION) to assess its detectability on MRI.

*Methods:*

The labeled adenovirus was assessed by electron microscopy. U87 glioma and normal human astrocyte (NHA) cell lines were infected with Ad5/3 cRGD-GFP +/- nanoparticles at 1x10<sup>5</sup> vp/cell. Fluorescent microscopy and flow cytometry were performed 48h post infection. Serial dilutions of free SPION were suspended in 0.5% agarose and imaged with a 3T MRI. An in vivo study was performed by intracranial injection of 1x10<sup>9</sup> nanoparticle labeled Ad-5/3 cRGD-GFP in 0.5ml PBS into the subcortical white matter of a non-tumor bearing pig. This was compared using 3T MRI to a contralateral PBS injection over 72 hours.

*Results:*

GFP expression by Ad5/3 cRGD-GFP was significantly higher in U87 glioma cells (26.5%) compared to NHA (11.2%) by flow cytometry. Further, SPION labeled adenovirus retained the ability for transgene expression of GFP similar to unlabeled virus. Imaging of the nanoparticles in serial dilution yielded a concentration related change in intensity using a T2 sequence. The in vivo MRI characteristics post-injection included a T2 hyperintensity and a T2-gradient echo hypointensity at the site of injection, which was not seen on the PBS-only injected side.

*Conclusion:*

We describe a glioma-targeting adenoviral vector (Ad5/3 cRGD) that is labeled with a Fe<sub>3</sub>O<sub>4</sub> nanoparticle. The labeling process does not affect the transduction efficiency of the vector. Further, such coating allows the *in vitro* and *in vivo* detection of this vector by MRI.

**Future Work:**

The current work represents a technological advancement that might provide an insight into the biodistribution of gene therapy vectors upon intracranial injection, an essential step for the optimization of gene therapy delivery into the brain. By demonstrating the detectability of the labeled vector with no affect on transduction efficiency, we are now able to employ various methods of delivery to enhance the distribution of the viral vectors for therapeutic purposes.

**Acknowledgments.**

Use of the Center for Nanoscale Materials was supported by the U. S. Department of Energy, Office of Science, Office of Basic Energy Sciences, under Contract No. DE-AC02-06CH11357.

**References:**

1. Szerlip NJ, Walbridge S, Yang L, Morrison PF, Degen JW, Jarrell ST, et al. Real-time imaging of convection-enhanced delivery of viruses and virus-sized particles. *J Neurosurg.* 2007 Sep;107(3):560-7.
2. Tyler MA, Ulasov IV, Borovjagin A, Sonabend AM, Khramtsov A, Han Y, et al. Enhanced transduction of malignant glioma with a double targeted Ad5/3-RGD fiber-modified adenovirus. *Mol Cancer Ther.* 2006 Sep;5(9):2408-16.
3. Lang FF, Bruner JM, Fuller GN, Aldape K, Prados MD, Chang S, et al. Phase I trial of adenovirus-mediated p53 gene therapy for recurrent glioma: biological and clinical results. *J Clin Oncol.* 2003 Jul 1;21(13):2508-18.
4. Li D, Duan L, Freimuth P, O'Malley BW, Jr. Variability of adenovirus receptor density influences gene transfer efficiency and therapeutic response in head and neck cancer. *Clin Cancer Res.* 1999 Dec;5(12):4175-81.
5. Sun S, Zeng H, Robinson DB, Raoux S, Rice PM, Wang SX, et al. Monodisperse MFe<sub>2</sub>O<sub>4</sub> (M = Fe, Co, Mn) nanoparticles. *J Am Chem Soc.* 2004 Jan 14;126(1):273-9.

## Mimicking Biological Membrane Function: Lipid Membrane Architectures Supported on Nanoporous Metal Films

Gautam Gupta, John K. Baldwin, Amit Misra and Andrew M. Dattelbaum

Center for Integrated Nanotechnologies, Los Alamos National Laboratory, Los Alamos New Mexico 87545

**Scientific Thrust Area:** The Soft, Biological and Composite Nanomaterials Thrust at the Center for Integrated Nanotechnologies (CINT) carries out activities that involve solution-based “bottom-up” materials synthesis, processing, characterization and integration. The work described here involves integrating soft materials, i.e., lipid membranes, with hard surfaces, i.e., nanoporous metals. This work supports two main goals of this CINT thrust area, including 1) Controlling interfaces and interactions between disparate classes of materials across multiple length scales and 2) Exploring the roles of disorder and dynamics in controlling the performance of functional soft, biological and composite materials.

**Scientific Challenge and Research Achievement:** Black lipid membranes,<sup>1</sup> liposomes,<sup>2</sup> and solid supported membrane<sup>3,4</sup> are common model lipid systems used to mimic cell membranes, as well as study transmembrane proteins. Of all these model systems, solid supported membranes exhibit the greatest stability for potentially longer term studies on transmembrane proteins embedded within membranes.<sup>5</sup> However, the thin cushion of water (less than a nanometer) between the supported lipid membrane and the substrate generally precludes the incorporation of functional transmembrane proteins with extra-membrane components, which can interact with the supporting surface resulting in loss of protein function.<sup>3</sup> Use of a porous substrate may minimize these denaturing interactions by providing an aqueous pocket for the extra-membrane piece to reside. Further, supported lipid membranes should be fluid in two dimensions and resistive to ion transport to study some important protein functions. Explicit demonstration of fluidity and resistivity of supported lipid membranes has not been shown.

Here we present a new class of supported lipid membranes on nanoporous gold that are both fluid and electrically resistive, which are two of the primary functions of naturally occurring lipid membranes. We make use of several techniques, including imaging fluorescence microscopy and electrochemical impedance spectroscopy, to characterize the supported lipid membranes. Development of fluid lipid membranes on conducting supports is broadly applicable for studying transmembrane protein function and may be potentially useful for new device applications.

Nanoporous metals have received significant attention over the last decade due to their unusually high surface area per unit volume, exceptional mechanical strength, and ease of synthesis.<sup>6-10</sup> However, due to the

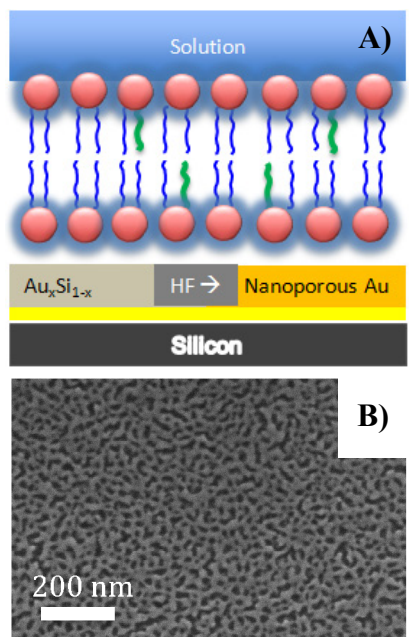


Fig. 1. (A) Formation of lipid bilayers on nanoporous gold. (B) SEM image of nanoporous gold.

fragile nature and non-uniform pore size distribution of the nanoporous Au films the goal to support lipids membranes has not been realized. We have developed a new procedure to synthesize exceptionally uniform nanoporous gold and platinum electrodes by dealloying a co-deposited Metal-Si thin film. Specifically, we developed a two-step etching process that prevents pitting and cracking, which are generally present in a typically used electrochemical etching process, during nanoporous metal preparation. An SEM image of a nanoporous Au film with pore sizes ranging from 10-20 nm is shown in Figure 1B. This process yields exceptional properties of the nanoporous gold including porosity, conductivity and stability.

We have also developed a simple technique to form fluid, stable and resistive bilayers on the nanoporous metal substrates. We note that the etching process is critical in formation of uniform pore-spanning lipid membranes over the nanoporous substrate. We used a mixture of thiol and phosphatidylcholine terminated lipids to prepare vesicles that were fused onto the nanoporous metal surface. The thiol-terminated lipids, which have a high affinity for noble metals surfaces,<sup>11,12</sup> were instrumental in forming a fluid and resistive membrane. Fluorescence recovery after photo-bleaching (FRAP) measurements were performed to demonstrate fluidity of the lipid membranes supported on nanoporous gold. Typical FRAP data are shown in Figure 2A. From these data we calculated a diffusion constant of  $0.25 \mu\text{m}^2/\text{s}$  at room temperature. Electrochemical Impedance Spectroscopy was used to study the resistivity of the supported membranes. As shown in Figure 2B, a significant increase in impedance was observed after membrane formation. The data were modeled using a R(RC)(RC) circuit diagram in a Zview software package.

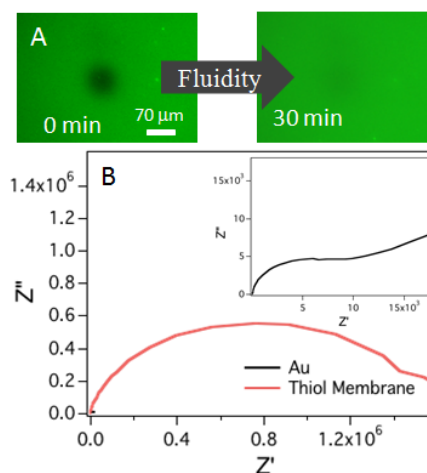


Fig.2 (A) FRAP images of thiolated lipid bilayers at 0 min and after 30 min. (B) Nyquist plot of nanoporous Au before and after thiolated lipid bilayer. Inset show the plot for the bare nanoporous Au surface.

**Future Work:** Further experiments will be performed to incorporate transmembrane proteins in the resulting lipid bilayers on various nanoporous metal substrates, e.g., gold and platinum. We plan to use gramicidin and bacteriorhodopsin as model systems.

## References:

- (1) Boheim, G. *Journal of Membrane Biology* **1974**, *19*, 277.
- (2) Bangham, A. D.; Standish, M. M.; Watkins, J. C. *Journal of Molecular Biology* **1965**, *13*, 238.
- (3) Castellana, E. T.; Cremer, P. S. *Surface Science Reports* **2006**, *61*, 429.
- (4) Jass, J.; Tjarnhage, T.; Puu, G. *Biophysical Journal* **2000**, *79*, 3153.
- (5) Wagner, M. L.; Tamm, L. K. *Biophysical Journal* **2000**, *79*, 1400.
- (6) Erlebacher, J.; Aziz, M. J.; Karma, A.; Dimitrov, N.; Sieradzki, K. *Nature* **2001**, *410*, 450.
- (7) Hakamada, M.; Mabuchi, M. *Scr. Mater.* **2007**, *56*, 1003.
- (8) Mathur, A.; Erlebacher, J. *Appl. Phys. Lett.* **2007**, *90*, 61910.
- (9) Jia, F. L.; Yu, C. F.; Deng, K. J.; Zhang, L. Z. *J Phys Chem C* **2007**, *111*, 8424.
- (10) Erlebacher, J.; Sieradzki, K. *Scr. Mater.* **2003**, *49*, 991.
- (11) Plant, A. L.; Gueguetchkeri, M.; Yap, W. *Biophysical Journal* **1994**, *67*, 1126.
- (12) Steinem, C.; Janshoff, A.; Ulrich, W. P.; Sieber, M.; Galla, H. J. *Biochimica Et Biophysica Acta-Biomembranes* **1996**, *1279*, 169.

## Tip functionalization of silicon probes to study inner ear mechanics

*K. Domenica Karavitaki*

Department of Neurobiology, Harvard Medical School, Boston, MA 02115

*Kamil Godula*

Department of Chemistry, University of California and The Molecular Foundry, Lawrence Berkeley National Laboratory, Berkeley, CA 94720

*Carolyn R. Bertozzi*

Department of Chemistry and Molecular and Cell Biology and Howard Hughes Medical Institute, University of California and The Molecular Foundry, Lawrence Berkeley National Laboratory, Berkeley, CA 94720

*David P. Corey*

Department of Neurobiology and Howard Hughes Medical Institute, Harvard Medical School, Boston, MA 02115

**Proposal Title:** Tip functionalization of silicon probes to study inner ear mechanics

### Scientific Challenge and Research Achievement:

Sound is a mechanical stimulus which is detected by about 40,000 specialized mechanosensory receptor cells of the inner ear. These hair cells have a bundle of 50-100 rod-like stereocilia which is vibrated by sound; the vibration is detected with force-gated ion channels located near the tips of stereocilia, which can open and close in microseconds. Work in the compact hair bundles from lower vertebrates (e.g. Karavitaki and Corey, 2010) indicates that these ion channels are mechanically in parallel, which has important implications for interpreting physiological data. However this may not hold true for the more distributed array of stereocilia in mammalian cochlear hair cells

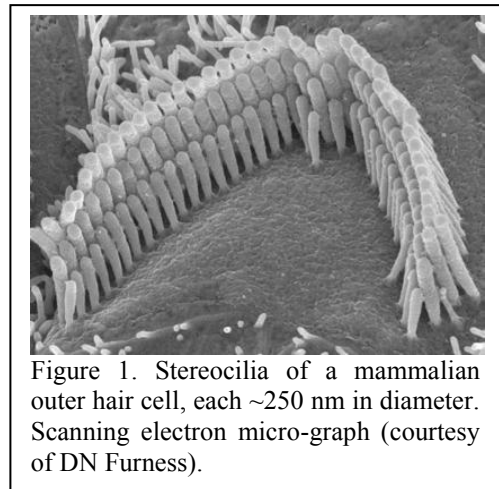


Figure 1. Stereocilia of a mammalian outer hair cell, each ~250 nm in diameter. Scanning electron micro-graph (courtesy of DN Furness).

(Figure 1). In addition, most cochlear cells not only respond to sound, but also mechanically amplify the vibration of quiet sounds to enhance sensitivity and to create extremely sharp frequency tuning. Yet the exact mechanical measurements needed both to test the parallel mechanics of auditory stereocilia and to explore the mechanical correlates of amplification require better coupling of stimulus probes to the stereocilia than currently exists. Specifically, it is difficult to simultaneously stimulate all the tallest stereocilia, which are each just 3 $\mu$ m in length and distributed in an extended V shape (Figure 1). We propose to exploit semiconductor-etch technology to microfabricate a V-shaped stimulus probe that would fit tightly the profile of the tallest stereociliary row. The specific aim of this project was to coat the silicon surface of these probes with lectins that would adhere to the glycocalyx of the stereociliary membrane.

The original protocol of Godula et al., 2009, was modified to synthesize glycopolymers which can be covalently arrayed onto azide-functionalized silicon surfaces and which bind to lectins in a ligand-specific manner. The methodology was first tested on silicon wafers. The wafers were first cleaned and oxidized and immediately placed in toluene solution of (3-azidopropyl)trimethoxy silane and heated for 18-24 hours. The wafers were then washed with dry toluene and methanol and dried in a stream of nitrogen. They were then incubated in a 1X Sea Block blocker solution for 2 hours, to prevent non-specific binding between the glycopolymer and the silicon surface. The fluorescently labeled glycopolymer (product  $\alpha$ -P4 in Godula et al., 2009) was then dissolved in aqueous sodium ascorbate, tris[(1-benzyl-1H-1,2,3-triazol-4-yl)methyl]amine in DMSO, and aqueous  $\text{CuSO}_4 \cdot 5\text{H}_2\text{O}$ . The resulting mixture was vortexed and a drop of the solution was placed for  $\sim 1$  hour on the azide-functionalized silicon surface. The wafers were then washed with distilled water and dried in a stream of nitrogen. In the presence of the copper catalyst ( $\text{CuSO}_4 \cdot 5\text{H}_2\text{O}$ ) the glycopolymers react with the azide-treated silicon surface in a covalent way to form stable triazol linkages. The resulting drop-like patterns of the Alexa-488 fluorescent polymer  $\alpha$ -P4 were directly observed using a fluorescence microscope. Fluorescence was not detected in the absence of the copper. We then tested the interaction between the glycopolymer and soybean agglutinin (SBA), a glycan-binding protein that binds the surface of mouse stereocilia. The lectin was also fluorescently labeled with Cy5 and thus we were able to compare the binding of the polymer and the lectin. SBA was not detected in the absence of the catalyst, indicating specific binding to the glycopolymer. The same protocol was repeated on the polysilicon wafers that had the V-shaped probes. Increased fluorescence was seen on the outer edges of the probes coated with the glycopolymer (as above) indicating binding of the glycopolymer.

**Future Work:** The glycopolymer synthesis will be modified to allow binding of a wider variety of lectins that might be more effective in the binding of the silicon probe to the stereociliary membrane. The probes developed in this project will be used to stimulate the hair bundles of mammalian inner ear hair cells. Such experiments have two goals: First, we wish to understand how the individual stereocilia move together so that we can generate quantitative biophysical models for how hearing works in the kilohertz range. Second, we will use these probes to identify the links that permit stereocilia to slide against each other while keeping them together. Mutation of similar links is known to cause inherited deafness in mice and humans.

**References:**

Karavitaki, K.D. and Corey, D.P. (2010) Sliding adhesion confers coherent motion to hair cell stereocilia and parallel gating to transduction channels. *J. Neuroscience* 30: 9051-9063 (featured on the cover)

Godula, K., Rabuka, D., Nam, K.T. and Bertozzi C. R. (2009) Synthesis and microcontact printing of dual end-functionalized mucin-like glycopolymers for microarray applications. *Angew. Chem. Int. Ed.* 48:4973-4976.

**Publications:** N/A

## Effects of aggregation on the properties of oligomers used for organic LEDs

L. A. Peteanu<sup>1</sup>, G. A. Sherwood<sup>1</sup>, T. M. Smith<sup>2</sup>, J. Wildeman<sup>3</sup>, J. H. Werner<sup>4</sup>, and A. P. Shreve<sup>4</sup>, M. Sfeir<sup>5</sup>

<sup>1</sup> Department of Chemistry, Carnegie Mellon University, 4400 Fifth Avenue Pittsburgh PA 15213

<sup>2</sup> Department of Chemistry, Biology and Environmental Science Christopher Newport University, Newport News, VA 23606

<sup>3</sup> Zernike Institute of Advanced Materials Nijenborgh 49747 AG Groningen, The Netherlands

<sup>4</sup> Materials Physics and Applications Division and Center for Integrated Nanotechnologies, Los Alamos National Laboratories, Los Alamos, NM 87544

<sup>5</sup> Center for Functional Nanomaterials, Brookhaven National Laboratories, Upton, NY 11973

### Scientific Challenge and Research Achievement

Recently, there has been an upsurge in applications using fluorescent conjugated polymers such as MEH-PPV in areas ranging from display technologies to sensitive analytical detection. Likewise, MEH-PPVs, CN-PPVs, and polythiophenes are promising materials currently being used in organic photovoltaic devices. Optimization for these and future uses requires understanding morphology and how it affects emission and charge migration. A detailed analysis of the interactions that lead to aggregate-induced fluorescence quenching in conjugated polymers is challenging due to the heterogeneity of their structures and the possibility of having both aggregated and un-aggregated regions present on a single chain. This has driven an effort to analyze the effects of chain-chain interactions on the emission spectra *via* a detailed study of short-chain oligomers and their aggregates formed in solution by ‘poisoning’ a solution of the oligomers in a good solvent, such as methyl tetrahydrofuran (MeTHF), with a small amount of methanol. An example of an oligomer used to model MEH-PPV is shown in Figure 1a. The aggregates formed *via* this method are in the size range 100-1000 nm and exhibit remarkably uniform and reproducible spectral properties making detailed analysis possible. The effects of aggregation on the intensity and vibronic structure of the emission vary reproducibly with the oligomer chain length and with the aggregate size as determined by dynamic light scattering (DLS).[1]

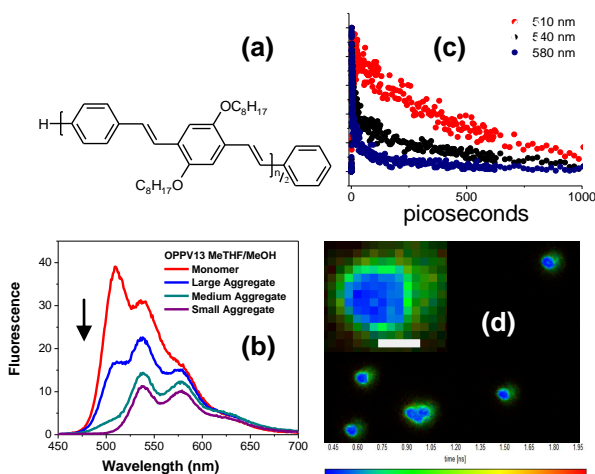


**Fig. 1** (a) Repeat unit of OPPV oligomers,  $n=4-12$  (b) Emission spectra of OPPV13 oligomer monomer (red) and aggregates. The arrow shows the trend in the 0-0 band intensity (510 nm) as a function of decreasing aggregate size and increasing methanol percentage. (c) Ultrafast fluorescence decay of OPPV13 aggregates as a function of collection wavelength. (d) FLIM microscopy images of OPPV13 aggregates. Inset shows detail and 500 nm scale bar. The image is coded by a rainbow scale in which blue corresponds to lifetimes in the range 0.2-0.55 ns and green corresponds to the range 0.6-1 ns.

Decreasing the ratio of good to poor solvent decreases the size of the aggregates formed. In their emission spectra, the intensity of the 510 nm band relative to that of the vibronic replicates decreases concomitantly (Fig. 1b). These spectral variations are strikingly similar to those observed in MEH-

PPV itself as a function of its degree of aggregation. As the 510 nm band is coincident with the electronic origin of the free monomer (red trace, Fig 1b), its intensity is diagnostic of the presence of unaggregated or weakly aggregated chains in the preparation. This assignment is confirmed *via* fluorescence lifetime studies on the bulk aggregate samples (Fig. 1c) which show that the lifetime of the emission at 510 nm is similar to that of the monomer ( $\sim 600$  ps) while that of the longer wavelength bands is significantly shorter (Fig. 1c). The rapid decay of the emission at 540 and 580 nm indicates that it arises predominantly from aggregated chains and is consistent with their lower emission yield relative to the isolated chains.

On the basis of these results, we proposed that the OPPV aggregates are best described as a “core-shell” structure in which monomer-like chains surround a core of tightly packed (highly aggregated) chains.[1] Direct experimental evidence for this model was obtained *via* fluorescence lifetime imaging (FLIM) of the aggregates performed at CINT.[5] The spatial distribution (Fig. 1d) of the short- and long-lived emitters at the center and at the surface of the aggregates, respectively, is consistent with the proposed “core-shell” model. In addition, images obtained as a function of distance from the slide surface (Fig. 2) show an increasing percentage of long lived monomer-like chains as the focus moves from the center of the aggregates (Fig. 2a) to their outer surface (Fig. 2c) as would be expected for the proposed “core-shell” structure.

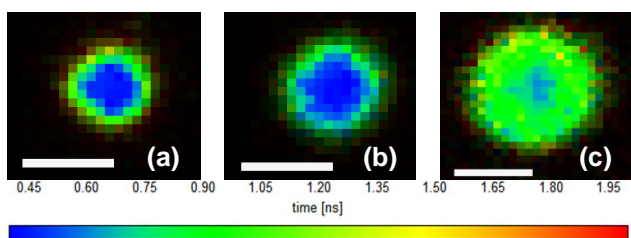


**Fig. 2** FLIM images of a single aggregate with the focus (a) at the microscope slide surface, (b) 1000 nm above the surface, and (c) 1500 nm above the surface. The image was obtained through a 510 nm filter (10 nm band pass) and the scale bar is 1500 nm long.

### Future Work

The universality of the “core-shell” model to describe the structure of aggregates formed by other conjugated systems such as CN-PPVs, thiophenes, and fluorenes is currently being investigated.[3] In addition, the mechanism of the fast decay process that leads to a drop in emission efficiency when chains are aggregated remains an important unanswered question and one that is particularly important for the optimization OLED devices. Our ongoing ultrafast studies of the aggregate emission dynamics at the CFN (Dr. Matthew Sfeir, collaborator) address this issue. Finally, FLIM show promise towards imaging variations in morphology in *polymer* films and we are developing the unique capabilities of this technique for depth profiling to characterize films within sandwich device structures in collaboration with a local industrial partner (Plextronics).

### References

- [1] Sherwood, G. A. Cheng, R., Smith, T. M., Werner, J. H., Shreve, A. P., Peteanu, L. A., Wildeman, J. *J. Phys. Chem. C*, **113**, 18851-18862 (2009)
- [2] Peteanu, L. A.; Sherwood, G. A.; Werner, J. H.; Shreve, A. P.; Smith, T. M.; and Wildeman, J., *J. Phys. Chem. C* (submitted)
- [3] Sherwood, G. A.; Cheng, R.; Chacon-Madrid, K.; Smith, T. M.; Wildeman, J.; and Peteanu, L. A. *J. Phys. Chem. C* **114**, 12078-12089 (2010)

The first two references are publications co-authored by CINT collaborators and acknowledge use of the CINT facility.

## The Hard X-ray Nanoprobe: Seeing Advanced Nanomaterials

R. P. Winarski<sup>1</sup>, M. V. Holt<sup>1</sup>, V. Rose<sup>2</sup>, J. Maser<sup>1,2</sup>, F. Brushett<sup>3</sup>, L. Trahey<sup>3</sup>, C. S. Johnson<sup>3</sup>

<sup>1</sup>Center for Nanoscale Materials, Argonne National Laboratory,  
9700 South Cass Avenue, Argonne, USA

<sup>2</sup>Advanced Photon Source, Argonne National Laboratory,  
9700 South Cass Avenue, Argonne, USA

<sup>3</sup>Chemical Sciences & Engineering, Argonne National Laboratory,  
9700 South Cass Avenue, Argonne, USA

### Scientific Thrust Area: X-ray Characterization of Electrochemical Nanostructures

One of the major challenges in the field of nanoscience is determining the electrochemical behavior of nanoarchitectures, particularly in the vicinity of interfaces. Understanding these properties requires the ability to observe system changes *in operando* as local structure and composition evolve because of the influence of electrochemical potentials. Equally important is the nanoscale control of the constituents in an electrochemical system, which offers the possibility of tailoring electronic, ionic, and molecular channels for novel or enhanced device functionality. Research in this area is essential for the advancement of the science underlying fuel cell and advanced battery designs and for the nation's future energy infrastructure.

Three-dimensional (3D) multifunctional battery structures show promise for improved storage capacity and scaling. We are using the unique combined x-ray nanotomography and x-ray fluorescence technologies that we have developed to study *in-situ* morphological and compositional changes of 3D battery structures in order to better understand advanced battery performance.

### Scientific Challenge and Research Achievement: In-Situ Study of 3D Battery Nanostructures

The anode of choice for lithium ion batteries is currently graphitic carbon. Its main advantages include stability, modest capacity, reversibility and low cost. It's theoretical capacity of 372 mAh/g ( $\text{LiC}_6$ ) results in Li-ion cells that possess high gravimetric energy density. On the other hand, the low insertion voltage vs. metallic Li of  $< 0.1$  V can cause a safety issue as lithium plating can occur under certain fast charge or shorting conditions. In today's batteries this is alleviated by incorporating sensors and other electronics in order to monitor the charge state of the graphite anode. The need for additional safety and improved electrochemical performance therefore has generated interest in alternative anodes to graphite. Alloys that insert lithium into interstitial holes in the structure [1-5], for example  $\text{Cu}_6\text{Sn}_5$  have notable positive attributes. First, they have only a limited volume expansion during lithiation of 59% compared to pure Sn that lithiates to a composition of  $\text{Li}_{4.4}\text{Sn}$  which results in a 400% volume change. This swelling process causes particle stress, and pulverization. This leads to loss of electrical inter-particle contact and a drastic drop in capacity. Second, since  $\text{Cu}_6\text{Sn}_5$  is a dense alloy ( $\sim 8 \text{ g/cm}^3$ ) the volumetric energy density is twice that of graphite;  $\sim 1800 \text{ mAh/cm}^3$  ( $\text{Cu}_6\text{Sn}_5$ ) versus  $\sim 800 \text{ mAh/cm}^3$  which is

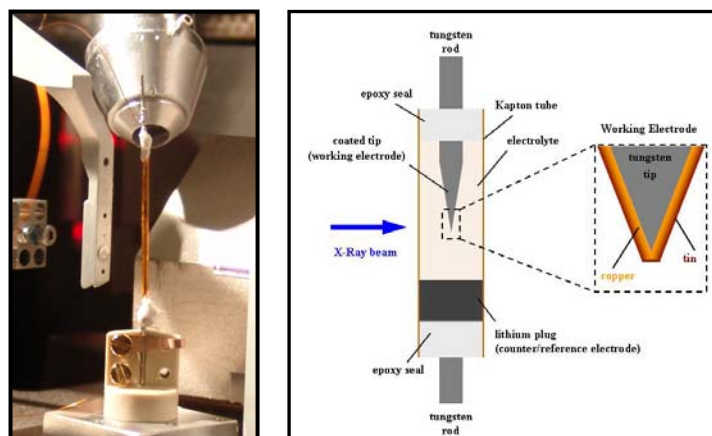
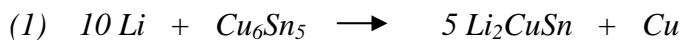


Figure 1. Photo and schematic of battery test cell inside the Nanoprobe.

attractive. Finally metal electrodes are preferable to graphite since the metal can act as a heat sink in case the battery was to heat up. This translates into an inherently safer battery system.

The mechanism of  $\text{Cu}_6\text{Sn}_5$  lithiation is the following:



This insertion reaction has a theoretical capacity of 275 mAh/g, and 50% of the Sn atoms are displaced into available interstitial sites in the structure during this reaction.

If the voltage of the anode is dropped below about 0.4 V versus metallic Li, then the  $\text{Li}_2\text{CuSn}$  lattice is destroyed, displacement occurs, and the Sn exiting the structure itself lithiates. As was discussed, this process results in a substantial ~ 400% volume expansion:



A nanosized real-time in-situ visualization of the comparison of reaction (1) versus reaction (2) in an operating Li battery cell is the objective of this work. This method will delineate the mechanism of these reactions and the volume change may be quantitatively measured. Furthermore the relationship of the mechanism to the voltages at which these lithiation reactions occur should be distinguishable from each other due solely to visualization of transmission x-ray images and reconstructed dynamic nanotomographic movies. The Hard X-ray Nanoprobe is ideally suited to monitor electrochemical reactions and can be used to determine Li-ion battery electrode reactions.

The specialized Li battery cell is mounted in the Nanoprobe chamber, as shown in Figure 1. The vertically mounted cell is fully contained inside a Kapton (polyimide) tube. The tube contains a W tip with a Cu-Sn electroplated coating, and a Li counter electrode. The non-aqueous electrolyte bathes the electrodes. Finally, insulated Cu wire leads are used to connect the electrodes to a galvanostat which controls the electrochemical cycling. An example of a discharge curve from such a cell is shown in Figure 2. Note that the voltage decreases as Li reacts with the Cu-Sn coating.

## Future Work

As we have demonstrated the potential of these types of in-situ imaging techniques, we will extend our measurements to include newly developed Li battery systems, and even Na based battery cells.

## Publications

1. Thackeray M. M., Vaughey J. T., Kahaian A. J., Kepler K. D., Benedek R., *Electrochem. Comm.* **1**, 111 (1999)
2. Tostmann H., Kropf A. J., Johnson C. S., Vaughey J. T., Thackeray M. M., *Phys. Rev. B* **66**, 014106, (2002)
3. Fransson L., Vaughey J. T., Benedek R., Edstrom K., Thomas J. O., Thackeray M. M., *Electrochem. Comm.* **3**, 317 (2001)
4. Fransson L., Nordstrom E., Edstrom K., Haggstrom L., Vaughey J. T., Thackeray M. M., *J. Electrochem. Soc.* **149**, A736 (2002)
5. Trahey L., Vaughey J. T., Kung H. H., and Thackeray M. M., *J. Electrochem. Soc.* **156** (5) A385 (2009)

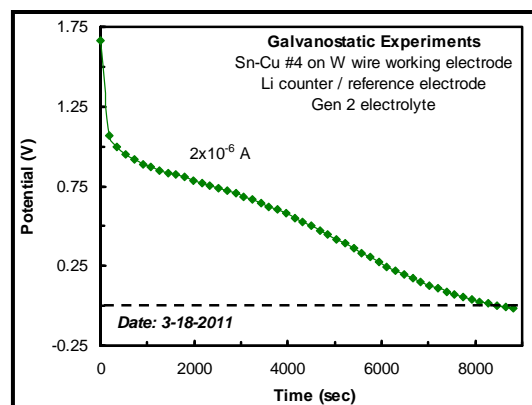


Figure 2. Voltage profile of Li/Cu-Sn electrode in cell.

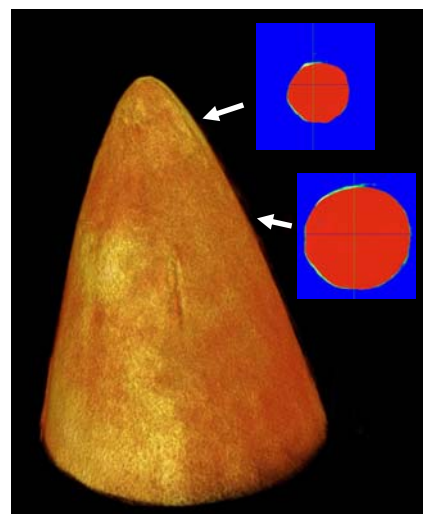


Figure 3. Nanotomographic reconstruction of Sn-Cu coated W tip. Inset images are two horizontal slices through the reconstructed tip showing volume changes along the surface of the coated tip during the initial stages of the discharge cycle (green edge regions).

# X-ray Spectral Fingerprints of Aqueous Chemical Processes from First-Principles Simulations

David Prendergast

*The Molecular Foundry, Lawrence Berkeley National Laboratory, Berkeley, CA 94720*

Gregory Dallinger, Andrew Duffin, Alice England, Craig Schwartz, Orion Shih, Janel Uejio,  
and Richard J. Saykally

*Chemistry Dept, UC Berkeley and Chemical Sciences Division, LBNL*

**Scientific Thrust Area:** Nanointerfaces, Multimodal in situ Nanoimaging

## Associated User Proposal Titles:

247: X-ray spectroscopy of biological nanostructures

527: Continued investigation of the X-ray Spectroscopy of Hydrated Biological Nanostructures

1197: X-ray spectroscopy of solution phase processes relevant to biology and energy storage

## Scientific Challenge and Research Achievement

Understanding chemical conversion of energy-relevant materials under working conditions can be complicated by solvent interactions. For example: (1) Hydrogen production from borohydride salts in water is dependent on solution pH; (2) the conversion of carbon dioxide to carbonate in water is also driven by pH, as in the geologic carbon cycle, or it can regulate pH, for example, in our own blood chemistry; additionally, (3) in biological systems, dissolved salts can impact the conformation of biomolecules through the Hofmeister effect. To study these three systems, we have employed Near-Edge X-ray Absorption Fine Structure (NEXAFS) spectroscopy of liquid microjets. This *in situ* probe of core-electron spectra reveals element-specific, local, chemical information which can expand our understanding of materials properties and dynamical processes in these solutions. However, this technique is strongly dependent on theoretical interpretation to make direct connections between measured spectra, which probe electronic properties, and atomistic, molecular, or conformational details. We have developed a suite of first-principles techniques capable of accurately predicting the spectra of solvated systems by carefully reproducing details of the electronic structure, condensed phase environment, and thermodynamic conditions [1-3].

We have applied this suite to interpret and predict details of the solution phase chemistry of the three systems described above. (1) We have successfully mapped the pH dependent spectra of boron oxides verifying the formation of polyborate species with combinations of trigonal planar and tetrahedrally coordinated boron. We find that boron K-edge NEXAFS of boron oxides is not particularly sensitive to interactions with the surrounding water, and, in fact, resembles the spectra of corresponding solid phases [4]. In contrast, we find that borohydride ( $\text{BH}_4$ ) is particularly sensitive to water interactions through the formation of di-hydrogen bonds, evident in measurements and simulations as drastic changes in the spectra with respect to gas phase predictions (Fig. 1) [5]. (2) Examining the subtle differences in the simulated carbon K-edge spectra of carbon dioxide, carbonic acid, bicarbonate, and carbonate, we reveal a transition from hydrophobic to hydrophilic interactions in this chemical sequence which is supported by experiment. We also provide benchmark spectra for future ultrafast x-ray experiments which may glimpse the brief formation of carbonic acid during the chemical decomposition of  $\text{CO}_2$  in water [6]. (3) Molecular dynamics simulations reveal conformational changes in the model peptide, triglycine, in varying salt solutions. These changes have associated subtle signatures in nitrogen K-edge NEXAFS simulations which correlate with microjet measurements and with predictions for structure making vs. structure breaking extracted from the Hofmeister series.

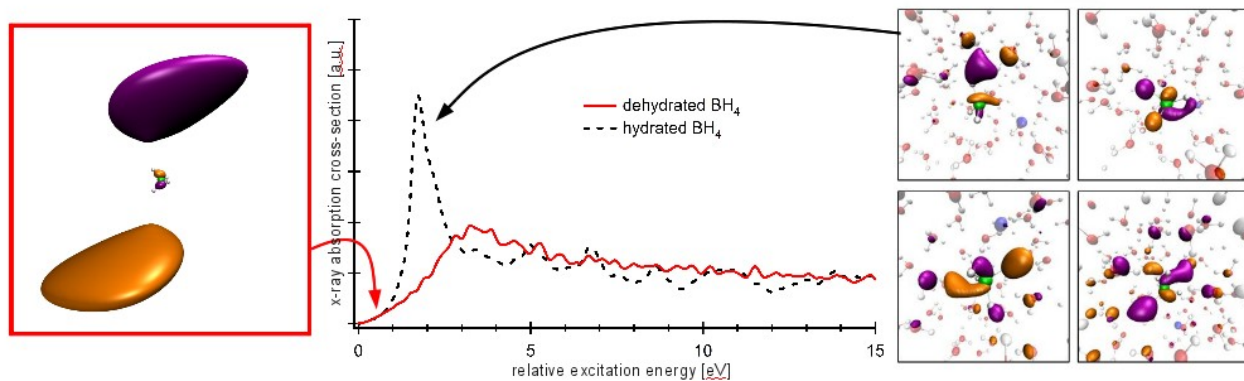


Figure 1: The sensitivity of boron K-edge NEXAFS of borohydride to water interactions (center) due to electronic confinement of excited states of the isolated species (left) and strong hybridization with nearby water molecules (right).

## Future Work

We will continue to apply these simulation techniques to analyze and predict spectra which reveal details of complex processes in aqueous solutions: (1) The association of various anions with N-methylacetamide: halide anions are predicted to associate with the hydrophobic methyl group of this small organic molecule. We will verify this prediction using a combination of microjet NEXAFS and first-principles simulations and extend the work to more complex hydrophobic species in solution; (2) The existence of contact-ion-pairs in concentrated solutions will be verified in the case of ammonium halide salts. These complexes are the seeds of molecular clusters that ultimately lead to crystal growth and precipitation; (3) We will explore the sensitivity of NEXAFS measurements to density variations and hydrogen-bonding rearrangements at water interfaces using first-principles molecular dynamics and spectral simulations.

## Publications

- [1] **X-ray absorption spectra of water from first-principles calculations.** David Prendergast and Giulia Galli, *Physical Review Letters*, 96, 215502 (2006).
- [2] **Effects of vibrational motion on core-level spectra of prototype organic molecules.** J. S. Uejio, C. P. Schwartz, R. J. Saykally, and D. Prendergast, *Chemical Physics Letters* 467, 195 (2008).
- [3] **Bloch-state-based interpolation: An efficient generalization of the Shirley approach to interpolating electronic structure.** David Prendergast and Steven G. Louie, *Physical Review B* 80, 235126 (2009).
- [4] **pH-Dependent X-ray Absorption Spectra of Aqueous Boron Oxides** Andrew Duffin, Craig Schwartz, Alice England, Janel Uejio, David Prendergast, and Richard Saykally, *J. Chem. Phys.* (accepted March 2011).
- [5] **Borohydride-Water Interactions Characterized by X-ray Absorption Spectroscopy.** Andrew Duffin, Alice England, Craig Schwartz, Janel Uejio, Gregory Dallinger, Orion Shih, David Prendergast, and Richard Saykally, (submitted April 2011).
- [6] **On the Hydration and Hydrolysis of Carbon Dioxide.** Alice Engalnd, Andrew Duffin, Craig Schwartz, Janel Uejio, David Prendergast, and Richard Saykally (in preparation).
- [7] **Investigation of Protein Conformation and Interactions with Salts via X-ray Absorption Spectroscopy.** Craig Schwartz, Janel Uejio, Andrew Duffin, Alice England, Daniel Kelly, David Prendergast, and Richard Saykally, *Proceedings of the National Academy of Scientists* 107, 14008 (2010).

# Manipulating Nanophase Separation in P3HT/PCBM System with a P3HT-*b*-PEO

## Block Copolymer Compatibilizer

Jihua Chen<sup>1\*</sup>, Xiang Yu<sup>2</sup>, Kunlun Hong<sup>1</sup>, Deanna L. Pickel<sup>1</sup>,  
Adam J. Rondinone<sup>1</sup>, Kai Xiao<sup>1</sup>, Mark Dadmun<sup>2,3</sup>, Jimmy W. Mays<sup>1,2,3</sup>,  
Bobby Sumpter<sup>1,4</sup>, and S. Michael Kilbey II<sup>1,3\*</sup>

<sup>1</sup> Center for Nanophase Materials Sciences, Oak Ridge National Laboratory, Oak Ridge, TN 37831

<sup>2</sup> Chemical Sciences Division, Oak Ridge National Laboratory, Oak Ridge, TN 37831

<sup>3</sup> Department of Chemistry, University of Tennessee, Knoxville, TN 37996

<sup>4</sup> Computer Science & Mathematics Division, Oak Ridge National Laboratory, Oak Ridge, TN 37831

### Scientific Thrust: Functional polymer architecture, organic photovoltaics

**Scientific Challenges:** Nanophase separation plays a critical role in the performance and stability of donor-acceptor based organic photovoltaics. However, the ability to exert precise control over the phase separated domains remains elusive.

**Research Achievement:** A poly(3-hexylthiophene)-*b*-poly(ethylene oxide) (P3HT-*b*-PEO) diblock copolymer is added to a binary blend of P3HT and 6,6-phenyl C<sub>61</sub>-butyric acid methyl ester (PCBM) to systematically modify the donor-acceptor interface. Adding 5-10wt% P3HT-*b*-PEO into a 1:1 P3HT/PCBM blend systematically decreases the size of PCBM- and P3HT-rich domains after thermal annealing, as evidenced from a combination of atomic force microscopy, transmission electron microscopy, wide-angle and small angle X-ray analysis (Fig 1), while in as-cast films the compatibilizer addition did not lead to reduced domain sizes (Fig 2). The impact of the compatibilizer is further rationalized through quantum density functional theory calculations. In the end, available solar cell device results suggest that adding P3HT-*b*-PEO compatibilizer to P3HT/PCBM blends has both positive and negative consequences: bulk heterojunction films show enhanced Voc but reduced current density.

**Future Work:** We wish to better understand the underlying compatibilizing effect on nanomorphology of P3HT/PCBM system and further improve performance through the choice of compatibilizer type and block copolymer composition.

**Publication:** *Tailoring P3HT/PCBM Donor/Acceptor Nano-Phase Separation with a Conjugated Diblock Copolymer Compatibilizer*, 2011, Submitted to *ACS Nano*

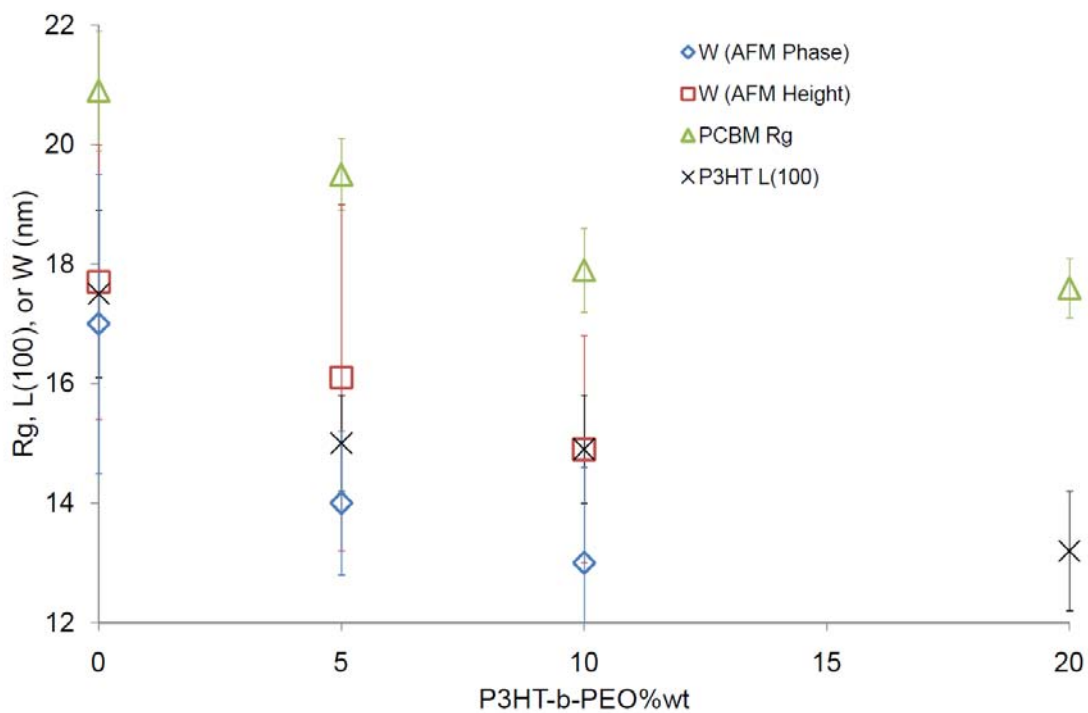


Figure 1. Domain size analysis in thermally annealed (120°C, 30 min) P3HT/PCBM 1:1 films with various amounts of P3HT-*b*-PEO compatibilizer.

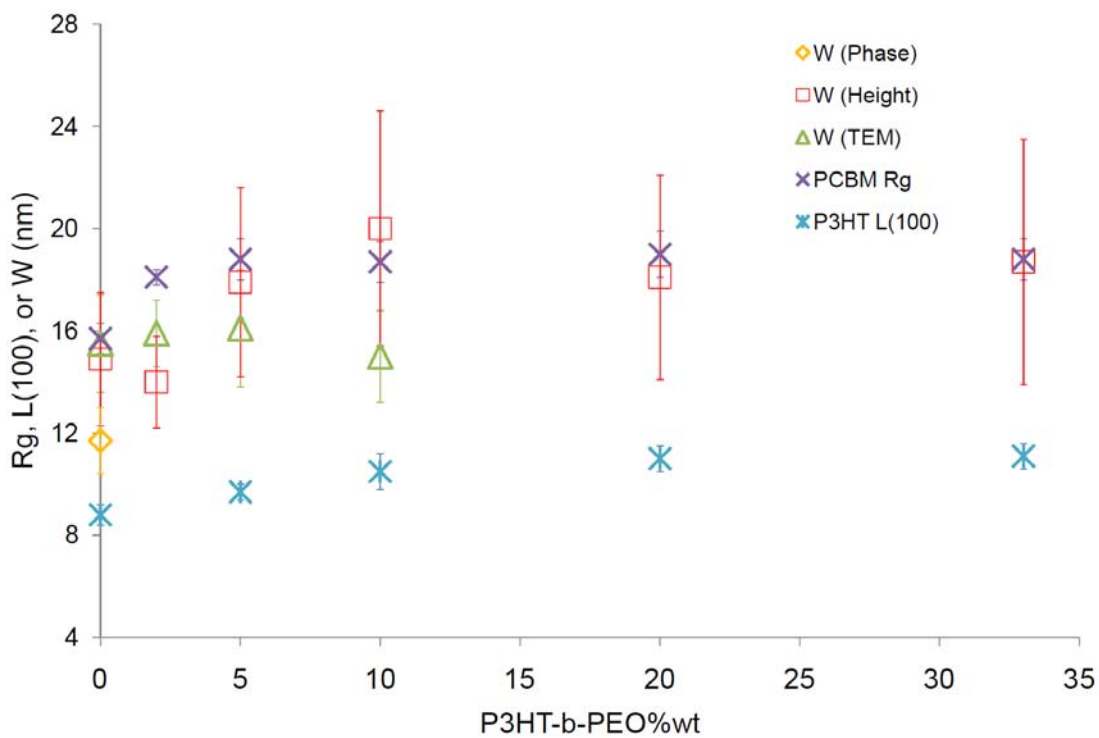


Figure 2. Domain size analysis in as cast P3HT/PCBM 1:1 films with various amounts of P3HT-*b*-PEO compatibilizer

## Phonon, exciton, and light interactions in Semiconducting Single Walled Carbon Nanotubes

Primary Investigator: Anna Swan Boston University, [swan@bu.edu](mailto:swan@bu.edu), Primary CINT Contact: Stephen K. Doorn, LANL, [skdoorn@lanl.gov](mailto:skdoorn@lanl.gov), Co-Investigators: Andrew Shreve, Serguei Tretiak

**CINT Proposal Title:** “Phonon, exciton, and light interactions in Semiconducting Single Walled Carbon Nanotubes”

**Scientific Challenge and Research Achievement** Single-walled carbon nanotubes (SWNTs) exhibit a large array of behaviors in optical and electronic properties due to the diverse array of chiral structures found for grown SWNTs. These behaviors are fundamental to anticipated applications in nano-electronics<sup>1, 2</sup>, optoelectronics<sup>3</sup> and sensing<sup>4, 5</sup>. Resonant Raman scattering is one of the major tools for determining the chirality of carbon nanotubes as well as exploring the effect of different perturbations (screening, strain, temperature variations, etc) to the nanotube on the physical nanotube properties (bandgap, exciton energy, dipole strength, quantum efficiency, mobility). Raman excitation profiles (plots of intensity in a vibrational mode vs. excitation energy) provide information on the CNT exciton energy and band-structure, exciton-phonon interaction, band interactions. Peaks in the profiles (appearing from resonances between discrete excited states and “ingoing” (excitation) or “outgoing” (scattered) photons) indicate the exciton energy, the strength of the electron phonon coupling, the electronic and phonon dephasing. However, the model dependent interpretation<sup>6, 7</sup> of such excitation profiles gives very different answers and physical understanding of these interactions that are fundamental to so many implementations of practical applications.

In order to test the models of Raman excitation profiles and clearly resolve the ingoing and outgoing resonance, we use the SWNT G band, which has sufficiently large energy to allow model based interpretations and to explore the physics of measured profiles. The G band is found at a common Raman frequency for all chiralities and it is therefore instrumental to isolate only a single SWNT species for measurements, achieved by our NIST collaborators, Ming Zheng and Xiamin Tu<sup>8</sup>. Our preliminary BU/LANL collaboration with measurements of the E<sub>22</sub> G band Raman excitation profiles for a large number of isolated semiconducting SWNTs has clearly demonstrated that the basis for all Raman scattering interpretation we have found that the assumption of unchanged dipole transition moment for the incoming and outgoing resonance is violated. This is illustrated in Fig. 1 which shows that the outgoing resonance (the second peak) is much weaker than the incoming resonance. This finding has ramifications not only SWNT optics, but also for SWNT electronic transport properties. For example, suspended nanotubes exhibit negative differential conductance with non-equilibrium phonon populations<sup>9</sup>. Measurements of the coherent phonon dynamics in the time domain by femto-second pump probe techniques demonstrates the very unusual vibrational structure, and yield a resonance profile where current models have not been able to reproduce the complex experimental results<sup>10</sup>.

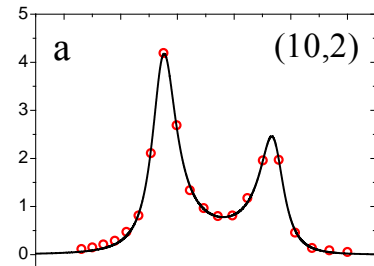


**Fig.1** Resonance Raman profile of G band for E<sub>22</sub> resonance for (10,2) SWNT.

**Future Work** The goal of this work is to predict and understand the chirality and energy level dependent exciton phonon interaction via measurements, models and quantum chemical

calculations. The strength of the G band e-ph interaction as a function of chirality will be explored, but more importantly, the physical understanding of the interaction (Non-Condon contribution, 1D vs 0D physics,) will be gained from the combined resonance Raman profile measurements for many different chiralities and theoretical modeling efforts. We will measure the resonant Raman Profiles for samples enriched in specific semiconducting chiralities via DNA wrapped SWNTs and ion chromatography<sup>11</sup>. We are particularly interested in the G band (~1600 cm<sup>-1</sup>) for the E<sub>33</sub> and E<sub>44</sub> transitions since the role of Raman interference can be tested for these transitions and applied to other transitions. In addition we will also attempt to measure the Raman excitation profiles of the highly dispersive 2D band (~2600 cm<sup>-1</sup>) that maps the phonon dispersion, since these vibrations are strongly interacting with electrons in transport. G-band and 2D-band profiles will allow testing of different models for the Raman scattering process and reveal new evidence for the importance of non-Condon effects in the Raman response.

**Theory and models** The strengths of the electron phonon coupling depend on the Raman profile intensity. However, the actual value of the e-phonon coupling is subject to the physical interpretation of the interaction. The measurement of the G band profiles for several electronic resonances will make it possible to determine how to model the Raman interaction, for example, the 4 level model (electronic and vibrational levels) can be explored to determine the degree of non-Condon effect and the role of interference (BU), and be compared with the results of the Raman transform method (Andy Shreve). Quantum Chemical calculations will explore from first principles the changes in the transition dipole moments for excited states of E<sub>11</sub>, E<sub>22</sub>, E<sub>33</sub> and E<sub>44</sub> bands while displacing the tube geometries along G-band and lower-frequency vibrational modes that show strong coupling to the electronic system (Tretiak). These computations will allow us to quantify the magnitudes of non-Condon effects to be directly compared with the results of Raman profile results. The results will provide insight to how the band structure and dipole moment is changed by vibrational motion of the atoms, with careful interpretations to avoid finite size effects.

## References

- <sup>1</sup> Baughman, R.H.; Zakhidov, A.A.; de Heer, W.A., *Science* **297**, 787-792, (2002).
- <sup>2</sup> Tans, S.J.; Devoret, M.H.; Dai, H.J., et al, *Natur*, **386**, 474-477 (1997).
- <sup>3</sup> Kind, H.; Yan, H.Q.; Messer, B., *Adv. Mat.* **14**, 158 (2002).
- <sup>4</sup> Kong, J.; Franklin, N.R.; Zhou, C.W., et al., *Science* **287**, 622, (2000).
- <sup>5</sup> Modi, A.; Koratkar, N.; Lass, E., et al. *Nature* **424**, 171-174 (2003).
- <sup>6</sup> Yin, Y., et al., *Phys. Rev. Lett.* **98**, 037404 (2007).
- <sup>7</sup> Shreve, A.P.; Haroz, E.H.; Bachilo, S.M., et al., *Phys. Rev. Lett.* **98**, 037405 (2007).
- <sup>8</sup> Hersam, M. C., *Nat. Nanotechnol.*, **3**, 387 (2008).
- <sup>9</sup> Bushmaker, A.W., et al., *Nano Lett.* **9**, 2862, (2009).
- <sup>10</sup> Luer, L., et al., *Phys. Rev. Lett.* **102**, 127401, (2009).
- <sup>11</sup> Tu, X.; Manohar, S.; Jagota, A.; Zheng, M., *Nature* **460**, 250 (2009).

## Publications:

1. Revealing new electronic behaviours in the Raman spectra of chirality-enriched carbon nanotube ensembles Duque JG, Chen H, Swan AK, Haroz EH, Kono J, Tu XM, Zheng M, Doorn SK, *PHYS. STAT. SOL. B* **247**, 2768-2773 (2010)
2. Violation of the Condon Approximation in Semiconducting Carbon Nanotubes Juan G. Duque, Hang Chen, Anna K. Swan, Andrew P. Shreve, Svetlana Kilina, Sergei Tretiak, Xiaomin Tu, Ming Zheng, Stephen K. Doorn, *Submitted to ACS Nano* (2011)

## LT-STM Investigations of Self-assembled 1D Molecular Chains: Aromatic Diisocyanides on Au(111)

J. Zhou,<sup>1</sup> P. Zahl,<sup>4</sup> D. Stacchiola,<sup>2</sup> Y. Li,<sup>3</sup> P. Sutter,<sup>4</sup> M. G. White<sup>1,2</sup>

<sup>1</sup> Department of Chemistry, Stony Brook University, Stony Brook, NY 11794

<sup>2</sup> Chemistry Department, Brookhaven National Laboratory, Upton, NY 11973

<sup>3</sup> Computational Science Center, Brookhaven National Laboratory, Upton, NY 11973

<sup>4</sup> Center for Functional Nanomaterials, Brookhaven National Laboratory, Upton, NY 11973

**Proposal Title:** “Investigations of the electronic structure of isocyanide molecules on Au(111)”

### Scientific Challenge

The electronic properties of organic molecules on metal substrates are of significant interest for their central role in the development of molecular-based electronic and optical devices.<sup>1</sup> Of particular importance are the energy positions of the HOMO and LUMO levels of the molecule relative to the Fermi edge ( $E_F$ ) of the metal contact, which are indicative of the junction bias required for hole and electron conduction, respectively. The thiol-gold interaction is the most extensively studied contact in molecular electronics applications, as the strong chemical bond between the sulfur and gold atoms drives the formation of ordered overlayers, e.g., self-assembled monolayers (SAMs). However, susceptibility to oxidation and a high electron transfer barrier have motivated the search for new molecular junctions. Molecular isocyanides have attracted widespread interest for this application as the  $N\equiv C$  triple bond is expected to act as an effective bridge for connecting  $p\pi$  orbitals of aromatic molecules with  $d\pi$  orbitals of the metal contact. These qualitative expectations are supported by conductance measurements and theoretical calculations which indicate that molecules with isocyanide groups exhibit higher conductance compared to the same molecule with a terminal thiol group.<sup>2</sup> Despite these promising results, direct spectroscopic determinations of the HOMO/LUMO level positions of adsorbed aromatic isocyanides are lacking, as well as detailed information on surface bonding morphology from low to high coverage leading to SAM formation. Such information is crucial for understanding and optimizing the charge transport properties of aromatic isocyanides for molecular electronics applications.

### Research Achievement

In this work, we used the Createc LT-STM at the Center for Functional Nanomaterials to explore the bonding morphology and electronic structure of two simple aromatic isocyanides, 1,4-phenyldiisocyanide (PDI) and 4,4'-biphenyldiisocyanide (BPDI), deposited on a Au(111) surface. Initial experiments on PDI/Au(111) were motivated by photoemission experiments in our laboratory that showed an unusually large drop in the work function for PDI/Au(111) surfaces prepared at low temperature (<100 K) that were subsequently annealed to room temperature. STM images show that annealing PDI/Au(111) surfaces to 300 K results in the formation of 1D structures that extend the length of the Au terraces (see Figure 1). The chains are oriented along the  $\langle 1\bar{1}0 \rangle$  directions of the Au(111) surface and are composed of alternating small and large spots with a repeat distance of  $11.7 \pm 0.2$  Å. These results are inconsistent with previous studies which suggest that PDI molecules bind end on via only one NC-Au bond. An alternative bonding arrangement was recently proposed in which Au adatoms are used to link PDI molecules into 1D chains.<sup>3</sup> The measured repeat distance is consistent with a [-Au-PDI-]

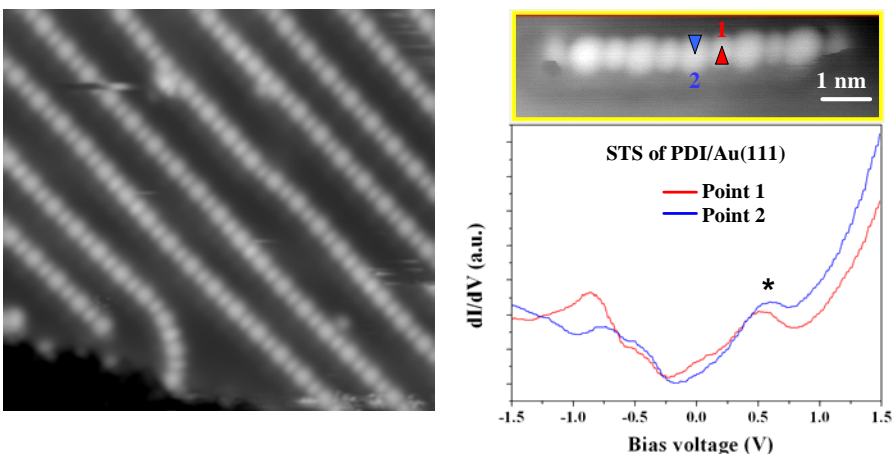


**Figure 1:** Left: STM image of a 0.33ML of PDI deposited on Au(111) at 90 K and annealed. Image size  $17.5 \times 14.8 \text{ nm}^2$ . Right:  $dI/dV$  curves at points along a short molecular chain at 5 K. Upper image taken at a bias of  $-0.7 \text{ V}$ .

Figure 2, BPDI molecules also self-assemble into 1D structures when dosed or annealed at room temperature. Images acquired at low temperature (5 K) reveal a repeating monomer distance which is longer than PDI by exactly what would be expected for the addition of the second phenyl ring. These experiments confirm that the diisocyanide molecules lie flat on the surface and provide strong support for molecular chains involving Au adatoms. Density functional calculations support the favorable energetics for Au adatom formation and PDI-Au<sub>ad</sub> bonding (Figure 2).

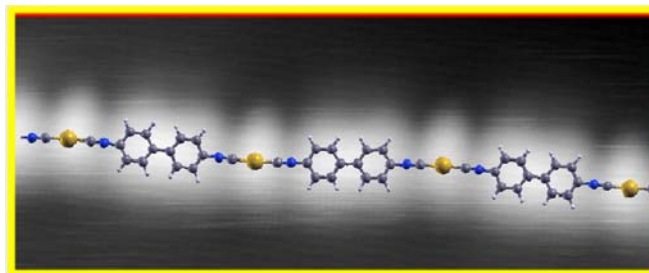


**Figure 2:** Superposition of a DFT calculated structure of a  $[\text{BPDI-Au}]_n$  molecular chain onto a STM image acquired at 5 K and a bias of  $-1.6 \text{ V}$ . Image size:  $5.4 \times 2.2 \text{ nm}^2$

### Future Work

In the near future, LT-STM will be used to explore the morphology and electronic structure of 1D diisocyanide-metal chains deposited on a thin insulating layer, i.e., NaCl on Au(111). These experiments will test if co-deposited Au atoms and diisocyanide molecules self-assemble into 1D chains in the absence of a Au surface template, and allow a more detailed STS characterization of the molecular chains by reducing the contributions from the Au substrate.

### References

1. Wang, W.; Lee, T.; Reed, M. A. *Rep. Prog. Phys.* **2005**, *68*, 523–544.
2. Chu, C.; Ayres, J.A.; Stefanescu, D.M.; Walker, B.R.; Gorman, C.B.; Parsons, G.N. *J. Phys. Chem. C* **2007**, *111*, 8080-8085 and references therein.
3. Boscoboinik, J.A.; Calaza, F.C.; Habeeb, Z.; Bennett, D.W.; Stacchiola, D.J.; Purino, M.A.; Tysoe, W.T. *Phys. Chem. Chem. Phys.* **2010**, *12*, 11624-11629.

### Publications

“Adsorption structure and electronic properties of phenyl diisocyanide (PDI) on Au(111),” J. Zhou, N. Camillone III, D. P. Acharya, P. Sutter and M.G. White, in preparation.

subunit. STS measurements also provided a detailed map of the PDI/Au(111) density-of-states including the observation of spatially resolved occupied levels near the Fermi edge. Our most recent experiments focused on BPDI, in which another phenyl group is inserted between the two isocyanide groups. As shown in

# Self-assembly of soft materials driven by competing specific and nonspecific interactions

Stephen Whitelam<sup>1\*</sup>, Thomas K. Haxton<sup>1</sup>, Caroline Ajo-Franklin<sup>2</sup> and Behzad Rad<sup>2</sup>

<sup>1</sup>*Theory of Nanostructured Materials Facility and* <sup>2</sup>*Biological Nanostructures Facility*

*The Molecular Foundry,*

*Lawrence Berkeley National Laboratory,*

*1 Cyclotron Road, Berkeley, CA 94720, USA*

\* [swhitelam@lbl.gov](mailto:swhitelam@lbl.gov)

## Scientific Thrust Area

*Multimodal in situ Nanoimaging; Understanding design rules for self-assembly.* Proteins and patchy nanoparticles possess interactions that are ‘specific’, able to stabilize ordered structures more complicated than simple close-packed crystals, and interactions that are ‘nonspecific’, which allow them to bind in a disordered way. I will show how molecular models of self-assembly that acknowledge *only* these microscopic details suggest strategies for controlling dynamical pathways and yields of assembly.

## Scientific Challenge and Research Achievement

Controlling the crystallization of molecular and nanoscale systems remains a principal challenge of physics and chemistry. Controlling protein crystallization in particular is central to protein characterization, but despite advances in our understanding of protein phase behavior and association dynamics we lack a set of rules for rational production of protein crystals *in vitro*. Some proteins crystallize *in vivo*. S (‘surface’)-layer proteins form functional crystalline lattices on the outsides of many bacteria and archaea, and were among the first protein structures used to organize nanomaterials in a ‘bottom-up’ fashion. The sbpA S-layer protein from the bacterium *Lysinibacillus sphaericus* forms a square crystalline lattice of tetramers, and has been shown to crystallize in a ‘multistage’ fashion on supported lipid bilayers *in vitro* [Chung, Shin, Bertozzi, De Yoreo, PNAS 2010]: order emerges from dense amorphous clusters, rather than directly from crystalline nuclei (see Figure). A similar dynamics is thought to operate during crystallization of the globular protein lysozyme.

We have used computer simulation to study a model of S-layer proteins equipped with interactions that are both nonspecific, in an orientational and chemical sense, and specific. Distinct dynamical pathways of crystal formation can be selected by tuning the strengths of these interactions (see Figure). Fluctuations of density and structure sometimes cooperate (enhancing assembly), and sometimes conflict (impairing assembly). While both scenarios are suggested by simulations of isotropic model proteins, here the presence of two types of interaction allows such fluctuations to be varied in strength, at fixed temperature and concentration, with a high degree of independence. Our results suggest that trading specific- for nonspecific interaction strength can alter assembly pathways and can optimize the yield of the resulting material.

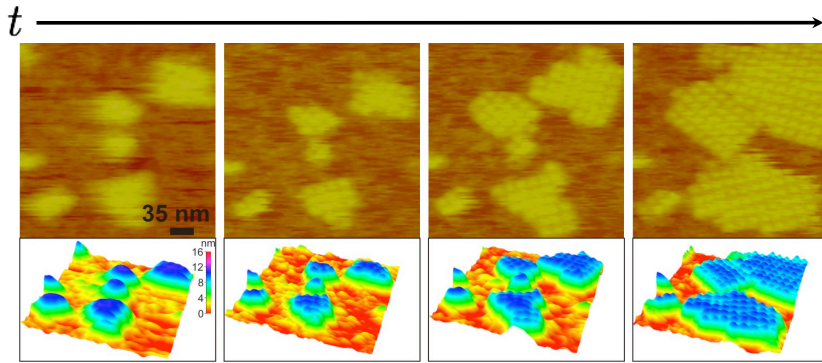
## Future Work

Our joint theory-experiment collaboration at the Molecular Foundry [Molecular Foundry Challenge Grant, S. Whitelam and C. Ajo-Franklin] is exploring ways of addressing S-layer proteins’ specific and nonspecific interactions in order to change their phase behavior and their dynamical pathway of assembly. Our preliminary work reveals that by varying protein concentration and calcium concentration we can identify phase boundaries of crystal stability, parameter regimes of robust self-assembly, and regimes in which kinetically-trapped, networked structures form.

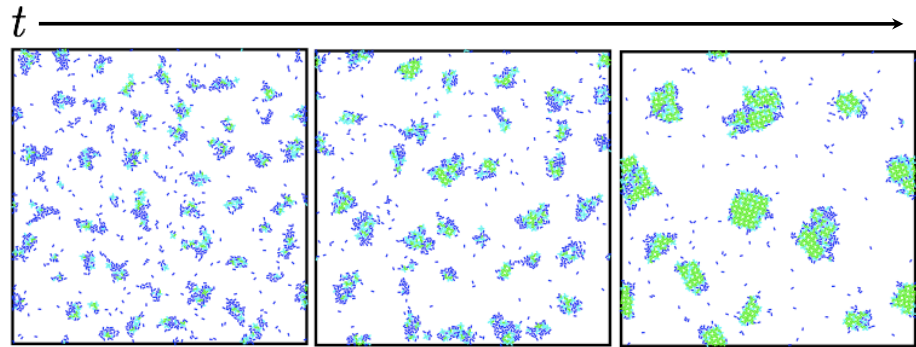
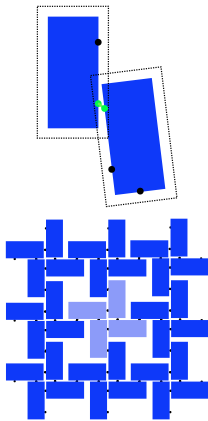
## References

2

S. Whitelam, *Control of pathways and yields of protein crystallization through the interplay of nonspecific and specific attractions*, Phys. Rev. Lett. 105, 088102 (2010)



Chung, Shin, Bertozzi, DeYoreo PNAS 2010



Whitelam PRL 2010

Multistage pathway of assembly of S-layer protein (top), and molecular model designed to explore where in parameter space such dynamics emerges (bottom).

## Surface-enhanced Raman spectroelectrochemistry of TTF-modified self-assembled monolayers

Walter F. Paxton,<sup>†</sup> Samuel L. Kleinman,<sup>\*</sup> Ashish N. Basuray,<sup>\*</sup>  
J. Fraser Stoddart,<sup>\*</sup> Richard P. Van Duyne<sup>\*</sup>

<sup>†</sup> Center for Integrated Nanotechnologies  
Sandia National Laboratories, Albuquerque, New Mexico 87185  
<sup>\*</sup> Department of Chemistry, Northwestern University  
2145 Sheridan Road, Evanston, Illinois 60208-3113

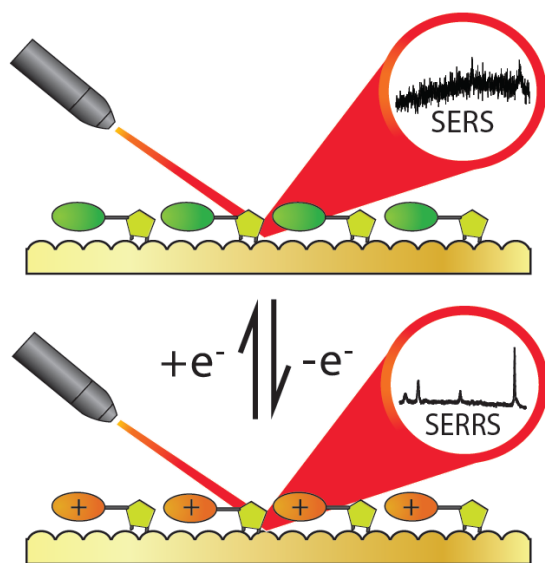
**Scientific Thrust Area:** Soft Biological and Composite Nanomaterials

### Scientific Challenge and Research Achievement:

Tetrathiafulvalene (TTF) is an electron-rich redox-active molecule that has been utilized extensively in mechanostereochemical systems and molecular electronic devices (MEDs). Neutral TTF is capable of donating one or two electrons to yield stable singly and doubly charged states, permitting access to electrochemically addressable electronic and magnetic properties. It also has the benefit of preserving its electrochemical properties following substitution at any or all four of its exterior carbons, thus enriching its chemical diversity by extending its utility to functional TTF molecules. For these reasons, TTF has been investigated extensively as

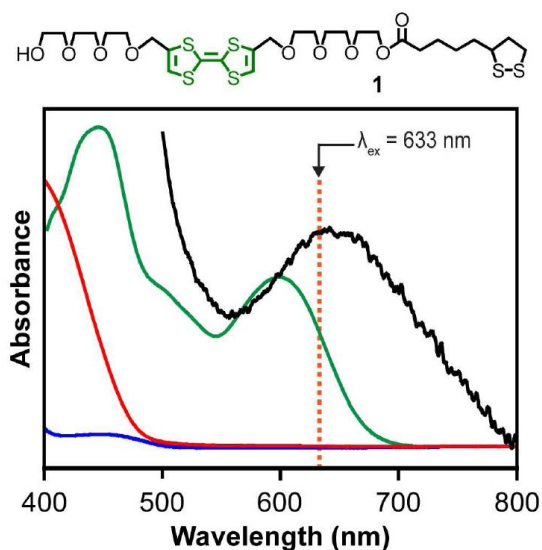
an electroactive recognition element in bistable mechanically interlocked molecules (MIMs) in solution, in polymer matrices, in self-assembled monolayers (SAMs) on gold electrodes and on gold nanoparticles, in closely packed condensed monolayers, in Langmuir-Blodgett films mounted on solid supports and in molecular switch tunnel junctions (MSTJs). Over the past decade, numerous reports, supported by molecular dynamics simulations, have documented the integration of bistable MIMs – where TTF is one of the key electroactive recognition elements – into MSTJs in solid-state MEDs. Although the incorporation of the bistable MIMs containing TTF as the switching trigger in the integrated systems and devices is a highly promising development offering considerable potential for the future growth of MEDs, direct real-time evidence for physical motion in response to electrochemical stimulation in these devices remains sparse.

We have demonstrated that a synergy of both surface and resonance Raman enhancement can be exploited to elucidate chemical information in real-time about the oxidation state of molecules at an electrode interface. Electrochemical investigations indicate that nonidealities in the electrochemistry can be suppressed by diluting the surface concentration of redox active with an inert compound – suggesting that they arise as a result of the interactions between neighboring TTF units. The SER(R)S investigations revealed changes in vibrational frequencies of the TTF



unit as a result of changes in oxidation state. Upon oxidation to the radical cation the spectrum of **1** is greatly enhanced by resonance between  $\lambda_{ex}$  and the electronic absorbance of **1**. This observation provides a highly sensitive contrast mechanism which can be used to probe the state of the TTF-bearing components in functional MEDs. The enhancement is sufficient to allow the observation of the first and second overtones of the C–S stretching mode.

**Future Work:** These results highlight the value of SER(R)S in future investigations of electroactive switchable molecular electronics. This nondestructive approach may allow the chemical investigations of molecular switching events at interfaces in working MEDs *in situ* to enable the elucidation of processes involved in the response of switchable molecules to electronic stimulation.



Structural formula of the TTF derivative **1** (top), and the truncated UV-vis absorbance spectra of 0.1 mM **1** in MeCN in its neutral (**1**, blue trace), radical cationic (**1**<sup>+</sup>, green trace) and dicationic (**1**<sup>2+</sup>, red trace) forms. Also shown is the wave-length ( $\lambda_{ex}$ ) of the excitation source and the normalized absorbance spectrum of the SERS active AuFON electrode (black trace), revealing the LSPR band centered at 640 nm. Taken together, this figure illustrates the matching between the **1**<sup>+</sup> absorbance, the AuFON LSPR, and  $\lambda_{ex}$ .

**Publications:** Walter F. Paxton, Samuel L. Kleinman, Ashish N. Basuray, J. Fraser Stoddart, Richard P. Van Duyne “Surface-enhanced Raman spectroelectrochemistry of TTF-modified self-assembled monolayers,” *submitted*.

## Direct surface imaging of model oxide catalytic supports

J. Ciston, C. Kisielowski, D. Su\*, Y. Zhu\* and L.D. Marks\*\*

National Center for Electron Microscopy, Materials Sciences Division, LBNL, Berkeley, CA 94720

\* Center for Functional Nanomaterials, Brookhaven National Laboratory, Upton, NY 11973

\*\* Department of Materials Science and Engineering, Northwestern University, Evanston, IL 60208

### Scientific Thrust Area

It is well-known that both the activity and selectivity of supported noble metal catalysts is highly dependent upon both the support material and the catalyst particle size [1]. Although relatively well characterized in their bulk state, the surface structure of catalytic materials in nanocrystalline form can deviate greatly from ideal terminations, and offers the key to understanding why the choice of support material is so critical.

### Scientific Challenge and Research Achievement

While the identification of surface structures at atomic resolution as proposed has been shown to be achievable in the profile geometry [2], this technique can only yield incomplete, one dimensional information. However, many two dimensional surface techniques cannot be straightforwardly applied to oxide materials, especially in nanoparticle systems relevant to actual catalysis. For example, scanning tunneling microscopy (STM), a staple technique for the identification of surface structures, experiences great difficulty with insulating materials. Surface diffraction techniques have been successful in solving oxide structures, but the phase retrieval methods used are prone to non-unique solutions. Recent work has shown that the Hitachi HD2700C STEM is capable of 0.1 nm resolution and single-atom sensitivity in secondary electron (SE) imaging of surface atoms ranging from carbon to uranium in isolated atom and crystalline materials [3]. Even more critically, we have been able to distinguish between SrO and TiO<sub>2</sub> terminations at the SrTiO<sub>3</sub> (001) surface as shown in Figure 1 [5].

### Future work

This work has been extended further to the study of surface reconstructions on the (001) and (111) surfaces of the model SrTiO<sub>3</sub> system with known and unknown atomic structures. Aberration-corrected surface imaging in TEM, STEM, and SE modes have been compared in their ability to retrieve quantitative atomic information from these structures. Surface structure imaging is not typically a resolution-limited problem, but these experiments are able to take full advantage of the monochromation, energy filtering, and exceptional stability of the TEAM instruments to maximize the signal to noise ratios required for quantitative imaging of these monolayer systems. Furthermore, the absence of image delocalization in aberration corrected instrumentation eliminates the apparent shift in registration of the surface with respect to the bulk as a function of defocus. Initial results indicate phase contrast TEM imaging to be most promising, exhibiting the highest signal to noise ratio of the three techniques. While the transmission geometry yields convoluted information from both top and bottom surfaces as well as the bulk, translational and rotational averaging in the manner of [4] has been used to elucidate the surface contribution (Figure 2). It is important to note that this technique may also be applied directly to facets of nanocrystals provided that the surface planes may be tilted perpendicular to the electron beam, enabling surface structure solution of materials for which it is not possible to grow large single crystals.

## References

- [1] S.K. Shaikhutdinov *et al.*, *Catalysis Letters* **86**, 211 (2003).
- [2] L. D. Marks, and D. J. Smith, *Nature* **303**, 316 (1983).
- [3] Y. Zhu *et al.*, *Nature Materials* **8**, 808 (2009).
- [4] E. Bengu *et al.*, *Physical Review Letters* **77**, 4228 (1996).

## Publications

- [5] H. Inada *et al.*, *Untramicroscopy*, In Press (2011) doi:10.1016/j.ultramic.2010.10.002

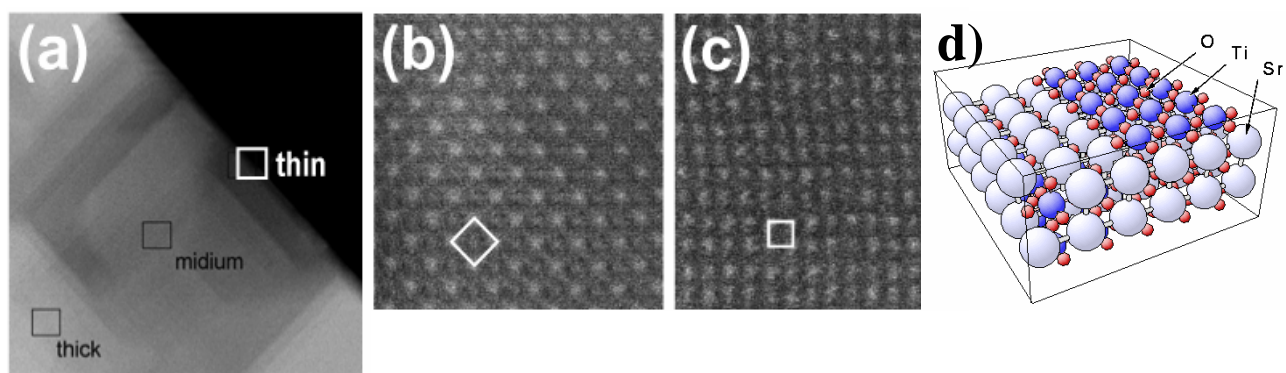


FIG 1: a) STEM-ADF image of heat treated SrTiO<sub>3</sub> single crystal exhibiting distinct (001) facets and steps b) Secondary electron image exhibiting SrO surface termination c) Secondary electron image exhibiting TiO<sub>2</sub> surface termination d) model structure of the SrTiO<sub>3</sub> (001) surface

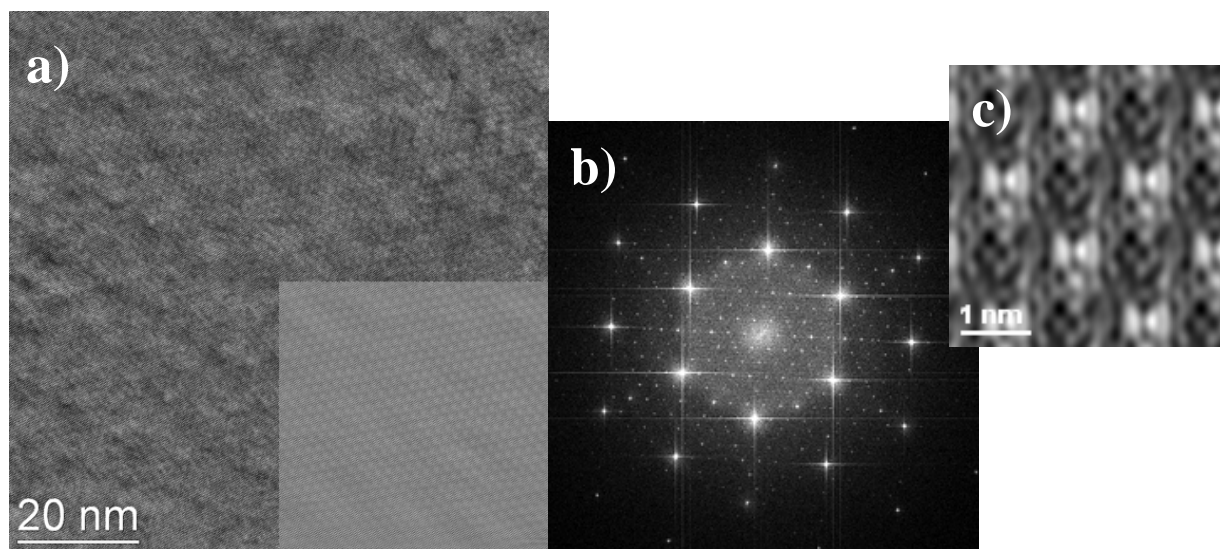


FIG 2: a) HRTEM image of SrTiO<sub>3</sub> (111) 3x3 surface reconstruction. Inset shows wiener filtered image. b) FFT of (a) exhibiting transfer of both bulk and surface information c) surface image after removal of bulk contribution and translational averaging.

## Nanofabrication Research Laboratory: Development of Unique Functionality at the Nanoscale

Pat Collier<sup>1</sup>, Seung-Yong Jung<sup>1</sup>, Scott Retterer<sup>1,2</sup>

Oak Ridge National Laboratory, <sup>1</sup>Center for Nanophase Materials Sciences, <sup>2</sup>Biosciences Division, Oak Ridge TN 37831

### Scientific Thrust Area

#### *Control of Mass Transport and Chemical Reaction Kinetics in Ultrasmall Volumes*

Chemical reactions that occur at or within nanoscale structures, interfaces and architectures take place under highly crowded and confined conditions, which significantly affect thermodynamic and kinetic properties. A better understanding of how confinement and reduced dimensionality modulate chemical reactivity and reaction dynamics will aid in the rational and systematic discovery of functionality unique to nanoscale systems. This poster describes the on-demand generation and fusion of femtoliter ( $10^{-15}$  L) volume water-in-oil droplets as a means for triggering chemical reactions and studying reaction kinetics under extreme confinement, with sub-millisecond temporal resolution.

### Research Achievement

#### *Overview*

Nanofluidics and microfluidics platforms are being developed to study chemical and biochemical reaction kinetics in dimensionally-restricted, confined or crowded conditions. Current state-of-the-art microfluidic sampling strategies for creating ultrasmall reaction volumes can be characterized as steady-state, such as trapping steady-state concentration profiles of reactants and products in a microfluidic channel in small nanoliter to femtoliter volume wells defined with soft-lithography, or in discrete water-in-oil droplets created with continuous segmented flows on chip. With these methods, it is difficult to trap reacting species in ultrasmall discrete reaction volume with a well-defined time-zero for initiation of chemical reactions. Instead of relying on steady-state formation of ultrasmall reaction volumes in microfluidic channels, our strategy is to confine and trigger chemical and biochemical reactions on demand, by integrating microfluidics for precise spatiotemporal control of molecular/mass transport with nanofabricated structures. Examples of systems fabricated at the Nanofabrication Research Laboratory at the CNMS include nanoporous reaction vessels as confined volumes with tunable chemical specificity and size selectivity at molecular scales, “channels within channels” consisting of nanopore arrays addressable with surface micromachined channels, and multiscale fluidics consisting of intersections of nano-scale and micro-scale channels for on-demand generation of water-in-oil droplets with confined volumes two orders of magnitude lower than the current state-of-the-art.

#### *Approach*

We have developed a method for creating discrete femtoliter-volume water-in-oil droplets on demand, based only on a geometrically induced reduction in interfacial area between oil and water phases at microfabricated junction orifices. This on-demand generation method is driven by self-shear of droplets due to interfacial tension induced forces resulting from a localized transition in microchannel height. The magnitudes of shear stresses involved appear to be significantly less than the shearing instabilities used to split off daughter droplets from aqueous mother plugs at microfabricated junctions in continuous water-in-oil segmented flows, which implies that this method may be better suited for studying

biochemical reactions and reaction kinetics in droplets of decreased volume without loss of chemical reactivity due to redistribution of surfactant density used to passivate the oil/water interface. We fabricate devices using molding in poly(dimethylsiloxane) (PDMS). First, electron beam lithography and reactive ion etching are used to define an aqueous nanochannel (500-900 nm radius) on a silicon master. A larger main oil channel (20  $\mu\text{m}$ ) was created in SU-8 photoresist with optical lithography. These raised features were then transferred by curing PDMS on the mold, followed by creation of inlet holes for introduction of water and oil. The PDMS was permanently bonded to a glass coverslip by plasma oxidation.

### *Results and Discussion*

The abrupt change in channel height at the junction orifice allows rapidly growing aqueous droplets room to expand both vertically and horizontally away from the orifice in order to minimize surface area by approximating a spherical shape. However, droplet shapes are distorted from spherical due to steric hindrance at the hydrophobic floor and wall of the channel. The local Laplace pressure at the nose of a distorted droplet becomes less than that at the neck due to differences in the radii of curvature. The resulting pressure gradient generates local extensional and shear stresses at the oil-water interface that results in droplets splitting off from the orifice. While the time intervals between successive droplet generation events depend linearly on the pressure difference across the oil-water interface, droplet size is independent of backing pressure, consistent with the fact that droplet size is determined more by interfacial tension than flow rates at this length scale. Slow and predictable droplet generation rates allowed the use of fixed pressure pulses to gate the formation of one, two, or more droplets at a time, depending on the length and magnitude of the pulse. We find that mixing triggered by droplet fusion is more rapid than can be explained by purely diffusive contributions, and must include convection from inertial effects. Chemical reactions due to fusion of two or more droplets can be triggered at sub-millisecond time scales. We demonstrate a reversible chemical toggle switch based on alternating fusion of droplets containing acidic or basic solution, monitored with the pH-dependent emission of fluorescein, as well as enzymatic reactions in confined volumes triggered on demand by droplet fusion.

### **Future Work**

Inclusion of surfactants or surface active solutes will stabilize droplets against fusion and slow down droplet fusion dynamics, to the point where real time imaging of transient droplet shape changes may become possible. In addition to control of droplet fusion, this method may enable precise control of droplet separation without fusing in order to quantitatively study diffusion of molecules across the oil/water interfaces separating the droplets. The demonstration here of a reversible chemical toggle switch lays the groundwork for exploring more complex chemical and biochemical reaction sequences triggered and monitored in real time in discrete ultras-small reactors, such as sequential and coupled enzymatic reactions.

### **Publications**

“Interfacial Tension Controlled Fusion of Individual Femtolitre Droplets and Triggering of Confined Chemical Reactions On Demand”, S.-Y. Jung, S.T. Retterer, and C.P. Collier, *Lab Chip* **10**, 3373 (2010).

“On-Demand Generation of Monodisperse Femtoliter Droplets by Shape-Induced Shear”, S.-Y. Jung, S.T. Retterer, and C.P. Collier, *Lab Chip* **10**, 2688 (2010).

“Shear-Driven Redistribution of Surfactant Affects Enzyme Activity in Well-Mixed Femtoliter Droplets,” Y. Liu, S.-Y. Jung, and C. P. Collier, *Anal. Chem.* **81**, 4922 (2009).

# Toward Capturing Membrane Protein Dynamics with the Fiber Force Probe

Babak Sanii<sup>\*</sup>, Martin Hennig<sup>†</sup>, Masahiro Nakajima<sup>‡</sup>, Jim DeYoreo<sup>\*</sup>, Andreas Frank<sup>#</sup>, Sindy Frank<sup>#</sup>, Ivo Rangelow<sup>#</sup>, Alex Chen<sup>††</sup>, Jef Huang<sup>††</sup>, Andrea Bertozzi<sup>††</sup>, Paul Ashby<sup>\*+</sup>

<sup>\*</sup>Imaging and Manipulation Facility, Molecular Foundry, Lawrence Berkeley National Laboratory, Berkeley, California, USA, 94720.

<sup>†</sup>Department für Physik, Ludwig-Maximilians-Universität, München, Germany, 80539.

<sup>‡</sup>Center for Micro-nano Mechatronics, Nagoya University, Nagoya, Japan, 464-8603.

<sup>#</sup>Institut für Mikro- und Nano-Elektronik, Technical University Ilmenau, Ilmenau, Germany, 98684.

<sup>††</sup> Department of Mathematics, University California Los Angeles, Los Angeles, California, USA, 90095.

<sup>+</sup>pdashby@lbl.gov

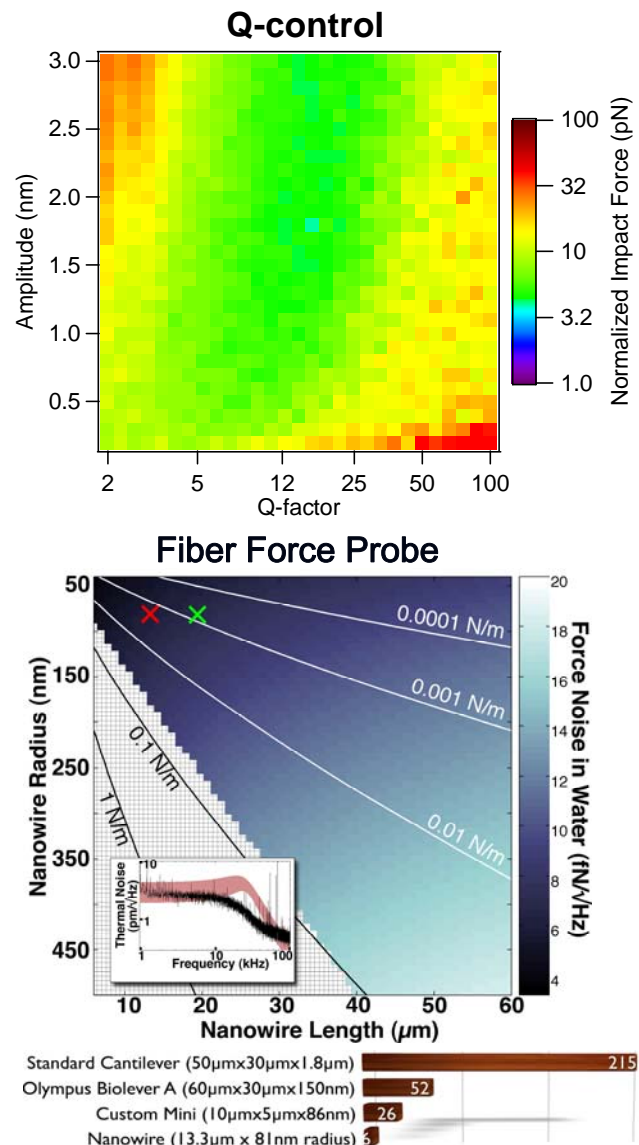
## Biological Atomic Force Microscopy

### Scientific Challenge

Living cells readily deform under the minimum force required to perform an AFM measurement precluding the imaging of membrane protein complexes at high temporal and spatial resolution. Methods to reduce significantly the minimum detectable force and increase imaging rate are required.

### Research Achievement

Although quite fashionable, attempts to use feedback methods such as Q-control and frequency modulation have failed to improve the image quality when in solution. Q-control amplifies weak tip-sample interactions and the thermal noise equally providing no overall advantage.<sup>1</sup> Frequency modulation also amplifies weak tip-sample interactions but controls the amplitude noise. However, the feedback shifts the amplitude noise to the time domain precluding a precise measurement of frequency providing no overall advantage either.<sup>2</sup> Instead, the thermal force-noise of the cantilever is the principal limitation to reducing sample deformation. Minimizing a cantilever's cross-section reduces its noise significantly and the minimum size of the cantilever is currently limited by a conventional deflection detection scheme, which requires a large surface area for laser specular reflection. A forward scattering

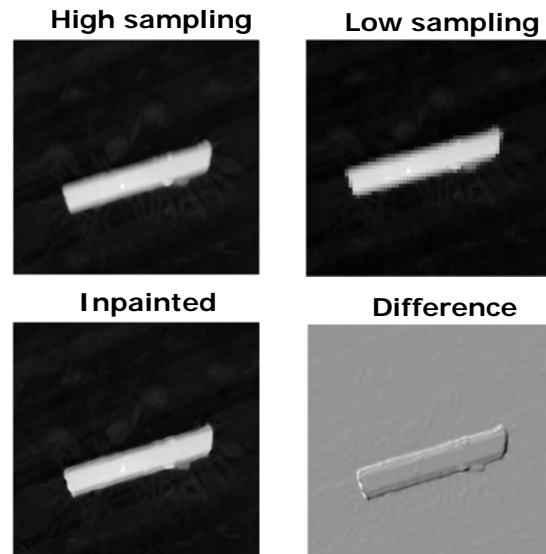


optical deflection detection technique enables the use of nanowires as cantilevers. We achieved a force noise in water of  $6 \text{ fN}/\sqrt{\text{Hz}}$  that is orders of magnitude gentler than conventional AFM. This is a significant milestone towards non-invasive scanning probe imaging of biological processes on the surfaces of vesicles and cell membranes.<sup>3</sup> Present raster scan techniques are poorly matched to the instrument limitations of Atomic Force Microscopy. Serial data collection from the local probe makes image collection slow and unable to match the timescales of many chemical and biological processes. One basic issue is the propensity of scientist oversampled data. We have used advanced image processing tools such as inpainting to recover high-resolution images from sparse quickly collected images to improve temporal resolution without applying more force or increasing bandwidth.<sup>4</sup>

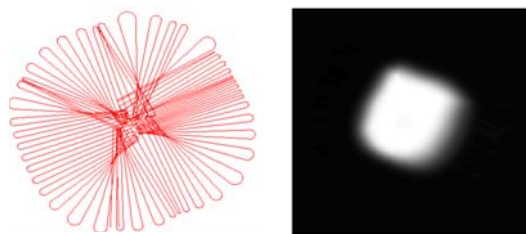
### Future Work

In the future, we will develop active scan algorithms that follow features of interest using boundary tracking and higher tip velocity low bandwidth scanner motions while accurately tracking the surface. We continue to develop gentle high resonant frequency probes for work in solution.

## Inpainting



## Non-raster Scanning



## References

- [1] Paul D. Ashby, Gentle imaging of soft materials in solution with amplitude modulation atomic force microscopy: Q control and thermal noise, *Appl. Phys. Lett.*, **2007**, *91*, 254102.
- [2] Paul D. Ashby, Impact force noise in Frequency Modulation Atomic Force Microscopy, in preparation.
- [3] Babak Sanii, Paul D. Ashby, High Sensitivity Deflection Detection of Nanowires, *Physical Review Letters*, **2010**, *104*, 147203.
- [4] Alex Chen, Paul D. Ashby, Andrea Bertozzi, Enhancement and Recovery in Atomic Force Microscopy Images, in preparation.

# Poster Group B



## Correlating Microstructure and Current Transport in High Temperature Superconductor Wires

D.J. Miller,<sup>1</sup> N.J. Zaluzec,<sup>1</sup> X. Li,<sup>2</sup> S. Sathyamurthy,<sup>2</sup> M. Rupich<sup>2</sup>

<sup>1</sup> Electron Microscopy Center, Argonne National Laboratory, Argonne, IL 60439

<sup>2</sup> American Superconductor Corporation, Devens, MA 01434

**Proposal Title:** Correlating Microstructure and Current Transport in HTS Materials

### Scientific Challenge and Research Achievement:

Phase evolution of rare-earth cuprate superconductor (REBCO) wires using a post-deposition *ex situ* conversion of metal-organic deposited (MOD) precursors has been studied using spectral imaging. In this process, an MOD precursor crystallizes to the superconducting phase with initial nucleation at the template followed by homoepitaxial growth through the thickness of the coating. [1,2] In order to achieve thicker conductor layers that can carry more current, multiple coatings are often used. However, a chemically segregated layer invariably forms at the interface between coatings. This chemically-segregated interlayer disrupts the propagation of the growth front and causes a loss of texture quality in the succeeding layer.[3] In this work using electron beam imaging and elemental mapping, we identified a mechanism by which the REBCO grows past the interlayer in two-layer films that also provides an explanation for degraded texture above the interlayer.

Double-layer precursor films were quenched at various stages of conversion and examined in cross-section by SEM and TEM/STEM. Fig. 1 shows an SEM cross-section of a film in which the conversion to REBCO has completed through the bottom layer but not yet completely proceeded into the top layer. At the interface between the layers an interlayer region consisting of various phases is observed, as marked with a dashed line. In this region, the light phase below that layer is fully converted REBCO. Above that layer, the film remains unconverted. To each side, however, REBCO is seen to have grown through and over the interlayer.

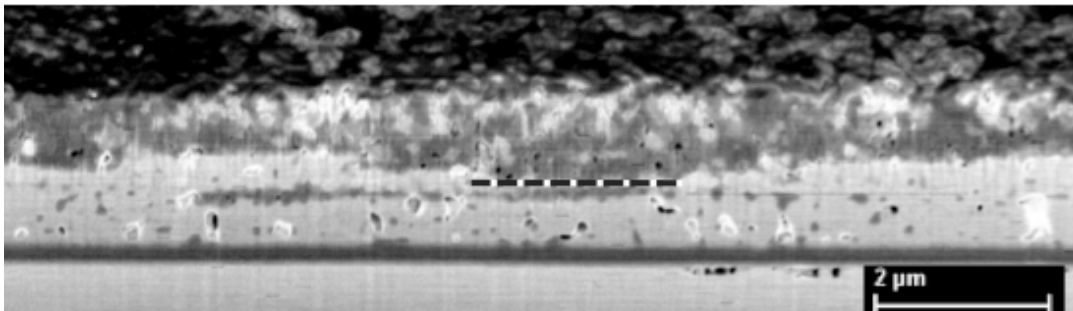


Figure 1: Cross-sectional scanning electron micrograph of a partially converted REBCO film. Although some regions have not grown past the interlayer (dashed line), in other regions the REBCO is seen to be growing through and over the interlayer.

The spectral images in Fig. 2 show the chemical segregation at the interlayer and reveal that the interlayer consists primarily of a mixture of Ba-(O,F) and Cu-O (oxygen not shown). The specific identify of the phases comprising the interlayer have been established through a variety of techniques including spectroscopy and electron diffraction.

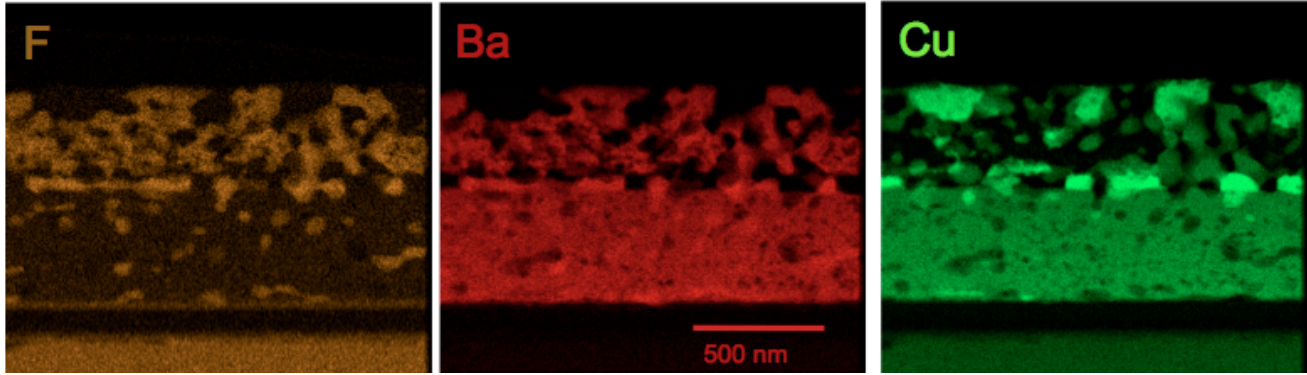


Figure 2: Spectral images revealing the chemical segregation at the interlayer.

Fig. 3 shows spectral images of three films quenched at slightly different times in the conversion process. These images that combine Ba and Cu signals show that as the REBCO growth front moves past the interlayer, REBCO growth takes place by dissolution of the Cu-O phase while the Ba-(O,F) phase remains relatively intact. Thus, a mechanism by which the REBCO surpasses the interlayer involves growth through a “channel” in the interlayer, followed by the resumption of lateral growth on top of the interlayer. This mechanism can be observed in Fig. 1. It is evident that the REBCO visible above the interlayer on either side of the dashed line grew through a channel in the interlayer and then spread laterally atop the interlayer.

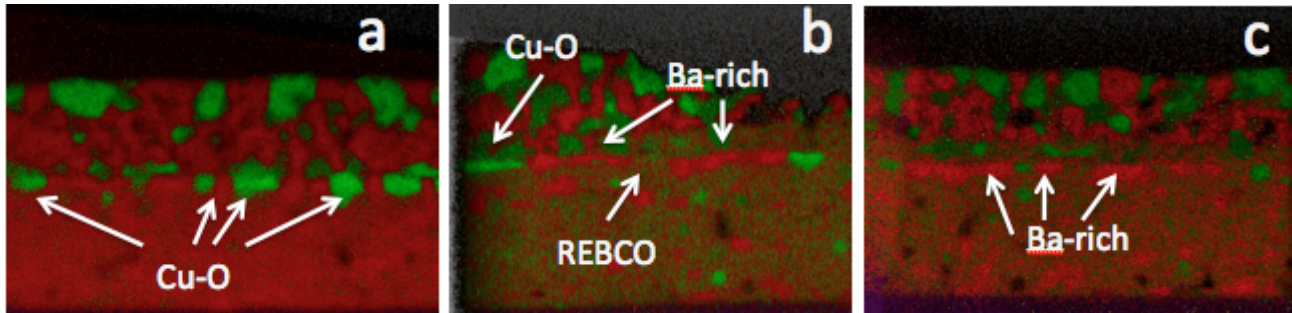


FIG. 3. Correlation maps of Ba and Cu for quenched films. Before the start of conversion (a) the interlayer consists primarily of Cu-O and Ba-rich phases. In (b), the REBCO (mottled contrast) just begun to penetrate the interlayer by dissolving Cu-O. In (c) REBCO has completely surpassed the interlayer, and the complete dissolution of Cu-O is apparent.

This growth mechanism, revealed by spectrum imaging, provides an explanation for the degradation of current-carrying capacity for the REBCO above the interlayer. The lateral growth of the REBCO above the interlayer does not take place by homoepitaxial growth on pre-existing REBCO. Instead, the REBCO grows through “channels” in the interlayer and then spreads laterally where it grows upon the interlayer phases. Without the influence of epitaxial growth on pre-existing REBCO, small deviations in orientation can develop leading to poorer texture and a decrease in performance.

#### References:

- [1] T. Izumi, et al. *IEEE Trans. Appl. Superconductivity* 19 (2009) 3119-3122
- [2] M.W. Rupich, et al. *Physica C* 412 (2004) 887-884

## Hybridization and Kondo Hole Effects in Hidden Order Phase of URu<sub>2</sub>Si<sub>2</sub>

A.V. Balatsky<sup>1</sup>, J. Haraldsen<sup>1</sup>, Y. Dubi<sup>2</sup>, P. Wolfle<sup>3</sup>, J.C. Davis<sup>4,5,6</sup>

<sup>1</sup> Center for Integrated Nanotechnologies and Theory Division, Los Alamos, NM 87545, USA

<sup>2</sup> School of Physics and Astronomy, Tel Aviv University, Tel Aviv 69978, Israel

<sup>3</sup> Institute for Theory of Condensed Matter and Center for Functional Nanostructures, Karlsruhe Institute of Technology, D-76128 Karlsruhe, Germany

<sup>4</sup> Laboratory for Atomic and Solid State Physics, Department of Physics, Cornell University, Ithaca, NY 14853, USA.

<sup>5</sup> Condensed Matter Physics and Materials Science Department, Brookhaven National Laboratory, Upton, NY 11973, USA.

<sup>6</sup> School of Physics and Astronomy, University of St. Andrews, St. Andrews, Fife KY16 9SS, Scotland.

### Scientific Thrust Area: Theory and Simulation of Nanoscale Phenomena. Integrated Modeling of Novel Materials.

**Challenge and Research Achievement.** We present recent result on Kondo and Fano lattice effects in the hybridized f-electron materials as revealed by ARPES and STM experiments [1,2]. To explain these result we introduce a phenomenological model for the “hidden order” transition in the heavy-Fermion material URu<sub>2</sub>Si<sub>2</sub> at  $T_{HO} = 17K$ . The hidden order is identified as an incommensurate, momentum-carrying hybridization between the light hole band and the heavy electron band. This modulated hybridization appears after a Fano hybridization at higher temperatures takes place. We focus on the hybridization wave as the order parameter in URu<sub>2</sub>Si<sub>2</sub> and possibly other materials with similar band structures. The model, Fig.1 is qualitatively consistent with numerous experimental results obtained from, e.g., neutron scattering and scanning tunneling microscopy [1,2,3], Fig.2.

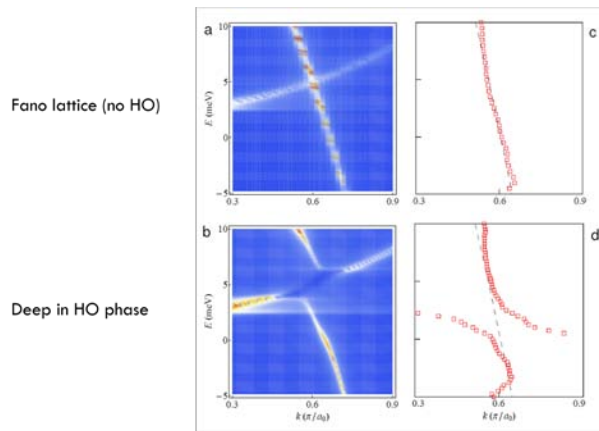


Fig.1 Comparison of Quasiparticle Interference pattern in a) Fano lattice regime above  $T_{HO}$  transition, our model calculation [1,3]; b) in the Hybridization Wave model,[3]; c) as seen in STM, above  $T_{HO}$ , data[2]; and d)  $T \ll T_{HO}$ , data [2].

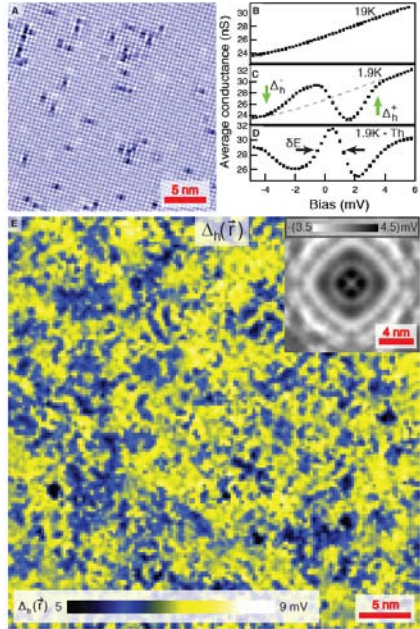


Fig.2 Kondo Hole modulation seen in STS in Hidden Order phase [2].

**Future Work.** We plan to extend this work to address possible pseudogap (PG) regime as a precursor to the Hidden Order phase. We find that the bulk of the data are consistent with the onset of PG at about  $T_{PG} \sim 25$  K, significantly higher than the Hidden Order phase transition temperature  $T_{HO} = 17$  K [4]. The schematic of the PG regime is illustrated in Fig.3.

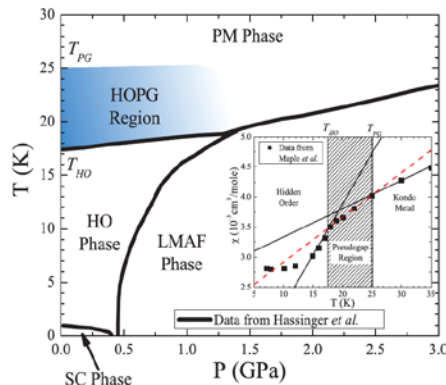


Fig.3 Schematics of the PG regime of Hidden Order phase of  $URu_2Si_2$ .

## References and Publications

- [1] P. Wolfle et al, Phys. Rev. Lett. v 105, p 24640 (2010).
- [2] M. Hamidian et al, submitted; A. Schmidt, Nature, v 465, p 570, (2010).
- [3] Y. Dubi and A.V. Balatsky, Phys. Rev. Lett. v 106, p 086401 (2011).
- [4] J. Haraldsen et.al., arXiv.1104.2931 (2011).

# Transition Metal Catalyzed Graphene: Growth, Interface Chemistry, Catalysis

P. Sutter, E. Sutter, J.T. Sadowski, M.S. Hybertsen

Center for Functional Nanomaterials, Brookhaven National Laboratory, Upton NY 11973, USA

**Scientific Thrust Area:** Interface Science & Catalysis

## Scientific Challenge and Research Achievement

Epitaxial growth on transition metals has recently become one of the most promising methods for large-scale graphene synthesis. We have studied the fundamental mechanisms of graphene growth on transition metals, using primarily powerful real-time and *in-situ* surface microscopy. Observations by low-energy electron microscopy (LEEM) demonstrate that epitaxy on Ru(0001) produces arrays of macroscopic monolayer graphene domains, whose coalescence is followed by the formation of bilayer and trilayer graphene in a controlled layer-by-layer fashion (Fig. 1). Combined *in-situ* microscopy methods, including LEEM imaging, diffraction, selected-area angle resolved photoemission spectroscopy (micro-ARPES), and scanning tunneling microscopy (STM) have been used to explore the interaction between graphene and the transition metal substrate, key to the synthesis of macroscopic graphene domains. A strong coupling between monolayer graphene and Ru(0001), and a weak interaction with Pt(111), manifest themselves in distinctly different metal-graphene spacings, graphene domain orientation, and electronic band structure. While epitaxy on Pt(111) preserves  $\pi$ -bands with linear dispersion, the interaction with metal d-states lifts the Dirac cones for graphene on Ru(0001). However, a distinct decoupling occurs as graphene sheets are added layer by layer: the top sheet of a bilayer has the electronic structure of isolated (doped) monolayer graphene, and a trilayer shows the characteristic band splitting and parabolic dispersion of isolated bilayer graphene.

Practical applications will ultimately require graphene synthesis on inexpensive substrates that can be patterned by lithographic processes and allow facile transfer to insulating supports. We have demonstrated epitaxial graphene growth on polycrystalline Ru thin films on SiO<sub>2</sub>/Si supports, as well as on epitaxial Ru(0001) films on sapphire. Our results show that graphene on thin Ru films becomes indeed transferable, while the growth still provides large domain sizes, high crystalline quality, and precise thickness control observed on single crystals.

Finally, sp<sup>2</sup> bonded graphene sheets on metal surfaces provide unique opportunities for surface and interface chemistry, as well as catalysis. The low chemical reactivity of graphene allows studying selective chemical reactions at the metal-graphene interface that can be used to tune the mechanical and electronic coupling of graphene sheets to the underlying metal, while site-dependent differences in the binding energy of metal atoms on top of epitaxial graphene provide avenues for the templated growth of monodisperse metal nanoparticle catalysts.

## Publications

- [1] P. Sutter, J.I. Flege, and E. Sutter, *Epitaxial Graphene on Ruthenium*, Nature Materials **7**, 406 (2008).
- [2] E. Sutter, D.P. Acharya, J.T. Sadowski, and P. Sutter, *Scanning tunneling microscopy on epitaxial bilayer graphene on ruthenium (0001)*, Appl. Phys. Lett. **94**, 133101 (2009).
- [3] P. Sutter, M.S. Hybertsen, J.T. Sadowski, and E. Sutter, *Electronic structure of few-layer epitaxial graphene on Ru(0001)*, Nano Lett. **9**, 2654 (2009).
- [4] P. Sutter, J.T. Sadowski, and E. Sutter, *Graphene on Pt(111): Growth and Substrate Interaction*, Phys. Rev. B **80**, 245411 (2009).

- [5] E. Sutter, P. Albrecht, and P. Sutter, *Graphene growth on polycrystalline Ru thin films*, Appl. Phys. Lett. **95**, 133109 (2009).
- [6] P. Sutter, *Epitaxial graphene: How silicon leaves the scene*, Nature Materials **8**, 171 (2009).
- [7] E. Sutter, P. Albrecht, F. Camino, and P. Sutter, *Monolayer Graphene as Ultimate Chemical Passivation Layer for Arbitrarily Shaped Metal Surfaces*, Carbon **48**, 4414 (2010).
- [8] P. Sutter, J. T. Sadowski, and E. Sutter, *Chemistry under Cover – Tuning Metal-Graphene Interaction by Reactive Intercalation*, J. Am. Chem. Soc. **132**, 8175 (2010).
- [9] G. Nazin, Y. Zhang, L. Zhang, E. Sutter, and P. Sutter, *Visualization of Charge Transport through Landau Levels in Graphene*, Nature Physics **6**, 870 (2010).
- [10] P. Sutter, P.M. Albrecht, and E. Sutter, *Graphene Growth on Epitaxial Ru Thin Films on Sapphire*, Appl. Phys. Lett. **97**, 213101 (2010).
- [11] E. Sutter, P. Albrecht, B. Wang, M.-L. Bocquet, L. Wu, Y. Zhu, and P. Sutter, *Monodisperse Ru Nanocluster Arrays Templated by Monolayer Graphene on Ru*, Surf. Sci. (2011), doi:10.1016/j.susc.2011.01.02

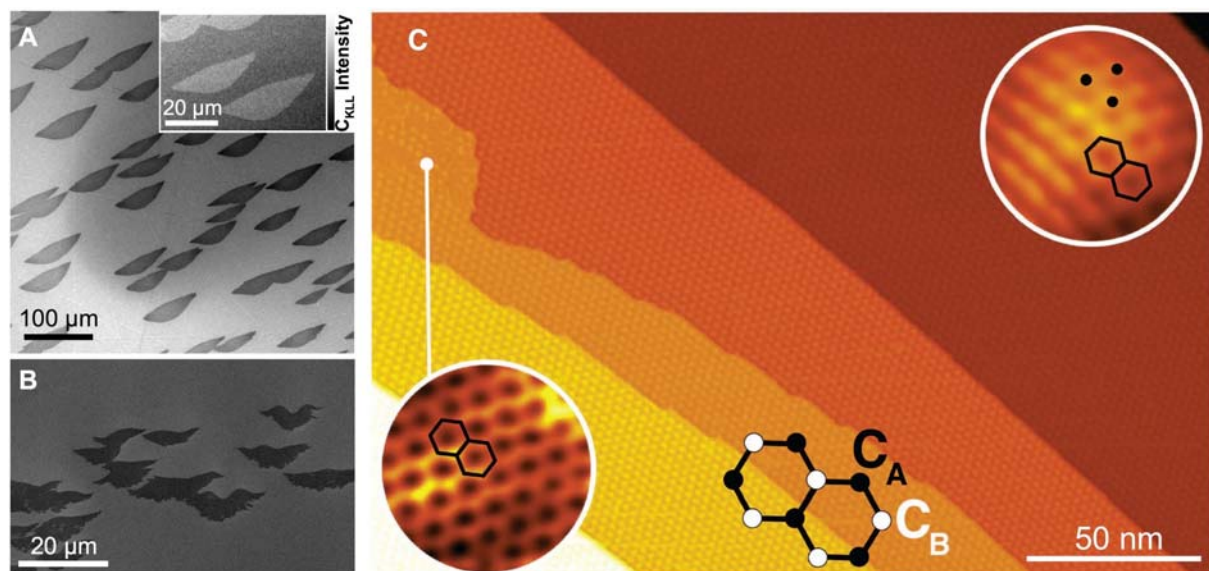


**FIG. 1. Epitaxial graphene on Ru(0001).** A – Morphology of macroscopic monolayer graphene domains. B – Bilayer graphene, grown in a layer-by-layer fashion on a completed monolayer. C – STM analysis showing a highly corrugated moiré structure of monolayer graphene, and honeycomb contrast similar to free-standing graphene on the top sheet of a bilayer.

## Poster 21 (Group B)

Title: **Electronic Transport in Graphene and Graphene Nanoribbons**

Authors: **Guangyu Xu<sup>1</sup>, Yuegang Zhang<sup>2</sup>, Fei Liu<sup>3</sup>, Xiangfeng Duan<sup>4</sup>, Yu Huang<sup>5</sup> and Kang L. Wang<sup>1</sup>**

<sup>1</sup>Department of Electrical Engineering, University of California at Los Angeles, Los Angeles, California 90095, USA; <sup>2</sup>Molecular Foundry, Lawrence Berkeley National Laboratory, 1 Cyclotron Road, Berkeley, California 94720, USA; <sup>3</sup>IBM T. J. Watson Research Center, Yorktown Heights, New York 10598, USA; <sup>4</sup>Department of Material Science and Engineering, <sup>5</sup>Department of Chemistry and Biochemistry, University of California at Los Angeles, Los Angeles, California 90095, USA

**Proposal Title:** Variability Effects of Graphene Nanoribbon Devices

### **Scientific Challenge and Research Achievement:**

An often-challenged question about nanoscale devices is the variability issue resulting from either the environment or the material itself. With no exceptions, carbon-based devices usually have enhanced variability effects inherent from their large surface-volume ratios in low-dimensions. Adversely, these variabilities cause device fluctuations and limit the reliability in large-scale production. On the contrary, these variability effects can be beneficial for applications in metrology, when the large fluctuations in nanoscale devices can be implemented as the 'signal' to achieve high sensitivities. We conducted the research of several typical variabilities in graphene-based devices through measuring their electrical properties, from the consideration of device designs in the presence of these variabilities to their implementation and potential applications as novel probing mechanisms.

Through multi-institutional collaboration among Lawrence Berkeley National Lab (LBNL), UCLA (Electrical Engineering, Materials, Chemistry and Biochemistry) and IBM T. J. Watson Research Center, we achieved the following results:

Variability effects in graphene electronics: 1) Revealed an abnormal  $1/f$  noise pattern in graphene devices originating from the non-uniform carrier distribution; proposed a new noise model that can benefit future all-graphene circuit modeling. 2) Revealed a strong correlation between  $1/f$  noise in graphene nanoribbon (GNR) devices with their band structures; provided a noise-based metrology to probe the quantum transport in GNRs

Resistance scaling rules in graphene electronics: Revealed the critical role of edge effect on the resistance scaling behavior (R-L relations) in graphene devices; the scaling behavior can be tuned by varying the gate bias, the number of layers, or the width of graphene devices. These findings are critical in realizing top-down scalable graphene electronics.

## Publications

- (1) G. Xu, C. M. Torres, Jr., J. Tang, J. Bai, E. B. Song, Y. Huang, X. Duan, Y. Zhang\*, and K. Wang, "Edge Effect on Resistance Scaling Rules in Graphene Nanostructures", ***Nano Letters*** 11, 1082-1086 (2011).
- (2) G. Xu, C. M. Torres, Jr., E. B. Song, J. Tang, J. Bai, X. Duan, Y. Zhang\*, and K. Wang, "Enhanced conductance fluctuation by quantum confinement effect in graphene nanoribbons", ***Nano Letters*** 10, 4590–4594 (2010).
- (3) G. Xu, J. Bai, C. M. Torres, Jr., E. B. Song, J. Tang, Y. Zhou, X. Duan, Y. Zhang, and K. L. Wang, "Low-noise submicron channel graphene nanoribbons", ***Applied Physics Letters*** 97, 073107 (2010).
- (4) G. Xu, C. M. Torres Jr., Y. Zhang\*, F. Liu, E. B. Song, M. Wang, Y. Zhou, C. Zeng, and K. L. Wang, "Effect of spatial charge inhomogeneity on  $1/f$  noise behavior in graphene", ***Nano Letters*** 10, 3312-3317 (2010).

## Nanostructured Graphene for Applications in Optoelectronics

Milan Begliarbekov<sup>a</sup>, Onejae Sul<sup>b</sup>, Nan Ai<sup>a</sup>, Xi Zhang<sup>a</sup>, John Santanello<sup>a</sup>, Nilam Jadav<sup>a</sup>, Sokratis Kalliakos<sup>a</sup>, Kitu Kumar<sup>b</sup>, Vikram Patil<sup>b</sup>, Eui-Hyeok Yang<sup>b</sup> and Stefan Strauf<sup>a</sup>

<sup>a</sup>Department of Physics and Engineering Physics, Stevens Institute of Technology, Castle Point on Hudson, Hoboken, NJ, USA, 07030; <sup>b</sup>Department of Mechanical Engineering, Stevens Institute of Technology, Castle Point on Hudson, Hoboken, NJ, USA, 07030

### Proposal Titles

- 1) Investigation of Bandgaps in Graphene Antidot Superlattices (CFN user proposal #30067)
- 2) Graphene based Tunable High efficiency Solar cell (CFN user proposal #604)

### Scientific Challenge and Research Achievement

Graphene is well known for its outstanding electronic, thermal, and mechanical properties, and has recently gained tremendous interest as a nanomaterial for optoelectronic devices. The near perfect transmission combined with a high sheet conductivity make graphene an ideal material for transparent contacts for flexible solar cells and displays. Other optoelectronic devices such as photodetectors rely on direct conversion of photons into charge carriers. While first demonstrations of ultrafast (100GHz) graphene photodetectors are very promising, graphene's low absorption strongly limits the achievable wall plug efficiency. Consequently, efficient photocarrier separation within graphene as well as exploration of new routes to enhance the device efficiencies becomes particularly important. To this end, nanostructured graphene in form of nanoribbons (GNRs) or in form of antidot superlattices offers new possibilities to create band gaps and to explore light harvesting and carrier separation. In both cases the underlying edge chiralities, i.e. zigzag, armchair, or mixed type edges, are very important since the atomic edge composition influences the electronic structure and thus optical and transport properties.

We have utilized the clean rooms at the Center for Functional Nanomaterials (CFN) at Brookhaven National lab to fabricate GNRs and antidot superlattices from exfoliated and CVD grown graphene by electron beam lithography.

In a first project we demonstrated that Raman spectroscopy can not only be used for layer metrology but also to monitor edge chirality [1]. In particular, we found that the G band polarization contrast reflects the fractional composition of armchair and zigzag edges and provides thus information about the purity of the edge, which serves as a convenient all-optical process monitor to characterize the degree of edge state purity in patterned graphene [1]. We furthermore fabricated double-gated field effect transistors from GNRs and discovered a new signature of Klein-tunneling in form of aperiodic conductivity oscillations in the electrical device characteristics [2].

Another project focused to elucidate the role of the localized edge state density on the optical properties [3,4]. To this end we fabricated dye sensitized antidot superlattices, i.e. nanopatterned graphene with adsorbed rhodamine 6G molecules. The fluorescence from deposited dye molecules was found to quench strongly as a function of increasing antidot filling fraction, whereas it was enhanced in unpatterned but electrically back-gated samples. This contrasting behavior is strongly indicative of a built-in lateral electric field of up to 260 mV accounting for p-type doping as well as fluorescence quenching due to dissociation of electron-hole pairs from attached dye molecules. Our study provided new insights into the interplay of localized edge states in antidot superlattices and the resulting band bending, which are critical properties to enable novel applications of nanostructured graphene for light harvesting and photovoltaic devices.

### **Future Work**

Our current efforts focus on determining the band gap of the fabricated GNRs and antidot superlattices using low-temperature differential conductivity measurements with the particular goal to study its dependence on edge chirality and filling fraction. Another goal is to directly control the edge chirality by transforming unwanted zigzag into the preferred armchair type edges, which are predicted to display higher bandgaps. We furthermore work on implementing on-chip strain tunability of the band gap of nanostructured graphene for applications in IR-LWIR photodetectors.

### **Publications** specific to work done at CFN

- [1] M. Begliarbekov, O. Sul, S. Kalliakos, E.-H. Yang, and S. Strauf, “Determination of edge purity in bilayer graphene using  $\mu$ -Raman spectroscopy”, *Appl. Phys. Lett.* **97**, 031908 (2010).
- [2] M. Begliarbekov, O. Sul, N. Ai, E.-H. Yang, and S. Strauf, “Aperiodic conductivity oscillations in quasiballistic graphene heterojunctions”, *Appl. Phys. Lett.* **97**, 122106 (2010).
- [3] M. Begliarbekov, O. Sul, J. Santanello, N. Ai, Z. Zhang, E.H. Yang, and S. Strauf, “Localized States and Resultant Band Bending in Graphene Antidot Superlattices”, *Nano Lett.* **11** 1254 (2011).
- [4] S. Strauf and E.-H. Yang, “Graphene Optoelectronics based on Antidot Superlattices”, invited paper, SPIE Defense, Security, and Sensing (2011), in print.

## Revealing the electronic structure of complex materials at the atomic scale with single atom sensitivity

Juan C. Idrobo,<sup>1</sup> W. Zhou,<sup>2,1</sup> J. Nanda,<sup>1</sup> and S. Pennycook<sup>1</sup>

<sup>1</sup>Materials Science and Technology Division, Oak Ridge National Laboratory

<sup>2</sup>Department of Physics and Astronomy, Vanderbilt University

**Scientific Thrust Area:** Advanced Microscopy and Microanalysis (Scientific User Facilities Division) and STEM: Atomic Structure and Properties of Materials (Materials Science and Engineering Division) SHaRE Proposal ID 09\_IdroboJC\_01.

**Scientific Challenge and Research Achievement:** The research summarized will be focused on two studies – (i) atomically localized Plasmon resonance in monolayer graphene and (ii) vortex beams for atomic resolution dichroism.

(i) *Atomically Localized Plasmon Resonance in Monolayer Graphene:* A long-term goal for electronics has been to make devices smaller, faster, lighter, and cheaper. After several decades of continuous development, the size of transistors is approaching the limit due to physical restrictions and cost. One promising solution is to integrate optics with nanoelectronic devices and use light to transmit data. The major drawback, however, is the orders of magnitude mismatch between the  $\mu\text{m}$ -sized optical waveguides and the nm-sized active electronic components.

Using electron energy-loss (EEL) spectrum imaging in scanning transmission electron microscopy (STEM), we observe that a single point defect (substitutional Si atom) in monolayer graphene can act as an “atomic antenna” in the petaHertz ( $10^{15}$  Hz) frequency range, leading to surface plasmon resonances at the sub-nm scale (see Fig. 1), which suggests that by atomically engineering or self-assembling substitutional Si atoms in graphene, *e.g.* along grain boundaries or into linear arrays, high frequency signals could be transmitted along these atomically confined paths, and atomic scale plasmonic/optoelectronic devices would be made possible [\*].

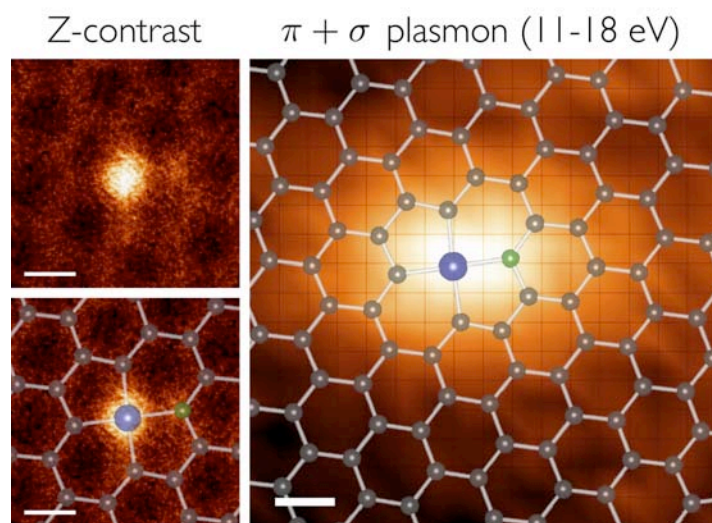


**Figure 1.** (Left) Z-contrast image of monolayer graphene in the presence of substitutional Si and N. The C, Si, and N atoms are shown schematically as gray, blue and green, respectively. (Right) Integrated signal of  $\pi + \sigma$  surface plasmons in the energy range of 11-18 eV. A localized, sub-nm scale enhancement in the  $\pi + \sigma$  plasmon is observed in graphene due to the presence of Si and N atoms. Scale bar is 0.2 nm.

(ii) *Vortex beams for atomic resolution dichroism*: It is now possible, using state-of-the-art electron microscopes, to obtain direct chemical identification of individual atoms based on image intensity together with spectroscopic fine-structure information. However, it has not yet been feasible to measure magnetic properties of individual atoms or single atomic columns. A way to obtain atomic-scale magnetic information within an electron microscope would be to polarize the electron beam such that each electron carries a specific orbital angular momentum (OAM). During the last year, research groups in Japan [1], Europe [2], and the U.S.A. [3], have shown experimentally that the interference of an electron plane wave with a fork dislocation grid splits the incident wave into a series of transmitted electron vortex beams that carry OAM.

Here, by directly evaluating the diffracted pattern formed by a plane wave that has passed through a grid containing fork dislocations, we will present an analytical description of vortex beams carrying OAM. We will show the optical conditions under which small probes with OAM can be achieved and discuss the parameters necessary to design an atomic-resolution scanning transmission electron microscope using vortex beams.

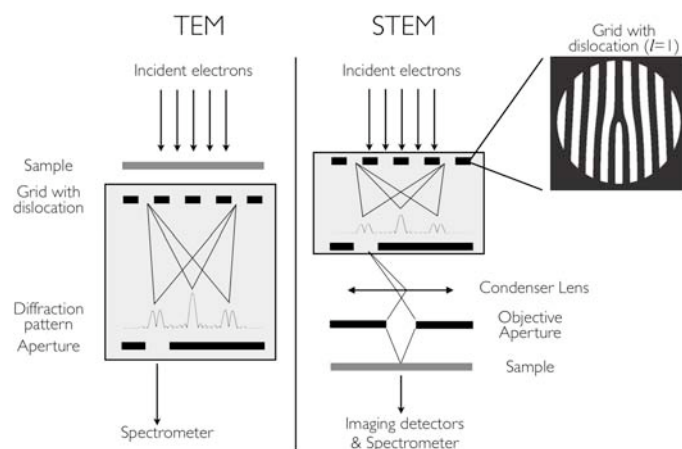


**Figure 2:** Schematic of how electron vortex beams can be produced in the (S)TEM. In TEM, a grid with fork dislocations is placed after the sample and then an aperture is used to select a single electron vortex beam with the desired OAM [2]. In STEM, the dislocation grid and the beam-selecting aperture (highlighted inside the gray rectangle) are placed before the sample. Extra condenser lenses are also required to magnify the electron vortex before the probe forming objective aperture. The resulting electron probe can be used as in any other STEM, but with the added benefit that since it carries an effective OAM, magnetic properties of the sample could also be studied directly.

**Future Work:** Research will focus on (i) revealing the electronic and optical properties of different adatoms in graphene and (ii) producing concentric vortex beams that carry simultaneously different OAMs.

**Support:** Research supported by the SHaRE User Facility (JCI) and the Materials Science and Engineering Division (SJP), both sponsored by the Office of Basic Energy Sciences, U.S. Department of Energy.

#### References:

- [1] M. Uchida and A. Tonomura, *Nature* **464** 737 (2010).
- [2] J. Verbeeck, H. Tian, and P. Schattschneider, *Nature* **467** 301 (2010).
- [3] B.J. McMorran et al., *Science* **331** 192 (2011).

#### Publications:

1. W. Zhou, J. Nanda, S.J. Pennycook, and J.C. Idrobo, "Atomically Localized Plasmon Resonance in Monolayer Graphene," submitted to *Nature Nanotechnology* (April 2011).
2. J.C. Idrobo and S.J. Pennycook, "Vortex beams for atomic resolution dichroism," submitted to *Physical Review Letters* (February 2011).

# Chemical Imaging of Functional Nanostructures Fabricated by Thermochemical Nanolithography

Debin Wang<sup>1,2</sup>, Marcel Lucas<sup>2</sup>, Suenne Kim<sup>2</sup>, Vamsi K. Kodali<sup>2</sup>, Simon C. Jones<sup>3</sup>, Zhongqing Wei<sup>4</sup>, Walter A. de Heer<sup>2</sup>, Paul E. Sheehan<sup>4</sup>, P. James Schuck<sup>1</sup>, D. Frank Ogletree<sup>1</sup>, Jennifer E. Curtis<sup>2</sup>, Seth R. Marder<sup>3</sup>, William P. King<sup>5</sup>, Elisa Riedo<sup>2</sup>

<sup>1</sup>Materials Sciences Division and The Molecular Foundry, Lawrence Berkeley National Laboratory, Berkeley, CA 94706

<sup>2</sup>School of Physics, Georgia Institute of Technology, Atlanta, Georgia 30332

<sup>3</sup>School of Chemistry and Biochemistry, Georgia Institute of Technology, Atlanta, Georgia 30332

<sup>4</sup>Chemistry Division, U.S. Naval Research Laboratory, Code 6177, Washington, D.C. 20375

<sup>5</sup>Department of Mechanical Science and Engineering, University of Illinois Urbana-Champaign, Urbana, IL 61801

**User Proposal:** Molecular Foundry #396: Quantitative imaging of chemical nanopatterns written by thermochemical nanolithography

## Scientific Challenge and Research Achievement

Recently, we have developed a novel atomic force microscope (AFM) based nanofabrication technique called thermochemical nanolithography (TCNL). TCNL uses a resistively heated AFM cantilever to thermally activate chemical reactions on a surface with nanometer resolution and at high speeds (up to 1.4 mm/s). This technique can be used for fabrication of functional nanostructures that are appealing for various applications in nanofluidics, nanoelectronics, nanophotonics, and biosensing devices. We have demonstrated that TCNL can be employed to (1) modify the wettability of a polymer surface at the nanoscale, (2) fabricate nanoscale templates on polymer films for assembly of nano-objects, such as proteins and DNA, (3) fabricate conjugated polymer semiconducting nanowires, and (4) control the extent of reduction of graphene oxide and pattern nanoscale regions of reduced graphene oxide within a graphene oxide sheet.

The characterization of the TCNL generated patterns and the measurement of the reaction efficiency calls for the use of surface-sensitive, non-invasive chemical imaging techniques with  $\mu\text{m}/\text{nm}$  spatial resolution. We have employed a variety of direct chemical imaging techniques to characterize TCNL generated micrometer scale structures, such as Raman spectroscopy, infrared spectroscopy, and fluorescence microscopy. AFM based indirect chemical imaging techniques have also been employed to characterize nanometer scale structures, such as friction force microscopy, tapping mode phase imaging. However, direct chemical characterization of as-prepared nanostructures still remains as a challenge. Most of the conventional optical microscopy methods cannot be applied to chemical patterns on nanometer scale, due to their relatively low spatial resolution hindered by diffraction limit. Raman microscopy has emerged as an extremely chemically-sensitive technique with sub-micron spatial resolution. It offers numerous advantages over infrared or fluorescence spectroscopy. The development of new optics and laser sources, as well as the discovery of surface enhanced Raman spectroscopy (SERS) has enabled *in situ* study of electrochemical reactions, fingerprinting of a wide range of proteins and bacteria, mapping of cell membrane proteins, and study of adsorption of biomolecules on various surfaces, including self-assembled monolayers.

In the first stage of the proposed work, we have correlated the intensity and position of the Raman bands with the concentration of the groups monitored. Confocal Raman spectroscopic maps were collected from TCNL-generated polymer nanopatterns and reduced graphene oxide nanopatterns. The Raman spectra from the nanopatterns were compared with the spectra collected from bulk standard samples. For example, the growth of characteristic Raman peaks as a function of a variety of parameters, such as heating temperature, polymer thickness, contact time, has been monitored by confocal Raman for the conversion of a sulfonium salt precursor to PPV.

### **Future Work**

In the future, we are planning to use tip-enhanced Raman microscopy (TERS) to characterize quantitatively and image chemical nanopatterns of sizes down to several tens of nanometers in various types of materials. Amides bands from polymers, proteins and bacteria were previously detected by TERS. SERS of self-assembled monolayers of 4-aminothiophenol with exposed amino groups was also reported, showing that TERS has the potential chemical and surface sensitivity required.

Another useful technique for the characterization of surface chemical modifications is the Sum Frequency Generation vibrational spectroscopy (SFG). Since the selection rules for Raman and SFG are different, SFG can serve as a complementary surface-sensitive technique and detect additional characteristic bands or enhance detected bands from the chemical nanopatterns. The order and orientation dependence of the SFG signal can also provide information about the conformation of the polymer chains on the surface.

### **References**

1. R. Szożkiewicz, T. Okada, S. C. Jones, T.-D. Li, W. P. King, S. R. Marder, and E. Riedo, *Nano Lett.* 7, 1064 (2007).
2. D. Wang, T. Okada, R. Szożkiewicz, S. C. Jones, M. Lucas, J. Lee, W. P. King, S. R. Marder, E. Riedo, *Applied Physics Letters* 91, 243104 (2007).
3. D. Wang, V. K. Kodali, W. D. Underwood, J. Jarvholm, T. Okada, S. C. Jones, M. Rumi, Z. Dai, W. P. King, S. R. Marder, J. E. Curtis, E. Riedo, *Advanced Functional Materials*, 19, 3696 (2009).
4. D. Wang, S. Kim, W. D. Underwood, W. P. King, C. L. Henderson, S. R. Marder, E. Riedo, *Applied Physics Letters*, 95, 233108 (2009)
5. Z. Wei, D. Wang, S. Kim, S.-Y., Kim, C. Berger, Y. Hu, A. R. Laracuente, S. R. Marder, W. P. King, W. A. de Heer, P. E. Sheehan, E. Riedo, *Science*, 328, 1373 (2010).

**Characterizing a novel form of carbon with advanced electron  
microscopy techniques**

**Eric Stach**

**Center for Functional Nanomaterials, Brookhaven National Lab**

**Scientific Thrust Area**

Electron Microscopy

**Scientific Challenge and Research Achievement**

We will describe characterization efforts concerning a novel form of carbon prepared by structural modification of graphene.



## Carbon-based Nanomaterials: Spectroscopic Studies on Single-walled Carbon Nanotubes and Graphene

Pulikel M. Ajayan,<sup>1</sup> Jared J. Crochet,<sup>2</sup> Andrew M. Dattelbaum,<sup>2</sup> Stephen K. Doorn,<sup>2</sup> Charudatta Galande,<sup>1</sup> Dani M. Keshav,<sup>2</sup> Junichiro Kono,<sup>1</sup> Jinho Lee,<sup>2</sup> Aditya Mohite,<sup>2</sup> Rohit P. Prasad,<sup>2</sup> and James H. Werner<sup>2</sup>

<sup>1</sup>Rice University, Houston, TX 77005

<sup>2</sup>Center for Integrated Nanotechnologies, Los Alamos National Laboratory, Los Alamos New Mexico 87545

**Scientific Thrust Area:** We will present several examples of the capabilities and expertise at the Center for Integrated Nanotechnologies (CINT) available in the field of carbon-based nanomaterials. The work presented demonstrates synergy between multiple thrusts at CINT, including the Soft, Biological and Composite Nanomaterials Thrust and the Nanophotonics and Optical Nanomaterials Thrust. We will highlight some user project interactions, as well.

**Scientific Challenge and Research Achievement:** CINT carries out an active program in carbon nanotube research, with efforts in spectroscopic studies of fundamental electronic structure and optical properties, noncovalent functionalization chemistry, redox behavior, separations, optical sensing, and nanoelectronic devices. Our presentation will highlight some of our capabilities in the context of enrichment and fundamental spectroscopy of metallic “armchair” structures, and in presenting recent studies of defect and dopant imaging and dynamic 1-D surface behavior on single semiconducting nanotubes. Specifically, we will

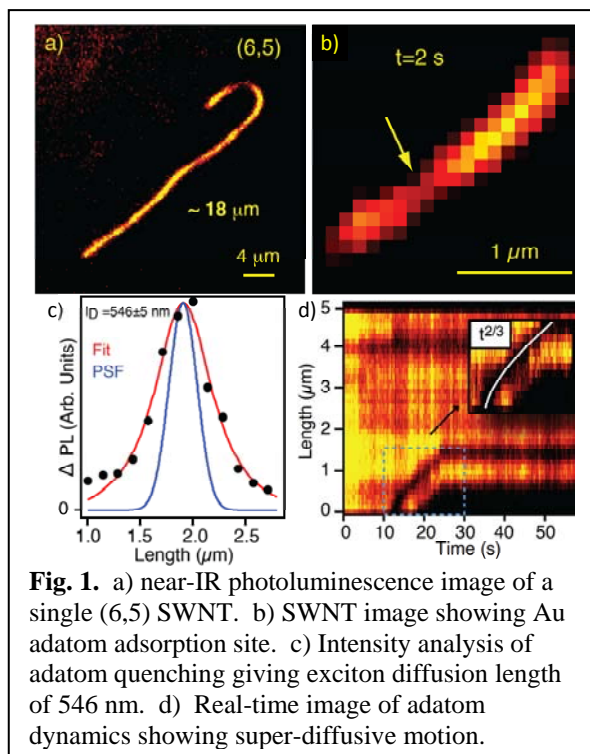


**Fig. 1.** a) near-IR photoluminescence image of a single (6,5) SWNT. b) SWNT image showing Au adatom adsorption site. c) Intensity analysis of adatom quenching giving exciton diffusion length of 546 nm. d) Real-time image of adatom dynamics showing super-diffusive motion.

present results demonstrating the use of density gradient ultracentrifugation for enrichment of nanotube samples in armchair structures. Raman spectroscopic evidence will be given as evidence of enrichment. Further, Raman investigations of these enriched samples focus on behavior of the G-band in the region of  $\sim 1550\text{-}1590\text{ cm}^{-1}$ . The appearance of a broad peak at  $\sim 1550\text{ cm}^{-1}$  (G-minus peak) has conventionally been attributed to the presence of metallic nanotubes. We present evidence that for the only true metallic nanotubes (the armchair structures) this peak is actually absent and only a high frequency (G-plus peak) at  $\sim 1590\text{ cm}^{-1}$  is observed. Furthermore, by demonstrating this behavior at the ensemble level, we show that the absence of the G-minus peak is a general result for all armchair structures.

Significant challenges also exist at the nanoscale in understanding electronic impurities associated with adatom defects due to lack of

imaging probes of dynamical surface behaviors. We will present direct imaging results of adatom dopant behavior in the 1-D nanotube surface environment. As seen in Figure 1, direct imaging of long bright nanotubes allows evaluation of dynamic surface quenching and diffusion behaviors. We will demonstrate how this capability allows direct determination of exciton diffusion behavior. Additionally, we will discuss the dynamic behavior of adatom diffusion. Specifically, diffusion kinetics of gold adatoms suggests a superdiffusive mechanism driven by environmental and surface structure fluctuations.

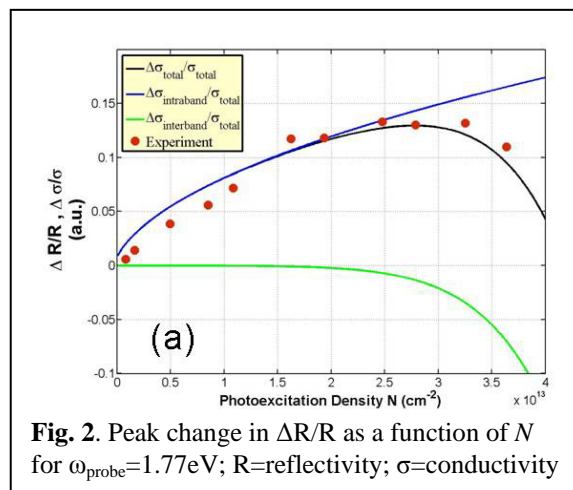
In addition to carbon nanotube research, CINT has an active program in graphene. We will describe our recent work establishing a large area graphene growth capability for CINT

users and CINT scientists, as well as some recent spectroscopic results on these films. In particular, we will show results from an ultrafast pump-probe experiment with *high* photon energies that isolate the Drude-like *intraband dynamics* of photoexcited carriers. We directly demonstrate the relativistic nature of the photoexcited Dirac quasiparticles by observing a nonlinear scaling of the response with the density of photoexcited carriers as shown in Figure 2. The intraband conductivity dominates the signal for all but the highest carrier densities, and the data thus follows the  $\sqrt{N}$  dependence (solid blue line) exhibited by relativistic two-dimensional Dirac quasiparticles.

This is in striking contrast to the linear scaling that is usually observed in tabletop experiments for non-relativistic charge carriers. Our results also indicate strong electron-phonon coupling in graphene, leading to a sub-100 femtosecond thermalization between high energy photoexcited carriers and optical phonons.

We have also used CINT capabilities to characterize functionalized graphene, such as graphene oxide (GO). Users working, in part, at CINT demonstrated that graphene emits a structured, strongly pH-dependent visible fluorescence. Based on experimental results and model computations, this fluorescence was proposed to arise from quasi-molecular fluorophores, similar to polycyclic aromatic compounds formed by the electronic coupling of carboxylic acid groups with nearby carbon atoms of graphene. Sharp and structured emission and excitation features resembling the spectra of molecular fluorophores are present near 500 nm in basic conditions. The GO emission reversibly broadens and red-shifts to ca. 680 nm in acidic conditions, while the excitation spectra remain very similar in shape and position, consistent with excited state protonation of the emitting species in acidic media. The sharp and structured emission and excitation features suggest that the effective fluorophore size in the GO samples is remarkably well defined.

**Future Work:** Future experiments in carbon-based nanomaterials will involve functionalization and characterization of single walled carbon nanotubes and graphene samples. In addition, we will continue to develop new imaging tools to characterize carbon-based nanomaterials for the user community to promote nanoscience in this rapidly expanding area.



## Combinatorial Discovery & Characterization of Upconverting Nanocrystal Probes

Emory Chan, Gang Han, Bruce Cohen, and Delia Milliron  
*The Molecular Foundry, Lawrence Berkeley National Laboratory, Berkeley, CA 94720*

**Scientific Thrust Area:** Nanoparticle synthesis, combinatorial nanoscience,  
upconverting nanomaterials

### Scientific Challenge and Research Achievement

Lanthanide-doped nanocrystals can exhibit visible upconversion luminescence when excited with near-infrared (NIR) laser excitation, enabling their use as non-toxic, non-photobleaching probes in cells and tissue. Existing upconverting materials, however, have narrow excitation ranges and exhibit multiple emission peaks that are not optimal for multi-probe biological imaging. Tuning the emission of upconverting materials is hindered by the insensitivity of lanthanide  $f$ -orbitals, and energy transfer between ions in multiply doped systems is difficult to predict due to the complex  $4f$  energy levels of lanthanide ions. Thus, optimizing upconverting probes over this expansive parameter space presents sizeable synthetic and analytical challenges.

We describe the high-throughput discovery and optimization of upconverting nanoparticle (UCNP) probes with tunable emission spectra. To perform combinatorial screening of these materials, we used an automated platform capable of synthesizing a library of high quality upconverting nanocrystals (e.g. NaYF<sub>4</sub>) with various lanthanide dopant combinations and concentrations. To characterize the optical properties of these materials, we constructed a high-throughput spectroscopic apparatus that can acquire upconversion spectra of samples in a 96-well microplate using excitation from eight NIR laser diodes. We demonstrate that by using non-standard pairs of lanthanide dopants, we can enhance the spectral selectivity of upconverting probes by selectively populating energy levels or selectively quenching undesired transitions via energy transfer. Finally, we will discuss the underlying mechanisms behind the selectivity of these materials and will discuss the advantages of these properties in robust biological probes.

### Future Work

We will use our high-throughput combinatorial approach to screen large libraries of ternary and quaternary-doped upconverting materials for unique physical properties. Materials with high quantum yields and selectivities will be used for multi-probe biological imaging.

### Publications:

1. Chan, E. M.; Xu, C.; Mao, A.W.; Han, G.; Owen, J. S.; Cohen, B. E.; Milliron, D. J. *Nano Letters* **2010**, *10*, 1874-1885.
2. Wu, S.; Han, G.; Milliron, D. J.; Aloni, S.; Altoe, V.; Talapin, D. V.; Cohen, B. E.; Schuck, P. J. *Proc. Natl. Acad. Sci. U.S.A.* **2009**, *106*, 10917-10921.



# Advanced Materials Science: Scanning Tunneling Microscopy of Complex Oxides and Chiral Molecular Superstructures

Nathan P. Guisinger

Center for Nanoscale Materials, Argonne National Laboratory

**Scientific Thrust Area** - Scanning tunneling microscopy (STM) is a powerful tool for characterizing material systems at the atomic-scale. In addition to structural information, its dependence on a tunneling current for feedback makes the STM sensitive to the electronic local density of states (LDOS) of the substrate, which can be extracted via scanning tunneling spectroscopy (STS). Furthermore, coating an STM probe with a magnetic thin film makes the instrument sensitive to the magnetic structure of the surface (spin-polarized STM).<sup>1</sup> Here we present examples of our state-of-the-art STM research using both commercial and custom home-built instruments. This fundamental research is critical for advanced energy storage, generation, performance and efficiency.

**Scientific Challenge and Research Achievement** - Oxides containing transition elements within the d-block of the periodic table exhibit a wide range of physical properties and structure, while comprising one of the most interesting set of materials currently studied. Striking phenomena have been observed in oxide thin films, heterostructures, and superlattices, in which some layered oxide structures result in material attributes that are not observed in the individual constituents. Many of these effects are believed to be governed by interface physics, which is very difficult to probe locally. As shown in Fig. 1, we have developed a novel cross-sectional STM technique, applied for the first time to complex oxide thin films, heterostructures, and superlattices.<sup>2-4</sup> In addition to atomic-scale topographic imaging, we can spatially map the electronic structure across these interfaces. We will show results for LCMO and LNO thin films grown on STO as well as an LCMO-YBCO superlattice.

Molecular technology has attracted scientists by the great opportunities and versatility it offers as a replacement for standard semiconductor electronics with organic materials, thus bringing down the cost, and opening endless possibilities for chemical synthesis, and scientific breakthrough. Of particular interest is the use of chiral molecules, such as alanine (the simplest chiral amino acid), to build self-assembled nanoscale structures for electron confinement.<sup>5</sup> L- and D-alanine on Cu(111) were studied using scanning tunneling microscopy and spectroscopy revealing the formation of a uniform hexagon porous network of average dimension  $\sim 12$  Å. Each pore acts as a tiny quantum corral, which confines the surface state of the Cu(111) free electron gas, as illustrated in Fig. 2. Furthermore, excess alanine molecules become trapped at the perimeter within the pores of the molecular network and are observed as rotating or immobile spatial states moving around the perimeter.

**Future Research** - We will be extending our studies to new oxide superlattices, also being grown using our unique oxide MBE system, and chiral molecular systems for spin-filter applications.

## References

1. P. Sessi, N. P. Guisinger, J. R. Guest, and M. Bode: Temperature and Size Dependence of Antiferromagnetism in Mn Nanostructures; *Phys. Rev. Lett.* 103, 167201 (2009).
2. N. P. Guisinger, T. S. Santos, J. R. Guest, T.-Y. Chien, A. Bhattacharya, J. W. Freeland, and M. Bode: Nanometer-Scale Striped Surface Terminations on Fractured SrTiO<sub>3</sub> Surfaces, *ACS Nano* 12, 4132 (2009).
3. T. Y. Chien, T. S. Santos, M. Bode, N. P. Guisinger, and J. W. Freeland: Controllable local modification of fractured Nb-doped SrTiO<sub>3</sub> surfaces, *Appl. Phys. Lett.* 95, 163107 (2009).
4. T. Y. Chien, J. A. Liu, J. Chakhalian, N. P. Guisinger, J. W. Freeland: Visualizing nanoscale electronic band alignment at the La<sub>2/3</sub>Ca<sub>1/3</sub>MnO<sub>3</sub>/ONb:SrTiO<sub>3</sub> interface, *Phys. Rev. B* 82, 041101 (2010).

5. E. N. Yitamben, R. A. Rosenberg, N. P. Guisinger: Molecular motion confined to self-assembled quantum corrals, submitted *Nature Chemistry* (2011).

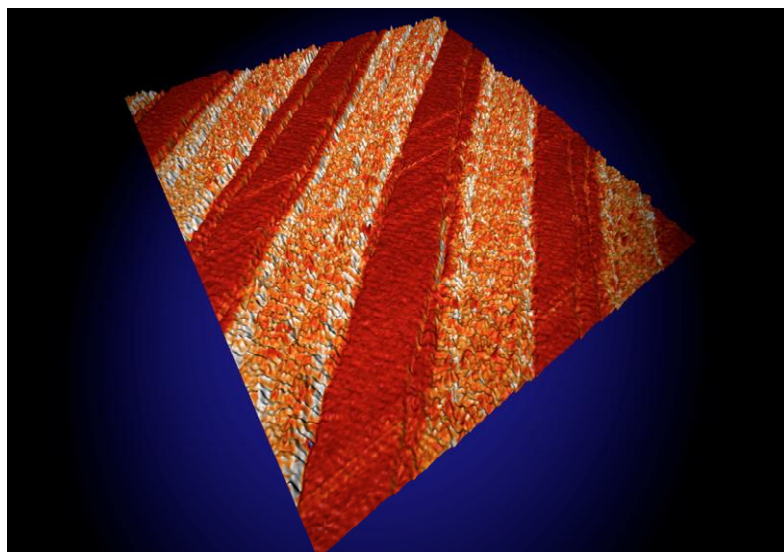


Figure 1: UHV-STM topographic image of fractured STO. The surface is atomically flat and the overlaid spatial conductance map shows electronic contrast between SrO and TiO<sub>2</sub> surface terminations forming striped domains.

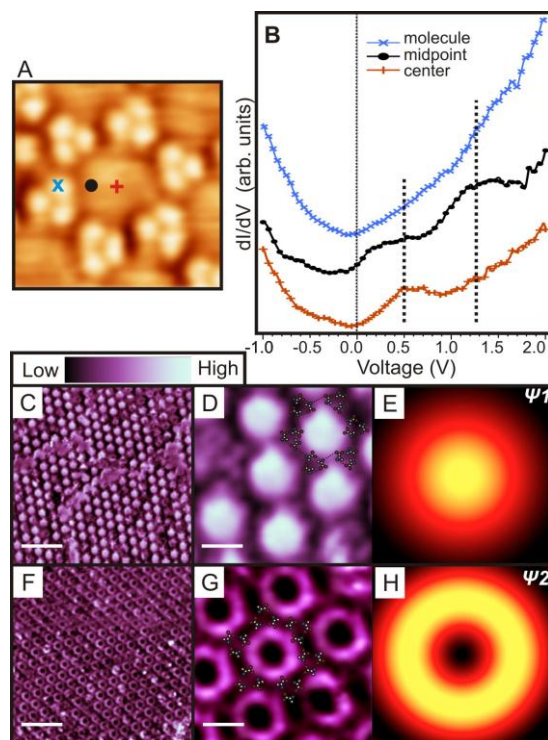


Figure 2: Probing the confined states of quantum corrals formed in the hexagonal pores of the molecular superstructure. (A) Filled states image of a single unit cell. (B)  $dI/dV$  spectra showing position dependence of the confined local density of states. (C) Spatial conductance ( $dI/dV$ ) map of the D-alanine molecular superstructure at the lower energy state. (D) Zoom-in image showing the hexagonal pores with a maximum LDOS at the center of the pore. (E) Calculated LDOS map of the first eigenstate ( $\psi_1$ ) at +0.5 V for a 1.2 nm pore. (F) Spatial conductance map of the L-alanine molecular superstructure probing the higher energy state. (G) Zoom-in image showing the donut structure of the higher energy confined state. (H) Calculated LDOS map for higher energy eigenstate ( $\psi_2$ ).

## Novel Approaches to Size Control in the Synthesis of Magnetic Nanoparticles

Dale L. Huber<sup>1</sup>, Danielle L. Fegan<sup>2</sup>, Natalie L. Adophi<sup>3</sup>, Jason E. Trujillo<sup>3</sup>, Todd C. Monson<sup>1</sup>, H. C. Bryant<sup>2</sup>, Helen J. Hathaway<sup>3</sup>, Debbie M. Lovato<sup>3</sup>, Kimberly S. Butler<sup>3</sup>, Trace E. Tessier<sup>2</sup>, Richard S. Larson<sup>3</sup>, Edward R. Flynn<sup>2</sup>

<sup>1</sup> Center for Integrated Nanotechnologies, <sup>2</sup> Senior Scientific LLC, <sup>3</sup> University of New Mexico

Proposal Title: Superparamagnetic Nanoparticles for Biomagnetic Imaging

### Scientific Challenge and Research Achievement

The SQUID remanence technique has been demonstrated to be a powerful new mode of biomedical imaging. The details of the approach have been published elsewhere<sup>1</sup>, but it relies on the Néel relaxation of superparamagnetic nanoparticles. While there are significant biological and medical issues in developing this technique for the clinical setting, at its heart this is a nanotechnology problem. Due to instrumental and clinical constraints, only Néel relaxations that occur between 50 msec and 2 sec can be detected. Despite a relatively large time window, this sets extremely narrow constraints on the particle sizes that are useful. The Néel relaxation time,  $\tau_N$  is governed by the equation:  $\tau_N = \tau_0 \exp(KV/(k_B T))$ .<sup>2</sup> Where  $\tau_0$  is a constant prefactor, K is the magnetocrystalline anisotropy of the material, and V is the volume of an individual nanoparticle. Inserting the values for magnetite means that to have a relaxation time in the window of interest, a nanoparticle must have a diameter between 23.5 and 24.5 nm.

Initial experiments focused on the use of commercially available particles that were already functionalized and had known behavior in physiological conditions. The best commercial particles available at the time yielded a signal of only 0.1% of what would be expected for the magnetic mass if the particle sizes were optimal. This is a result of the extremely broad size dispersity of commercially available nanoparticles. Clearly, optimization of this technique requires custom synthesis of nanoparticles.

There are many ways to make nanoparticles, but most wet chemical approaches are made following what is generally referred to as the LaMer mechanism.<sup>3</sup> In this approach, there is a brief initial stage where particles nucleate and a relatively long stage where these particles grow without significant nucleation. The difficulty with this approach is that in a closed system, the final particle size is determined by the amount of product divided by the number of nuclei. As a practical matter, most size control approaches attempt to control the number of nuclei formed by, for example, controlling heating rate. Nucleation is a complex and chaotic process, and this size control can be extended only through a limited range, and with limited batch to batch reproducibility.

For these reasons, we have developed an approach we refer to as the Extended LaMer Mechanism. Instead of a closed system, we synthesize particles using a continuous addition of precursor. The beginning of the reaction is similar in that nuclei are produced in a short burst. Following this burst of nucleation, we achieve a pseudo-steady state, where concentration of precursor stabilizes as does the rate of product formation. Systematic size control then is a

matter of time of addition, a parameter that is obviously quite easy to control. Fig. 1 shows the result of a reaction of this type, where particles were grown to the desired size and achieved a greater than 100 fold improvement in signal over commercial particles (>10% of the particles are in the size window).

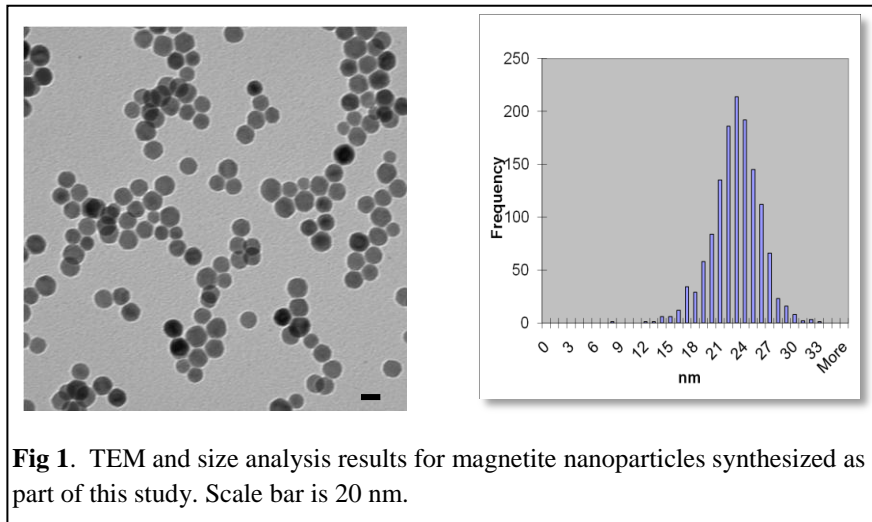


**Fig 1.** TEM and size analysis results for magnetite nanoparticles synthesized as part of this study. Scale bar is 20 nm.

## Future Work

Proof of concept work is complete and we believe the Extended LaMer Mechanism is an excellent way to control size in nanoparticle synthesis, particularly large nanoparticles such as are shown here. Still, much work must be done to demonstrate the general utility of this synthetic approach, and improve size control and polydispersity. For application in a medical setting, it is critical to demonstrate a high level of synthetic control and reproducibility before one could envision FDA approval.

## References

1. Flynn, E.R. and Bryant, H.C., *A biomagnetic system for in vivo cancer imaging*. Physics in Medicine and Biology, 2005. **50**(6): p. 1273-1293.
2. Neel, L., *Influence des Fluctuations Thermiques sur Laimantation de Grains Ferromagnetiques Tres Fins*. Comptes Rendus Hebdomadaires des Seances de l Academie des Sciences, 1949. **228**(8): p. 664-666.
3. Lamer, V.K. and Dinigar, R.H., *Theory, Production and Mechanism of Formation of Monodispersed Hydrosols*. Journal of the American Chemical Society, 1950. **72**(11): p. 4847-4854.

## Publications

1. Adolphi, N.L., Huber, D.L., Jaetao, J.E., Bryant, H.C., Lovato, D.M., Fegan, D.L., Venturini, E.L., Monson, T.C., Tessier, T.E., Hathaway, H.J., Bergemann, C., Larson, R.S., and Flynn, E.R., *Characterization of magnetite nanoparticles for SQUID-relaxometry and magnetic needle biopsy*. Journal of Magnetism and Magnetic Materials, 2009. **321**(10): p. 1459-1464.
2. Adolphi, N.L., Huber, D.L., Bryant, H.C., Monson, T.C., Fegan, D.L., Lim, J., Trujillo, J.E., Tessier, T.E., Lovato, D.M., Butler, K.S., Provencio, P.P., Hathaway, H.J., Majetich, S.A., Larson, R.S., and Flynn, E.R., *Characterization of single-core magnetite nanoparticles for magnetic imaging by SQUID relaxometry*. Physics in Medicine and Biology, 2010. **55**(19): p. 5985-6003.
3. Bryant, H.C., Adolphi, N.L., Huber, D.L., Fegan, D.L., Monson, T.C., Tessier, T.E., and Flynn, E.R., *Magnetic properties of nanoparticles useful for SQUID relaxometry in biomedical applications*. Journal of Magnetism and Magnetic Materials, 2011. **323**(6): p. 767-774.

## **Vortex behavior in patterned magnetic heterostructures with circular exchange-bias**

M Tanase<sup>1\*</sup>, A K Petford-Long<sup>1</sup>, O G Heinonen<sup>2\*\*</sup>, K S Buchanan<sup>3</sup>, J Sort<sup>4</sup>, J Nogues<sup>4</sup>

<sup>1</sup>Materials Science Division, Argonne National Laboratory (ANL), Lemont, IL; <sup>\*</sup>currently at the National Institute of Standards and Technology, Gaithersburg MD 20899; <sup>2</sup>Seagate Technology, Bloomington, MN; <sup>\*\*</sup>currently at ANL; <sup>3</sup>Center for Nanoscale Materials, ANL; <sup>4</sup>Universitat Autònoma de Barcelona, Bellaterra, Spain.

### **Electron Microscopy Center (ANL) Proposal title: Quantitative in-plane magnetization mapping in lithographically patterned magnetic nanostructures**

Magnetization processes in patterned magnetic heterostructures are of fundamental interest and have important potential applications in high-density magnetic recording media, magnetic random access memories, miniature magnetic field sensors and spintronic logic devices. Simultaneous magnetic and structural characterization of nanostructures with multiple magnetic layers, such as can be encountered in functioning devices is an incipient field and extensive fundamental research is needed for the understanding of magnetism at very small scales.

#### **Scientific Challenge and Research Achievement:**

The nanoscale confinement of the magnetization leads to the existence of novel magnetic configurations (onion, flower and vortex) and new reversal mechanisms. Exchange biasing to an antiferromagnetic (AF) layer can offer a mechanism of controlling the reversal behavior of the ferromagnetic (FM) vortex. Our Lorentz TEM study of lithographically patterned magnetic nanostructures has brought important insights in understanding the influence of microstructure on magnetization reversal mechanisms. Using Lorentz transmission electron microscopy (LTEM), magneto-optic Kerr (MOKE) magnetometry and micromagnetic simulations, we have characterized the reversal in vortex supporting nanostructures of CoFe and NiFe, both as single layers and exchange-biased to antiferromagnetic (AF) IrMn. 1  $\mu\text{m}$  diameter disks were fabricated by electron lithography and lift-off, on 50 nm thick SiN windows set into a 300  $\mu\text{m}$ -thick Si wafer frame. Four different configurations were sputter-deposited: Ta/Ni<sub>80</sub>Fe<sub>20</sub>/Cr (Py); Cr/Co<sub>90</sub>Fe<sub>10</sub>/Cr (CF); Ta/Ni<sub>80</sub>Fe<sub>20</sub>/IrMn/Cr (Py/IrMn); Cr/Co<sub>90</sub>Fe<sub>10</sub>/IrMn/Cr (CF/IrMn).  $t_{\text{Py}}=12\text{nm}$  and  $t_{\text{CF}}=10\text{nm}$ . An exchange-bias (EB) was imprinted in a vortex geometry in some of the bilayer disks by zero field cooling (ZFC) through the Néel temperature of IrMn from 240°C, as described previously by Sort et al. [1]. The exchange bias was set in the AF layer in a vortex shape using the molecular field from the adjacent FM layer. MOKE magnetometry confirmed that exchange-bias was indeed set circularly and the strength of the exchange-bias was determined from micromagnetic simulations. LTEM shows that reversal takes place via vortex states only for Py, whereas for CoFe both domain wall motion and a vortex state are observed. In Py/IrMn disks the reversal takes place via vortex motion only and the behavior is controlled by the exchange bias; it is reversible over a range of small fields and the vortex maintains a single chirality throughout reversal, determined by the chirality of the exchange bias. In CoFe/IrMn disks

the non-negligible magnetocrystalline anisotropy causes a reversal via both vortices and domain walls resulting in a finite coercivity, and the behavior is controlled by microstructure. Exchange-bias stabilizes the vortex over a wider applied field range in both Py and CoFe disks, and the variation in reversal behavior observed in single FM layer disks, as a result of thermal activation, is suppressed in the exchange-biased (FM/AF) disks. Unlike linear exchange bias, circular exchange-bias decreases the coercivity of the FM layer and even produces reversibility in the magnetic behavior of Py/IrMn disks.

**Future work:** an investigation of the sources of vortex pinning and the vortex pinning behavior in multilayered magnetic heterostructures will be carried out; as part of this project, point defects will be induced in a controlled manner in these heterostructures using either in the form of holes or by local implantation of Ga, and the changes induced in the magnetization reversal mechanisms observed will be investigated.

**References:** [1] J Sort et al., APL 88, 042502(2006)

**Selected publications and talks:**

M. Tanase, A. K. Petford-Long, O. Heinonen, K. S. Buchanan, J. Sort, and J. Nogués, “Magnetization reversal in circularly exchange-biased ferromagnetic disks”, Physical Review B 79, 014436 (2009)

M Tanase, A K Petford-Long, M De Graef, K Buchanan, J Sort, J Nogués, “Magnetization Reversal in Nanostructures with Circular Exchange Bias”, INTERMAG May 4-8th 2008, Madrid, Spain (contributed talk)

M Tanase, D K Schreiber, A K Petford-Long, O G Heinonen, J Sort, “Vortex Behavior in Patterned Magnetic Heterostructures with Circular Exchange Bias”, The Advanced Photon Source, Center for Nanoscale Materials and the Electron Microscopy Center Joint Users Meeting, Argonne National Laboratory, May 5-9th, 2008 (invited talk)

M Tanase, A K Petford-Long, M De Graef, K Buchanan, J Sort, “Exchange-Biased Magnetic Heterostructures”, 52nd Magnetism and Magnetic Materials Conference, Nov. 5-9th, Tampa FL 2007 (contributed talk)

M Tanase, A K Petford-Long, M De Graef, K Buchanan, J Sort, “Magnetization Reversal in Exchange-Biased Nanostructures”, University of Michigan Ann Arbor, CM/AMO Seminar, Dec. 11, 2007 (invited talk)

M Tanase, A K Petford-Long, O G Heinonen, M De Graef, J Sort, “Magnetization behavior in exchange biased patterned nanostructures”, Center for Materials for Information Technology (MINT Center), University of Alabama, Tuscaloosa, AL, July 14, 2008 (invited talk)

**Acknowledgments:** Work carried out in part by UChicago Argonne, LLC, Operator of Argonne National Laboratory. Argonne, a U.S. Department of Energy Office of Science laboratory, is operated under Contract No. DE-AC02-06CH11357. We gratefully acknowledge the use of the Electron Microscopy Center and the Center for Nanoscale Materials.

## Colloidal GeTe Nanoparticles as a Solution Processable Route to Phase Change Materials

Marissa A. Caldwell<sup>1</sup>, Simone Raoux<sup>2</sup>, Rakesh G. D. Jeyasingh<sup>3</sup>, Robert Y. Wang<sup>4</sup>, Delia J. Milliron<sup>4</sup> and H.-S. Philip Wong<sup>3</sup>

Departments of Chemistry<sup>1</sup> and Electrical Engineering<sup>3</sup>, Stanford University, Stanford CA 94005

<sup>2</sup>IBM T.J. Watson Research Center, Yorktown Heights NY 10598

<sup>4</sup>The Molecular Foundry, Lawrence Berkeley National Laboratory, Berkeley CA 94720

**Proposal Title:** Synthesis, characterization and device integration of GeTe nanoparticles

### Scientific Challenge and Research Achievement:

One of the significant challenges facing electronic memory storage is the ability to scale; as demand for higher capacity continues to grow, memory cells must continue to shrink. Phase change random access memory (PCRAM) not only has the potential to scale to extremely small dimensions, but is also predicted to improve in several key device characteristics including endurance and RESET power as programming volume decreases. PCRAM stores information through the reversible transition between the amorphous and crystalline states of a phase change material (PCM), which intrinsically links the fundamental scaling limit of PCRAM to the relative phase stability of the PCM. Our work focuses on investigating this fundamental limit by probing the size dependent properties of phase change nanoparticles.

In order to investigate the size dependence of phase stability below the 20nm range, monodisperse nanoparticles of different sizes are required. To this end, we developed the first colloidal nanoparticle synthesis of GeTe, a prototypical PCM. In addition to elemental and structural characterization of the nanoparticles, nanoparticle films retained both a high and low resistance state where the transition temperature correlated to a measured crystallization temperature ( $T_{\text{cryst}}$ ) over 100°C above the bulk value. The elevated  $T_{\text{cryst}}$  indicated that the amorphous phase was significantly more stable in the nanoparticles than the bulk counterpart. To further elucidate this trend, the 1.5-4nm nanoparticles were separated into narrower size distributions through a post-synthetic size selection process and the size dependent  $T_{\text{cryst}}$  was measured. It was observed that  $T_{\text{cryst}}$  increased with decreasing average diameter, implying that the stability of the amorphous phase increases with decreasing size. The increased stability predicts favorable trends for data retention with scaling.

Finally, we demonstrate the fabrication of PCRAM cells utilizing the nanoparticles as solution processable PCM. In order for PCRAM to become commercially viable, the cell size must shrink, as current performance limiting characteristics such as RESET power consumption have been shown to scale with programming volume. However, small features are difficult to fill via the traditional physical processes (such as RF sputtering or chemical vapor deposition) that PCMs are deposited from. Solution processing offers an alternative route to PCM deposition that allows for efficient deposition into small features. To demonstrate the potential of colloidal GeTe nanoparticles as a solution precursor we built vertical PCRAM cells patterned by conventional optical lithography. The PCM was

deposited by drop-casting a nanoparticle solution, and patterned by photoresist lift-off. After fabrication, the  $5 \mu\text{m}^2$  cells showed reversible switching between high and low resistive states for up to 100 cycles before failing, currently the best performance reported of a solution processed PCM. By applying a DC sweep, the cells also demonstrated threshold switching characteristic of PCMs.

### **Future Work:**

Our immediate focus is to leverage the solution processability of the nanoparticle solutions to fabricate smaller PCRAM cells. Using block copolymer lithography, we will pattern arrays of small ( $\sim 20\text{nm}$  in diameter) vias and use the nanoparticle colloids to deposit the PCM. These smaller devices should show significantly enhanced device characteristics, illustrating the potential for depositing PCMs into previously challenging geometries.

In addition to the practical demonstration, our work continues to be focused on understanding the scaling limitations of PCMs. Further size dependent studies cannot be completed unless we can prevent the sintering of the nanoparticles into a continuous film during the phase transitions. Previous work described for other systems [1] have been shown to prevent sintering by incorporating the nanoparticles into an inorganic matrix. We are currently working on synthesizing such a composite material with the GeTe nanoparticles. By incorporating the GeTe nanoparticles into a matrix, we will be able to measure the effect of different interface materials on  $T_{\text{cryst}}$  and investigate the size dependence of reamorphization.

### **References:**

[1] Tangirala, J., Baker, J.L., Alivisatos, A.P., Milliron, D.J. *Angew. Chem. Int. Ed.* **49**. 2878 (2010).

### **Publications:**

1. Caldwell, M., Raoux, S., Wang, R.Y., Wong, H.-S.P., Milliron, D. "Synthesis and size-dependent crystallization of colloidal germanium telluride nanoparticles" *J. Mater. Chem.* **20**. (2010) 1285.
2. Caldwell, M., Raoux, S., Milliron, D.J., Wong, H.-S.P. "GeTe nanoparticles: A colloidal route to phase change materials" *Invited Talk/Proceedings Paper*. European Phase Change and Ovonic Symposium 2010. Milan, Italy.
3. Caldwell, M., Raoux, S., Wang, R.Y., Milliron, D., Wong, H.-S.P. "Synthesis and Electrical Characterization of GeTe Nanoparticles" *Invited Talk*. Materials Research Symposium Spring Meeting 2010. San Francisco CA.
4. Caldwell, M., Wong, H.-S.P., Raoux, S., Tangirala, R., Wang, R., Milliron, D.J. "Size-dependent phase transitions and morphological control over phase change properties using colloidal nanoparticle building blocks" *Invited Talk/Proceedings Paper*. European Phase Change and Ovonic Symposium 2009. Aachen, Germany.
5. Caldwell, M., Raoux, S., Wang, R.Y., Milliron, D., Wong, H.-S.P. "Synthesis of amorphous germanium telluride nanoparticles and characterization of their structural phase stability" *Invited talk*. The Molecular Foundry/Advanced Light Source User Meeting 2009. Berkeley, CA.
6. Raoux, S., Zhang, Y., Milliron, D., Caldwell, M., Rettner, C., Jordan-Sweet, J., Wong, H.-S.P. "X-Ray Diffraction Studies of the Crystallization of Phase Change Nanoparticles Produced by Self-Assembly Techniques" *Proceedings Paper/Presented Talk*. European Phase Change and Ovonic Symposium 2007. Zermatt, Switzerland.

## Synthesis, Local Structure and Size-Dependent Crystallization of Colloidal Germanium Telluride Nanoparticles

Indika U. Arachchige,<sup>1</sup> Ronald Soriano,<sup>2</sup> Christos D. Malliakas,<sup>2</sup> Mercuri G. Kanatzidis<sup>2</sup> and Sergei A. Ivanov<sup>1</sup>

<sup>1</sup>*Center for Integrated Nanotechnologies, Los Alamos National Laboratory,  
Los Alamos, NM 87545 (USA)*

<sup>2</sup>*Department of Chemistry, Northwestern University, Evanston, IL 60208 (USA)*

**Scientific Trust Area:** Nanophotonics and optical nanomaterials

**User Proposal:** Synthesis of germanium chalcogenide (GeE, E = S, Se, Te) nanomaterials

### Scientific Challenge and Research Achievement

Chalcogenide compounds and alloys displaying thermally or electrically induced, reversible, amorphous-to-crystalline phase transitions associated with distinct property states are important for a wide range of technological applications.<sup>1-2</sup> The phase transitions in these materials are generally followed by a significant change in reflectivity, enabling their use as optical data storage materials.<sup>2</sup> Moreover, the decrease in resistivity upon crystallization forms the basis for their relevance in next-generation phase-change random access memory devices.<sup>3</sup> Among phase-change materials, GeTe is archetypal and is known as a narrow gap semiconductor and a ferroelectric material with the simplest atomic composition. Although many synthetic strategies have been developed for the preparation and phase change property characterization of GeTe microcrystals ( $1.0 \pm 0.2 \mu\text{m}$ ),<sup>4</sup> nanowires ( $50\text{-}500 \text{ nm}$ )<sup>5</sup> and thin films ( $0.5\text{-}7.5 \mu\text{m}$ ),<sup>3</sup> no considerable effort have been devoted to the synthesis and study of dimensionally controlled small nanocrystals. Furthermore, small colloidal nanocrystals ( $2\text{-}30 \text{ nm}$ ) have long been used to study the dependence of phase stability and transitions on size, and both structural stability and phase transitions have been shown to change dramatically in the nano-size regime.<sup>6</sup> In an effort to study the phase change properties of GeTe in the nanoscale, we have recently developed a colloidal synthetic route for the preparation of amorphous and crystalline GeTe nanoparticles. Herein, we describe the structure, morphology, optoelectronic, and phase change properties of the resultant GeTe nanocrystals as a function of primary particle size. Furthermore, our recent efforts on investigating the local structure of amorphous GeTe using X-ray pair distribution function analysis will also be discussed.

### Future Work

Amorphous and crystalline GeTe particles prepared by this colloidal route display excellent solution stability and processability as well as size dependent phase change properties. Hence, they could potentially be viable candidates for phase-change memory applications. Our current

efforts are devoted to the assembly of GeTe colloids into dense thin films to investigate further the phase change characteristics.

### References

- (1) Raoux, S.; Welnic, W.; Ielmini, D. *Chem. Rev.* **2010**, *110*, 240-267.
- (2) Yamada, N.; Ohno, K.; Nishiuchi, K.; Akahira, N.; Takao, M. *J. Appl. Phys.* **1991**, *69*, 2849-2856.
- (3) Lankhorst, M. H. R.; Ketelaars, B. W. S. M. M.; Wolters, R. A. M. *Nat. Mater.* **2005**, *4*, 347-352.
- (4) Buck, M. R.; Sines, I. T.; Schaak, R. E. *Chem. Mater.* **2010**, *22*, 3236-3240.
- (5) Yu, D.; Wu, J.; Park, H. *J. Am. Chem. Soc.* **2006**, *128*, 8148-8149.
- (6) Goldstein, A. N.; Echer, C. M.; Alivasatos, A. P. *Science* **1992**, *256*, 1425-1427.

### Publications

- (1) Arachchige, I. U.; Soriano, R.; Malliakas, C. D.; Ivanov, S. A.; Kanatzidis, M. G. *Adv. Funct. Mater.* **2011**, accepted. (DOI: adfm.201100633)

### Acknowledgements

This research was supported by Office of Naval Research (grant N00014-10-1-0331) and partially performed at the Center for Integrated Nanotechnologies, a U.S. Department of Energy, Office of Basic Energy Sciences user facility at Los Alamos National Laboratory (Contract DE-AC52-06NA25396) and Sandia National Laboratories (Contract DE-AC04-94AL85000). We thank Dr. Darrick Williams at LANL for his help with the PXRD measurements. Use of the Advanced Photon Source for PDF measurements was supported by the U. S. DOE-BES, under Contract No. DE-AC02-06CH11357.

## Structure and Properties of Thermoelectrics from Computation and Neutron Scattering

Paul R. C. Kent

kentpr@ornl.gov

Center for Nanophase Material Sciences, Oak Ridge National Laboratory

**Scientific Thrust Area:** Understanding Emergent Phenomena

### Scientific Challenge and Research Achievement

High efficiency thermoelectric materials are of considerable current interest. Nanostructuring of a bulk material provides a route to an enhanced figure of merit, ZT. For example  $(\text{PbTe})_x(\text{AgSbTe}_2)_{1-x}$  ( $x \sim 0.05$ ) nanocomposites display  $ZT \sim 2.1$  at 800K. The underlying principle governing the role of nanoprecipitates on electron and phonon transport, and therefore, thermoelectricity, is still lacking in these materials, primarily due to the material complexity. The scientific challenge is to obtain (i) an accurate description of the microstructure of complex nanocomposites and link this to the resulting (ii) electronic transport and (iii) phonon-transport properties. A linked solution would facilitate discovery of high performance thermoelectric materials by design, rather than by serendipity. At the same time, new neutron scattering measurements of bulk materials provide new insight into the phonon transport in better-defined systems.

In two complementary user projects we have recently obtained new insight into bulk and nanostructured thermoelectric materials,[1-3] building towards the ability to model all aspects of these systems. The studies leverage multiple user facilities including the CNMS, SNS, HFIR, and NCCS.

*Bulk materials* -- We have shown how,[1] in some materials, there can be a surprisingly strong coupling between certain features of the electronic structure and the way the atoms in a solid vibrate. Inelastic neutron scattering measurements of  $\text{Fe}_{1-x}\text{Co}_x\text{Si}$  alloys were combined quantum mechanics based calculations to show why the alloys exhibit unusual softening as the temperature is increased. Our results show that for alloys with a rapidly changing concentration of electrons near the chemical potential, there are likely to be strong temperature-dependent interactions between the atom vibrations and electrons.

By combining extensive neutron scattering based analysis with the results of first principles molecular dynamics calculations, Fig. 1, we have clearly demonstrated a strong coupling between the phonon and electron states when there are sharp electronic features around the Fermi level. These effects are likely to be common to many narrow gap materials including some superconductors, heavy-Fermion compounds, and many thermoelectric materials.

*Nanostructured materials* – To study the structure, electronic, and phonon transport properties of nanostructured thermoelectric materials requires the use of very large supercells, which pushes the limit of current computing capability. By combining extensive large scale calculations at NCCS with the results of HRTEM, we have been able to make unambiguous structural assignments for  $(\text{PbTe})_x(\text{AgSbTe}_2)_{1-x}$ , identifying the mechanisms for nucleation and atomic arrangement of the nanoprecipitates[2].

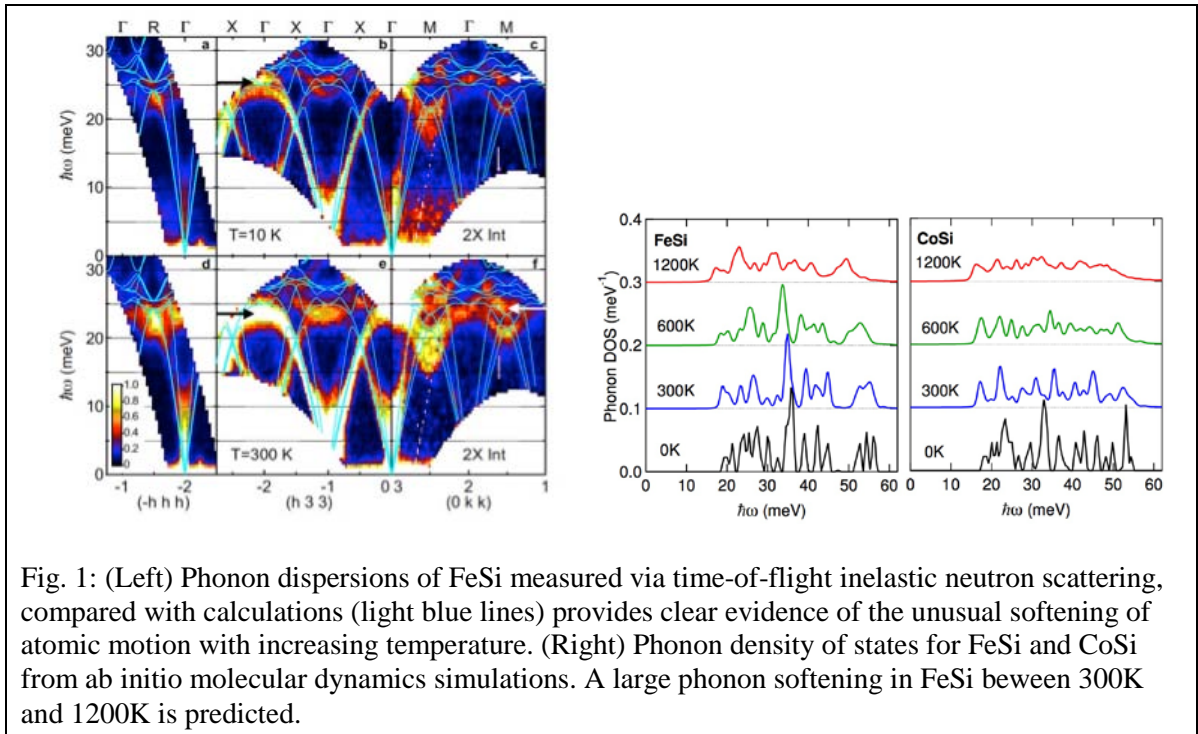


Fig. 1: (Left) Phonon dispersions of FeSi measured via time-of-flight inelastic neutron scattering, compared with calculations (light blue lines) provides clear evidence of the unusual softening of atomic motion with increasing temperature. (Right) Phonon density of states for FeSi and CoSi from ab initio molecular dynamics simulations. A large phonon softening in FeSi between 300K and 1200K is predicted.

This work is currently being extended to include the phonon properties and electronic transport[3] in realistic models of nanostructured materials. The techniques developed will be broadly applicable to thermoelectric materials.

## Publications

1. “Phonon softening and metallization of a narrow-gap semiconductor by thermal disorder”. O. Delaire, K. Marty, M. B. Stone, P. R. C. Kent, M. S. Lucas, D. L. Abernathy, D. Mandrus, B. C. Sales. Proceedings of the National Academy of Sciences 108 4725-4730 (2011)
2. “Microstructure and a nucleation mechanism for nanoprecipitates in  $PbTe-AgSbTe_2$ ”. X. Ke, C. Chen, J. Yang, L. Wu, J. Zhou, Y. Zhu, P. R. C. Kent. Physical Review Letters 103 145502 (2009)
3. “Nanodopant-induced band modulation in  $AgPb_mSbTe_{2+m}$ -type thermoelectrics”. Y. Zhang, X. Ke, C. Chen, J. Yang, and P. R. C. Kent. Submitted to Physical Review Letters (2011)

## Acknowledgements

Research at ORNL’s Spallation Neutron Source, High Flux Isotope Reactor, and Center for Nanophase Materials Sciences (PRCK) research was sponsored by the U. S. Department of Energy, Division of Scientific User Facilities. Computations by PRCK used resources of the National Energy Research Scientific Computing Center, as well as the Oak Ridge Leadership Computing Facility, located in the National Center for Computational Sciences at Oak Ridge National Laboratory, which are supported by the Office of Science, U.S. Department of Energy.

## New Tools to Exploit Density Functional Theory for Large-Scale Simulations of Nanomaterials

Qin Wu

Center for Functional Nanomaterials, Brookhaven National Laboratory,  
Upton, NY 11973

### Scientific Thrust Area - Theory and Computation

**Scientific Challenge and Research Achievement** – The success of density functional theory (DFT) methods in materials simulations leads to growing interests of applying them to larger and more complex systems. But direct applications are prohibited by the high computational cost of *ab initio* calculations and alternative strategies have to be sought. We have been developing new DFT methods that can be used to construct more efficient computational schemes. In one project, together with Prof. Adam Wasserman of Purdue University, we are implementing the idea of partition DFT [1], where a large system is divided into smaller subsystems and only subsystems need to be solved directly. This is essentially a “divide-and-conquer” strategy. Our initial tests on small molecules are shown to be successful. In another project, collaborating with Prof. Yingkai Zhang of New York University and Prof. Paul Ayers of McMaster University, we have developed a density-based energy decomposition analysis [2] that breaks the interaction energies from DFT calculations into non-overlapping terms that are basic elements in classical force fields. We are using this method to generate a large amount of accurate data (DFT level) that will be fed into parameterization of force fields (classical molecular mechanics level). This is thus a multiscale approach. We will show some results of hydrogen bonding in water.

**Future Work** – In partition DFT, we will further develop the method on the equilibration of subsystems. Ultimately, Prof. Wasserman will apply the method to determine the pore-size distributions that maximize the capacitance of nanoporous carbon materials used in electrochemical capacitors. In energy decomposition analysis, we are working intramolecular interactions and applying it to simulations of semiconducting polymers. This is part of our research effort on improving organic photovoltaics at CFN.

### References:

[1] P. Elliott, K. Burke, M. H. Cohen and A. Wasserman, “Partition density-functional theory”, *Phys. Rev. A*, **82**, 024501 (2010)

### Publications:

[2] Q. Wu, P. W. Ayers and Y. Zhang, “Density-based energy decomposition analysis for intermolecular interactions with variationally determined intermediate state energies”, *J. Chem. Phys.*, **131**, 164112 (2009)



## ***Growth mode and electronic structure of Nb nano-islands on Cu***

C. Clavero<sup>1</sup>, N. Guisinger<sup>2</sup>, R. A. Lukaszew<sup>1,3</sup>

*1 Dept. of Applied Science, The College of William & Mary, Williamsburg, VA, 23187, USA.*

*2 Center for Nanoscale Materials, Argonne National Laboratory, Argonne, IL 60439, USA.*

*3 Department of Physics, The College of William & Mary, Williamsburg, VA, 23187, USA.*

Center for Nanoscale Materials (Argonne National Laboratory) proposal CNM 22172  
“Growth mode and electronic structure of Nb nano-islands on Cu”

### **Scientific Challenge and Research Achievement**

Among the large range of possible applications for superconducting Nb thin films, coatings for superconducting radio-frequency (SRF) cavities in linear accelerators have greatly aroused the interest of researchers in the last years<sup>1</sup>. Superconducting thin films and multilayer coatings are expected to increase further the maximum field gradients that SRF cavities can withstand, pushing them above 100 MeV/m [2]. In this regard, Nb coated Cu cavities have been proposed as a prototypical system for this purpose since they combine the better thermal stability of Cu due to its much higher thermal conductivity and the superconducting properties of Nb thin films<sup>3</sup>. Nevertheless, it is well known that structural dislocations and localized surface resistive defects on the thin films have a dramatically negative influence on their superconducting properties and resonator quality. Indeed, the quality of the films is strongly conditioned by the growth mode below the single atomic layer coverage at the very early stages of growth, and thus special attention needs to be devoted to this range. Here we present a complete study on the early stages of growth of Nb on Cu(111). Different growth and annealing temperatures ranging from room temperature (RT) to 600 °C were used in order to investigate the characteristic growth mode of Nb in the sub-monoatomic coverage range. Scanning tunneling microscopy (STM) and scanning tunneling spectroscopy (STS) were used to investigate morphology and chemical composition of the surfaces with atomic resolution. Growth of sub-monolayer coverages at RT leads to amorphous Nb islands

with 1 and 2 AL heights. Annealing at 350 °C gives rise to crystallization of the islands pseudomorphically with the substrate, *i.e.* Nb(111). Further annealing at 600 °C promotes interdiffusion of Nb atoms into the Cu substrate and alloying of the islands. Growth of higher coverages above 1 AL at 350 °C reveals preferential Volmer-Weber growth mode.

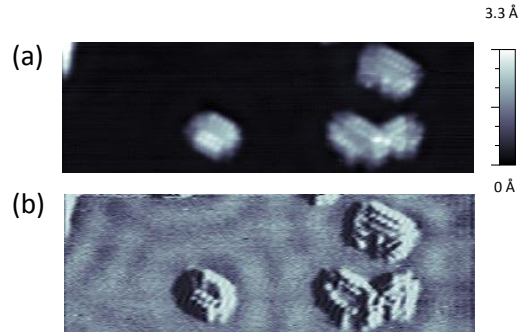


Fig. 1. (a) Topography STM map of Nb islands deposited on Cu (111). (b) Differential conductance ( $dI/dU$ ) map measured at a bias voltage of  $U = -0.2$  V featuring Friedel electronic standing waves.

### Future Work

Once we have investigated the growth mode and electronic structure of the Nb islands, we will carry out the second part of this study following similar strategy but below the Nb transition temperature ( $T_c = 9.2$  K) in order to investigate the evolution of the electronic structure of sub-monolayer Nb on Cu, the onset of superconductivity and proximity effects. For this second part, a cryogenic STM will be required to achieve temperatures below the transition temperature. These studies will be performed at the CNM depending of its availability or in collaboration with the CFM at BNL.

### References

1. H. Padamsee, Annual Review of Nuclear and Particle Science **43**, 635 (1993).
2. A. Gurevich, Applied Physics Letters **88** (1), 012511 (2006).
3. C. Benvenuti, S. Calatroni, I. E. Campisi, P. Darriulat, M. A. Peck, R. Russo and A. M. Valente, Physica C: Superconductivity **316** (3-4), 153-188 (1999).

### Publications

“Morphology and electronic structure of Nb nano-islands on Cu(111)”, C. Clavero, N. Guisinger, R. A. Lukaszew. In preparation.

“Island-assisted interface alloying and magnetic polarization at submonolayer V/Cr(001) interfaces” C. Clavero, M. Bode, G. Bihlmayer, S. Blügel and R. A. Lukaszew, Physical Review B **82** (8), 085445 (2010).

# Poster Group C



## **Elucidating the atomic-scale corrosion mechanisms of catalysts, supports, and polymers in proton exchange membrane (PEM) fuel cell cathodes**

Karren L. More, Juan Carlos Idrobo, Miaofang Chi, and David C. Cullen

Materials Science and Technology Division, Oak Ridge National Laboratory

**Proposal:** “Characterization of the Individual Material Constituents in PEM Fuel Cells”  
SHaRE Proposal ID: 2011\_More\_87

**Scientific Challenge and Research Achievement:** Proton exchange (or polymer electrolyte) membrane fuel cells (PEMFCs) are being developed for future use as efficient, zero-emission power sources. However, the performance of PEMFCs degrades rapidly with time at elevated temperature during electrochemical aging. Performance degradation can be attributed to the durability of individual components comprising the membrane electrode assembly (MEA), such as the electrocatalyst, catalyst support, and/or the proton-conducting polymer membrane. Degradation within the cathode is particularly aggressive as a result of the highly acidic, oxidative environment. Unfortunately, many of the mechanisms contributing to decreased stability within the cathode (and the MEA in general) during long-term electrochemical aging are not fully understood and strategies to mitigate the instabilities have yet to be fully realized.

Research at ORNL has been focused on correlating the observation of microstructure-related degradation phenomena with performance during/after PEMFC durability testing. This characterization effort has required an understanding of the interplay between the different MEA material constituents as a function of both processing (electrode architecture) and aging protocol (including temperature, potential cycling conditions, relative humidity, etc.). In general, there are five primary degradation mechanisms that are considered life-limiting:

- i) Pt-based catalyst coarsening (loss a catalyst surface area)
- ii) Pt dissolution and migration from cathode into membrane (loss of Pt)
- iii) Leaching of alloying elements from catalyst particles (poisoning of electrode and membrane)
- iv) Catalyst support corrosion (usually carbon-based supports)
- v) Membrane degradation (de-fluorination accompanied by loss of proton conductivity)

Depending on the PEMFC architecture and/or aging conditions, one or more of these mechanisms can contribute to performance loss, and under certain aggressive, transient operating conditions (e.g., automotive start-up/shut-down cycling resulting in open circuit voltage conditions), the excessive degradation of only one or two components of the cathode (severe corrosion of the carbon catalyst support structure, for instance) can result in complete collapse of the electrode and ultimately, fuel cell failure.

Extensive Å-scale microstructural and chemical characterization via combined high-resolution TEM, Z-contrast STEM, and electron energy loss spectroscopy (EELS) have provided new insight into the fundamental material’s degradation mechanisms that contribute to loss of PEM fuel cell performance, which will be discussed/presented. These include (as demonstrated in Figure 1) determination of the mechanism of catalyst coarsening in fuel cell cathodes, Pt migration profiles, mechanism of carbon support corrosion, and polymer degradation.

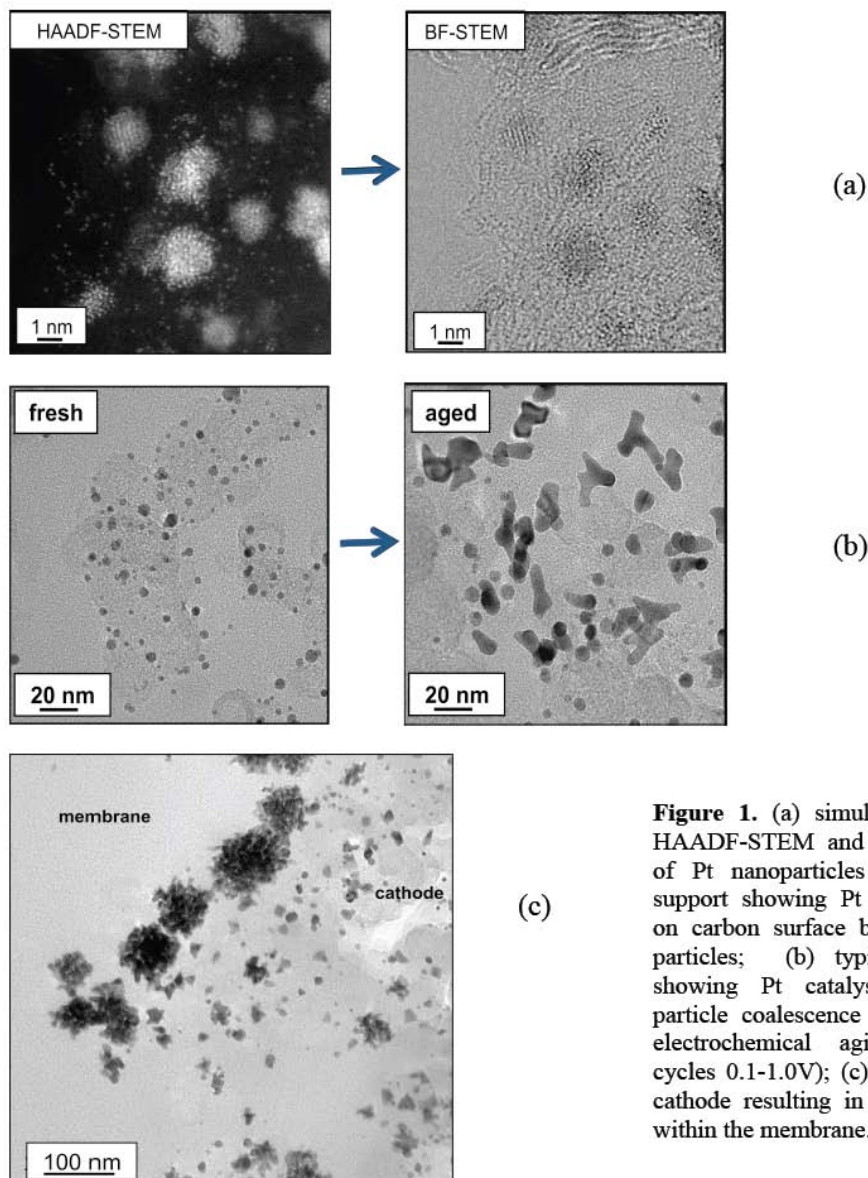


**Figure 1.** (a) simultaneously acquired HAADF-STEM and BF-STEM images of Pt nanoparticles on carbon black support showing Pt adatoms dispersed on carbon surface between Pt catalyst particles; (b) typical TEM images showing Pt catalyst coarsening via particle coalescence mechanism during electrochemical aging (80°C, 3000 cycles 0.1-1.0V); (c) Pt migration from cathode resulting in Pt agglomeration within the membrane.

**Future work:** Research will focus on correlating Pt nucleation and growth observations with nanoparticle stability during fuel cell operation and understanding support degradation mechanisms resulting in performance loss.

**Support:** Research supported by (1) Fuel Cell Technologies Program, Office of Energy Efficiency and Renewable Energy, U.S. Department of Energy and (2) ORNL's Shared Research Equipment (SHaRE) User Facility, Office of Basic Energy Sciences, U.S. Department of Energy.

**Publications:**

1. M.P. Brady, et al., *Journal of Power Sources* **195**[17] 5610-5618 (2010).
2. L.F Xiong, K.L. More, and T. He, *Journal of Power Sources* **195**[9] 2570-2578 (2010).
3. J.A. Xie, et al., *Electrochim Acta* **55**[24] 7404-7412 (2010).
4. Z.Y. Liu, et al., *Journal of the Electrochemical Society* **157**[6] B906-B913 (2010).
5. Y. Garsany, et al., *Journal of Physical Chemistry Letters* **1**[13] 1977-1981 (2010).
6. P. Strasser, et al., *Nature Chemistry* **2**[6] 454-460 (2010).

## Novel Nanomaterials as Anodes for Li-ion Batteries

Wei-Qiang Han, Xiao-Liang Wang

Center for Functional Nanomaterials, Brookhaven National Laboratory, Upton, New York 11973

**Scientific Thrust Area:** Nanoelectrodes for Li-ion Batteries

### Scientific Challenge and Research Achievement

Advances in electrochemical energy storage are essential for widespread adoption of renewable sources of electrical energy. We work on new chemical synthesis approaches to nanostructured materials for use as anodes in lithium-ion (Li-ion) batteries. Nanostructured forms have been demonstrated to perform better, due in large part to stress relief and facile lithium diffusion within the material. We focus on novel nanostructures, especially those of high capacity anodes (*vs.* the state-of-the-art graphite,  $372 \text{ mAh g}^{-1}$ ), such as Si, Ge, and Sn.

(1) Nanosphere of Sn-M (M=Fe, Co, Ni, Cu)

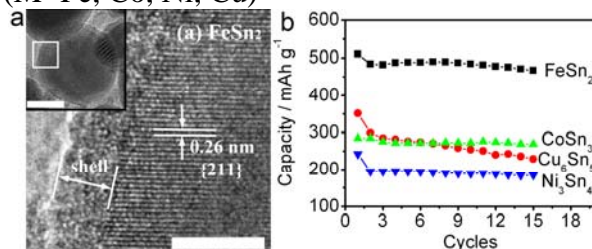


**Figure 1** (a) HRTEM images of  $\text{FeSn}_2$ . The scale bars are 5 nm and 20 nm (insets); (b) Reversible ( $\text{Li}^+$  removal) capacities of coin cells with intermetallic nanospheres as the working electrodes and lithium metal as both the reference and counter electrodes. The cycling rate was  $C/20$ . The voltage range was 0.05-1.5 V.

Forming intermetallic M-Sn compounds has long been believed as a solution to the poor cyclabilities of high-capacity Sn-based anodes. During electrochemical processes, M can form a buffering framework that ameliorates the disastrous lithium-driven volume changes and stabilizes the integration of single particles, and can enhance the electrical conductivity. We synthesized  $\text{FeSn}_2$ ,  $\text{Cu}_6\text{Sn}_5$ ,  $\text{CoSn}_3$  and  $\text{Ni}_3\text{Sn}_4$  single crystalline nanospheres characteristic with uniform particle size of  $\sim 40 \text{ nm}$  have been synthesized via a modified polyol process,<sup>1</sup> aiming at determining and understanding their intrinsic cycling performance as electrode materials for lithium-ion batteries. We find that the reversible capacities follow  $\text{FeSn}_2 > \text{Cu}_6\text{Sn}_5 \approx \text{CoSn}_3 > \text{Ni}_3\text{Sn}_4$ , which is not directly decided by their theoretical capacities or lithium-driven volume swings.  $\text{FeSn}_2$  exhibits the best electrochemical activity among these intermetallic nanospheres because it has opened crystal structure.<sup>2</sup>

(2) Graphene sheets/porous Si nanowires

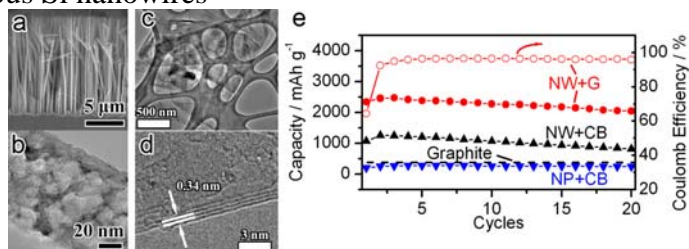


**Figure 2** (a) SEM images of porous single-crystalline Si nanowires; (b) TEM image of a porous Si nanowire; (c) & (d) TEM images of graphene sheets; (e) Charge capacities and Coulomb efficiency of cells for 20 cycles. NW: Si nanowires; G: graphene; CB: carbon black; NP: Si nanoparticles.

We demonstrated that graphene significantly enhances the reversible capacity of porous silicon nanowires used as the anode in Li-ion batteries. We prepared our experimental nanomaterials, viz. porous single-crystalline silicon nanowires (Figure 2(a) and (b)) and graphene (Figure 2(c) & (d)), respectively, using a liquid-phase graphite exfoliation method, and an electroless HF/AgNO<sub>3</sub> etching process. The Si porous nanowire/graphene electrode realized a charge capacity of 2470 mAh g<sup>-1</sup> that is much higher than the 1256 mAh g<sup>-1</sup> of porous Si nanowire/C-black electrode, and 6.6 times the theoretical capacity of commercial graphite.<sup>3</sup> This relatively high capacity could originate from the favorable charge-transportation characteristics of the combination of graphene with the porous Si 1D nanostructure.

### (3) Carbon-coated Magnéli phase Ti<sub>n</sub>O<sub>2n-1</sub> nanobelts

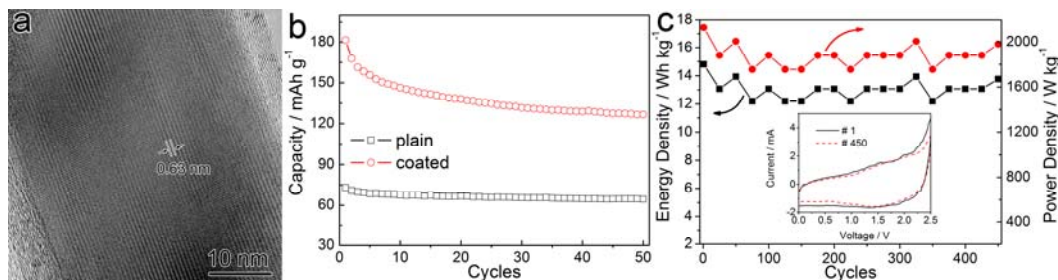


**Figure 3**(a) TEM image of a carbon-coated Ti<sub>9</sub>O<sub>17</sub> nanobelt; (b) Reversible (Li<sup>+</sup> removal) capacities of coin cells with the carbon-coated Ti<sub>9</sub>O<sub>17</sub> nanobelts as the working electrodes, and lithium metal as both the reference- and counter- electrodes. The cycling rate was C/10 based on theoretical capacity; (c) Cycling performance of the hybrid electrochemical-cell at 100 mV s<sup>-1</sup>, where the inset shows the CV profiles at the 1st and 450th cycles.

This is the first work of using nanostructured Magnéli phase Ti<sub>n</sub>O<sub>2n-1</sub> as anodes for Li-ion batteries and hybrid electrochemical cells.<sup>4</sup> We used a novel synthesis for preparing carbon-coated Ti<sub>9</sub>O<sub>17</sub> nanowires using H<sub>2</sub>Ti<sub>3</sub>O<sub>7</sub> nanobelts as precursors to react with ethylene and hydrogen at high-temperature. The carbon-coating layers play a key role in restraining the sintering growth of the core during the phase-transformation from H<sub>2</sub>Ti<sub>3</sub>O<sub>7</sub> to Magnéli phase Ti<sub>n</sub>O<sub>2n-1</sub>, and in retaining the morphology of nanobelts. We demonstrated that the initial reversible capacity of these Ti<sub>9</sub>O<sub>17</sub> nanobelts attained 182 mAh g<sup>-1</sup>, a value even higher than the theoretical value of α-TiO<sub>2</sub> (167 mAh g<sup>-1</sup>). Cyclic-voltammetry measurement supports the pseudocapacitive lithium-storage behavior of these Magnéli phases Ti<sub>9</sub>O<sub>17</sub> nanobelts. Furthermore, the nanobelts exhibit high power density along with excellent cycling stability in their application as hybrid electrochemical cells.

**Future work:** Pursue new nanomaterials as high performance anodes and understand the mechanism.

**Acknowledgement:** This work is supported by the U. S. DOE under contract DE-AC02-98CH10886 and E-LDRD Fund of Brookhaven National Laboratory.

### Publications

<sup>1</sup> X. L. Wang, M. Feyngenson, M. C. Aronson, and W. Q. Han, *Journal of Physical Chemistry C* 114, 14697 (2010).

<sup>2</sup> X. L. Wang, W. Q. Han, J. J. Chen, and J. Graetz, *Acs Applied Materials & Interfaces* 2, 1548 (2010).

<sup>3</sup> X. L. Wang and W. Q. Han, *Acs Applied Materials & Interfaces* 2, 3709 (2010).

<sup>4</sup> W. Q. Han and X. L. Wang, *Appl. Phys. Lett.* 97 (2010).

## SILICON NANOWIRES FOR NOVEL THERMAL BATTERY ANODE

Vojtech Svoboda<sup>1</sup>, George Gomes<sup>1</sup>, Jeong-Hyun Cho<sup>3</sup>, S. Tom Picraux<sup>3</sup> and Mark Temmen<sup>2</sup>

1: CFD Research Corp., 215 Wynn Drive, Huntsville, Alabama 35805  
vxs@cfdr.com, PH: (256) 327-0681, FAX: (256) 327-0985

2: US Army RDECOM, AMRDEC, RDMR-WSI, Redstone Arsenal, AL 35898  
Mark.temmen@us.army.mil

3: CINT, Los Alamos National Laboratory, K771, Los Alamos, NM 87545  
picraux@lanl.gov, PH: (505) 665-8554

Proposal title: *Silicon Nanowire Materials for Reserve Thermal Batteries*

Thermal batteries are single discharge reserve batteries, which have been primarily used in a wide range of military applications. The technology based on molten salt electrolyte offers a long shelf life, a wide range operating temperature, and high power performance. Modern military applications call for advanced thermal batteries that provide higher power and capacity with a smaller footprint. The principal avenue for increasing thermal battery specific energy and power is to identify and develop new electrode materials which provide higher specific capacity at high operating voltage with lower internal resistance.

Various chemistries have been developed for thermal battery application, we are focusing on improvement of the state of the art Li(Si)/FeS<sub>2</sub> system, particularly on the silicon based anode. The overall objective of our research is to develop novel nano-structured anode materials for thermal battery with enhanced electronic conductivity and Li<sup>+</sup> ions storage capacity.

Thermal batteries are inactive at room temperature due to solid phase electrolyte that has a low ionic conductivity and thus minimal kinetics of self discharge and degradation processes. The solid phase electrolyte promotes the ability for this type of battery to be stored for times greater than 20 years with practically no charge loss and performance fade. When needed, the subsequent activation occurs in time range of 0.1 – 1.0 sec. For battery activation, internal pyrotechnics are ignited that generate thermal energy to raise the battery internal temperature to >500°C which melts the electrolyte causing a large increase in its ionic conductivity thus allowing the battery to operate. The typical electrolyte is eutectic mixture of LiCl and KCl or halide mixtures like LiCl-LiBr-LiF. Additive of MgO functions as binder and separator between anode and cathode pallets.

We are developing novel nano-structured anode materials for thermal batteries with enhanced electronic conductivity and Li<sup>+</sup> ions storage capacity. Our concept is based on the application of nanostructured silicon and silicon composite material. Silicon has the highest known theoretical capacity for lithium storage of 4.2 Ah/g and a low discharge potential [1]. The volume change with Li<sup>+</sup> intercalation is more than 300% and such expansion causes strong mechanical strain in the material resulting in pulverization, which causes mechanical damage of the electrode material [2]. We are applying the recent discovery that silicon synthesized at the nanometer scale and particularly in the form of nanowires can withstand the strain without structural damage of the material [3, 4].

We synthesized CVD grown Si nanowires (Si NW) from 2nm thick Au seed film directly on stainless steel disk current collector. This minimizes contact resistance between the Si NW and the current collector. The synthesized nanowires have diameter 40 to 100 nm and length 20 to 50  $\mu\text{m}$ . SEM micrographs of the synthesized material is shown in Figure 1.

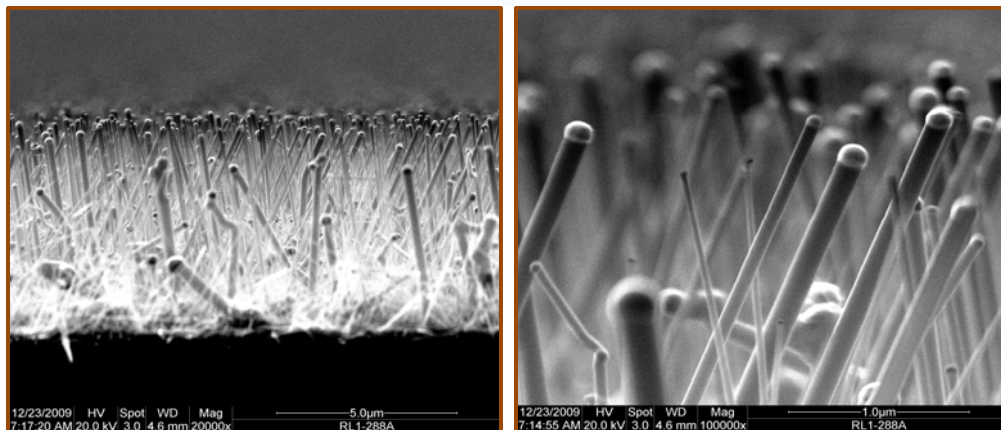


Figure 1: SEM Micrographs of Aligned CVD Grown Si Nanowires, S. Tom Picraux, CINT.

We have electrochemically tested the Si NW electrodes in a half cell setup with  $\text{LiPF}_6$  electrolyte and Li metal counter electrode in room temperature. Providing enhanced electronic conductivity and high mechanical stability, we report the  $\text{Li}^+$  ions storage capacity of 2.2 Ah/g, the intercalation process reversibility for more than 100 cycles, coulombic efficiency over 95%, and current rates up to 4C.

We have tested the electrode's structural endurance in high temperature environment of 700  $^{\circ}\text{C}$  and did not observe any physical damage. We have tested contact angle of both the eutectic mixture of LiCl and KCl (at 450  $^{\circ}\text{C}$ ) and halide mixtures LiCl-LiBr-LiF (at 500  $^{\circ}\text{C}$ ) molten salt electrolyte. The measured contact angles were totally different 134 $^{\circ}$  versus 2 $^{\circ}$  for the eutectic and halide mixture respectively. This clearly identifies the selection of halide mixture electrolyte for the Si NW anode that readily and completely flooded the Si nanowires.

Future work: We are developing computational model of the Si NW anode to optimally design and experimentally validate the electrode parameters. We are now synthesizing  $\text{FeS}_2$  cathode to demonstrate complete cell operation with molten salt electrolyte at high temperature.

#### References:

1. Boukamp, B.A., C.G. Lesh, and R.A. Huggins, *All-solid lithium electrodes with mixed-conductor matrix*. J. Electrochem. Soc., 1981. **128**: p. 725-729.
2. Kasavajjula, U., C. Wang, and A.J. Appleby, *Silicon Anodes for Li-ion Battery – A Review*. Journal of Power Sources, 2007. **163**: p. 1003-1039.
3. Chan, C.K., et al., *High-performance lithium battery anodes using silicon nanowires*. Nature Nanotechnology, 2008. **3**: p. 31-35.
4. Cui, L.-F., et al., *Crystalline-Amorphous Core - Shell Silicon Nanowires for High Capacity and High Current Battery Electrodes*. Nano Letters, 2009. **9**(1): p. 491-495.

#### Publications:

1. Svoboda, V., et al., Towards the development of silicon nanostructure based anode for thermal batteries. 2010 Power Sources Conference, Las Vegas, NV, June 14-17, 2010.
2. Svoboda, V., et al., Silicon nanostructure anode for thermal batteries. Pacific Power Source Symposium, Waikoloa, HI, January 10-14, 2011.

# Transient Reflectivity and Ion Production from Silicon Nanopost Arrays

Jessica A. Stolee<sup>1</sup>, Ralu Divan<sup>2</sup>, Leonidas E. Ocola<sup>2</sup>, David Gosztola<sup>3</sup>, Gary Wiederrecht<sup>3</sup> and Akos Vertes<sup>1\*</sup>

<sup>1</sup>*Department of Chemistry, George Washington University, Washington, DC 20052*

<sup>2</sup>*Nanofabrication Group, Center for Nanoscale Materials, Argonne National Laboratory, Argonne, IL 60439*

<sup>3</sup>*Nanophotonics Group, Center for Nanoscale Materials, Argonne National Laboratory, Argonne, IL 60439*

## Proposal Title

Nanopost Arrays and Plasmonic Structures for Laser Desorption Ionization

## Scientific Challenge and Research Achievement

Recently we have demonstrated that silicon nanopost arrays (NAPA) act as nanophotonic ion sources and can be tailored to exhibit resonant ion production upon laser irradiation.<sup>1</sup> Localized electromagnetic fields around and energy deposition into the posts are thought to contribute to the desorption and ionization of adsorbates.<sup>2</sup> Due to the unique interactions of the posts with the laser radiation, the ion yields and ion fragmentation can be modulated by rotating the plane of polarization of the desorption laser.<sup>3</sup> However, these experiments do not provide insight into the dynamic optical properties that are thought to play a role in nanophotonic ion production.

In this work, the transient reflectance of NAPA is probed to investigate energy deposition into the posts and the interplay between the generated charge carriers, the local fields, and the nanostructure. Gold-coated NAPA that exhibit plasmon resonances are used to study the effects of local field enhancements on their optical properties and ion production. Since ion production in NAPA shows a strong dependence on post aspect ratio, the dynamic optical properties of NAPA with similar heights,  $H$ , and a range of diameters ( $D = 100\text{-}400\text{ nm}$ ) were studied. An example of gold-coated NAPA with  $H = 1350\text{ nm}$  and  $D = 200\text{ nm}$  ( $H/D = 6.75$ ) is shown in Figure 1.

The ultrafast transient reflectance of native and gold-coated NAPA was measured via a pump-probe experiment in which 130 fs laser pulses were used to excite the charge carriers in the nanostructures and, as the system returned to an equilibrium state, the change in reflectance was measured. The transient reflectance from NAPA exhibits an abundance of fine spectral features that are not present for unstructured silicon. It was found that the post aspect ratio had a large impact on the nature of the spectral features, shown in Figure 2. For gold-coated structures with different diameters, shifting of the plasmon resonance peak was observed. Additional peaks were also present that were absent in gold-coated unstructured silicon. These large differences in the spectra from NAPA with varying diameters point to altered carrier dynamics and relaxation processes that may play a role in the desorption and ionization of adsorbates.

Due to the oxidation of the structures during the nanofabrication process, the ion production from these structures was reduced. However, by modifying the surface chemistry via derivatization of the native and gold-coated NAPA using silane chemistry ion production was restored on these structures. The results show that gold coated NAPA exhibit slightly higher ion

yields than uncoated NAPA, and this may be attributed to the enhanced local fields due to the presence of surface plasmon resonances.

### Future Work

Further studies will focus on the relationship between the transient optical properties of the nanostructures and their ionization efficiency. In order to directly correlate the effects of the structure and its corresponding optical properties on the ion yields, it is critical that the structures do not become oxidized in the nanofabrication process. We also plan to create plasmonic structures that are tailored to maximize the electric field intensity enhancements for higher ion yields. Because NAPA exhibit high sensitivity in mass spectrometry experiments, they have many applications in single cell analysis, bioanalysis, metabolomics and forensics.

### Figures

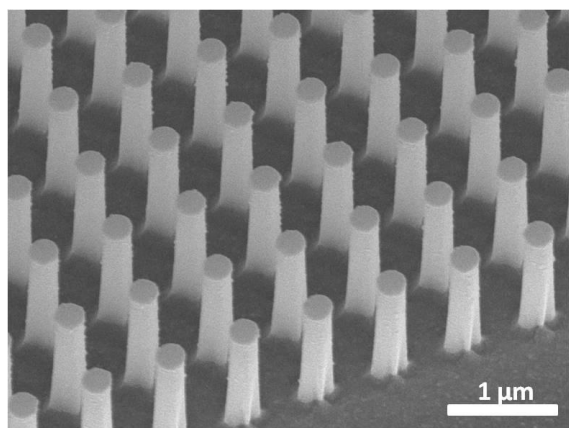


**Figure 1.** SEM image of silicon NAPA with  $D = 200$  nm,  $P = 674$  nm, and  $H = 1350$  nm coated with a 50 nm layer of gold.

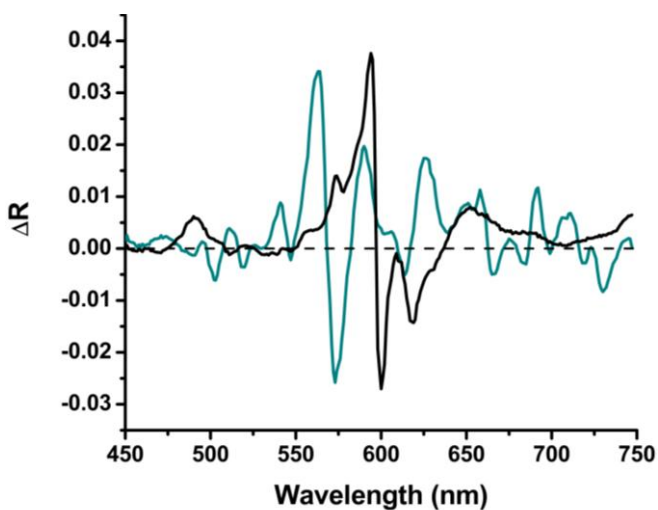


**Figure 2.** Comparison of transient reflectance spectra from low resistivity NAPA of  $D = 100$  nm,  $P = 337$  nm, and  $H/D = 15.5$  (blue trace), and of  $D = 200$  nm,  $P = 674$  nm, and  $H/D = 6.75$  (black trace) at 1.5 ps shows a strong dependence on the post aspect ratio.

### References

1. Walker, B. N.; Stolee, J. A.; Pickel, D. L.; Retterer, S. T.; Vertes, A., Tailored Silicon Nanopost Arrays for Resonant Nanophotonic Ion Production. *J. Phys. Chem. C* **2010**, *114* (11), 4835-4840.
2. Stolee, J. A.; Walker, B. N.; Chen, Y.; Vertes, A., Nanophotonic Ion Sources. *AIP Conference Proceedings* **2010**, *1278* (1), 98-110.
3. Stolee, J. A.; Vertes, A., Polarization dependent fragmentation of ions produced by laser desorption from nanopost arrays. *Physical Chemistry Chemical Physics* **2011**, Advance Article.

## Core-Protected Platinum Monolayer Shell High-Stability Electrocatalysts for Fuel-Cell Cathode

Kotaro Sasaki<sup>a</sup>, Kurian A. Kuttiyiel<sup>a</sup>, Dong Su<sup>b</sup> and Radoslav R. Adzic<sup>a</sup>

<sup>a</sup>Chemistry Department and <sup>b</sup>Center for Functional Nanomaterials,  
Brookhaven National Laboratory, Upton, NY 11973, US

**Proposal Title:** Ultra-low Pt on non-noble metal electrocatalysts for fuel cells

**Scientific Challenge and Research Achievement:** The last decade has seen considerable advances made in fuel cell electrocatalysis, yielding improved electrocatalysts, and increasing our understanding of the kinetics of the oxygen-reduction reaction (ORR) along with affording significant advances in theoretical treatments. However, some technological difficulties that hamper the automotive applications of fuel cells have not been removed and further research and development efforts are underway. Improving efficiency and reducing overall cost are two key issues to the commercialization of proton exchange fuel cell. Over the last several years we inaugurated a new class of electrocatalysts for ORR based on a monolayer of Pt deposited on metal or alloy carbon-supported nanoparticles.<sup>1-5</sup> We synthesized a low-Pt electrocatalyst consisting of a Pt monolayer deposited on carbon-supported Ir-M (M = Ni, Fe) core-shell nanoparticles by the galvanic displacement of a Cu monolayer obtained by under potential deposition.<sup>6-7</sup> The formation of Ir shells on Ir-M solid solution alloy cores has been verified by scanning transmission electron microscopy (STEM) coupled with energy-loss spectroscopy (EELS) and *in situ* X-ray absorption spectroscopy (XAS) (Figure 1). The Pt specific and mass activities for the Pt<sub>ML</sub>/IrFe/C electrocatalyst are 0.46 mA/cm<sup>2</sup> and 1.1 A/mg<sub>Pt</sub>, which are much higher than those on a commercial Pt/C electrocatalyst (Figure 2). High durability of Pt<sub>ML</sub>/Ir-M/C has also been demonstrated by potential cycle tests. These high activity and durability observed can be ascribed to the structural- and electronic interaction between the Pt monolayer and the Ir-M core-shell nanoparticle. The results have demonstrated an effective way of using Pt that can resolve key ORR problems which include inadequate activity and durability while minimizing the Pt loading.

**Future Work:** We will explore new electrocatalysts that have cores comprising non-noble metals only (or oxides, carbides, etc) to further (i) reduce the total precious-metal loadings, and (ii) enhance specific activity and durability for ORR by tuning the structural- and electronic interactions between Pt shells and non-noble material cores.

### Publications

1. Adzic, R. R.; Zhang, J.; Sasaki, K.; Vukmirovic, M. B.; Shao, M.; Wang, J. X.; Nilekar, A. U.; Mavrikakis, M.; Uribe, F. *Top. Catal.* 2007, 46, 249.
2. J. Zhang, M.B. Vukmirovic, K. Sasaki, A.U. Nilekar, M. Mavrilakis, R.R. Adzic, *J. Am. Chem. Soc.*, 127(36) (2005) 12480.
3. K. Sasaki, J.X. Wang, H. Naohara, N. Marinkovic, K. More, H. Inada and R.R. Adzic, *Electrochimica. Acta*, 55 (2010) 2645–2652.
4. K. Sasaki, H. Naohara, Y. Cai, Y.M. Choi, P. Liu, M.B. Vukmirovic, J. Wang, and R.R. Adzic *Angew. Chem. Int. Ed.* 2010, 49, 8602 –8607.

5. J. X. Wang, H. Inada, L. Wu, Y. Zhu, Y. Choi, P. Liu, W.-P. Zhou and R. R. Adzic, *J. Am. Chem. Soc.*, 2009, **131**, 17298-17302.
6. K. Sasaki, K.A. Kuttiyiel, D. Su and R. R. Adzic, accepted to *Electrocatalysis*
7. K. Sasaki, K. A. Kuttiyiel, L. Barrio, Dong Su, A. I. Frenkel, N. Marinkovic, D. Mahajan, R.R. Adzic, submitted to *J. Phys. Chem. C*.

**ACKNOWLEDGEMENT:** This work is supported by U.S. Department of Energy, Divisions of Chemical and Material Sciences under the Contract No. DE-AC02-98CH10886. Beamlines X19A at the NSLS are supported in part by the Synchrotron Catalysis Consortium, U. S. Department of Energy Grant No DE-FG02-05ER15688.

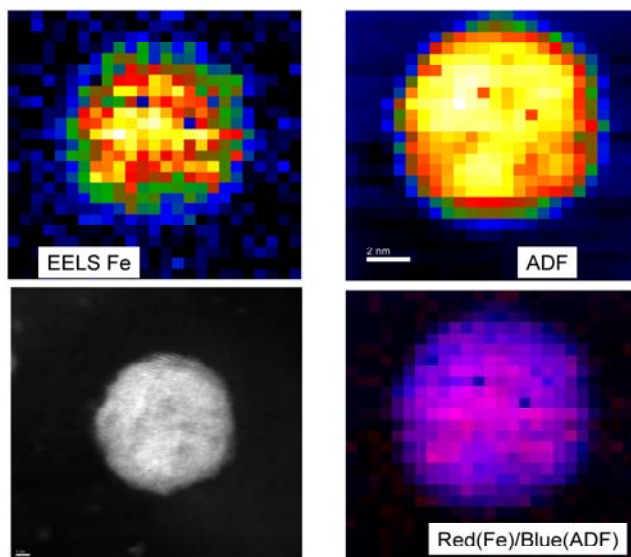


Figure 1. Two-dimensional mappings of (a) Fe EELS signal and (b) HAADF intensity on (c) a IrFe nanoparticle (HAADF-STEM image). (d) depicts an image overlapping the Fe EELS (red) on the HAADF signal (blue).

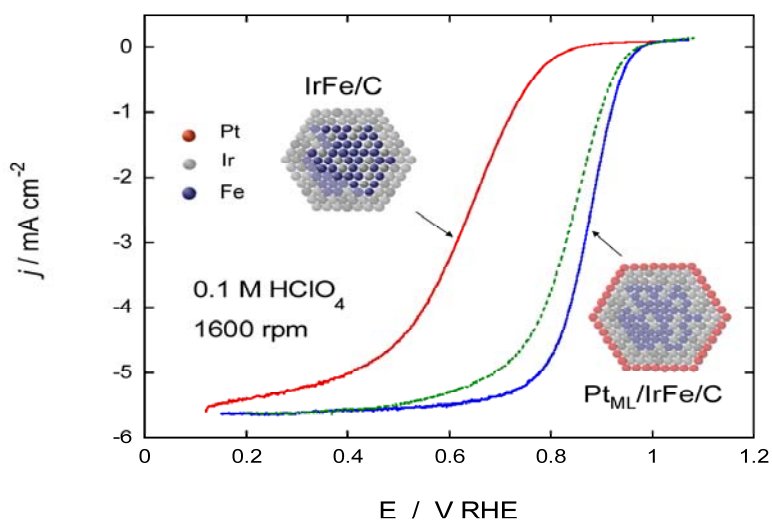


Figure 2. Comparison of polarization curves for the ORR on the IrFe/C and Pt<sub>ML</sub>/IrFe/C electrocatalysts in oxygen-saturated 0.1 M HClO<sub>4</sub> at a rotation speed of 1600 rpm. Also shown (dotted green curve) is that from a commercial Pt/C.

## Investigating Active Sites on Carbon Based Catalysts

Chengdu Liang, Wujun Fu, Viviane Schwartz, and Steve Overbury  
Center for Nanophase Materials Sciences, Oak Ridge National Laboratory

**Scientific Thrust Area:** Origins of functionality at the nanoscale

### Scientific Challenge and Research Achievement

The identification of the active sites is essential for achieving fundamental understanding of the origin of catalytic behavior and therefore guiding the search of advanced catalysts for energy efficient chemical reactions. Carbon-based materials have been widely used in catalysis, but the active sites are not well-understood due to the structural complexity and heterogeneity in practical carbons. This problem is complicated by the fact that there are almost no appropriate research tools to characterize their surface chemical and structural properties. This program addresses the challenges of identifying the active sites in carbon catalysts. Specifically, we focus on the relationship between catalytic function and the carbon morphology, surface structure and termination. The synthesis of model compounds along with established characterization techniques have been used as tools to probe the catalytic functionalities. We derived the following basic understanding of carbon based catalysts: (1) the open edge sites are the active center for carbon catalysts; (2) the selectivity for oxidative dehydrogenation (ODH) reaction to isobutene does not clearly correlate to the amount of surface quinone that initially decorate the carbon surface; (3) phosphorous groups at the carbon edges passivate the active centers that are highly reactive but less selective; and (4) oxygenated groups on the basal plane of graphene can lead to high reactivity with moderate selectivity. These discoveries clarify the role of different sites on carbon based catalysis. The essence of the research is the utilization of model compounds with well-defined structure and surface-functionalities that simplify the reaction system and thus enable the investigation of active sites on carbon surfaces. Therefore, synthesis of model carbon catalysts with variable nanostructures is a key component of this research.

*Open edge sites—the active center for carbon catalysts:* We developed a facile synthesis approach of fullerene-like cages, which can be opened and closed through simple thermal treatments. A glassy carbon with enclosed fullerene-like cages of 2-3 nm was synthesized through a soft-template approach that created open mesopores of 7 nm. The open mesopores provided access to the fullerene-like cages, which were opened and closed through heat treatments in air and inert gas at various temperatures. Catalytic measurements showed that the open cages displayed strikingly higher activity for the oxidative dehydrogenation of isobutane in comparison to the closed ones.

*Quinone-type oxygen—the functional group that controls selectivity in ODH reactions:* Reaction network analysis of the oxidative dehydrogenation (ODH) reaction of isobutane over model carbon catalysts with tailored open-edge graphitic structure and quinone-type oxygenated functionalities was used to identify the selective pathways for the formation of isobutene. Our studies reveal that the ODH reaction of isobutane on carbon catalysts is a parallel-consecutive pathway with partial oxidative dehydrogenation for the formation of isobutene and deep oxidation pathway for the direct formation of CO and CO<sub>2</sub> from isobutane. These two pathways show different dependence on the quinone-type oxygen sites: the rate constant leading to the desired partial oxidation product does not show a strong correlation to the density of the oxygen

sites, whereas the rate constant leading to the unselective CO<sub>x</sub> products increase continuously with the density of oxygen sites.

*Phosphorous modification—tuning the selectivity of carbon catalysts:*

Graphitic mesoporous carbon was modified with phosphorous groups in order to tune the catalytic selectivity and to investigate the roles of quinone and adsorbed oxygen for the oxidative dehydrogenation reaction of isobutane to isobutene. Small changes in the apparent activation energy for isobutene conversion are consistent with the notion that the phosphorous groups do not change the nature of the active sites. Instead, they interfere with the availability of the sites. Our results show that the improvement in selectivity is not proportional to the amount of phosphorous added. Small phosphorous content improved the selectivity by suppressing the combustion of isobutane. However, a higher amount of phosphorous groups leads to blocking of sites that are selective to isobutene and/or creation of active sites favorable to total oxidation.

*Graphene based catalysts—how do oxygen atoms on the basal plane affect the catalytic behavior:*

Graphite oxide was synthesized by the Hummer method and multilayer graphene was subsequently obtained by a novel exfoliation technique. The resulting graphene contained residual oxygen and was reduced under by various methods to produce a sequence of graphene-like carbons with successively lower concentrations of oxygen. Temperature programmed desorption was used to probe the nature of the remaining oxygen and the catalytic activity and selectivity in ODH reactions was measured. Initial analysis of the data reveals that the catalytic activity and selectivity do not correlate well with initial surface oxygen concentration.

**Future work:** We will continue to use and alter model carbon materials to probe the effects of structural alteration on catalytic activity in ODH reactions. Highly dispersed carbon nano-onions, will be examined as catalysts. The initially closed surfaces and surfaces opened by chemical treatment will be examined to further probe effects of basal plane vs defect sites. Doping heteroatoms such as nitrogen and boron will be added to see how they could alter catalytic activity by providing sites with variable acid/base properties or electron affinities that may activate reactant C-H bonds. Neutron scattering will be applied to probe H and functional groups on the model carbons.

This research was conducted at the Center for Nanophase Materials Sciences, which is sponsored at Oak Ridge National Laboratory by the Office of Basic Energy Sciences, U.S. Department of Energy.

### **Publications**

W. Fu, J. Kiggans, S. H. Overbury, V. Schwartz,\* C. D. Liang\*; *Low-temperature Exfoliation of Multilayer-Graphene Material from FeCl<sub>3</sub> and CH<sub>3</sub>NO<sub>2</sub> Co-intercalated Graphite Compound*, **Chemical Communications** 2011, ASAP

V. Schwartz\*, H. Xie, H. M Meyer, S. Overbury, C.D. Liang; *Oxidative dehydrogenation of isobutane on phosphorous-modified graphitic mesoporous carbon*, **Carbon** 2011, 49, 659-668

H. Xie, Z. L. Wu, S. Overbury, C. D. Liang\*, V. Schwartz\*; *Investigation of the selective sites on graphitic carbons for oxidative dehydrogenation of isobutene*, **Journal of catalysis**, 2009, 267, 158-166

C. D. Liang\*, H. Xie, V. Schwartz\*, J. Howe, S. Dai, S. Overbury; *Open-cage Fullerene-like Graphitic Carbons as Catalysts for Oxidative Dehydrogenation of Isobutane*, **Journal of the American Chemical Society**, 2009,131, 7735-7741.

## Nanocatalysis from First Principles

Jeffrey A. Herron<sup>1</sup>, Carrie A. Farberow<sup>1</sup>, Guowen Peng<sup>1</sup>, Jeff Greeley<sup>2</sup>, Maria Flytzani-Stephanopoulos<sup>3</sup>, and Manos Mavrikakis<sup>1</sup>

<sup>1</sup> Department of Chemical and Biological Engineering, University of Wisconsin – Madison, Madison, WI 53706; <sup>2</sup> Center for Nanoscale Materials, Argonne National Laboratory, Argonne, IL 60439; <sup>3</sup> Department of Chemical and Biological Engineering, Tufts University, Medford, MA 02155

**Proposal Title:** First-principles studies of heterogeneous nano-catalysis

### Scientific Challenge and Research Achievement

1. The water-gas shift reaction is an essential reaction in the purification and production of hydrogen from fossil fuel sources.<sup>1</sup> WGS catalysts, within *fuel cells*, must be stable over a number of cycles, be non-pyrophoric and active over a wide temperature range. To meet these criteria, Pt-based catalysts are essential. We have recently discovered a novel class of low-temperature WGS catalysts featuring alkali-stabilized, atomically-dispersed, oxidized Pt ( $\text{Pt}^{2+}$ ,  $\text{Pt}^{4+}$ ) over common supports ( $\text{Al}_2\text{O}_3$ ,  $\text{SiO}_2$ ).

Using first-principles, density functional theory calculations we sought to identify the active site of these catalysts.<sup>2</sup> We examined a wide range of  $\text{PtK}_n\text{O}_x(\text{OH})_y$  clusters to identify those which mirror the experimental characteristics. That is: (1) atomically dispersed Pt, (2) high alkali:Pt ratio, (3) an oxidized Pt state and (4) high WGS activity. We calculate the charge state of Pt through Bader Charge<sup>3</sup> analysis and benchmark the WGS activity using the calculated thermochemistry of key WGS steps on these clusters versus Pt(111) and Cu(111) extended surfaces. Our results identify a number of candidate structures which meet this criteria with  $\text{PtK}_6\text{O}_4(\text{OH})_2$  being the most promising active site.

2. Nitric Oxide (NO) is a harmful pollutant that is produced during the combustion of fossil fuels. Using  $\text{H}_2$  as a reductant may improve selectivity towards  $\text{N}_2$ , the desired product, and decrease  $\text{N}_2\text{O}$  formation. Experimental results<sup>4</sup> at low-temperature, over Pt catalysts, have shown high NO surface coverage and the involvement of H-atoms in the activation of NO. These findings have led us to begin studies on the importance and influence of (1) spectator species and (2) hydrogen-assisted mechanisms towards the experimentally observed chemistry.

Using first principles, density functional theory calculations we have studied the kinetics and thermochemistry of NO reduction by  $\text{H}_2$  over Pt(111) extended surfaces. Using the differential binding energy as a guide, we probe a wide-range of possible pathways in the presence of 0.50 ML of NO spectator species. We discuss the hydrogen-assisted nature of key reactions within the network and the effects of high surface coverage.

## Future Work

Currently, we are exploring additional pathways in the NO reduction network and expanding the studies onto other catalysts.

## Publications

1. L. C. Grabow, M. Mavrikakis, *ACS Catalysis* **1**, 365 (2011).
2. L. R. Merte, L. C. Grabow, G. Peng, J. Knudsen, H. Zeuthen, W. Kudernatsch, S. Porsgaard, E. Lægsgaard, M. Mavrikakis, F. Besenbacher, *Journal of Physical Chemistry C* **115**, 2089 (2011).
3. S. Kandoi, J. Greeley, D. Simonetti, J. Shabaker, J. A. Dumesic, M. Mavrikakis, *Journal of Physical Chemistry C* **115**, 961 (2011).
4. Y. P. Zhai, D. Pierre, R. Si, W. L. Deng, P. Ferrin, A. U. Nilekar, G. W. Peng, J. A. Herron, D. C. Bell, H. Saltsburg, M. Mavrikakis, M. Flytzani-Stephanopoulos, *Science* **329**, 1633 (2010).
5. J. Knudsen, L. R. Merte, G. W. Peng, R. T. Vang, A. Resta, E. Laegsgaard, J. N. Andersen, M. Mavrikakis, F. Besenbacher, *ACS Nano* **4**, 4380 (2010).
6. G. Peng, L. R. Merte, J. Knudsen, R. T. Vang, E. Laegsgaard, F. Besenbacher, M. Mavrikakis, *Journal of Physical Chemistry C* **114**, 21579 (2010).
7. S. L. Knupp, M. B. Vukmirovic, P. Haldar, J. A. Herron, M. Mavrikakis, R. R. Adzic, *Electrocatalysis* **1**, 213 (2010).
8. M. Ojeda, A. W. Li, R. Nabar, A. U. Nilekar, M. Mavrikakis, E. Iglesia, *Journal of Physical Chemistry C* **114**, 19761 (2010).
9. D. C. Ford, A. U. Nilekar, Y. Xu, M. Mavrikakis, *Surface Science* **604**, 1565 (2010).
10. A. U. Nilekar, S. Alayoglu, B. Eichhorn, M. Mavrikakis, *Journal of the American Chemical Society* **132**, 7418 (2010).
11. M. Ojeda, R. Nabar, A. U. Nilekar, A. Ishikawa, M. Mavrikakis, E. Iglesia, *Journal of Catalysis* **272**, 287 (2010).
12. S. Kandoi, P. A. Ferrin, M. Mavrikakis, *Topics in Catalysis* **53**, 384 (2010).
13. J. Rempel, J. Greeley, L. B. Hansen, O. H. Nielsen, J. K. Nørskov, M. Mavrikakis, *Journal of Physical Chemistry C* **113**, 20623 (2009).
14. P. Ferrin, M. Mavrikakis, *Journal of the American Chemical Society* **131**, 14381 (2009).
15. W. P. Zhou, X. F. Yang, M. B. Vukmirovic, B. E. Koel, J. Jiao, G. W. Peng, M. Mavrikakis, R. R. Adzic, *Journal of the American Chemical Society* **131**, 12755 (2009).
16. L. W. Bruch, R. P. Nabar, M. Mavrikakis, *Journal of Physics-Condensed Matter* **21**, 264009 (2009).
17. P. Ferrin, D. Simonetti, S. Kandoi, E. Kunkes, J. A. Dumesic, J. K. Nørskov, M. Mavrikakis, *Journal of the American Chemical Society* **131**, 5809 (2009).
18. A. U. Nilekar, A. V. Ruban, M. Mavrikakis, *Surface Science* **603**, 91 (2009).
19. P. Ferrin, A. U. Nilekar, J. Greeley, M. Mavrikakis, J. Rossmeisl, *Surface Science* **602**, 3424 (2008).

## References

1. C. N. Satterfield, *Heterogeneous catalysis in industrial practice*, 2nd Ed., McGraw-Hill, New York (1991).
2. Y. P. Zhai, D. Pierre, R. Si, W. L. Deng, P. Ferrin, A. U. Nilekar, G. W. Peng, J. A. Herron, D. C. Bell, H. Saltsburg, M. Mavrikakis, M. Flytzani-Stephanopoulos, *Science* **329**, 1633, (2010).
3. G. Henkelman, A. Arnaldsson, H. Jonsson, *Comput. Mater. Sci.* **36**, 354 (2006).
4. All experimental information obtained from personal communication with Prof. Iglesia's group at the University of California, Berkeley

# Anisotropic Volume Expansion and Ultrafast Lithiation of Si Nanowires Revealed

## by In-Situ Transmission Electron Microscopy

Xiao Hua Liu,<sup>1</sup> He Zheng,<sup>2</sup> Li Zhong,<sup>2</sup> Shan Huang,<sup>3</sup> Khim Karki,<sup>4</sup> Li Qiang Zhang,<sup>2</sup> Yang Liu,<sup>1</sup> Akihiro Kushima,<sup>5</sup> Wen Tao Liang,<sup>6</sup> Jiang Wei Wang,<sup>2</sup> Jeong-Hyun Cho,<sup>7</sup> Eric Epstein,<sup>4</sup> S. Tom Picraux,<sup>7</sup> Ting Zhu,<sup>3</sup> Ju Li,<sup>5</sup> John P. Sullivan,<sup>1</sup> John Cumings,<sup>4</sup> Scott X. Mao,<sup>2</sup> Sulin Zhang<sup>6</sup>, Jian Yu Huang<sup>1</sup>

<sup>1</sup>CINT, Sandia National Laboratories, Albuquerque, New Mexico 87185, USA

<sup>2</sup>University of Pittsburgh, Pittsburgh, Pennsylvania 15261, USA

<sup>3</sup>Georgia Institute of Technology, Atlanta, Georgia 30332, USA

<sup>4</sup>University of Maryland, College Park, Maryland 20740, USA

<sup>5</sup>University of Pennsylvania, Philadelphia, Pennsylvania 19104, USA

<sup>6</sup>Pennsylvania State University, University Park, Pennsylvania 16802, USA

<sup>7</sup>CINT, Los Alamos National Laboratory, Los Alamos, New Mexico 87545, USA

**Scientific Thrust Area:** *Nanoscale Electronics and Mechanics*

**Related User Proposal:** *In-Situ Experiment and Modeling of Electrode Failures in Li Ion Nano-Batteries*

**Scientific Challenge and Research Achievement:** Silicon has attracted much interest because it has the highest theoretical capacity (4200 mAh/g for  $\text{Li}_{22}\text{Si}_5$ ) among the anode materials for lithium ion batteries (LIBs). However, the large volume change during cycling causes pulverization of Si and loss of electrical contact between Si and the electrode. Understanding the atomic scale mechanism of the lithiation behavior will help to develop strategies to mitigate these adverse effects. *In situ* transmission electron microscopy (TEM) enables real-time observations of microstructural evolution of the electrode materials during battery operation, providing important insight about the electrochemical reactions.<sup>1,2</sup> We have constructed successfully two types of working nano-batteries inside the high vacuum of a TEM to test the lithiation behavior of individual Si nanowires, *i.e.* a solid cell and a liquid cell. The former consisted of a Si nanowire electrode, a solid-state  $\text{Li}_2\text{O}$  electrolyte, and a Li metal electrode, while the latter used an ionic liquid electrolyte and a bulk  $\text{LiCoO}_2$  cathode. We made two important discoveries recently in the electrochemical lithiation of Si nanowires.

*1. Anisotropic Volume Expansion upon Lithiation:* Upon lithiation of  $\langle 112 \rangle$  orientated Si nanowires, the diameter expanded by 200% along the  $\langle 110 \rangle$  directions but by less than 20% along the  $\langle 111 \rangle$  directions, resulting in a unique dumbbell shaped cross section (Figs. 1 & 2). The fully lithiated phase was  $\text{Li}_{15}\text{Si}_4$  as identified by electron diffraction, corresponding to an achievable capacity of 3579 mAh/g.<sup>3</sup> The results uncover previously unknown anisotropic deformation mechanism and highlight the critical role of plastic flow in the lithiation and fracture of Si nanostructures.

*2. Ultrafast Lithiation by Phosphorus Doping and Carbon Coating:* Si nanowires either coated with carbon or doped with phosphorus each leads to about 2 to 3 orders improvement of the electrical conductivity, and in turn one order of magnitude higher lithiation rate each than the

intrinsic Si nanowires in the first charging process. Combining both doping and coating, a further increase in the lithiation rate by one order of magnitude over the carbon coated or phosphorus doped Si nanowires can be achieved. These results showed great promise of using Si electrode in high power LIBs, and provide important science in guiding the development of high energy density Si anode in LIBs for electrical vehicle and portable electronics applications.

**Future Work:** The charging current of single nanowires is in femto ampere scale, which is beyond the measurement limit of most electrochemical devices. We are developing techniques to enable cyclic voltammetry and galvanostatic cycling of individual nanostructures, in the *in situ* TEM platform. Our next goal is to create a nanoscale electrochemistry lab inside the TEM that enables rigorous electrochemical characterizations as well as structure analysis of individual nanowires, nanoparticles and other nanostructured electrodes. If successful, the technique will revolutionize the nano-electrochemistry and lead to the development of high power batteries.

**References:** [1] Jian Yu Huang, *et al.* In situ observation of the electrochemical lithiation of a single SnO<sub>2</sub> nanowire electrode. *Science* **330**, 1515-1520 (2010). [2] Yet-Ming Chiang. Building a better battery. *Science* **330**, 1485 (2010). [3] M. N. Obrovac, *et al.* Structural changes in silicon anodes during lithium insertion/extraction. *Electrochemical and Solid-State Letters* **7** (5), A93-A96 (2004).

**Publications:** [1] Xiao Hua Liu, *et al.* Anisotropic volume expansion of silicon nanowires during lithiation, submitted, (2011). [2] Xiao Hua Liu, *et al.* Ultrafast electrochemical lithiation of individual Si nanowire anodes, *Nano Letters*, revised submitted, (2011).

**Acknowledgement:** This work was performed, in part, at the Center for Integrated Nanotechnologies, a U.S. Department of Energy, Office of Basic Energy Sciences user facility. Sandia National Laboratories is a multi-program laboratory operated by Sandia Corporation, a Lockheed-Martin Company, for the U. S. Department of Energy under Contract No. DE-AC04-94AL85000. Portions of this work was supported by the Science of Precision Multifunctional Nanostructures for Electrical Energy Storage (NEES), an Energy Frontier Research Center funded by the U.S. Department of Energy, Office of Science, Office of Basic Energy Sciences under Award Number DESC0001160. The NEES center supported the development of TEM techniques, and some of the platform development, and fabrication and materials characterization. CINT supported the TEM capability and the fabrication capabilities that were used for the TEM characterization, in addition, this work represents the efforts of several CINT users, primarily those with affiliation external to Sandia National Labs.

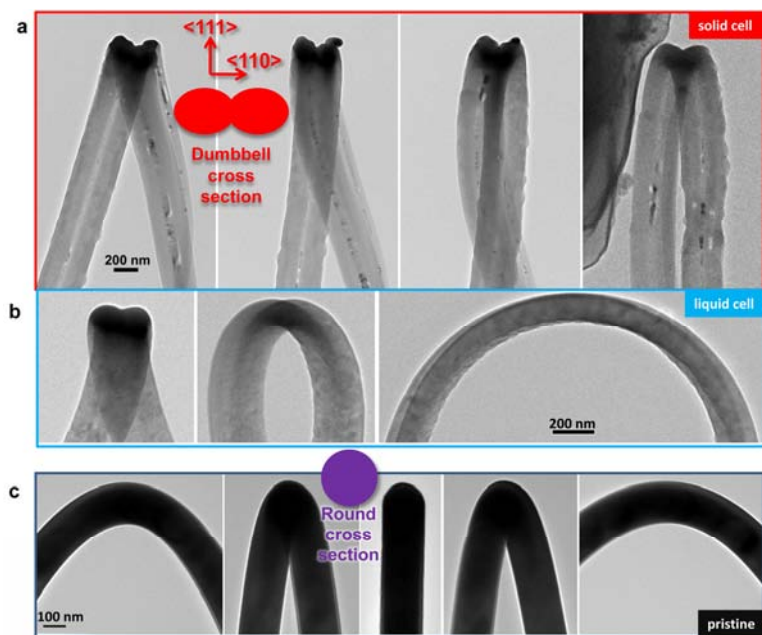


**Fig. 1** (a-b) Dumbbell shaped cross sections of the lithiated nanowires. The expansion is anisotropic, much larger along the <110> directions than along the <111> directions. (c) Round cross section of the pristine Si nanowire.

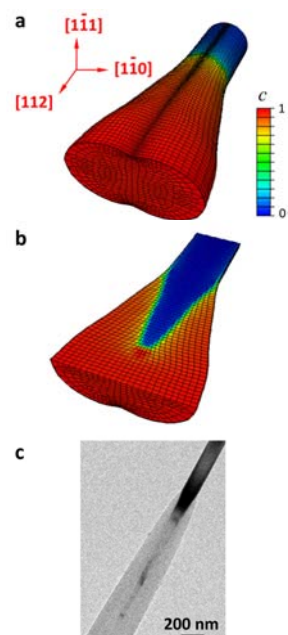


**Fig. 2** (a-b) Simulated Li distribution and anisotropic volume expansion in the <112>-oriented Si nanowire during lithiation. (c) TEM image showing the reaction front and the conical Si core.

## In-situ LEEM Study of Ceria-Copper Based Water-Gas Shift Catalysts

Jerzy T. Sadowski<sup>1</sup>, Sanjaya D. Senanayake<sup>2</sup>, Jan I. Flege<sup>3</sup>, Jose A. Rodriguez<sup>2</sup> and Jan Hrbek<sup>2</sup>

<sup>1</sup>*Center for Functional Nanomaterials, Brookhaven National Laboratory, Upton, NY 11973*

<sup>2</sup>*Chemistry Department, Brookhaven National Laboratory, Upton, NY 11973*

<sup>3</sup>*Institute of Solid State Physics, University of Bremen, 28359 Bremen, Germany*

### Scientific Thrust Area

This work has been performed through the *Interface Science and Catalysis* research theme of the Center for Functional Nanomaterials at Brookhaven National Laboratory in collaboration with staff in the Chemistry Department, Brookhaven National Laboratory, and the University of Bremen.

### Scientific Challenge and Research Achievement

At present, hydrogen is mainly produced from the reforming of crude oil, coal, natural gas, wood, organic waste, and biomass. The CO (1-10% content) present in the reformed fuel degrades the performance of the Pt electrode used in fuel cell systems. The water-gas shift (WGS) reaction ( $\text{CO} + \text{H}_2\text{O} \rightarrow \text{CO}_2 + \text{H}_2$ ) is a critical process for procuring pure hydrogen from an environmentally benign reaction. For each molecule of CO remediated, a molecule of hydrogen is produced. The WGS reaction then allows not only the removal of CO but simultaneously an upgrade in fuel cell efficiency by increasing the H<sub>2</sub> concentration.

There is a general desire to improve the configuration of industrial catalysts to take advantage of the intrinsic properties of metal oxides and achieve better catalytic performance. Oxide nanoparticles can exhibit unique physical, chemical and electronic properties due to their size, high density of defects and nature of available surface sites (corner or edge). What happens when nanoparticles of a given metal oxide are deposited on the surface of a metal? Recently, inverse model catalysts of CeO<sub>x</sub> nanoparticles supported over Au(111) or Cu(111) have shown a high catalytic performance in the water-gas shift reaction ahead of traditional industrial standards for this reaction [1].

The use of CeO<sub>2</sub>-based materials in catalysis has attracted considerable attention in recent years. Ceria has shown great potential as a novel reducible oxide support with excellent stability and unique oxygen storage capacity (OSC) [2]. Ceria can accommodate a large number of oxygen vacancies and the oxidation states of the Ce cation can be switched readily between Ce<sup>+3</sup> and Ce<sup>+4</sup> depending on the ambient conditions. Hence ceria can actively participate in redox chemical reactions.

The formation of well-ordered, flat CeO<sub>2</sub> films is a prerequisite in order to minimize substrate effects in the surface chemistry of ceria. An earlier successful approach to this problem involved growth of ceria films on Ru(0001) [3]. More recently, CeO<sub>2</sub>(111) was grown on a Cu(111) substrate [4]. High activity of ceria-based model catalysts was demonstrated on the inverse catalyst [1, 5] with ceria nanoparticles supported on noble metal substrates. However, there is still little known about the mechanism for the growth of ceria films on metal surfaces, its resulting structure and stoichiometry and the influence of catalyst structure to the observed chemistry.

In the present work the growth of thin ceria films on Cu(111) has been investigated *in-situ* by means of low-energy electron microscopy (LEEM). Ce was deposited from an e-beam evaporator onto Cu(111) under O<sub>2</sub> atmosphere (5x10<sup>-7</sup> Torr). Real-time observation of the film growth revealed that at relatively high substrate temperature (above 800K), a flat, highly crystalline, epitaxial

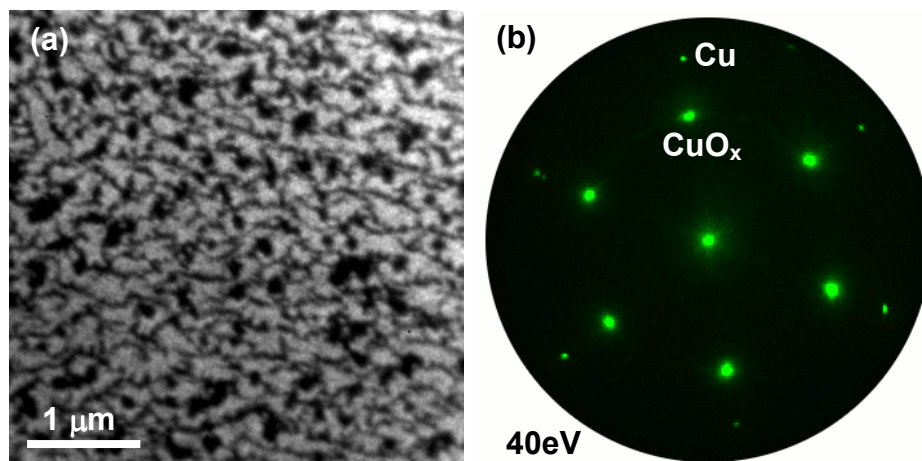


Fig.1. (a) A bright-field LEEM image showing a CeO<sub>x</sub> film (brighter contrast) grown on Cu(111) at 580K; (a) Micro-spot (2μm) LEED pattern obtained from the CeO<sub>x</sub> film shown in (a) – both, Cu and CuO<sub>x</sub> diffraction spots are visible, evidencing a high crystallinity of the epitaxial CeO<sub>x</sub> film.

CeO<sub>x</sub>(111) film (Fig. 1) has been formed. A control of the oxidation state of ceria, ie. CeO<sub>2</sub>/CeO<sub>x</sub> ratio, has been achieved by adjusting the growth conditions, namely the growth temperature and the initial oxidation state of the Cu(111) surface. Following the growth of CeO<sub>x</sub> films, the reaction of the CeO<sub>2</sub>-Cu(111) surface in the CO oxidation reaction (CO(g)+O(l)→CO<sub>2</sub>(g)) was observed *in situ* in LEEM.

In this poster presentation we will discuss in detail the mechanism of the nucleation and growth, and the atomistic structure of the CeO<sub>x</sub> film on Cu(111) under varying growth conditions and identify the CeO<sub>x</sub> and Cu(111) oxidation states.

### Future Work

In the future we plan to investigate the relation between the ceria film structure and morphology, with the efficiency of the CO-reduction reaction on the CeO<sub>2</sub>-Cu(111) surface. We anticipate that *in situ* observation of the reduction process will allow us to identify the intermediate surface structures formed during the dynamic reduction process and elucidate the role of Ce and Cu in this process.

### References

- [1] J. A. Rodriguez, S. Ma, P. Liu, J. Hrbek, J. Evans, and M. Pérez, *Science*, **318**, 1757 (2007).
- [2] A. Trovarelli, *Catalysis by Ceria and Related Metals*, Imperial College Press, London, 2002.
- [3] D. R. Mullins, P. V. Radulovic, S. H. Overbury, *Surf. Sci.* **429**, 186 (1999).
- [4] V. Matolin, J. Libra, I. Matolinova, V. Nehasil, L. Sedlacek, F. Sutara, *Appl. Surf. Sci.* **254**, 153 (2007).
- [5] J. A. Rodriguez, J. Hrbek, *Surf. Sci.*, **604**, 241 (2010).

## Ion Irradiation of Complex Perovskite Systems

Gregory R. Lumpkin<sup>1</sup>, Karl R. Whittle<sup>1</sup>, Katherine L. Smith<sup>1</sup> and Nestor J. Zaluzec<sup>2</sup>

<sup>1</sup>Australian Nuclear Science and Technology Organisation, Locked Bag 2001, Kirrawee DC, New South Wales, 2232, Australia

<sup>2</sup>Materials Science Division, Argonne National Laboratory, 9700 South Cass Avenue, Argonne, Illinois 60439, USA

### Proposal Title

Fundamental experimental and computational studies of radiation effects and defects in oxide based materials for applications in advanced nuclear systems.

### Scientific Challenge and Research Achievement

Perovskites are an important class of materials with a wide range of applications including nuclear waste forms, where they are potential host phases for trivalent lanthanides and actinides. The systems presented here are  $\text{Sr}_{1-1.5x}\text{La}_x\text{TiO}_3$  and  $\text{Ca}_{1-1.5x}\text{La}_x\text{TiO}_3$  [1,2], which have been irradiated at the IVEM-TANDEM facility, Argonne National Laboratory (ANL), with 1 MeV Kr ions at various temperatures [3]. The major challenge of this project is to understand the non-linear radiation response (Figure 1) as a function of composition in systems with phase transitions due to octahedral tilting and cation-vacancy ordering (for every two La atoms, one A-site vacancy is introduced). Although the octahedral tilting phase transitions are very different in the Ca and Sr based systems, both exhibit cation-vacancy ordering at  $x = 0.5-0.6$ . Ion irradiation results reveal a decrease in the critical temperature for amorphisation with increasing La content, with a minimum at  $x = 0.2$ , which begins to increase with further increases in La content in both systems.

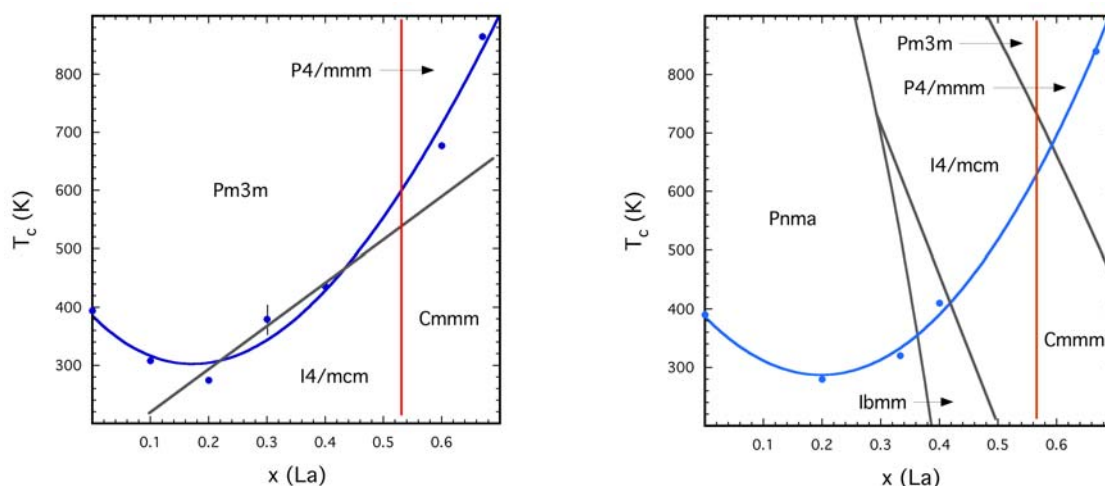


**Figure 1.** Radiation response in the Sr-La (left) and Ca-La defect perovskite systems. Gray lines are the phase transitions due to octahedral tilting and the red lines represent cation-vacancy ordering above  $x = 0.5-0.6$ . Blue curves approximate the trend of the critical dose for amorphization ( $T_c$ ).

A combination of *ab initio* and classical simulation techniques were used to characterise the energetics of A-site vacancy and cation interactions for the  $\text{Sr}_{1-1.5x}\text{La}_x\text{TiO}_3$  system [4]. When the La content is low, the A-site interactions follow intuitive electrostatic arguments, promoting association of La ions with vacancies and dissociation of vacancy-vacancy pairs. This mechanism explains why  $T_c$  decreases and the material becomes more radiation tolerant between  $x = 0.0$  and  $0.2$ , e.g., the increasing number of A-site vacancies accelerates the recovery of atoms displaced by radiation damage by providing more available sites and by lowering the energy barrier for the migration of atoms through the material.

For samples with high La content, the defect interactions are inverted due to strain forces arising from cooperative atomic relaxations and it is more energetically favourable for La atoms and vacancies to dissociate into separate layers. Although the reasons for reduced radiation tolerance at high La content are still open to debate, we believe that energy barriers for defect migration are higher in the strain-dominated region of the system (above  $x = 0.4$ ). For intermediate compositions with  $x = 0.2-0.4$ , our colleagues at the University of Cambridge suggested that there may be a coupling between the radiation damage recovery mechanism and the octahedral tilting phase transition. This hypothesis was tested during recent experiments described below.

Zhang et al. [2] found that the system  $\text{Ca}_{1-1.5x}\text{La}_x\text{TiO}_3$  has very different octahedral tilting transitions, although the La-vacancy ordering transition is still present at a slightly higher La content (Fig. 1). Therefore, we chose this system as a test of the proposed coupling between radiation damage recovery and phase transition boundaries. Results of ion-irradiation experiments obtained in December 2010 on selected samples of this system indicate that the  $T_c$  curve (light blue line in Fig. 1, right) mimics that found in the Sr-La system, but it cuts across all of the phase boundaries, thus providing evidence against the idea that damage recovery processes couple with phase transitions. In future work, we will attempt to measure the ionic conductivity in both perovskite systems, as it may give a general indication of the barriers to atomic migration (e.g., higher ionic conductivity is related to lower migration barriers).

## Future Work

Data sets will be completed. Then these data will be integrated with data from other systems to develop comprehensive models.

## Acknowledgements

Acknowledge funding by the Access to Major Research Facilities Programme that is a component of the International Science Linkages Programme established under the Australia Government's innovation statement, Backing Australia's Ability.

## References

- [1] C.J. Howard, G.R. Lumpkin, R.I. Smith, Z. Zhang, *J. Solid State Chem.* **177** (2004) 2733.
- [2] Z. Zhang, G.R. Lumpkin, C.J. Howard, K.S. Knight, K.R. Whittle, K. Osaka, *J. Solid State Chem.* **180** (2007) 1083.
- [3] K.L. Smith, G.R. Lumpkin, M.G. Blackford, M. Colella, N.J. Zaluzec, *J. Applied Phys.* **103** (2008) 083531.
- [4] B.S. Thomas, N.A. Marks, P. Harrowell, *Phys. Rev. B* **74** (2006) 214109.

## Publications

- Lumpkin G.R., Whittle K.R., Rios S., Smith K.L., and Zaluzec N.J. (2004) Temperature dependence of ion irradiation damage in the pyrochlores  $\text{La}_2\text{Zr}_2\text{O}_7$  and  $\text{La}_2\text{Hf}_2\text{O}_7$ . *Journal of Physics: Condensed Matter* **16**, 8557-8570.
- Lumpkin G.R., Pruneda M., Rios S., Smith K.L., Trachenko K., Whittle K.R., and Zaluzec N.J. (2007) Nature of the chemical bond and prediction of radiation tolerance in pyrochlore and defect fluorite compounds. *Journal of Solid State Chemistry* **180**, 1512-1518.
- Smith K.L., Lumpkin G.R., Blackford M.G., Colella M., and Zaluzec N.J. (2008) In situ radiation damage studies of  $\text{La}_x\text{Sr}_{1-3x/2}\text{TiO}_3$  perovskites. *Journal of Applied Physics* **103**, 083531.
- Lumpkin G.R., Smith K.L., Blackford M.G., Thomas B.S., Whittle K.R., Marks N.A., and Zaluzec N.J. (2008) Experimental and atomistic modelling study of ion irradiation damage in thin crystals of the  $\text{TiO}_2$  polymorphs. *Physical Review B* **77**, 214201.
- Lumpkin G.R., Smith K.L., Blackford M.G., Whittle K.R., Harvey E.J., Redfern S.A.T., and Zaluzec N.J. (2009) Ion irradiation of ternary pyrochlore oxides. *Chemistry of Materials* **21**, 2746-2754.
- Lumpkin G.R., Blackford M.G., Smith K.L., Whittle K.R., Zaluzec N.J., Ryan E.A., and Baldo P. (2010) Ion irradiation of the  $\text{TiO}_2$  polymorphs and cassiterite. *American Mineralogist* **95** 192-195.
- Whittle K.R., Lumpkin G.R., Blackford M.G., Aughterson R.D., Smith K.L., and Zaluzec N.J. (2010) Ion irradiation of lanthanum compounds in the systems  $\text{La}_2\text{O}_3\text{-Al}_2\text{O}_3$  and  $\text{La}_2\text{O}_3\text{-TiO}_2$ . *Journal of Solid State Chemistry* **183**, 2416-2420.

## High-resolution characterization of oxide scale grain boundaries

K. A. Unocic and B. A. Pint

Materials Science and Technology Division, Oak Ridge National Laboratory

**Proposal:** “Combined Use of Atom Probe Tomography and HR-STEM/EELS to Study Oxide Scale Formation and Growth.” SHaRE Proposal ID: 2011\_Unocic\_69

**Scientific Challenge and Research Achievement:** Significant efficiency improvements of land based gas turbines for power generation can be achieved by developing/modifying spray MCrAlY bond coatings (where M=transition metal). One strategy to improve coating performance is to use co-doped substrates and coatings. Depending on the specific alloy composition, various oxide surface scales can form during oxidation/exposure, but formation of an adherent, continuous, and slowly growing oxide scale leads to long-lasting and excellent oxidation resistance of the material when exposed to high temperatures. The formation of  $\alpha$ -Al<sub>2</sub>O<sub>3</sub> scales is highly preferred, as it is more stable in corrosive environments and grows at a much slower rate than other oxides. Further improvements in the high temperature oxidation properties can be achieved by the addition of reactive elements (RE), e.g. Hf, Y, Ti, Zr to the bond coating [1,2] or, as reported recently, the addition of small levels (ppm) of Y and La to current generation Ni-base superalloys [3]. However, there is little mechanistic understanding of the benefits from such RE additions.

In order to obtain a more fundamental understanding of the role of these dopants on oxide scale formation, RE segregation to the grain boundaries in the alumina scale formed on bare and coated superalloys were compared. Two versions of superalloy CMSX4 were used in this study: one La-free and one containing both Y and La additions. The surfaces of the specimens were polished before oxidation to a 0.3 $\mu$ m finish, then ultrasonically cleaned in acetone and ethanol, and inserted into a hot furnace for a 100h isothermal exposure at 1100°C in dry, flowing O<sub>2</sub>. After exposure, the specimens were characterized by a variety of electron microscopy methods and analytical techniques.

The scales formed on the surface of both alloys (alloy with La or La-free alloys) were microstructurally similar. Examination of the cross-sections of the exposed CMSX4 showed the presence of an oxide scale (~5 $\mu$ m thick) that formed on the surface of the bare metal, with an evident depletion region in the alloy beneath the scale due to Al consumption during scale formation. High-angle annular dark-field (HAADF) STEM provided Z-contrast imaging at fairly high-resolution. Figure 1a shows a HAADF-STEM cross-section image of an oxide scale formed on the bare CMSX4 that exhibits a bi-layer structure. The outer spinel layer was enriched in large precipitates close to the inner/outer layer interface, while the inner corundum layer was precipitate-free and contained columnar Al<sub>2</sub>O<sub>3</sub> grains aligned perpendicular to the metal/oxide interface. Figure 1b shows a selected-area diffraction pattern acquired from the outer layer oriented along the  $[\bar{1}11]$  zone axis, confirming the presence of the spinel phase (NiAl<sub>2</sub>O<sub>4</sub>). A bright-field STEM image and FFT confirmed that the inner layer was  $\alpha$ -Al<sub>2</sub>O<sub>3</sub> (Figure 1c). EDS elemental maps of an oxide scale grain boundary and metal/oxide interface showed only Hf enrichment at the grain boundaries (Figure 1d). Segregation of other REs (La or Y) to the metal/oxide interface was not observed. Also, Ti was present in the outer layer

(precipitates), suggesting Ti diffusion during the initial state of surface oxidation. Moreover, the presence of Ti in the scale formed on the bond coating was observed, indicating Ti diffusion through the bond coating. Techniques for quantifying dopant segregation will be discussed to better compare segregation in different systems.

**Future Work:** Additional HR-STEM, TEM, and APT work for understanding the microstructures of oxide grain boundaries.

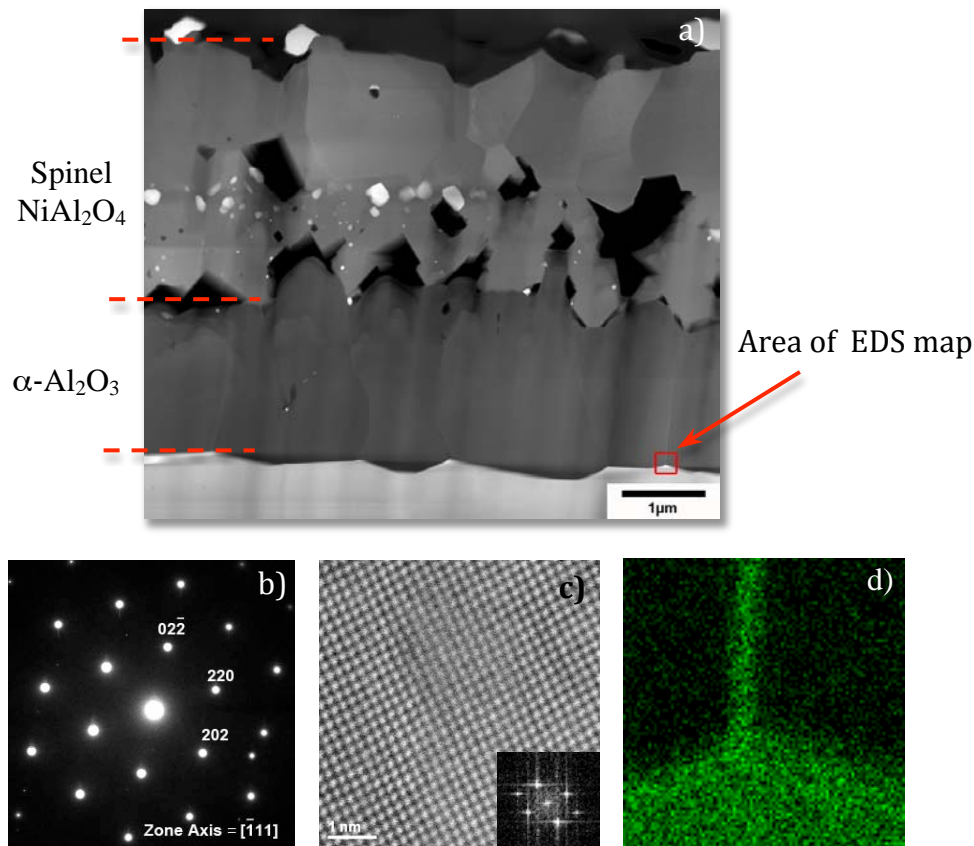


**Figure 1.** a) HAADF-STEM image showing the oxide scale formed on bare CMSX4 superalloy after 100h at 1100°C. b) Selected area diffraction pattern taken from the grain interior of outer layer of scale consistent with  $\text{NiAl}_2\text{O}_4$ . c) BF-STEM image of the grain interior of inner layer with associated FFT (inset). d) EDS Hf map acquired from the area marked on the HAADF-STEM image (1a).

**References:**

- [1] T.J. Nijdam, et al., *Acta Materialia* **55** 5980 (2007).
- [2] G.J. Tatlock, et al., *Materials Corrosion*. **56**[12] 867 (2005).
- [3] K. Harris and J.B. Wahl, *Superalloys 2004* p. 45 (2004).

**Support:** Research supported by U. S. Department of Energy, Office of Coal and Power R&D, Office of Fossil Energy and ORNL’s Shared Research Equipment (SHaRE) User Facility, which is sponsored by the Office of Basic Energy Sciences, U.S. Department of Energy.

**Publications:**

K.A. Unocic and B.A. Pint, “Study of Ionic Grain Boundary Segregation in Thermally Grown Alumina on Single-crystal Superalloys,” *Microscopy and Microanalysis* 2011 accepted.

## Imaging Bi<sub>2</sub>O<sub>3</sub> Nanostructures with the X-ray Nanoprobe

Dillon Fong<sup>1</sup>, Stephan Hruszkewycz<sup>1</sup>, Martin Holt<sup>1</sup>, Matthew Highland<sup>1</sup>, Jörg Maser<sup>1</sup>,  
Paul Fuoss<sup>1</sup>, Danielle Proffit<sup>2</sup>, Guo-ren Bai<sup>1</sup>, Jeffrey Eastman<sup>1</sup>

<sup>1</sup>Argonne National Laboratory

<sup>2</sup>Northwestern University

### Proposal Title

Zone Plate Focused Coherent Diffractive Imaging of Conductive Oxide Nanostructures:  
Mapping 3D Strain States Experimentally and Computationally

### Scientific Challenge and Research Achievement

We have used the CNM/APS Hard X-Ray Nanoprobe to measure coherent x-ray diffraction from samples of  $\delta$ -Bi<sub>2</sub>O<sub>3</sub> nanostructures grown on single crystal surfaces of SrTiO<sub>3</sub>(001).  $\delta$ -Bi<sub>2</sub>O<sub>3</sub> is an exceptionally good oxygen conductor that could greatly improve the performance of devices relying on high ionic conductivity. Unfortunately, bulk  $\delta$ -Bi<sub>2</sub>O<sub>3</sub> is only stable at high temperature (from  $\sim 729^\circ\text{C}$  to  $\sim 825^\circ\text{C}$  [1]), making fabrication of such devices problematic. We have recently succeeded in stabilizing this phase at room temperature via strained, epitaxial growth [2], but the exact role of strain and defects in the growth process remain unclear. To understand these stability issues in more detail, we have measured ptychographic Bragg CXDI data from isolated islands with hard x-rays focused to a 50 nm spot and are attempting to invert this data to obtain images and strain maps. A major advantage of nanofocused x-ray coherent imaging is that subvolumes within a targeted nanostructure can be illuminated; however, understanding and modelling the interaction of a complex focused wavefront with a faceted nanocrystal requires a departure from single processor fast Fourier transform based algorithms. We are developing parallel algorithms that compute kinematic focused diffraction patterns from finely sampled model nanocrystals and are integrating these algorithms into iterative phasing routines that will converge to unique images of the structure and internal strain of individual nanocrystals. While we have not yet succeeded in inverting the data, we will present simulations that reproduce the important features of our data and suggest possible paths towards successful reconstructions.

### Future Work

We are in the process of reconstructing the internal strain fields of Bi<sub>2</sub>O<sub>3</sub> nanocrystals from a large dataset of ptychographic coherent diffraction images. We plan to continue this research by exploring the effects of noise and beam position uncertainty on algorithm convergence and by introducing beam recovery into our 3D ptychographic iterative engine algorithm.

### References

- [1] H.A. Harwig and A.G. Gerards, *Thermochim. Acta* **28**, 121 (1979).
- [2] D.L. Proffit et al., *Applied Physics Letters* **96**, 021905 (2010).

### Publications

S.O. Hruszkewycz, M. V. Holt, A. Tripathi, J. Maser, P. H. Fuoss, "A framework for 3D coherent imaging by focused beam x-ray Bragg ptychography." *submitted to Optics Letters*, March 2011.

S.O. Hruszkewycz, M. V. Holt, D. L. Proffit, M. J. Highland, A. Imre, J. Maser, J. A. Eastman, G. R. Bai, P. H. Fuoss, "Bragg Coherent Diffraction Imaging of Epitaxial Nanostructures Using Focused Hard X-ray Ptychography." *in press, XRM-2010 Conf. Proc. AIP*.

## Quantitative STEM: Mapping Order Parameter Fields and Phase Separation on a Single Unit Cell Level

Albina Y. Borisevich

Materials Science and Technology Division, Oak Ridge National Laboratory, Oak Ridge, TN 37831

**Scientific Thrust:** Development of advanced automated aberration-corrected STEM image quantification methods and their application to studies of functional oxide interfaces, phase separated systems, and catalysts.

### Scientific Challenge and Research Achievements

Interfacial phenomena and phase transitions in solids can often be described through order-parameter based thermodynamic theories, which usually operate on length scales much larger than unit cell and are tied to structural changes in the material via diffraction characterization methods. However, modern device structures such as ferroelectric (FE) tunnel junctions and memristors often contain features that are just several unit cells in size, necessitating the development of local, real space approaches to structure/order parameter mapping. Same reasoning applies to phase separated systems with complex nanoscale morphologies, such as oxide compositions in the vicinity of morphotropic phase boundaries (MPB). Quantitative aberration corrected Scanning Transmission Electron Microscopy (STEM) is the perfect tool for this application, as its demonstrated sub-Angstrom spatial resolution combined with picometer-scale precision for atomic position determination can be used to map order parameters such as polarization, strain, and octahedral tilts.<sup>1,2</sup> With such data in hand, it is possible to understand and predict material and device behavior, as well as test mesoscale theories at the unit cell level and bridge the gap with first-principles calculations.

An example of such study is illustrated in Figure 1. Fig. 1(a) shows a HAADF STEM image of a 50nm BiFeO<sub>3</sub> (BFO) grown on SrTiO<sub>3</sub> substrate with (La, Sr)MnO<sub>3</sub> (LSMO) buffer. Figure 1(b) shows a map of Fe displacements calculated from the image in 1(a), with clear contrast at the interface between ferroelectric BFO and non-FE LSMO. A profile averaging the displacement map along the interface (Figure 1(c)) reveals more complex behavior, with the first few layers of LSMO showing small Mn displacement *opposite* to that in BFO. Combined with the data on the film with opposite polarization of BFO, we used Landau-Ginsburg-Devonshire fit to trace the origin of this behavior back to trapped charge at the interface. This approach allowed us to recreate polarization, charge, and electric field (Figure 1(d)) distribution for this system.

Figure 2 illustrates application of the quantitative STEM to phase-separated systems. Shown in Fig. 2(a) is a HAADF STEM image of 10% Sm-substituted BFO, which has antiferroelectric (AFE) properties. Figures 2 (b,c) give the maps of lattice spacings calculated from 2(a) for Bi/Sm (2(b)) and Fe (2(c)) sublattices. A considerable modulation of the Bi spacings in (110) direction is observed in the central area of the map in 2(b), while upper left and lower right corners have uniform spacings, showing the coexistence of the modulated AFE phase and parent FE phase. In contrast, the map of Fe spacings in Fig. 1 (c) appears quite featureless, suggesting uniform spacings for both modulated and unmodulated areas. This data clearly illustrates phase coexistence on a nanometer level and provides insight into the nature of antiferroelectric state in this system

## Future Work

To continue studies of phase-separated systems, we plan to investigate changes in the structure of the Sm-substituted BFO in the compositions at the morphotropic phase boundary in tandem with EXAFS and EELS studies. We further plan to employ quantitative STEM approach to study the origins of nanometer-scale superstructure in checkerboard- and stripe-ordered  $(\text{Na}_x\text{Nd}_{1-x})(\text{Mg}_y\text{W}_{1-y})\text{O}_3$  perovskites. Applications to different classes of materials, such as structure refinement for  $(\text{Mo},\text{V},\text{Ta})\text{Te}_2$  catalysts (Figure 3), are also being investigated.

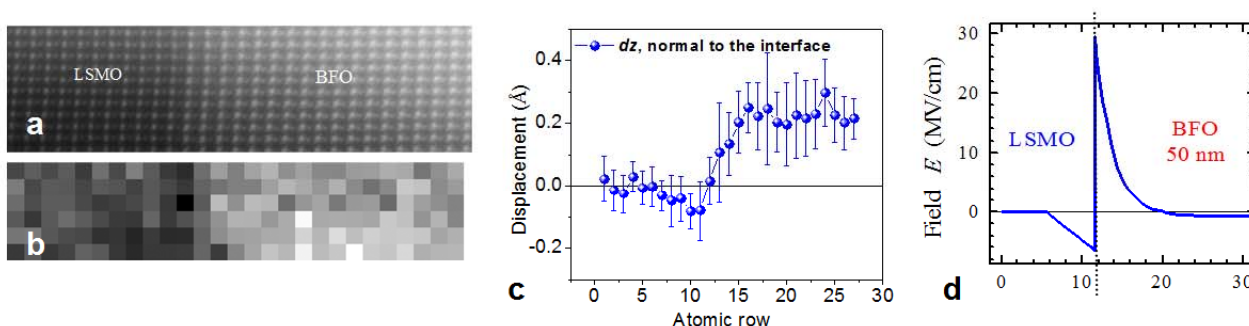


FIG.1 (a) HAADF image of the  $(\text{La}, \text{Sr})\text{MnO}_3/\text{BiFeO}_3$  interface in (110) pseudocubic projection; (b) map of ferroelectric displacements calculated from (a); (c) displacement profile obtained by averaging (b) along the interface; (d) atomically resolved electric field profile across the interface obtained from Landau-Ginsburg-Devonshire fit of data (c).

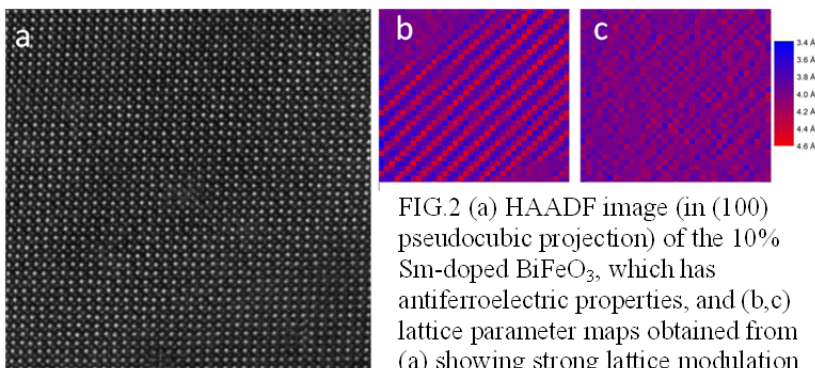


FIG.2 (a) HAADF image (in (100) pseudocubic projection) of the 10% Sm-doped  $\text{BiFeO}_3$ , which has antiferroelectric properties, and (b,c) lattice parameter maps obtained from (a) showing strong lattice modulation in the Bi sublattice (b) and no contrast in the Fe sublattice (c).

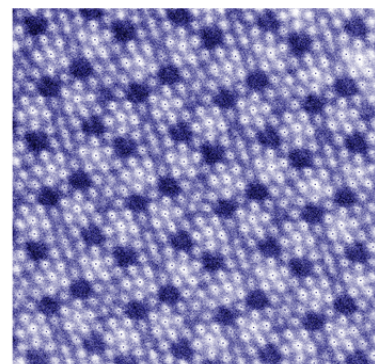


FIG.3 HAADF image of the M1  $(\text{Mo}, \text{V}, \text{Ta})\text{Te}_2$  catalyst with an overlay of refined atomic positions.

## References

- [1] \*A. Borisevich *et al.*, Phys. Rev. Lett., **105**, 087204 (2010)  
 [2] \*A. Borisevich *et al.*, ACS Nano, ACS Nano **4**, 6071 (2010).

## Publications:

†C.-J. Cheng, A. Y. Borisevich, D. Kan, I. Takeuchi and V. Nagarajan, Nanoscale Structural and Chemical Properties of Antipolar Clusters in Sm-Doped  $\text{BiFeO}_3$  Ferroelectric Epitaxial Thin Films, Chem. Mater. **22**, 2588 (2010).

\*# H.J. Chang, S.V. Kalinin, A.N. Morozovska, M. Huijben, Y.H. Chu, P. Yu, R. Ramesh, E.A. Eliseev, G.S. Svechnikov, S.J. Pennycook and A. Borisevich, Advanced Materials, in press (2011).

\*Supported by the Materials Science and Engineering Division, US DOE

#Supported by ORNL's Shared Research Equipment (SHaRE) User Facility, which is sponsored by the Office of Basic Energy Sciences, U.S. Department of Energy.

†SHaRE user research

## **Radiation Tolerance of Ceramics in Extreme Environments**

Karl R. Whittle<sup>1</sup>, Gregory R. Lumpkin<sup>1</sup>, Katherine L. Smith<sup>1</sup> and Nestor J. Zaluzec<sup>2</sup>

<sup>1</sup>Australian Nuclear Science and Technology Organisation, Locked Bag 2001, Kirrawee DC, New South Wales, 2232, Australia

<sup>2</sup>Materials Science Division, Argonne National Laboratory, 9700 South Cass Avenue, Argonne, Illinois 60439, USA

### **Proposal Title**

Predicting performance and properties of materials in extreme environments

### **Scientific Challenge and Research Achievement**

Inter-metallic compounds (ICs) and some oxides are of considerable interest in the sphere of clean energy production. For example, in fission and fusion reactors, ICs have been proposed as structural materials, wear coatings and in heat exchange devices; while some oxides have been proposed as actinide transmutation targets and radioactive waste management host phases. In such environments, ICs and oxides must exhibit robust performance under extreme conditions of temperature, irradiation, and chemical attack; and in the case of nuclear waste forms must be able to retain radioactive elements for long periods of time in geological repositories. In this paper, new experimental work will be presented on novel ICs which shows they are much more tolerant of heavy ion irradiation than most oxides. These results will be reviewed in the context of previous experimental studies and computational simulations of radiation tolerance. Commonalities and differences between proposed damage and recovery mechanisms at play in ICs and oxides will be discussed.

### **Future Work**

Irradiation of additional carbide and oxide based materials of relevance to both GenIV and Fusion technologies – coupled with atomistic modelling of radiation damage/recovery processes.

### **Acknowledgements**

Acknowledge funding by the Access to Major Research Facilities Programme that is a component of the International Science Linkages Programme established under the Australia Government's innovation statement, Backing Australia's Ability.

### **Publications**

Whittle K.R., Blackford M.G., Aughterson R.D., Moricca S., Lumpkin G.R., Riley D.P., and Zaluzec N.J. (2010) Radiation tolerance of  $M_{n+1}AX_n$  phases,  $Ti_3AlC_2$  and  $Ti_3SiC_2$ . *Acta Materialia* **58**, 4362-4368.



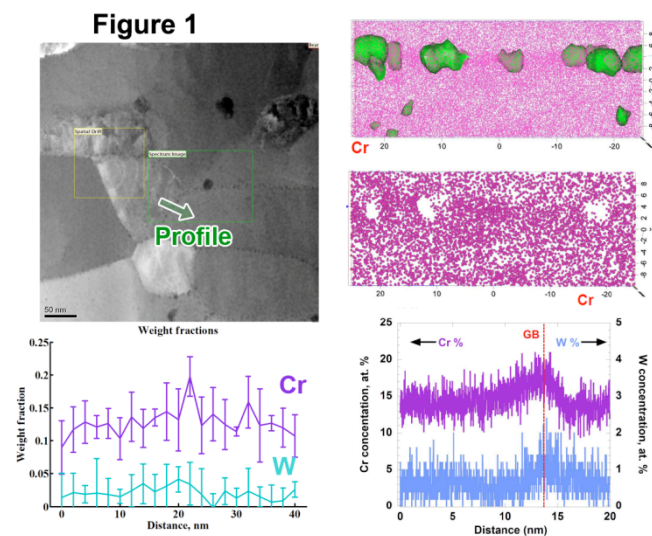
## A multi-technique approach to understand and develop radiation-tolerant nanostructures

C. M. Parish, P. D. Edmondson, and M. K. Miller  
Materials Science and Technology Division,  
Oak Ridge National Laboratory, Oak Ridge, TN 37831-6136

**Scientific Thrust Area:** Materials under extreme environments (Materials Science and Engineering Division)

**Scientific Challenge and Research Achievement:** Advanced nuclear energy systems (fission or fusion) will require materials that are resistant to corrosive environments, high temperatures, and extreme doses of radiation (hundreds of displacements per atom (dpa)) over decades of service [1]. Nanostructured ferritic alloys (NFAs) are strong candidate materials to meet these requirements. NFAs exhibit creep strength several orders of magnitude higher than conventional alloys, despite ultrafine grain sizes that would be expected to cause superplastic behavior and poor creep strength [2]. It has also been hypothesized that nanoclusters (NCs) may getter transmutation-induced He and form small, high-pressure bubbles, and thereby reduce the possibility of He embrittlement [3]. In order to gain a science-based understanding of the radiation tolerance, He embrittlement, and creep resistance of NFAs, combined scanning transmission electron microscopy (STEM) and atom probe tomography (APT) characterizations of ion irradiated and He implanted NFAs are in progress. For these studies, heavy ion irradiation was used as a rapid screening tool to simulate high dose neutron irradiation. This fundamental research should lay the groundwork for future engineering programs to design and fabricate NFAs for practical fission or fusion applications.

A 14YWT NFA was irradiated with 10 MeV Pt<sup>3+</sup> to 300 dpa at temperatures between -100 and 750°C to understand the effect of high-dose irradiation on the microstructure. To

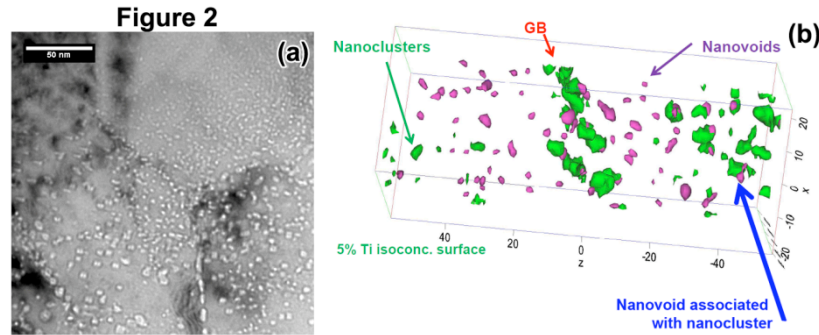


explain the unexpectedly good mechanical properties, the grain boundary (GB) structure and chemistry were characterized at the atomic level, as shown in Figure 1. In STEM (Figure 1, left column), simultaneous X-ray (EDS) and electron energy loss spectroscopy (EELS) spectrum images (SIs) were acquired from the boxed area, which contained several GBs. A GB profile (shown by arrow) was extracted from the EDS SI, and the Cr and W concentrations along the profile were quantified, indicating enrichment of Cr to the GB. EELS showed Ti-O enriched NCs at the GBs, and EDS showed Y was also present in the NCs.

Similarly, APT data from a GB (Figure 1, right column) shows a GB decorated with Ti-Y-O enriched NCs. Computationally removing the NC-associated atoms leaves the GB structure itself, and solute profiles of all the elements across

the GB can be computed. In this example, Cr and W segregation are prominent. APT provides higher resolution and smaller statistical and systematic uncertainties, whereas STEM provides a greater field of view, allowing more GBs to be studied and information on GB crystallography can be obtained. Combining STEM and APT indicates significant Cr-W segregation at GBs in addition to a large population of NCs. It is hypothesized that the nm-scale features and the solute segregation pin the GBs and are responsible for the high creep strength of NFA materials.

TEM indicates a high density of small He bubbles in NFA implanted with 335 keV He<sup>2+</sup>



at 400°C. However, because of the low contrast of the NCs in conventional TEM imaging (Figure 2a), it is difficult to tell if He bubbles nucleate heterogeneously on the NCs. Thus, APT methods were developed to identify nanovoids. The APT results indicated that some nanovoids were associated with NCs and others were not,

experimentally confirming the previously-hypothesized gettering of He to the surface of NCs (Figure 2b). APT of NCs and He bubbles complements TEM measurements of their number densities and sizes to provide a complete characterization.

**Future Work:** STEM, TEM, and APT methodologies for understanding the microstructures of ion-irradiated NFAs have been developed. Future work will involve He irradiations over a wider temperature range, as well as combined He and heavy ion irradiations, to more closely simulate in-reactor environments. Ion irradiations at varying dose rates will be performed to elucidate kinetic effects during irradiation. Additionally, STEM, TEM and APT of high dose HFIR neutron-irradiated specimens with the new dedicated focused ion beam tool will be performed to investigate and understand differences between ion and neutron irradiation effects.

**Support:** Research supported by the Materials Science and Engineering Division and the SHaRE User Facility, both sponsored by the Office of Basic Energy Sciences, U.S. Dept. of Energy.

#### References

- [1] Y. Guerin, G. S. Was and S. J. Zinkle: Materials Challenges for Advanced Nuclear Energy Systems. MRS Bulletin V34(1), (2009), P.10-14.
- [2] J. H. Schneibel, C. T. Liu, M. K. Miller, M. J. Mills, P. Sarosi, M. Heilmaier and D. Sturm: Ultrafine-grained nanocluster-strengthened alloys with unusually high creep strength. Scripta Materialia V61(8), (2009), P.793-796.
- [3] G. R. Odette and D. T. Hoelzer: Irradiation-tolerant Nanostructured Ferritic Alloys: Transforming Helium from a Liability to an Asset. JOM V62(9), (2010), P.84-92.

#### Publications

M.K. Miller and C. M. Parish, "The Role of Alloying Elements in Nanostructured Ferritic Steels," *Materials Science and Technology* 27[4] 729-734 (2011).

# Poster Group D



## Manipulating light-matter interactions in nanostructures

D. López, I. Jung, D. Gosztola, G. Wiederrecht

Center for Nanoscale Materials, Argonne National Laboratory, Lemont, IL – 60439

**Scientific Thrust Area:** Nanoscale materials and structures for new device functionality

### Scientific Challenge and Research Achievement

The future of nanoscale devices depends upon the scientific community's capacity to physically manipulate nanoscale structures and to integrate them into functional nanosystems. Conventional manipulation mechanisms that work very well in the micrometer size become extremely inefficient when scaled down to the nanometer size. The main reasons for this are as follows: electrostatic forces are difficult to control at the nanoscale due to the presence of strong fringe field effects and parasitic effects, optical forces become diffraction limited when device dimensions are scaled below the wavelength of the illumination used, and local interactions arising from surface potentials and quantum effects cause strong nonlocal force fluctuations that can modify the state of the nano-structures. The primary goal of this scientific trust is to explore the use of *plasmonic* forces to manipulate the optical properties of sub-wavelength nanostructures. Surface plasmons are localized electromagnetic fields that exist in the near-field vicinity of metallic bodies and could present novel ways to interact with nanostructures if a mechanism to manipulate them is developed. When two or more surface plasmon modes interact, new plasmonic modes can be created. The optical properties of these new modes are strongly dependent on the coupling of the individual plasmonic modes. These features of surface plasmons are being exploited to construct optical devices with highly reduced size, weight, and power consumption and enhanced capabilities for light manipulation. Although a broad variety of plasmonic nanostructures have been demonstrated in recent years, one of the critical barriers is the development and implementation of techniques to actively control the optical properties of these plasmonic nanodevices. Active control of the amplitude and phase of plasmonic signals is needed to produce elemental active devices such as plasmonic modulators and switches.

We have developed a novel approach to achieve active control of near-field plasmonic signals by integrating metallic nanostructures into Micro Electro Mechanical Devices (MEMS) devices. The optical properties of plasmonic nanostructures can be controlled by changing the relative distance between interacting metal nanostructures due to the presence of strong near-field coupling. If the separation between neighboring plasmonic elements can be actively controlled, very strong modulation and tuning of their local electromagnetic properties can be achieved. This requires control over important properties, such as the resonance wavelength, the degree of radiative and nonradiative decay components, and coherence of the plasmons, to name only a few. The MEMS actuators are ideal for mechanical tuning of plasmonic nanostructures because they can provide fast, stable, and precise control of their geometry in a continuous fashion for a large range of wavelengths.

In Figure 1 we shown a SEM image of a typical MEMS structures designed in our group. It consists of a set of voltage controlled "nano-needles" capable of unidirectional motion. By putting two of these "nano-needles" facing each other, we produced a nanopositioning device capable to control the gap between tips with nm positioning resolution. In this

way, the spacing between nanoparticles can be controlled in a reproducible and continuous manner and thus, the optical properties of this *two-particle* nanophotonic system can be precisely controlled and reversibly tuned.

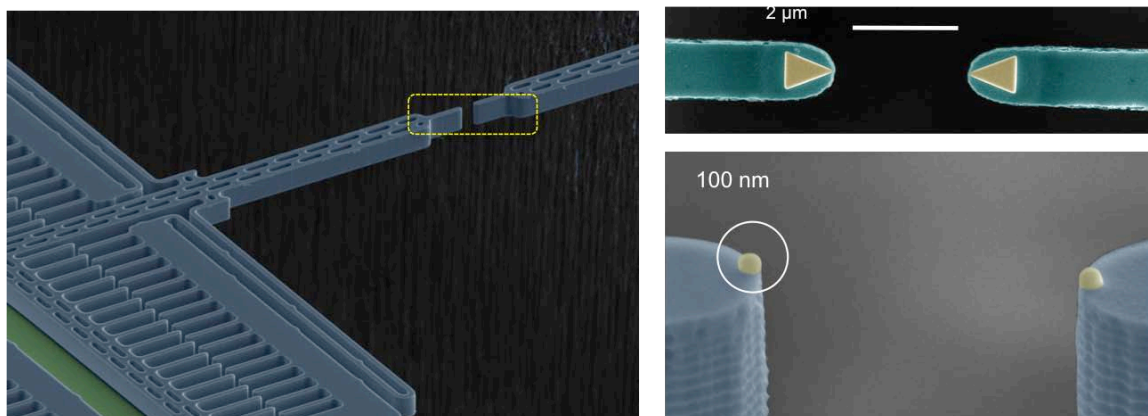


**Figure 1:** Left-side: SEM image of a typical MEMS actuator used to manipulate the optical interaction between metallic nanostructures. On the right side panel a magnified SEM image of the tip of the actuators with different nanostructures is shown.

Using a variety of deposition processes, we deposited a variety of metallic nanostructures at the ends of the nano-needles (Figure 1 – right side). Several fabrication processes were developed to reliably integrate nanoparticles onto the probes. We have used a maskless FIB fabrication approach to make individual metallic nanoparticles with diameters in the range of 50 nm to 300 nm. A combination of electron-beam evaporation and FIB etching was used to create Au-based nanostructures. No other research group has applied MEMS technologies to precisely control nanoparticle-nanoparticle coupling interactions.

In this poster we will describe the MEMS actuators we have developed, the nanofabrication processes used to integrate nanostructures onto MEMS actuators and the preliminary optical measurements performed on these structures.

### **Future Work**

In addition to study the optical properties of these devices under photonic illumination, we are developing the tools required to study them under electronic excitation. In order to do that, in collaboration with the Electron Microscopy Center at ANL, we are implementing an experiment that will allow the use of a TEM for direct visualization of plasmons interaction.

Use of the Center for Nanoscale Materials was supported by the U. S. Department of Energy, Office of Science, Office of Basic Energy Sciences, under Contract No. DE-AC02-06CH11357.

# Synthesis of Abrupt Interfaces without Kinking in VLS-Growth of Si-Ge Axial Nanowire Heterostructures by Novel *in situ* Catalyst Alloying

Daniel E. Perea<sup>†</sup>, Nan Li<sup>†</sup>, Robert M. Dickerson<sup>‡</sup>, Amit Misra<sup>†</sup>, and S. T. Picraux<sup>†</sup>

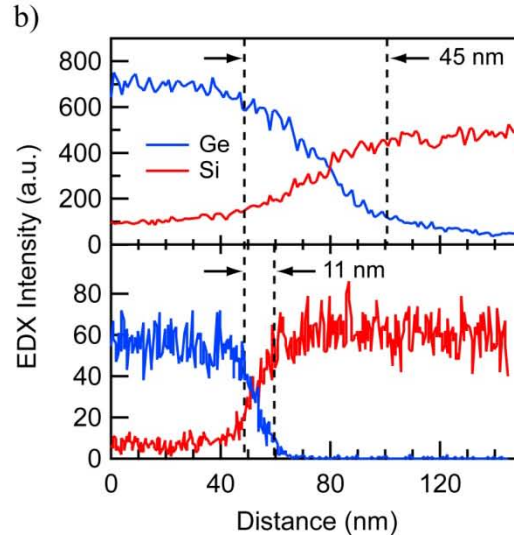
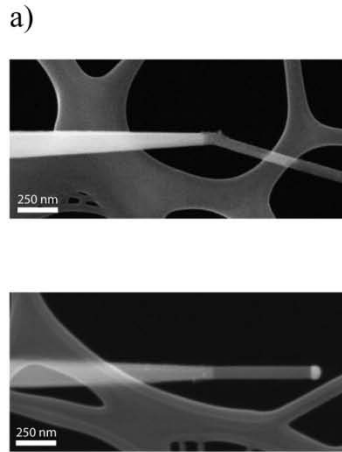
<sup>†</sup>Center for Integrated Nanotechnologies, <sup>‡</sup>Material Science and Technology-6; Los Alamos National Laboratory, Los Alamos, New Mexico 87545

## Proposal Title

Dopant Distribution and Interface Studies of Si and Ge Nanowire Heterostructures

## Challenge and Research Achievement

Vapor-liquid-solid (VLS) grown axial semiconductor heterostructures have garnered much attention due to their potential for novel or enhanced optical, electronic, and thermoelectric properties compared to conventional planar technology. Of particular interest are Si-SiGe and Si-Ge axial superlattice heterostructures which are being explored for thermoelectric and tunnel field-effect transistor applications. However, it is commonly found that due to the VLS growth process, the interfaces are significantly broadened and a high percentage of Si-Ge heterostructured nanowires form undesired structural kinks by changing growth direction shortly after the change in composition. Using electron beam based analysis, we report recent results in which the interfaces are much more abrupt and kinking is significantly reduced. The new process involves *in situ* alloying of the liquid Au catalyst with Ga by the introduction of trimethylgallium. This resulting novel liquid alloy catalyst significantly reduces the solubility of Si and Ge in the liquid which sharpens the interface, while at the same time reduces the growth rate at the higher precursor partial pressures favorable to nanowire growth, thus promoting a significant reduction in kinking. For example, considering a ~65nm diameter nanowire, for the transition from Ge to Si, the solubility of Ge is significantly decreased and the interface sharpness increases from a width of 45 nm to 11 nm for growth at 380 C using a Au<sub>0.67</sub>Ga<sub>0.33</sub> alloy, as compared to growth from pure Au. At the same time, the growth rate decreases from 2.8 nm/s for kinked Si segments grown from a pure Au catalyst, to 0.2 nm/s with a 10X increase in unkinked Ge/Si heterostructure growth from approximately 95% kinking to <10%. While the underlying mechanisms for kinking which drive a nanowire to change growth direction is not well understood, it is known that this effect is sensitive to the kinetics of growth and becomes a significant issue when changing the growth precursors or temperature. In this presentation we will present detailed results for this new approach to achieving high quality nanowire heterostructure interfaces, discuss the underlying mechanisms.



A high percentage of Si-Ge axial heterostructure nanowires grown from a pure 60 nm Au catalyst nanoparticle exhibit a kinked morphology (a-top) after the junction and have an average interfacial width of 45 nm (b-top) as measured by EDAX analysis. A high percentage of nanowires grown from a  $\text{Au}_{0.67}\text{Ga}_{0.33}$  catalyst alloy are straight, i.e. do not kink (a-bottom) and have a sharpened interface of 11 nm (b-bottom).

### Future work

Future directions include tailoring high quality compositionally-abrupt VLS-grown *doped* axial interfaces (eg. *pn*-junctions) based on this new understanding which is important for future nanowire device applications such as in tunnel field effect transistors. A combination of electron beam holography and atom probe tomography will be used to reveal the three-dimensional distribution of dopants and allow an understanding of the limits of dopant incorporation and interface abruptness in nanowire heterostructures. These techniques will provide a unique route to correlate the nanowire structure/composition with the electronic transport properties of heterojunction nanowires with sharpened interfaces.

### Related publications for work performed at LANL

D.E. Perea, N. Li, R.M. Dickerson, A. Misra, and S.T. Picraux, Controlling Heterojunction Abruptness in VLS-Grown Semiconductor Nanowires via in situ Catalyst Alloying; in submission (2011).

Acknowledgment: This research was funded in part by the Laboratory Directed Research and Development (LDRD) Program at Los Alamos National Laboratory and performed in part at the Center for Integrated Nanotechnologies, a U.S. Department of Energy, Office of Basic Energy Sciences user facility at Los Alamos National Laboratory (Contract DE-AC52-06NA25396). D.E.P. acknowledges funding from a LDRD-funded Postdoctoral Director's Fellowship at Los Alamos National Laboratory (LANL). Electron microscopy and EDX analysis was carried out at the MST-6 Electron Microscope Laboratory LANL. The authors would also like to acknowledge helpful discussions with E. J. Schwalbach and P. W. Voorhees at Northwestern University, and T. Lookman at LANL.

# Mechanism of plasmonic response of noble metal nanoparticles actuated by responsive polymer brush

Ihor Tokarev<sup>a</sup>, Yuri Roiter<sup>a</sup>, Iryna Minko<sup>a</sup>, Dmytro Nykypanchuk<sup>b</sup>, and Sergiy Minko<sup>a</sup>

<sup>a</sup> Department of Chemistry and Biomolecular Science, Clarkson University  
Potsdam, New York 13699-5810 (USA)

E-mail: [itokarev@clarkson.edu](mailto:itokarev@clarkson.edu), [sminko@clarkson.edu](mailto:sminko@clarkson.edu)

<sup>b</sup> Center for Functional Nanomaterials, Brookhaven National Laboratory  
Upton, New York 11973-5000 (USA)

## Proposal Title

Stimuli-responsive polymer brushes and polymer gel thin films. X-ray reflectivity characterization of the internal structure and swelling profiles

## Scientific Challenge and Research Achievement

The mechanism of the high spectral sensitivity of an ultrathin film composed of a grafted poly(2-vinylpyridine) layer (P2VP brush) that tunes the spacing between two kinds of nanoparticles—gold nanoislands immobilized on a transparent support and gold colloidal particles adsorbed on the brush—in response to changes in the solution pH was investigated in detail in this study. The optical response of the film relies on the phenomenon of localized surface plasmon resonances in the noble metal nanoparticles, giving rise to an extinction band in visible spectra, and a plasmon coupling—electromagnetic interactions between the particles and the islands that have a strong effect on the band position and intensity. Since the coupling is controlled by the interparticle spacing, the pH-triggered swelling-shrinking transition in the P2VP brush leads to pronounced changes in the transmission spectra of the hybrid film. The extinction band was deconvoluted into four spectrally separated and overlapping contributions that were attributed to different modes of interactions between the particles and the islands. These modes come into existence due to variations in the thickness of the grafted polymeric layer on the profiled surface of the islands. Atomic force microscopy (AFM) and X-ray reflectometry (the measurements were carried out in the Center for Functional Nanomaterials, Brookhaven National Laboratory) allowed us to explore the behavior of the Au particles as the P2VP brush switched between the swollen and collapsed states. In particular, we identified an interesting, previously unanticipated regime when a particle position in a polymer brush is switched between two distinct states: the particle exposed to the surface of the collapsed layer and the particle engulfed by the swollen brush. On average, the characteristic distance between the particles and the islands increased upon the brush swelling. The observed behavior is a result of the anchoring of the particles to polymeric chains that limit the particles' vertical motion range. The experimental findings provide a better understanding of the pronounced optical response of the studied hybrid film and will be used to design highly sensitive optical nanosensors based on a polymer-brush-modulated interparticle plasmon coupling.

## **Future Work**

Future work will involve studying phase behavior of inorganic nanoparticles interacting with polymer brushes. We will carry out *in-situ* X-ray reflectivity measurements of the vertical particle distribution in a swollen and collapsed brush. Unlike AFM, the X-ray reflectometry available at the Brookhaven National Laboratory will allow us to acquire statistically averaged information over a large sample area.

## **Publications**

1. Roiter, Y., Minko, I., Nykypanchuk, D., Tokarev, I., Minko, S. Mechanism of plasmonic response of noble metal nanoparticles actuated by responsive polymer brush. Submitted for publication in 2011.

## **Imaging Shape Dependent Surface Plasmon Resonances using Monochromated Electron Beams.**

**S. Aloni**<sup>1</sup>, E.C.Nelson<sup>2</sup>, R. Erni<sup>2</sup>, Y. Yin<sup>1</sup>.

<sup>1</sup>The Molecular Foundry, Lawrence Berkeley National Laboratory, Berkeley, CA 94706.

<sup>2</sup>National Center for Electron Microscopy, Lawrence Berkeley National Laboratory, Berkeley, CA 94706.

**NCEM Proposal No. 1365:** "Measuring Optical properties of individual nanostructures and their assemblies."

**Scientific Trust area:** "Multimodal in-situ nanoimaging"

**Scientific Challenge and Research Achievement:** Optical properties of noble metal nanoparticles stem from electric field distribution on nm length scale. Optical spectroscopy lacks the resolution to spatially resolve the shape dependent plasmonic resonances. In this work we developed methodology to map the surface plasmon resonances with sub nanometer and sub 100meV resolution linking the optical response of individual nanoparticle to the spatial distribution of the excited plasmon resonances.

Noble metal nanostructures are of great interest because of their unique optical properties. Their optical properties are determined by the surface plasmon resonance of conduction electrons, the frequency of which is determined not only by the nature of the metal or alloy of which the particle is made but also by the particle's size and shape. Moreover, the properties can be further tailored by forming nanoparticle assemblies and by controlling the surrounding dielectric medium [1]. For many metals the plasma frequency lies in the UV part of the spectrum and the nanoparticles do not display strong color effects. In noble metals, due to strong d-d band transitions, the plasma frequency is pushed into the visible part of the spectrum. Hence most of the surface plasmon experiments were carried out with gold silver and copper nanoparticles.

In this work we focus on study of the shape effects of the plasmonic excitations in silver and gold nanostructures. The silver and gold nanostructures were synthesized by solution phase synthesis [2] yielding highly faceted nanocrystals including spheres, cubes, triangular plates, bi-pyramids and rods of aspect ratios up to 1:15. The nanoparticle solutions were washed off the excess surfactant and suspended on commercially available carbon and SiO<sub>x</sub> and SiN support grids for analysis.

Due their small size, the correlation of the shape and optical properties of individual nanocrystals is not straightforward. Usually the geometrical shape is deduced from high-resolution TEM images while optical properties are measured via optical spectroscopy, which provides average information of large number of nanoparticles with varying sizes and shapes. We used high energy-resolution EELS spectral imaging in combination with Z-contrast imaging that was carried out using a FEI TEAM 0.5 microscope operated between 80 and 300kV. This microscope is equipped with a double-focusing Wien filter acting as a monochromator. This setup in combination with a high-resolution Gatan Imaging Filter (GIF) allows for a 2Å electron probe with an energy resolution of 0.14 eV or better, thus energy-loss information can unambiguously be accessed down to about .5 eV electron energy loss facilitating studies of optical properties of individual nanostructures in the visible and near infra-red part of the spectrum.

In a small spherical silver nanoparticle the optical response is defined by the dipole resonance mode at 3.1eV (395nm). This mode is size dependent exhibiting significant red-shift and broadening as the size increases. The contributions of the higher order modes, mainly quadrupole mode, dominate at sizes above 40 nm and are weakly size dependent. Figure 1c shows EEL spectra extracted from different positions in the spectral image of single spherical nanoparticle. When pointing the electron beam to the center of the nanoparticle the most significant energy loss mode can be observed at ~3.8eV, which was observed in silver thin

films and is attributed to the bulk silver plasmon. By pointing at the particles edge we increase our sensitivity to surface related phenomena revealing the SPR as expected at 3.15 eV. The spatial distribution of the energy loss intensity at these,(Fig 1c&d) reveals characteristic distribution for the bulk and surface plasmons as series of “energy filtered” images obtained by constant energy cuts through the 3d spectral image data cube.

The plasmons of a rod-shaped nanoparticle can be categorized into the longitudinal and transverse modes where the direction of the collective electronic oscillations is parallel and perpendicular to the rod axis, respectively. The longitudinal modes can be described as resonant modes of an antenna that are described by the wire’s length. Higher order transverse plasmons unlike their longitudinal counterpart, show little frequency dependence. Figure 2 displays energy-filtered images of the first 3 longitudinal modes (a) of a 30x300nm silver nanowire at 0.95,1.5 and 2.2 eV’s respectively. The transverse (b) and bulk(c) modes are similar to the ones observed for the spherical nanoparticle . Finally, the plasmon dispersion relation, i.e. the wavelength dependence of the modes energy, the silver plasmon dispersion relation, can be derived by measuring the wave number from the distinct modes and the associated mode energies (see figure 2d).

In summary, the unmatched lateral resolution modern microscopes combined with the high energy resolution of and spectrometers is a unique tool to understand optical properties of metallic nanostructures.

References

- [1] L.M. Liz-Marzan, *Langmuir* 22 (2006) 32.
- [2] Y. Yin, A. P. Alivisatos, *Nature* 437 (2005) 664.
- [3] S.Aloni et.al. *Microscopy and Microanalysis* 15 (2009) 136.

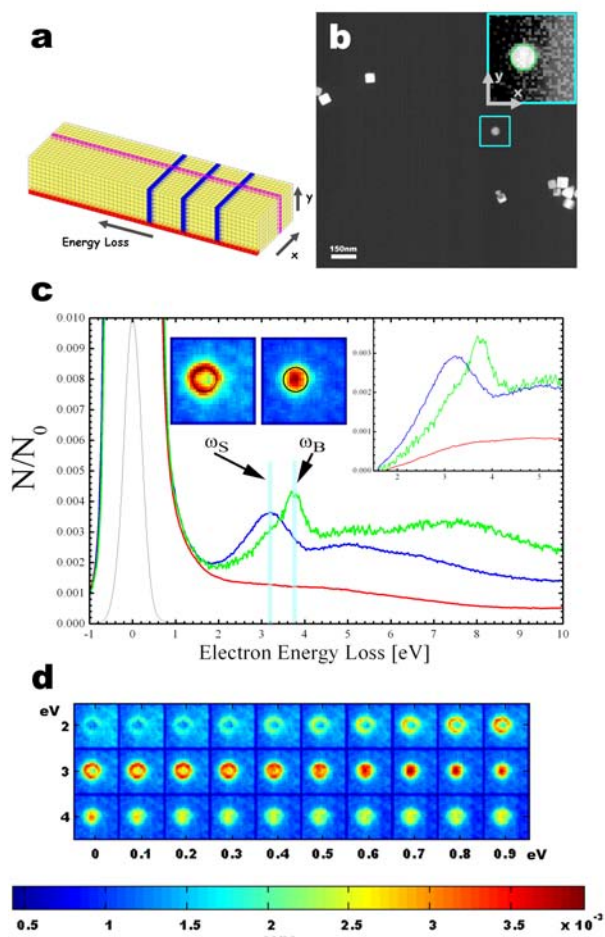


Figure 1. Spectral image of a spherical silver nanoparticle. Schematic description of the 3D EELS spectral image (a) and a high angle annular dark field image of the sample (b). The blue square indicates the area of the spectral image map around a spherical particle. (c) displays individual spectra representative of the the particle's center (green)and edge (blue) as well as the supporting film (red).In the insert spectra after subtraction of the ZLP. The left upper corner shows the spectra after subtraction of the ZLP. (d) spatial distribution of the energy loss signal as a function of energy in the 2 to 4 eV range.

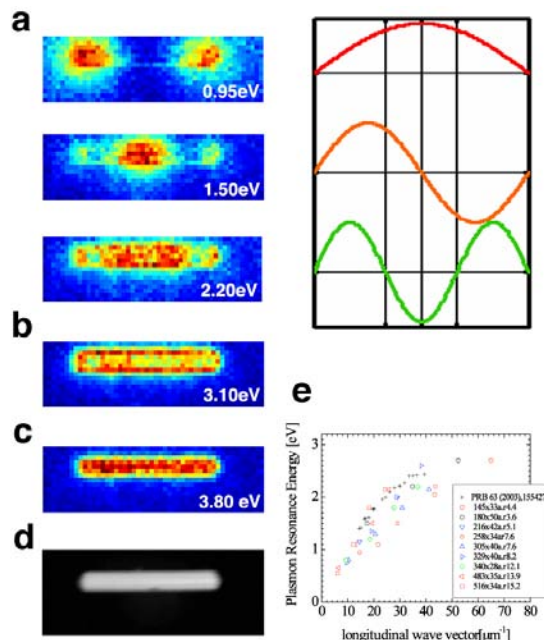


Figure2. Spectral imaging revealing the plasmonic modes of a 30x300nm silver nanorod. The characteristic signatures of the first 3 longitudinal modes (a) as well as the transverse (b) and bulk (c)plasmons can be clearly resolved. (d) The HAADF image. (e) the silver plasmon dispersion relation obtained from 9 different nanowires with aspect ratios of 3-15.

# Theoretical Studies of Quantum Dot – Plasmon Interactions

S. K. Gray and M. Pelton

Center for Nanoscale Materials, Argonne National Laboratory, Argonne, Illinois 60439

## Scientific Thrust Area

Theory and modeling of light-matter interactions at the nanoscale.

## Scientific Challenge and Research Achievement

The scientific challenge is to predict, based on theory and modeling, how light can interact with systems composed of metal nanoparticles and quantum dots to yield novel near and far field properties relevant to sensing, electronics and energy technologies. Much of our work has been based on rigorous computational electrodynamics modeling via the finite-difference time-domain (FDTD) method for which we have developed highly parallelized software adapted to these types of problems.

The metal nanoparticles, when exposed to appropriate radiation, can exhibit optical resonances known as surface plasmons (or simply “plasmons”) that are associated with relatively intense near fields around their surfaces. Quantum dots (semiconductor nanocrystals) placed near metal nanoparticles can have their emission properties significantly altered and affect the overall optical properties of the combined system. For example, we have previously shown that fluorescing quantum dots can excite dark plasmons [1], i.e., plasmons that cannot normally be excited by ordinary light. More recently we have illustrated the opposite extreme, a transparency

[2] wherein the system does not scatter or absorb any light for some spectral region.

We first considered a model system corresponding to a pair of ellipsoidal silver nanoparticles in air, as schematically illustrated in blue at the top of Figure 1. This represents a plasmonic resonator when exposed to light polarized along the dimer axis, with the FDTD-based extinction spectrum (green dots, Fig. 1) corresponding to a strong peak near photon energies 2.1 eV. (The particles are 40nm long and 10nm wide, and are separated by 6nm; the spherical, 4nm QD is modeled as a region of space that has a Lorentzian polarization response consistent with the CdSe absorption spectrum.) The extinction spectrum of the full system (black circles, Fig. 1) displays a remarkable dip or

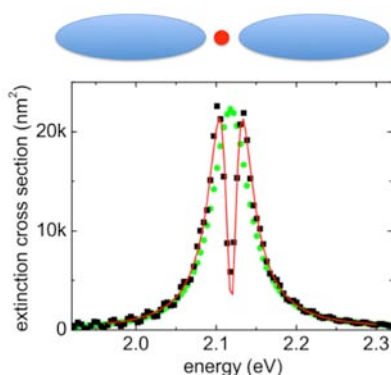


**Figure 1.** Placing a small quantum dot in a silver nanoparticle dimer system can lead to a transparency. Green symbols correspond to the extinction in the absence of the quantum dot, black symbols correspond to the full system, and the red curve is the result of a two-oscillator analytical model.

near-transparency just above 2.1 eV due to an interference effect that can be mimicked with an analytical, two-oscillator model (red line, Fig. 1). We have termed this effect a “quantum dot induced transparency.”

The system in Fig. 1 is somewhat idealized. Figure 2(a) displays a more realistic system that could be prepared lithographically, for example. The system consists of two silver hexahedrons with a uniform rhomboid cross-section, or “nanodiamonds,” on top of a glass surface with a quantum dot inserted between them. FDTD calculations were carried out and

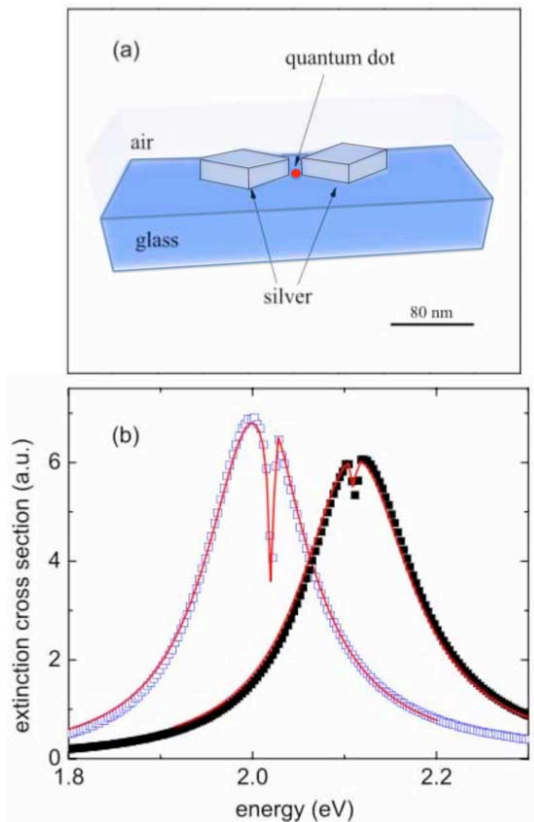


Figure 2. (a) Silver nanoparticles on glass with a quantum dot placed between them. (b) Optical spectra inferred from FDTD calculations assuming 2nm (left, open) and 5nm (right, filled) radii of curvature around the nanoparticle edges.

optical spectra were calculated. The same remarkable transparency is evident, Fig. 2(b). The degree of transparency depends on how rounded the corners of the nanoparticles are, with sharper (i.e., lower radius of curvature) corners leading to stronger interactions and a stronger effect. Furthermore, it is likely the effect could be enhanced via optimization of the system configuration, which we have not yet pursued.

### Future Work

We will explore and optimize quantum dot/metal nanoparticle systems such as those discussed above for the control of near and far field properties. Optimization techniques such as those we have recently introduced in the context of other problems should prove particularly useful [3]. Systems of long nanowires, which themselves have interesting properties in terms of exhibiting “plasmonic wave packets” [4], will also be considered. Other important directions are to develop and apply methods to incorporate quantum mechanical features of the quantum dots more accurately via, e.g., the Maxwell-Bloch equations. We will also investigate the importance of other phenomena such as the non-local dielectric constant behavior [5] and chemical interactions [6] that can become important as nanoparticle sizes are decreased.

Use of the Center for Nanoscale Materials was supported by the U. S. Department of Energy, Office of Science, Office of Basic Energy Sciences, under Contract No. DE-AC02-06CH11357.

### Publications

- [1] Excitation of dark plasmons in metal nanoparticles by a localized emitter  
M. Liu, T.-W. Lee, S. K. Gray, P. Guyot-Sionnest, and M. Pelton, *Phys. Rev. Lett.* **102**, 107401 (2009).
- [2] Quantum dot induced transparency in a nanoscale resonator  
X. Wu, S. K. Gray, and M. Pelton, *Optics Express* **18**, 23633 (2010).
- [3] Surrogate-based modeling of the optical response of metallic nanostructures  
R. L. Miller, Z. Xie, S. Leyffer, M. J. Davis, and S. K. Gray, *J. Phys. Chem. C* **114**, 207041 (2010).
- [4] Controlling plasmonic wave packets in silver nanowires  
L. Cao, R. A. Nome, J. M. Montgomery, S. K. Gray, and N. F. Scherer, *Nano Letters* **10**, 3389 (2010).
- [5] Optical properties of nanowire dimers with a spatially nonlocal dielectric function  
J. M. McMahon, S. K. Gray, and G. C. Schatz, *Nano Letters* **10**, 3473 (2010).
- [6] Reversing the size-dependence of surface plasmon resonances  
S. Peng, J. M. McMahon, G. C. Schatz, S. K. Gray, and Y. Sun, *Proc. Nat. Acad. Sci.* **107**, 14530-14534 (2010).

# PHOTON LOCALIZATION AND SUB-DIFFUSIVE LIGHT TRANSPORT IN APERIODIC NANOSTRUCTURES

Prof. Luca Dal Negro

*Department of Electrical and Computing Engineering & Photonics Center  
Boston University, 8 Saint Mary's street, Room 825  
Boston, MA 02215-2421 USA*

The ability to design and to control light-matter interactions at the nanoscale represents the core aspect of the rapidly growing field of nanophotonics. Efficient schemes for electromagnetic field localization and intensity enhancement are essential requirements for the design and engineering of novel optoelectronic components that leverage on broadband enhancement of optical cross sections, such as optical biosensors, photodetectors and light sources and on-chip nonlinear elements. Recent advancements in the design and fabrication of Deterministic Aperiodic Nanostructures (DANS) have provided novel opportunities for the generation of broadband field localization, enhancement, and light-matter coupling on the nanoscale.

DANS are optical media in which the refractive index fluctuates over length scales comparable or smaller than the wavelength of light. They include dielectric and metallic structures, metallo-dielectric nanostructures and metamaterials. In all cases, DANS are designed by deterministic algorithms that interpolate in a tunable fashion between periodicity and pseudo-randomness. As a result, DANS are readily fabricated using conventional nanolithographic techniques and display unique transport and localization properties akin to random media. In this talk, I will present our work on the design, fabrication, and optical characterization of DANS in the context of broadband nanophotonic devices for on-chip applications. Specifically, I will focus on the enhancement of nanoscale optical fields using aperiodic resonant nanoparticle arrays for multi-frequency light sources, plasmon enhanced photodetectors, optical biosensors, and nonlinear signal generation on optical chips<sup>1-11</sup>. I will also present our recent work on circularly symmetric multiple scattering of light in photonic-plasmonic aperiodic spiral arrays<sup>12</sup> and demonstrate its impact for broadband energy harvesting in thin-film plasmonic solar cells. Finally, I will present our preliminary work towards demonstration of a novel light transport regime, Sinai sub-diffusion, in aperiodic waveguide structures fabricated in collaboration with the Molecular Foundry at LBNL. Future work related to the fabrication of Coherent Perfect Absorbers (CPAs)<sup>13</sup> integrated into silicon-based waveguide structures will also be discussed.

## Selected References:

1. L. Dal Negro, N. Feng, "Spectral gaps and mode localization in Fibonacci chains of metal nanoparticles" **Optics Express**, **15**, 22, 14396, (2007)
2. L. Dal Negro, N.N. Feng, A. Gopinath "Electromagnetic coupling and plasmon localization in deterministic aperiodic arrays", **J. Opt. A: Pure Appl. Opt.** **10**, 064013, (2008)
3. R. Dallapiccola, A. Gopinath, F. Stellacci, L. Dal Negro, "Quasi-periodic distribution of plasmon modes in two-dimensional Fibonacci arrays of metal nanoparticles" **Optics Express**, **16**, 8, 5544, (2008)
4. A. Gopinath, S. Boriskina, N.N. Feng, B.M. Reinhard, L. Dal Negro, "Photonic-plasmonic scattering resonances in deterministic aperiodic structures", **Nano Letters**, **8**, 2423, (2008)
5. C. Forestiere, G. Miano, G. Rubinacci, and L. Dal Negro, "Role of aperiodic order in the spectral, localization, and scaling properties of plasmon modes for the design of nanoparticles arrays", **Phys. Rev. B.**, **79**, 085404 (2009)
6. C. Forestiere, G. F. Walsh, G. Miano, L. Dal Negro, "Nanoplasmonics of prime number arrays", **Optics Express**, **17**, 24288 (2009)
7. A. Gopinath, S. Boriskina, R. Premasiri, L. Ziegler, B. Reinhard, L. Dal Negro, "Plasmonic nano-galaxies: multi-scale aperiodic arrays for surface enhanced Raman sensing", **Nano Letters**, **9**, 11, 3922 (2009)
8. A. Gopinath, S. V. Boriskina, S. Selcuk, R. Li, and L. Dal Negro, "Enhancement of the 1.55 $\mu\text{m}$  Erbium<sup>3+</sup> emission from quasi-periodic plasmonic arrays" **Appl. Phys. Lett.**, **96**, 071113 (2010)

9. S. Y. K. Lee, J. J. Amsden, S. V. Boriskina, A. Gopinath, A. Mitropoulos, D. L. Kaplan, F. G. Omenetto, and L. Dal Negro, "*Spatial and spectral detection of protein monolayers with deterministic aperiodic arrays of metal nanoparticles*," **Proc. Natl. Acad. Sci. USA**, **107**, 12086 (2010).
10. J. Yang, S.V. Boriskina, H. Noh, M. J. Rooks, G.S. Solomon, L. Dal Negro, H. Cao, "*Demonstration of laser action in a pseudorandom medium*", Appl. Phys. Lett., **97**, 223101 (2010).
11. Forestiere, M. Donelli, G.F. Walsh, E. Zeni, G. Miano, L. Dal Negro, "*Particle swarm optimization of broadband nanoplasmonic arrays*", **Optics Letters** **35**, 133 (2010)
12. J. Trevino, H. Cao and L. Dal Negro, "*Circularly-symmetric light scattering from nanoplasmonic spirals*", **Nano Letters** DOI: 10.1021/nl2003736
13. W. Wan, Y. Chong, L. Ge, H. Noh, A. D. Stone, H., Cao, "*Time-reversed lasing and interferometric control of absorption*" **Science**, 331, 889 (2011)

# Hybrid Nanophotonic Structures for Energy Conversion

G. P. Wiederrecht, N. C. Giebink, J. Hranisavljevic

Center for Nanoscale Materials, Argonne National Laboratory, Argonne, Illinois

## Scientific Thrust Area

Experimental nanophotonics.

## Scientific Challenge and Research Achievement

The scientific challenge of this project is to create novel electronic and optical states in a hybrid nanomaterial in order to provide new routes for the collection and conversion of energy at the nanoscale. The motivation for this project is that basic studies in nanophotonics can reveal optical and optoelectronic phenomena that are useful for a range of critical technologies including solar energy collection and conversion, as well as impacting next generation optical microscopy and ultrasensitive spectroscopies.

The design of nanostructures to contain strongly localized optical fields is a central focus of this project. This is due to the fact that optical fields confined in at least one dimension provide the opportunity to couple optical near-fields to neighboring nanostructures. Doing so can produce strongly coupled states with very different optical and electronic properties than either constituent of the hybrid nanostructure. Furthermore, interfacial interactions can provide impetus for converting energy, such as the conversion of tightly bound excitons to long-lived charge separated states. Finally, confinement enables strong tunability of the optical resonances of the nanostructure based on nanomaterial size, shape, composition, and environment.

In this project, the confinement of optical fields is achieved through the fabrication of ultra-thin dielectric films to produce optical cavities. An initial example of an optical cavity containing nanostructures is shown in Figure 1. We have designed and fabricated these high- $Q$  cavities with a guide layer incorporating CdSe/ZnS core/shell quantum dots. We observe strong coupling and hybridization between two exciton states of the quantum dots that are mediated by the cavity photon. The nanofabrication approach we have taken greatly simplifies the creation of high- $Q$  planar nanocavities for organic and inorganic quantum dot thin films.

We have further utilized the optical cavities to realize a novel means to concentrate optical energy from luminescent chromophores by nanostructuring the surface of the cavity. The

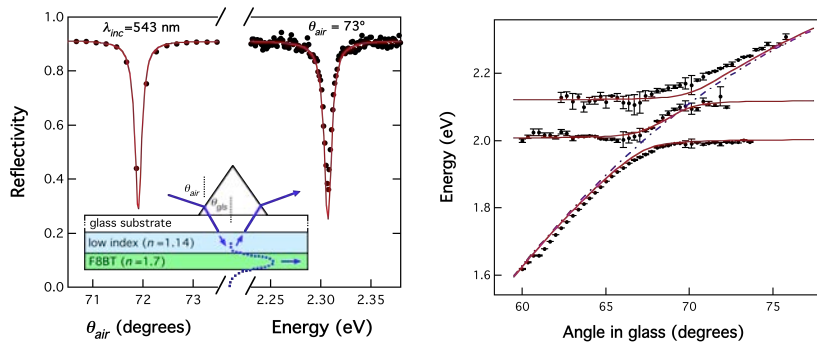


**Figure 1.** A schematic and polarized reflectivity plot for a prism-coupled optical cavity is shown (left). When quantum dots are added, anticrossing regions in the cavity dispersion is observed, which is a signature for strong exciton-photon coupling and the creation of mixed, hybrid electronic states.

project develops concepts related to luminescent solar concentrators that traditionally consist of a transparent slab embedded with a chromophore that absorbs sunlight and re-emits it back into the slab, where it is trapped by total internal reflection and absorbed by photovoltaic cells attached to the edges. In

practice, however, the overlap between chromophore absorption and emission spectra ultimately leads to unacceptable reabsorption losses that limit the concentration of optical energy and therefore the utility of luminescent solar concentrators to date. In this project, we nanostructured the thickness of the cavity in order to alter the optical resonance along the length of the cavity. Thus, sharply directed emission from the cavity continuously avoids the narrow reabsorption resonance at each subsequent bounce and hence propagates with low loss to the substrate edges. Using this approach, we have demonstrated near-lossless propagation for several different chromophores with varying reabsorption overlap that ultimately enables a more than two-fold increase in concentration of emission over that of the corresponding conventional luminescent solar concentrator. This work opens up new opportunities for energy collection and conversion with nanostructures, as well as studies of the impact of strong coupling on important optical processes such as nonlinear optical phenomena in nanomaterials.

### Future Work

Future work will be to realize new hybrid nanomaterials with novel optical properties that enable energy collection, concentration, and conversion. Specific targets at this time are functionalized plasmonic nanotubes for reducing plasmonic propagation losses (as opposed to solid plasmonic nanowires) and optical cavities with ultrahigh extinction emitters for energy concentration. Future work will be performed in continued collaboration with the theory and modeling group and will use the advanced lithography capabilities at the CNM.

Use of the Center for Nanoscale Materials was supported by the U. S. Department of Energy, Office of Science, Office of Basic Energy Sciences, under Contract No. DE-AC02-06CH11357.

### Publications

- Strong exciton-photon coupling with colloidal quantum dots in a high-Q bilayer microcavity. N. C. Giebink, G. P. Wiederrecht, and M. R. Wasielewski, *Appl. Phys. Lett.* **98**, 081103 (2011).
- Designed ultrafast optical nonlinearity in a plasmonic nanorod metamaterial enhanced by nonlocality. G. A. Wurtz, R. Pollard, W. Hendren, G. P. Wiederrecht, D. J. Gosztola, V. A. Podolskiy, and A. V. Zayats, *Nature Nanotech.* **6**, 107 (2011).
- The ideal diode equation for organic heterojunctions. I. Derivation and Application. N. C. Giebink, G. P. Wiederrecht, M. R. Wasielewski, and S. R. Forrest, *Phys. Rev. B* **82**, 155305 (2010).
- The ideal diode equation for organic heterojunctions. II. The role of polaron pair recombination. N. C. Giebink, B. E. Lassiter, G. P. Wiederrecht, M. R. Wasielewski, and S. R. Forrest, *Phys. Rev. B* **82**, 155306 (2010).
- Self-consistent model of light-induced molecular motion around metallic nanostructures. M. Juan, J. Plain, R. Bachelot, P. Royer, S. K. Gray, and G. P. Wiederrecht, *J. Phys. Chem. Lett.* **1**, 2228 (2010).
- External control of the scattering properties of a single optical antenna. C. Huang, A. Bouhelier, J. Berthelot, G. Colas-des Francs, J.-C. Weeber, A. Dereux, S. Kostcheev, A.-L. Baudrion, J. Plain, R. Bachelot, P. Royer, and G. P. Wiederrecht, *Appl. Phys. Lett.* **96**, 143116 (2010).
- Tuning of an optical dimer nanoantenna by electrically controlling its load impedance. J. Berthelot, A. Bouhelier, C. Huang, J. Margueritat, G. Colas-des Francs, E. Finot, J. Weeber, A. Dereux, S. Kostcheev, H. Ahrach, A. L. Baudrion, J. Plain, R. Bachelot, P. Royer, G. P. Wiederrecht, *Nano Letters* **9**, 3914 (2009).
- Electroluminescence from electrolyte-gated carbon nanotube field-effect transistors. J. Zaumseil, X. Ho, J. R. Guest, G. P. Wiederrecht, and J. A. Rogers, *ACS Nano* **3**, 2225 (2009).
- Multi-scale model for photo-induced molecular motion in azo-polymers. M. L. Juan, J. Plain, R. Bachelot, P. Royer, S. K. Gray, and G. P. Wiederrecht, *ACS Nano* **3**, 1573 (2009).

## From Atomic-Resolution Imaging towards Nano-Thermodynamics by Enabling Dynamic Experiments for Electron Microscopy with Single Atom Sensitivity at Controlled Temperature and Pressure

C. Kisielowski<sup>1</sup>, C. Song<sup>1</sup>, B. Barton<sup>2</sup>, P. Specht<sup>2</sup>, D. Detert<sup>2</sup>, O.D. Dubon<sup>2</sup>, H. Calderon<sup>1,3</sup>, J.H. Kang<sup>4</sup>, D. Barton<sup>4</sup>, R. Cieslinski<sup>4</sup>, B. Jiang<sup>5</sup>

1) NCEM, Helios SERC, and JCAP, One Cyclotron Rd., Berkeley CA 94720, USA

2) Materials Sciences Division, LBNL, One Cyclotron Road, Berkeley, CA 94720, USA

3) Escuela Superior de Física y Matemáticas, IPN, Ed. 9 UPALM Zacatenco, Mexico D.F. 07738

4) The Dow Chemical Company, Midland, MI, USA

5) FEI Company, NE Dawson Creek Drive, Hillsboro, Oregon 97124, USA

### Scientific Thrust Area

In recent years the LBNL dedicated significant resources for the quest to explore sustainable energy solutions with an existing sense of urgency. In this context, the Helios project, LBNL's initiative Carbon Cycle 2.0, and the Joint Center for Artificial Photosynthesis (JCAP) are established<sup>1</sup>. For materials and chemical sciences one key aspect is the discovery of new functional composites that are earth abundant, cheap, and can be manufactured into devices in scalable, chemical processes.

### Scientific Challenge and Research Achievement

This rapid development coincides with breakthroughs in instrumentation. Most noticeable is the development of the next generation electron microscopes within DoE's TEAM Project, which was recently concluded and yielded two aberration-corrected microscopes at the NCEM. The extraordinary performance of the TEAM I<sup>2,3</sup> and TEAM 0.5<sup>4-9</sup> microscopes is currently explored with great success. They are operated with single atom sensitivity at a resolution limit around 0.5 Å that is now controlled at a fundamental level by the electron scattering process itself and by beam-sample interactions. As a result, efforts to push for higher resolution are coming to an end and there is room for assessing the future of the field. One outstanding aspect in this discussion relates to ongoing efforts striving for sustainable energy solutions. In this context, it is desirable to enable experiments that would provide dynamic ( $\leq 1$  kHz) atomic-resolution microscopy with single atom sensitivity in chemically meaningful environments (pressure  $p$ , temperature  $T$ ) to advance our knowledge about functionality at the atomic level including pathways of catalytic reactions. While pressure control in electron microscopy is readily available, the control of temperature remained unsolved because it is intimately linked to uncontrolled beam-sample interactions. Figures 1 and 2 show recent implementations of new capabilities and concepts that minimize beam-sample interactions by developing low-voltage and low-dose electron microscopy. It is seen that atomic resolution microscopy is now available between 20 and 300 kV and we report that the phase contrast signal is drastically improved, materials integrity is better maintained even at surfaces, and soft or hard matter can be imaged in identical conditions by applying low-dose microscopy ( $< 100$  e/Å<sup>2</sup>). Sufficient temperature control ( $< 10$  K) is documented<sup>10</sup>.

### Future work

Thus, an opportunity exists to foster innovation and to accelerate the rate of discovery in energy related research by merging on a higher performance level the existing TEAM-technology with environmental electron microscopy. This development will enable nano-thermodynamic investigations with single atom sensitivity in controlled environments.<sup>11</sup>

[1] <http://carboncycle2.lbl.gov/>

[11] This work was supported by the DoE under Contract No. DE-AC02-05CH11231

## Publications

[2] N. Alem, O. V. Yazyev, C. Kisielowski, P. Denes, U. Dahmen, P. Hartel, M. Haider, S. Uhlemann, B. Jiang, S. G. Louie, A. Zettl, **Phys. Rev. Lett.** **106** (2011) 126102

[3] M. J. Polking, J.J. Urban, D.J. Milliron, H. Zheng, E. Chan, M. A. Caldwell, S. Raoux, C. F. Kisielowski, J.W. Ager, R Ramesh, A. P. Alivisatos, **Nano Letters** **11** (2011) 1147 – 1152

[4] S. Van Aert, K. J. Batenburg, M. D. Rossell, R. Erni, G. Van Tendeloo, **Nature** **470** (2011) 374 – 377.

[5] R. Erni, M. D. Rossell, C. Kisielowski, U. Dahmen, **Phys. Rev. Lett.** **102** (2009) 096101

[6] Ç. Ö. Girit, J. C. Meyer, R. Erni, M. D. Rossell, C. Kisielowski, L. Yang, C.-H. Park, M. F. Crommie, M. L. Cohen, S. G. Louie, A. Zettl, **Science** **323** (2009) 1705 - 1708

[7] K.-J. Jeon, H. R. Moon, A. M. Ruminski, B. Jiang, C. Kisielowski, R. Bardhan, J. J. Urban, **Nature Materials** **10** (2011) 286 – 290

[8] K.T.Nam, S. A. Shelby, P.H. Choi, A. B. Marciel, R. Chen, L.Tan, T.K. Chu, R. A. Mesch, B.-C. Lee, M. D. Connolly, C. Kisielowski, R.N. Zuckermann, **Nature Materials** **9** (2010) 454 – 460

[9] C. Kisielowski, Q. M. Ramasse, L. P. Hansen, M. Brorson, A. Carlsson, A. M. Molenbroek, H. Topsøe, S. Helveg, **Angewandte Chemie, International Edition** **49** (2010) 2708 – 2710

[10] H. Zheng, J. Baker, T. Miller, B. Sadtler, A. Lindenberg, L.-W. Wang, C. Kisielowski, A. P. Alivisatos, **Science in review**, 2011

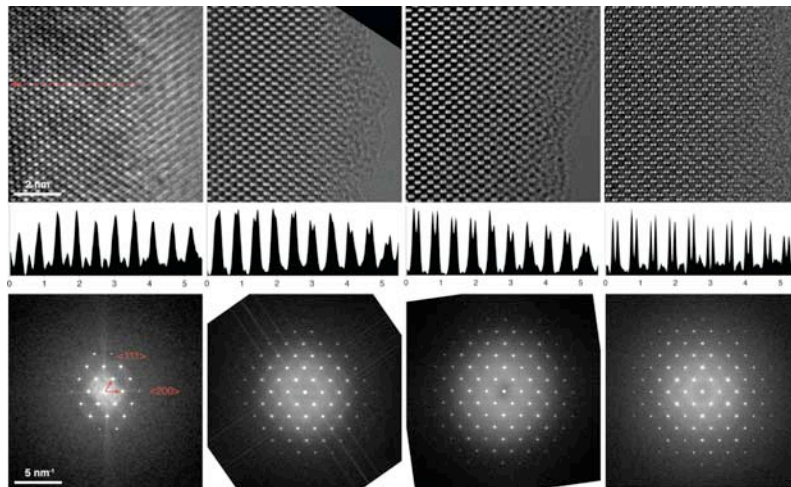


Figure 1: New capabilities - Atomic resolution microscopy at variable voltage is enabled by TEAM0.5. From left to right: 20, 50, 80, and 300 kV. Structural images of Si [110] are displayed together with their Fourier transform and line traces. It is feasible to resolve the Si [110] dumbbell distance of 136 pm across the entire energy range. At 20 kV the Cs corrector of TEAM 0.5 limits the information transfer.

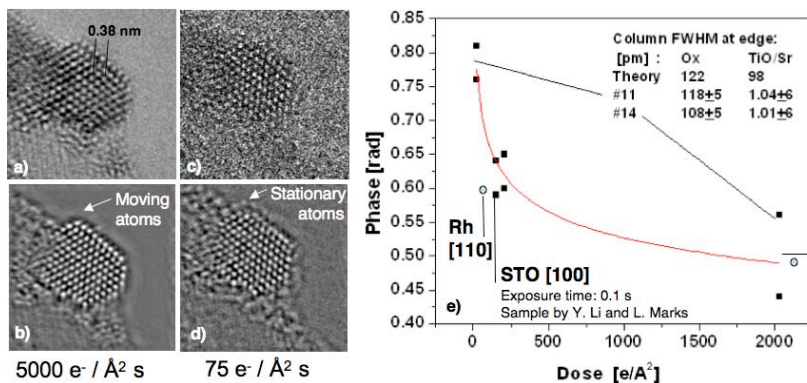


Figure 2: New concepts – Controlling beam-induced phonon excitations by dose variations. Reconstructing electron exit wave functions in low and high dose conditions from large image sets (currently  $\leq 200$  images) using in-line holography to solve the phase problem. Industry-style catalysts are imaged (Rh [110]:W on alumina,

The Dow Chemical Company). a) & c): Single, structural images of a Rh [110] particle recorded in high and low-dose conditions by TEAM 0.5 at 80 kV. b) & d): Phase of the reconstructed wave functions. Atoms are displaced and move across the surface of the catalyst in high-dose conditions, b). In contrast, atoms remain locked in place if low-dose conditions are applied, d). e): The signal enhancement with decreasing dose is caused by a suppression of phonon excitations during the image acquisition process and was observed in a variety of materials including  $\text{SrTi}_2\text{O}_3$  (STO).

## Nanomanipulation for Precise Placement of Individual Nanowires for Thermoelectric Characterization

Julio A. Martinez<sup>1</sup>, Paula P. Provencio<sup>1</sup>, John S. Sullivan<sup>1</sup>, S. T. Picraux<sup>2</sup>, B. S. Swartzentruber<sup>1</sup>

<sup>1</sup>Center for Integrated Nanotechnologies, Sandia National Laboratories, NM 87185

<sup>2</sup>Center for Integrated Nanotechnologies, Los Alamos National Laboratory, NM 87545

Scientific Thrust Area: *Nanoscale Electronics & Mechanics*

Thermoelectric power generation is presently receiving increasing interest as an approach to waste heat recovery and energy generation as part of a comprehensive plan for a clean-energy based economy. Nano-engineered materials, such as nanowires, are ideal candidates for the new generation of high figure of merit ( $ZT$ ) thermoelectrics due to the possibility of increasing phonon scattering by the small dimension of the nanowires increasing the thermal resistivity while not appreciably affecting the electrical conductivity and Seebeck coefficient. Silicon-germanium (SiGe) alloy nanowires are promising candidates to further reduce thermal conductivity by phonon scattering because bulk SiGe alloys already have thermal conductivity comparable to reported Silicon nanowires<sup>1</sup>

For the first time, we report the thermoelectric characteristics of boron-doped SiGe alloy (Si:Ge; 60:40) nanowires. In this work, we show that thermal and electrical conductivity can be measured for the same single nanowire eliminating the uncertainties in  $ZT$  estimation due to measuring the thermal conduction on one set of wires and the electrical conduction on another set. We employed nanomanipulation to place p-type SiGe nanowires on predefined surface structures and carried out in-situ contact-annealing to achieve negligible electrical contact resistance. This new methodology can be extended to other types of nanostructured materials. One of the direct consequences of our work is to estimate the influence of the free carrier concentration to the thermal conductivity of SiGe alloy nanowires. We observed that low frequency phonons are effectively scattered by boundary and hole-phonon scattering mechanisms<sup>2</sup>. This, combined with the scattering of high frequency phonons by the alloy, resulted in thermal conductivities as low as 1.1 W/m-K at 300 K, which is one of the lowest measured for SiGe alloys and is comparable to that of silica. The enhanced thermal properties observed in this work yielded  $ZT$  close to 0.18 at 300 K – more than a factor of 2 higher than the bulk alloy.

1. Dismukes J.P. et al. JAP, 1964.

2. Martinez J.A. et al. (*Submitted*)

This work was performed at the Center for Integrated Nanotechnologies, a U.S. Department of Energy, Office of Basic Energy Sciences user facility at Los Alamos National Laboratory (Contract DE-AC52-06NA25396) and Sandia National Laboratories (Contract DE-AC04-94AL85000).



## Understanding the Low Contact Resistance for Direct Au-C Links to Electrodes in Single Molecule Junctions

H. Vazquez<sup>1</sup>, J. Widawsky<sup>2</sup>, Z.-L. Chen<sup>3</sup>, S. Schneebeli<sup>3</sup>, R. Skouta<sup>3</sup>, W. Chen<sup>3</sup>, R. Breslow<sup>3</sup>, M.S. Hybertsen<sup>4</sup> and L. Venkataraman<sup>1,2</sup>

<sup>1</sup> Center for Electron Transport in Molecular Nanostructures, Columbia University, New York, NY

<sup>2</sup> Department of Applied Physics and Applied Mathematics, Columbia University, New York, NY

<sup>3</sup> Department of Chemistry, Columbia University, New York, NY

<sup>4</sup> Center for Functional Nanomaterials, Brookhaven, Upton, NY

### **Proposal Title:**

Understanding the correlation between bond breaking forces and chemistry at the single molecule scale

### **Background:**

Understanding and controlling electron transfer across metal/organic interfaces is of critical importance to the field of organic electronics and photovoltaics. Single molecule devices offer an ideal test bed for probing charge transfer details at these interfaces. These single-molecule measurements can be directly related directly theoretical models, unlike measurements at the ensemble level. The ability to fabricate single molecule devices and probe electron transfer reliably and reproducibly has enabled us to study and model transport through them. We have found that the conductance of such a junction is strongly affected by the molecular backbone chemistry, the metal-molecule link coupling and the structure at the interface. Unfortunately, the detailed role of these factors, and approaches to achieve highly-conducting molecular junctions, are not yet fully understood.

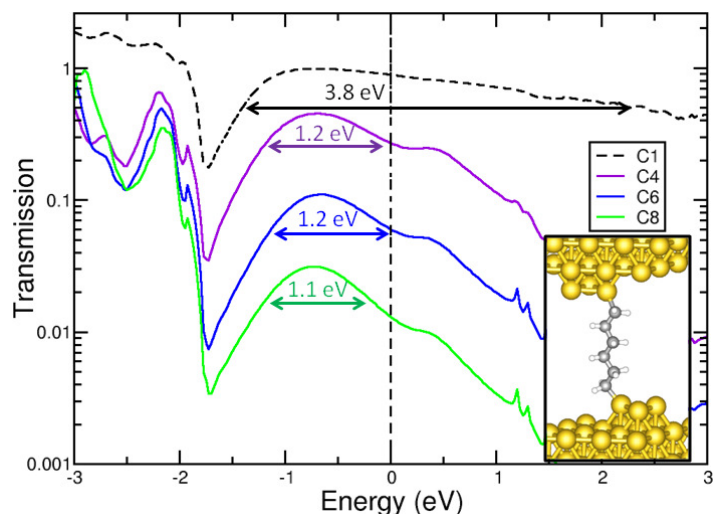
### **Scientific Challenge and Research Achievement:**

This work addresses a fundamental question in single-molecule transport; namely, how the chemical nature of the metal-molecule bond affects the junction structure and conductance. Strong bonds result in a high probability of a molecular junction being formed, but often increase the variability in molecular junction conductance. They, too, can reduce the molecular transport properties significantly by acting as an electronic “bottleneck”. Thus, achieving links that are strong, reproducible and highly-conducting has been and still is a key goal in the field.

In recent years, we have explored, in a combined experimental and theoretical approach, the effect on single molecule conductance of metal-molecule chemical linkers. The theoretical work was undertaken in collaboration with Dr. Mark Hybertsen using computing resources in the CFN through a series of CFN User Projects. Conductance measurements are carried out using STM break-junction techniques [1,2]. First-principles transport calculations are carried out within the Density-Functional Theory – Non-Equilibrium Green’s Functions (DFT-NEGF) method [3]. A major experimental breakthrough was achieved with the use of amine linkers, which enabled reproducible single molecule conductance measurements due to their selective binding to the Au electrodes [1,2,4]. This work was later extended to other link groups [4,5].

In our most recent project, we demonstrated selective, highly-conducting direct Au-C bonds for single molecule junctions [6]. Measurements were carried out using trimethyltin (SnMe<sub>3</sub>) terminated alkanes which were shown to be cleaved in-situ forming direct, covalently bonded Au-C coupled single molecule junctions. The resulting measured conductance for alkanes was found to be almost 100 times higher than with any other linker. Using ab-initio

calculations, a detailed understanding of these highly-conducting Au-C coupled single molecule junctions was developed. We first showed using total energy calculations that the Sn-backbone bond cleavage, followed by adsorption of the products on the Au substrate, was energetically



favorable. Second, transmission calculations for alkanes having direct Au-C bonds showed that a molecular end resonance, localized at the Au-C bond, governed transmission near the Fermi level. The position of this transmission resonance was found to be closer to  $E_F$  than similar resonance with other linkers, and also significantly broader. These resulted in a much higher metal-molecule electronic coupling, explaining the high conductance measured. These results were robust across alkanes of different lengths. Finally, the calculated

conductance of a single  $\text{CH}_2$  unit bonded to two Au electrodes was found to be close to  $G_0$ , indicating that these links exhibit near ideal contact resistance.

**Future work:**

We are currently investigating the conducting properties of direct Au-X bonds, for a variety of X atoms to theoretically determine an ideal linker with the aim of achieving resonant transport through a longer molecule. These results will then be used for the synthesis of a series of molecules for which conductance measurements will be carried out. These results will provide important feedback for chemists and experimentalists as to optimal metal-molecule bonds in single molecule junctions.

**Acknowledgements:**

This work was supported in part by the NSEC program of the NSF (Grant No. CHE-0641523), NYSTAR, and a NSF Career grant (No. CHE-07-44185). Part of this research was performed at the CFN at BNL and supported by DOE (Contract No. DE-AC02-98CH10886).

**References:**

[1] L. Venkataraman, J.E. Klare, I.W. Tam, C. Nuckolls, M.S. Hybertsen and M. Steigerwald, Nano Lett. 6, 458 (2006).  
 [2] L. Venkataraman, J.E. Klare, C. Nuckolls, M.S Hybertsen and M. Steigerwald, Nature, 442, 904-907 (2006).  
 [3] J. M. Soler et al. J. Phys.:Cond. Mat. 14, 2745-2779 (2002); M. Brandbyge, et al, Phys. Rev. B 65, 165401 (2002).  
 [4] M. Kamenetska, M. Koentopp, A. C. Whalley, Y. S. Park, M. L. Steigerwald, C. Nuckolls, M. S. Hybertsen, and L. Venkataraman, Phys. Rev. Lett. 102, 126803 (2009)  
 [5] R. Parameswaran, J. R. Widawsky, H. Vazquez, Y. S. Park, B. M. Boardman, C. Nuckolls, M. L. Steigerwald, M. S. Hybertsen, and L. Venkataraman, J. Phys. Chem. Lett., 1, 2114 (2010).

**Publications:**

[6] Z-L Cheng, R. Skouta, H. Vazquez, J. R. Widawsky, S. Schneebeli, W. Chen, M.S. Hybertsen, R. Breslow and L. Venkataraman, Accepted to Nature Nanotechnology (2011).

# Correlation between electron transport and local structures at the nanoscale revealed by four-probe scanning tunneling microscopy

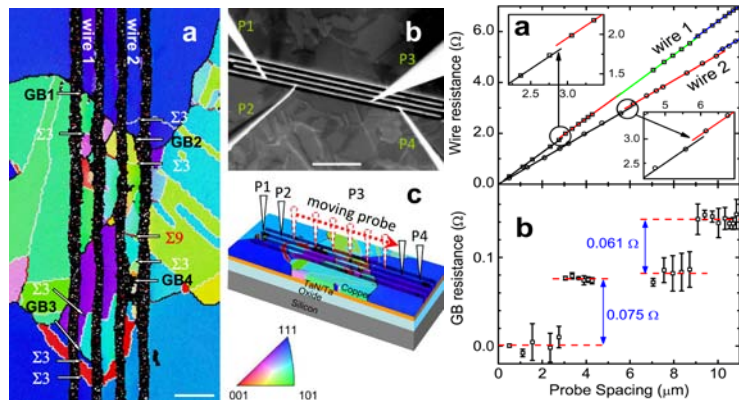
An-Ping Li, Tae-Hwan Kim, Xiaoguang Zhang, Arthur P. Baddorf, and John F. Wendelken  
 Center for Nanophase Materials Sciences, Oak Ridge National Laboratory

## Scientific Thrust Area:

Electron transport properties in nanostructures and the correlation with the local structures are of intense interest in both basic and applied research. The nanotransport research is in the Origins of Functionality at the Nanoscale thrust area in the Center for Nanophase Materials Sciences. Significant progress has been achieved recently in this area.

## Research Achievements:

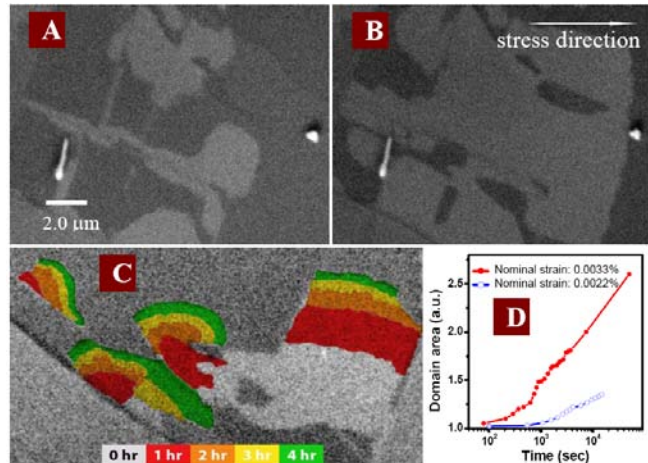
*Grain boundary resistance in Cu nanowire.* Copper nanowire is currently used as interconnect in integrated circuits. As interconnect dimensions decrease, the resistivity of copper increases dramatically because of electron scattering from surfaces, impurities, and grain boundaries (GBs), and threatens to stymie continued device scaling. Lacking direct measurements of individual scattering sources, understanding of the relative importance of these scattering mechanisms has largely relied on semiempirical modeling. We have made a first ever attempt to measure and calculate individual GB resistances in copper nanowires with one-to-one correspondence to the GB structure. By directly measuring both intra- and inter-grain resistance with a unique four-probe scanning tunneling microscope, we observed surprisingly large resistance jumps across high-angle random GBs, while the resistance of coincidence boundaries are negligibly small. Strikingly, the high resistance for random boundaries is found to be an intrinsic result arising from the scaling of the electron mean free path with the size of the relaxation region near the GBs.



Left Figure: Structures of copper nanowires. (a), The inverse pole figure of EBSD maps showing the orientations of grains and GBs. (b), SEM image showing four-probe STM contacted onto the same copper nanowire. (c), A schematic illustrating the resistance measurement procedure with 4-probe STM. Right Figure: resistance jumps near random GBs.

*Electronic inhomogeneity near Mott transition in complex oxide.* The complex interplay between electron and lattice degrees of freedom produces many nearly degenerate electronic states in correlated electron materials. These states determine the functionality of the system, but competition between these states produces highly variable properties whose mechanism remains

in debate. By imaging phase domains with electron microscopy and interrogating individual domains in situ via a point probe electron transport spectroscopy in double-layered  $\text{Sr}_3(\text{Ru}_{1-x}\text{Mn}_x)_2\text{O}_7$  ( $x = 0$  and  $0.2$ ), we have showed (right figure) the first real-space evidence that the microscopic phase competition and the Mott-type metal-insulator transition can be tuned by applying a mechanical stress. Studies were enabled by novel application of a cryogenic four-probe scanning tunneling microscope system, which both images the microscopic phase domains using a scanning electron microscope and simultaneously interrogates the electronic properties of each domain using the scanning tunneling probes in either spectroscopic or transport modes. Dramatic changes were observed in the size and shape of phase domains in response to thermal cycling and mechanical stress. A quantitative correlation between the macroscopic metal-insulator transition and the microscopic phase percolation has been revealed.



Strain-induced domain evolutions in the cleaved surface of a  $\text{Sr}_3(\text{Ru}_{0.8}\text{Mn}_{0.2})_2\text{O}_7$ . (A), Domain image before stress and (B), after applying an uniaxial compressive stress in the  $ab$  plane. (C), Domain evolution in time with nominal strain of 0.0022%. (D), Domain area change with time.

Dramatic changes were observed in the size and shape of phase domains in response to thermal cycling and mechanical stress. A quantitative correlation between the macroscopic metal-insulator transition and the microscopic phase percolation has been revealed.

### Future work:

The next step in our nanotransport research will be to control the electron transport by tuning the local structures at the atomic scale. The correlation between the transport and the local structures will be deterministically addressed.

### Publications:

- 1 Tae-Hwan Kim, X. G. Zhang, Don M. Nicholson, Boyd M. Evans, Nagraj S. Kulkarni, B. Radhakrishnan, Edward A. Kenik & An-Ping Li, *Large discrete resistance jump at grain boundary in copper nanowire*, Nano Lett., **10**, 3096 (2010).
- 2 Tae-Hwan Kim, M. Angst, B. Hu, R. Jin, X. G. Zhang, J. F. Wendelken, E. Ward Plummer, and An-Ping Li, *Imaging and Manipulation of the Competing Electronic Phases near the Mott Metal-Insulator Transition*, Proc. Nat. Acad. Sci., **101**, 5272 (2010).
- 3 T.-H. Kim, R. Jin, L.R. Walker, J.Y. Howe, M.H. Pan, J. F. Wendelken, J. R. Thompson, A. S. Sefat, M. A. McGuire, B. C. Sales, D. Mandrus, and A. P. Li, *Probing Microscopic Variations of Superconductivity on the Surface of  $\text{Ba}(\text{Fe}_{1-x}\text{Co}_x)_2\text{As}_2$  Single Crystals*, Phys. Rev. B, **80**, 214518 (2009).
- 4 Tae-Hwan Kim, D. M. Nicholson, X.-G. Zhang, B. M. Evans, N. S. Kulkarni, E. A. Kenik, H. M. Meyer, B. Radhakrishnan, and An-Ping Li, *Structural Dependence of Grain Boundary Resistivity in Copper Nanowires*, Jap. J. Appl. Phys., in press (2011).

## Single-Molecule Spectroscopy Study of Interfacial Charge Separation in Quantum Dot based Hybrid Systems

Mircea Cotlet<sup>1\*</sup>, Zhihua Xu<sup>1</sup> and Mathew M. Maye<sup>2</sup>

<sup>1</sup>Center for Functional Nanomaterials, Brookhaven National Laboratory, Upton, NY 11778, [cotlet@bnl.gov](mailto:cotlet@bnl.gov),

<sup>2</sup>Chemistry Department, Syracuse University, Syracuse NY 13244

**Scientific Thrust Area:** Soft and Biological Nanomaterials

**Scientific Challenge and Research Achievement.** Blends of semiconducting quantum dots with fullerenes and/or conjugated polymers (CPs) are promising materials for light-emitting diodes and photovoltaics. Effective design of optoelectronic devices relies on the understanding of photophysics of these hybrid materials, including charge separation and energy transfer.

We have studied the dynamics of single molecule electron transfer in a series of donor-bridge-acceptor conjugates based on core/shell CdSe/ZnS quantum dots and fullerenes. Using a surface-based stepwise self assembly method, we have engineered donor-bridge-acceptor systems with varying interparticle distance and varying quantum dot size to demonstrate control of the magnitude of electron transfer rate and of the fluctuations in electron transfer rate by controlling interparticle (quantum dot – fullerene) distance and electron transfer driving force. Furthermore, we have investigated the effect of fullerene on the photoluminescence blinking of quantum dots and provided a mechanistic view of the role of charge traps on regulating this process.

We have studied the dynamics of hole transfer as a function of intercomponent distance in hybrid systems based on core/shell CdSe/ZnS quantum dots and conjugated polymers. Using quantum dots with varying shell thickness, we demonstrated control of the rate of hole transfer in quantum dot/polymer blends and explained the effect of hole transfer on the blinking dynamics of quantum dots, namely suppression of Auger recombination in the quantum dot core due to the competing hole transfer between quantum dot and polymer.

**Future work.** Composite materials integrating quantum dots as light harvesters, fullerenes as electron acceptors and conjugated polymers as hole acceptors in the form presented above should provide efficient and controlled charge transfer and charge separation. Such composites are currently explored in our group in terms of active layers for photovoltaics.

### **Publications:**

1. Z.Xu, M.Cotlet, Quantum dot-bridge-fullerene heterodimers with controlled photoinduced electron transfer, *Angewandte Chemie Intl. Ed.*, 2011, in press.
2. Z.Xu, M.Cotlet, Photoluminescence blinking dynamics of colloidal quantum dots in the presence of controlled external traps, 2011, under review.
3. Z.Xu, M.M.Maye, H.L.Wang, M.Cotlet, Probing the dynamics of photoinduced hole transfer in colloidal quantum dot/ conjugated polymer nanocomposites by single molecule spectroscopy, 2011, under review.



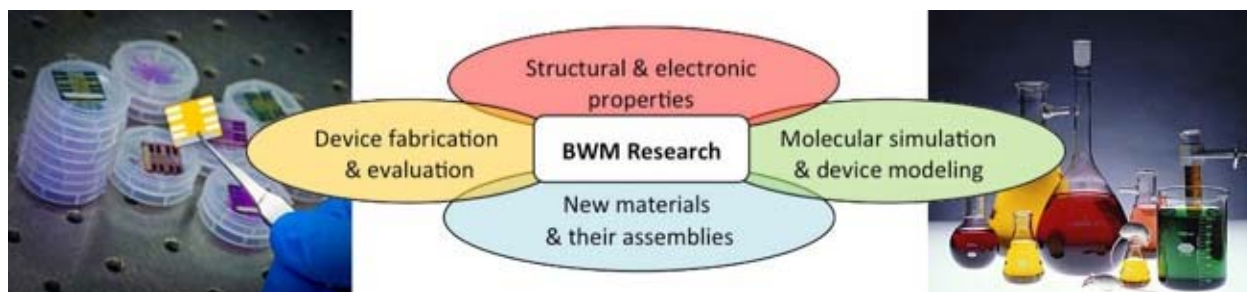
# Functional Organic Materials and Their Application in Solar Cells

Biwu Ma

The Molecular Foundry, Lawrence Berkeley National Laboratory

## Scientific Thrust Area: Organic Electronics

My research focuses on the development of new functional organic materials for applications in electronic devices, e.g. organic light emitting diodes (OLEDs), organic field effect transistors (OFETs) and organic solar cells (OSCs). It involves design, synthesis and characterization of new materials, as well as device fabrication and testing. The major purpose of my research is to study the underlying chemical and physical properties of new materials and understand how molecular structure affects material properties and device performance. Herein, I present our recent efforts on organic solar cells.



## Scientific Challenge and Research Achievement

Solar cells are among the most promising technologies for renewable clean energy. However, conventional silicon-based solar cells are too expensive for everyday use. Organic solar cells (OSCs) have substantial promise due to their low cost in materials and device fabrication, ca. roll-to-roll printing abundant carbon-based materials. Driven by the continuous development of new materials, processing techniques and advanced device concepts, the power conversion efficiencies of OSCs have steadily improved to the 6-8% range. Despite those achievements, many issues remain (e.g., efficiency, lifetime, stability, etc.) that need to be addressed before OSCs are widely utilized.

To realize OSCs with efficiencies exceeding 10%, we seek to develop new photo-/electro-active soft materials, real control on morphology leading to ideal donor/acceptor nanophase separation, and the fundamental understanding of device operation. Materials based on light absorbing organic pigments, which have been widely used in plastic coloration and paints, show great potential. We aim to make those low-cost, non-toxic, abundant and stable materials suitable for solar cells application. The synthetic approach will involve integrating multiple functional components into a pigment (dye) core to achieve new materials possessing high light absorbing, high solubility, high charge carrier mobility and nanoscale ordering functionality. For instance, BODIPY-based polymers possessing high absorption coefficient ( $\sim 10^5 \text{ cm}^{-1}$ ) and low bandgap ( $\sim 1.6 \text{ eV}$ ), have been demonstrated as effective electron donors in solution-processed bulk heterojunction (BHJ) solar cells with power conversion efficiencies (PCEs) of more than 2%. Small molecules, on the other hand, maintain many attractive advantages over typical polymeric materials, including monodispersity, high charge carrier mobility, and relatively simple synthesis and purification. A number of small molecule based soluble materials, such as subphthalocyanines (SubPcs) and quinacridones (QAs), have been designed, synthesized and

used for the fabrication of OSCs in various device structures ranging from planar to bulk and “ideal” heterojunctions. By utilizing functional QAs as electron donor, we have achieved the best device performance to date for as-cast small molecule blends (QAs and PC<sub>70</sub>BM) with PCEs of up to 2.2% and external quantum efficiencies exceeding 45%. Through the integration of new functional materials and well controlled nanostructures, our studies have provided the basis for the low-cost fabrication of efficient OSCs. Our efforts have also generated a comprehensive understanding of structure-property relationships and established guidelines for further development of high performance organic materials for solar energy conversion.

### Future Work

We propose to further develop families of solution processable organic molecules with controlled optical/electronic properties and structural features to self-assemble into ordered nanoscopic arrays for highly efficient photovoltaic cells, i.e. supramolecular photovoltaics. Several approaches will be developed, including  $\pi$ -stacked discotic semiconducting materials and polymer-assisted molecular assemblies, with a common theme of self-assembling into macroscopic patterns, instead of disordered constructs. Through the use of advanced characterization techniques, we will investigate the correlations among molecular structures, film morphology, electronic/photonics properties, and device performance; and address the basic photovoltaic operation processes including exciton diffusion, energy transfer, charge separation and recombination, as well as charge transport. We will also perform molecular level simulations to predict properties and to interpret the characterization results, and use device modeling to verify and predict the performance of the device structures. Concerted efforts in these specialties and concepts will contribute to the fundamental understandings of material-device integration and provide guidelines for the further development of new materials and their assemblies in a rational manner. The potential impact of our success will be high-performance, light-weight, flexible, and low-cost photovoltaic solar arrays that contain sustainable and nontoxic species.

### Publications

- Chen, T.; Zhang, Y.; Smith, P.; Liu, Y.; Tamayo, A.; Ma, B.\*; Diketopyrrolopyrrole-Containing Oligothiophene-Fullerene Triads and Their Use in Organic Solar Cells, **2011**, *ACS Applied Materials & Interfaces*, Accepted.
- Chen, T.; Chen, J.; Catane, L.; Ma, B.\*; Fully Solution Processed p-i-n Organic Solar Cells with An Industrial Pigment – Quinacridone, *Organic Electronics*, **2011**, In Press
- Chen, J.; Chen, T.; Kim, B.; Poulsen, D. A.; Mynar, J. L.; Fréchet, J. M. J.; Ma, B.\*; Quinacridone-Based Molecular Donors for Solution Processed Bulk-Heterojunction Organic Solar Cells, *ACS Applied Materials & Interfaces*, **2010**, *2*, 2679-2686.
- Mauldin, C. E.; Piliago, C.; Poulsen, D. A.; Unruh, D.; Woo, C. H.; Ma, B.\*; Mynar, J. L.; Fréchet, J. M. J.; Axial Thiophene – Boron(subphthalocyanine) Dyads and Their Application in Organic Photovoltaics, *ACS Applied Materials & Interfaces*, **2010**, *2*, 2833-2838.
- Kim, B.; Ma B.\*; Donuru, V. R.; Liu, H.; Fréchet J. M. J.; BODIPY-Backboned Polymers as Electron Donor in Bulk Heterojunction Solar Cells, *Chemical Communications*, **2010**, *46*, 4148-4150.
- Ma, B.\*; Woo, C. H.; Miyamoto, Y.; Fréchet, J. M. J.; Solution Processing of a Small Molecule, Subnaphthalocyanine, for Efficient Organic Photovoltaic Cells, *Chemistry of Materials*, **2009**, *21*, 1413–1417.
- Ma, B.\*; Miyamoto, Y.; Woo, C. H.; Fréchet, J. M. J.; Zhang, F.; Liu, Y. Solution Processable Boron Subphthalocyanine Derivatives as Active Materials for Organic Photovoltaics, *Proc. SPIE*, **2009**, *7416*, 74161E.

## Tailored Assemblies of PS-*b*-P3HT Diblock Copolymers: Adaptable Building Blocks for High-Performance Organic Transistors and Solar Cells

Kai Xiao, Xiang Yu, Jihua Chen, Nickolay V. Lavrik, Kunlun Hong, Bobby Sumpter, David B. Geohegan

Center for Nanophase Materials Sciences, Oak Ridge National Laboratory, 1 Bethel Valley Road, Oak Ridge, TN 37831

[xiaok@ornl.gov](mailto:xiaok@ornl.gov)

**Scientific Thrust Area:** Origins of Functionality at the Nanoscale

**Research Achievement:** To develop high-performance organic electronic devices, such as organic field-effect transistors (OFETs), or organic photovoltaic devices (OPVs), it is of crucial importance to develop methods to construct well-organized nanostructures of semiconducting polymers. In this work, we aim to use the conjugated block copolymers, promising molecular architectures, to self-assemble into a variety of segregated nanoscale structures, thereby providing an opportunity to tailor the morphology of an active layer and a powerful pathway to assemble charge carrier conductors into nanoscale segregated structures within organic electronic devices.

Diblock copolymers of polystyrene-*b*-poly[3-hexylthiophene] were synthesized and characterized using TEM, SAED, GIXD, AFM, and first principles modeling and simulation. A detailed analysis revealed how this diblock copolymers can self-assemble into different nanostructures based upon the molecular weight of the polythiophene block, with the P3HT blocks forming highly crystalline ordered domains dominated by intermolecular  $\pi$ - $\pi$  stacking and microphase separation. These domains, on the length scale of 10 – 20 nm, increase the carrier mobility in the fabricated transistors by up to a factor of two. This work demonstrates that the high degree of molecular order induced by block copolymer phase separation can improve the transport properties and stability of conjugated polymers, which are critical for high-performance

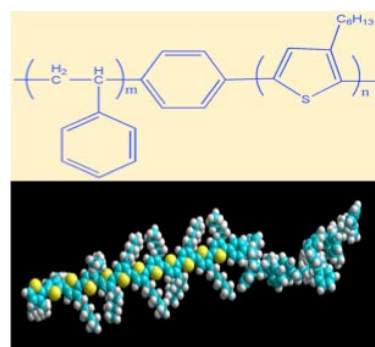


Figure 1 Chemical structure of the P3HT-*b*-PS diblock copolymer and semiempirical AM1 Hamiltonian-optimized structure of diblock copolymer

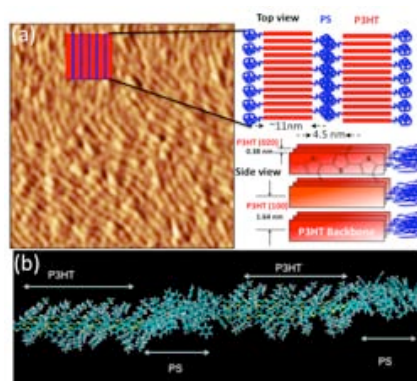


Figure 2 (a) AFM images (500 nm  $\times$  500 nm) of the lamellar structure of block copolymer film. Inset shows the schematic illustration of the lamellar nano-structures. Left images show the schematic illustrations of top view and side view of the lamellar structures of PS-*b*-P3HT film. (b) Optimized lamellar structure of PS-*b*-P3HT film

organic electronic transistors, photovoltaics, and displays.

**Future work:** To control the phase separation for more efficient organic bulk heterojunction photovoltaic cells, PS-*b*-P3HT diblock copolymer will be added to serve as compatibilizer in a P3HT/PCBM blend. We will systematically explore the relationship of the fraction of PS-*b*-P3HT polymer in P3HT/PCBM blend and device performance and understand how the interaction between the block copolymer and P3HT/PCBM as a major drive force to control the phase separation through absorption spectroscopy, GISAXS, neutron reflectivity combined with Quantum density functional theory calculations.

### References:

1. Wu, P.; Ren, G.; Kim, F. S.; Li, C.; Mezzenga, R.; Jenekhe, S. A. Poly(3-hexylthiophene)-*b*-Poly(3-cyclohexylthiophene): Synthesis, Microphase Separation, Thin Film Transistors, and Photovoltaic Applications. *J. Polym. Sci. Part A -Polym. Chem.* 2010, *48*, 614-626;
2. Chueh, C.; Higashihara, T.; Tsai, J.; Ueda, M.; Chen, W. All-Conjugated Diblock Copolymer of Poly(3-hexylthiophene)-*b*-Poly(3-phenoxyethylthiophene) for Field-Effect Transistor and Photovoltaic Applications *Organic Electronics* 2009, *10*, 1541-1548;
3. Zhang, Y.; Tajima, K.; Hiroa, K.; Hashimoto, K. Synthesis of All-conjugated Diblock Copolymers by Quasi-Living Polymerization and Observation of Their Microphase Separation. *J. Am. Chem. Soc.* 2008, *130*, 7812-7813.

### Publications:

1. Yu, X.; Xiao, K.; Chen, J.; Lavrik, N. V.; Hong, K.; Sumpter, B. G.; Geoghegan, D. B., High-Performance Field-Effect Transistors Based on Polystyrene-*b*-Poly(3-hexylthiophene) Diblock Copolymers, *ACS Nano* 2011, In press.

### Credit

This work is a collaboration of the following themes at CNMS: Origins of Functionality at the Nanoscale, Functional Polymer Architectures, Understanding Emergent Behavior, which was sponsored by the Scientific User Facilities Division, Office of Basic Energy Sciences, U. S. Department of Energy.

## Directed Self-Assembly of Organic Nanostructures from Tailor-Made Electron Donors and Acceptors

Yi Liu, Organic and Macromolecular Synthesis Facility  
The Molecular Foundry, Lawrence Berkeley National Laboratory

### Scientific Thrust Area

The objective of our research is to achieve controlled assembly of functional organic nanostructured materials through the design, synthesis and manipulation of tailor-made electron donors and acceptors. The growing needs for miniaturization and better efficiency of electronic devices have inspired enormous interests in obtaining novel semiconductor nanostructures. One particular challenge is to obtain nanostructures with continuous interface between electron donors and acceptors in order

to facilitate charge separation and charge transport. Here I will summarize our progress in utilizing the donor-acceptor interactions to direct the synthesis of nanostructured materials, both at the molecular and supramolecular level (Figure 1). I will also highlight one user program on the development of biocompatible Cu(I) catalyst for in vivo bioimaging (Figure 2).

### Research Achievement

Through a series of examples of assembling interlocked molecular switches, we have demonstrated how the challenges in multi-component assembly, i.e. *product specificity* and *conformational selectivity*, are addressed through deliberate molecular design. Moving from molecular structures to supramolecular electronic systems, we have made significant progress towards controlled donor-acceptor stacking geometry, including: phase-separated 1D nanostructures, alternating donor-acceptor (ADA) stacks, and donor-acceptor columnar hetero junctions (CHJ). The realization of these structures is accompanied by the development of novel electron donors and acceptors, the design of which takes account of both bandgap engineering and structural features affecting non-covalent interactions. These nanostructures will bring in promising materials properties that can find applications in organic photovoltaics (OPVs), novel organic ferroelectrics for nonvolatile memories, and flexible electronics.

In collaboration with Prof. Peng Wu from Albert Einstein School of

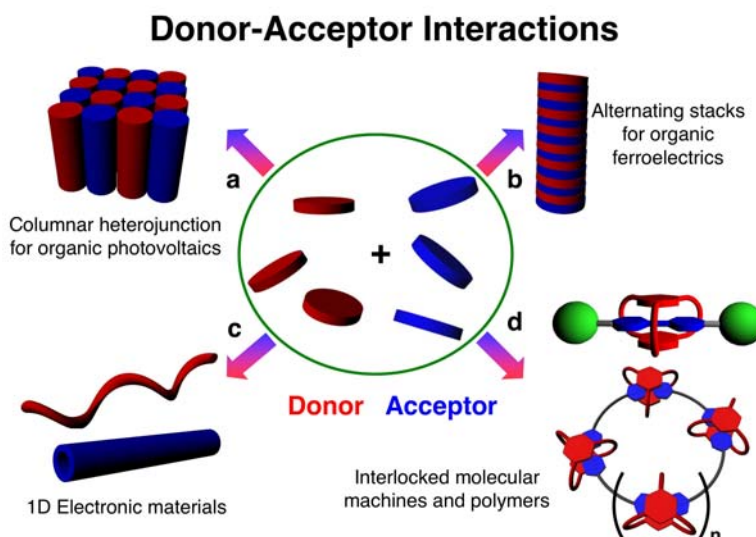


Figure 1. Self-assembled nanostructures from organic electron donors and acceptors.

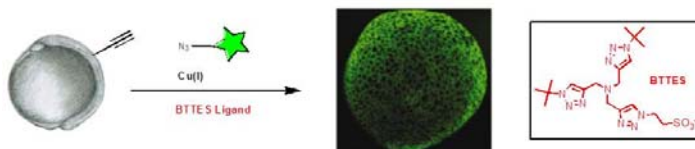


Figure 2. Novel Cu(I)-ligand catalysts for in vivo imaging using copper-catalyzed azide-alkyne cycloaddition (CuAAC).

Medicine, we have developed biocompatible catalysts that allow for expedient *in vivo* glycosylation on cell surfaces, and for *the first time* imaging of sialylated and fucosylated glycans in the enveloping layer of the zebrafish embryo *as early as 10 hours post fertilization*. An array of ligands have been developed and applied for different bioconjugation applications. Specific application-related guidelines are under development for the effective suppression of cytotoxicity or developmental abnormalities that are commonly associated with Cu(I) catalyst.

### Future Work

Our research will continue the existing efforts in the design and synthesis of donor and acceptor materials in order to tailor the self-assembly behavior to give highly ordered nanostructures. Particular efforts will be directed towards the development of organic semiconducting materials that are compatible with inorganic semiconductors and cheap carbon-based electronic materials to give high-efficiency hybrid photovoltaic cells. The knowledge obtained from the donor-acceptor systems will be applied on the exploration of small molecule based *p*-type and *n*-type electronic materials for photovoltaic applications.

### Selected Publications

- Besanceney, C.; Jiang, H.; Zheng, T.; Feng, L.; Soriano del Amo, D.; Wang, W.; Klivansky, L. M.; Marlow, F. L.\*; **Liu, Y.;**\* Wu, P.\* “Raising the Efficacy of Bioorthogonal Click Reactions for Bioconjugation: A Comparative Study”, *Angew. Chem. Int. Ed.* accepted.
- Zheng, T.; Jiang, H.; Gros, M.; **Liu, Y.;** Wu, P.\* “Tracking N-acetyllactosamine on Cell Surface Glycans *in vivo*”, *Angew. Chem. Int. Ed.* in press. (<http://onlinelibrary.wiley.com/doi/10.1002/ange.201100265/pdf>)
- Hanifi, D.; Cao, D.; Klivansky, L. M.; **Liu, Y.;**\* “Novel *n*-Type Tris(aryl)eneimidazole and Its Analogs: Synthesis, Physical Properties and Self-Assembly”, *Chem. Commun.* **2011**, 47, 3454-3456. (Top ten most accessed articles in February). (<http://pubs.rsc.org/en/Content/ArticleLanding/2011/CC/c0cc04753h>)
- Koshkaryan, G.; Jiang, P.; Cao, D.; Klivansky, L. M.; Altoe, V.; Zhang, Y.; Ma, B.; Salmeron, M.; Aloni, S.; **Liu, Y.;**\* “Multi-Layered Nanofibers from Stacks of Single-Molecular Thick Hexakis(alkoxy)triphenylenes”, *Chem. Commun.* **2010**, 46, 8579-8581. (Editor’s choice as ‘Hot Paper’) (<http://pubs.rsc.org/en/Content/ArticleLanding/2010/CC/c0cc03942j>)
- Amo, D. S.; Wang, W.; Jiang, H.; Besanceney, C.; Amos, Y.; Levy, M.; **Liu, Y.;** Marlow, F. L.; Wu, P.\* “Dynamic *in vivo* Imaging Using Biocompatible Copper(I) Catalysts”, *J. Am. Chem. Soc.* **2010**, 132, 16893-16899 (Highlighted by C&EN news “Imaging Molecules on Living Cells”). (<http://pubs.acs.org/doi/abs/10.1021/ja106553e>)
- Koshkaryan, G.; Cao, D.; Klivansky, L. M.; Teat, S. J.; Tran, J. L.; **Liu, Y.;**\* “Dual Selectivity Expressed in [2+2+1] Dynamic Clipping of Unsymmetrical [2]Catenanes”, *Org. Lett.* **2010**, 12, 1528-1531. (<http://pubs.acs.org/doi/abs/10.1021/ol100215c>)
- Cao, D.; Amelia, M.; Klivansky, L. M.; Koshkaryan, G.; Khan, S. I.; Semeraro, M.; Silvi, S.; Venturi, M.; Credi, A.\*; **Liu, Y.;**\* “Probing Donor-Acceptor Interactions and *Co*-Conformational Changes in Redox Active Desymmetrized [2]Catenanes”, *J. Am. Chem. Soc.* **2010**, 132, 1110-1122. (<http://pubs.acs.org/doi/abs/10.1021/ja909041g>)
- Klivansky, L. M.; Koshkaryan, G.; Cao, D.; **Liu, Y.;**\* “Linear  $\pi$ -Acceptor Templated Dynamic Clipping to Macrocycles and [2]Rotaxanes”, *Angew. Chem. Int. Ed.* **2009**, 48, 4185-4189. (<http://www3.interscience.wiley.com/cgi-bin/fulltext/122370856/PDFSTART>)
- Koshkaryan, G.; Klivansky, L. M.; Cao, D.; Snauko, M.; Teat, S. J.; Struppe, J. O.; **Liu, Y.;**\* “Alternative Donor-Acceptor Stacks from Crown Ethers and Naphthalene Diimide Derivatives: Rapid, Selective Formation from Solution and Solid State Grinding”, *J. Am. Chem. Soc.* **2009**, 131, 2078-2079. (<http://pubs.acs.org/doi/pdf/10.1021/ja809088v>)

# Synthesis and Characterization of Multifunctional Nanocomposite Materials

Q. X. Jia<sup>1)</sup>, H. Yang<sup>1)</sup>, P. Zerrer<sup>2)</sup>, Z. X. Bi<sup>3)</sup>, J. S. Yoon<sup>3)</sup>, J. L. MacManus-Driscoll<sup>2)</sup>, H. Wang<sup>3)</sup>

<sup>1)</sup>Center for Integrated Nanotechnologies, Los Alamos National Laboratory, Los Alamos, NM

<sup>2)</sup>Department of Materials Science, University of Cambridge, UK

<sup>3)</sup>Department of Electrical and Computer Engineering, Texas A&M University, TX

**Scientific Thrust Area:** Nanoscale Electronics and Mechanics

**Scientific Challenge and Research Achievement:** Epitaxial nanocomposites, in which emerging behaviors can be achieved through *interfacing* different materials at the nanoscale, provide a new design paradigm to produce enhanced and/or novel functionalities that cannot be obtained in the individual constituents.

Recent experimental results<sup>1-4</sup> have shown that either structural or electrostatic boundary conditions are the dominant factors in controlling the atomic and electronic structures at solid-solid interfaces. We have used pulsed laser deposition to synthesize and control the strain states in nanocomposite films by forming spontaneously ordered pillar structures (see Fig. 1).<sup>5</sup> We have made several discoveries: 1) the columns control the strain in one another in the vertical direction, *independent* of the lateral interface; 2) the strain is maintained in rather thick films; and 3) the strains of two phases can be tuned by the processing parameters during deposition. These results should allow an order of magnitude thicker strained films to be grown relative to *lateral* systems, enabling much improved properties of the materials.

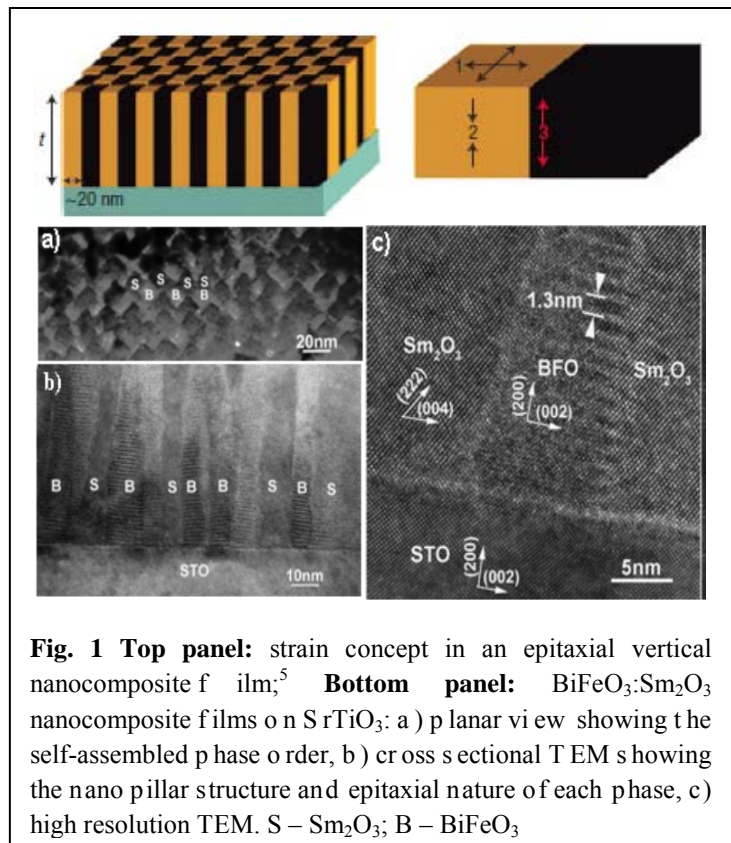


**Fig. 1** Top panel: strain concept in an epitaxial vertical nanocomposite film;<sup>5</sup> Bottom panel: BiFeO<sub>3</sub>:Sm<sub>2</sub>O<sub>3</sub> nanocomposite films on SrTiO<sub>3</sub>: a) planar view showing the self-assembled phase order, b) cross sectional TEM showing the nano pillar structure and epitaxial nature of each phase, c) high resolution TEM. S – Sm<sub>2</sub>O<sub>3</sub>; B – BiFeO<sub>3</sub>

**Future Work:** With remarkable worldwide advances in the epitaxial growth of high quality films based on both MBE and laser-MBE in the last several years, the construction of epitaxial nanocomposites has become possible. We will continue to explore the layered laminar-like and the vertically aligned pillar-like (Fig. 1) nanocomposites. Specifically, we will grow high quality BiFeO<sub>3</sub>/La<sub>0.7</sub>Sr<sub>0.3</sub>MnO<sub>3</sub> and La<sub>0.7</sub>Sr<sub>0.3</sub>MnO<sub>3</sub>/YBa<sub>2</sub>Cu<sub>3</sub>O<sub>7</sub> multilayers with mono-layer level control as well as vertically aligned BaTiO<sub>3</sub>:Sm<sub>2</sub>O<sub>3</sub> and La<sub>0.7</sub>Sr<sub>0.3</sub>MnO<sub>3</sub>:ZnO pillar structures using our laser-MBE, a technique particularly well suited for fabricating epitaxial complex oxide films and superlattices. We will systematically investigate the effect of strain on the

functionalities of the materials. A clear understanding of the relationship between the strain and the functionalities as well as how to manipulate the strain state in the nanocomposites are crucial for the application of these oxides in the next generation electronic devices.

## References

1. H. Zheng, J. Wang, S. E. Lofland, Z. Ma, L. Mohaddes-Ardabili, T. Zhao, L. Salamanca Riba, S. R. Shinde, S. B. Ogale, F. Bai, D. Viehland, Y. Jia, D. G. Schlom, M. Wuttig, A. Roytburd, and R. Ramesh, "Multiferroic BaTiO<sub>3</sub>-CoFe<sub>2</sub>O<sub>4</sub> nanostructures," *Science* **303**, 661 (2004).
2. A. Ohtomo and H. Y. Hwang, "A high-mobility electron gas at the LaAlO<sub>3</sub>/SrTiO<sub>3</sub> heterointerface," *Nature* **427**, 423 (2004).
3. A. Brinkman, M. Huijben, M. van Zalk, J. Huijben, U. Zeitler, J. C. Maan, W. G. van der Wiel, G. Rijnders, D. H. A. Blank, and H. Hilgenkamp, "Magnetic effects at the interface between non-magnetic oxides," *Nature Materials* **6**, 493 (2007).
4. N. Reyren, S. Thiel, A. D. Caviglia, A. F. Kourkoutis, G. Hammerl, C. Richter, C. W. Schneider, T. Hopp, A. S. Ruetschi, D. Jaccard, M. Gabay, D. A. Muller, J. M. Trusccone, and J. Mannhart, "Superconducting interface between insulating oxides," *Science* **317**, 1196(2007).
5. J. L. MacManus-Driscoll, P. Zerrer, H. Wang, H. Yang, J. Yoon, S. R. Foltyn, M. G. Blamire, and Q. X. Jia, "Spontaneous ordering, strain control and manipulation in vertical nanocomposite heteroepitaxial films," *Nature Materials* **7**, 314(2008).

## Publications

1. B. Bi, A. Chen, H. Wang, E. Weal, J. L. MacManus-Driscoll, H. Luo, and Q. X. Jia, "Microstructure and magnetic properties of (La<sub>0.7</sub>Sr<sub>0.3</sub>MnO<sub>3</sub>)<sub>0.7</sub>:(Mn<sub>3</sub>O<sub>4</sub>)<sub>0.3</sub> nanocomposite thin films", *J. Appl. Phys.*, accepted
2. E. M. Choi, S. Patnaik, E. Weal, S. L. Sahonta, H. Wang, Z. Bi, J. Xiong, M. G. Blamire, Q.X. Jia, and J. L. MacManus-Driscoll, "Strong room temperature magnetism in highly resistive strained thin films of BiFe<sub>0.5</sub>Mn<sub>0.5</sub>O<sub>3</sub>," *Appl. Phys. Lett.* **98**, 012509 (2011).
3. Z. Bi, O. Anderoglu, X. Zhang, J. L. MacManus-Driscoll, H. Yang, Q. X. Jia, and H. Wang, "Nanoporous thin films with controllable nanopores processed from vertically aligned nanocomposites," *Nanotechnology* **21**, 285606 (2010).

# Presenter Index



Ajo-Franklin, Caroline.....	67	Martinez, Julio.....	179
Aloni, Shaul.....	169	Mavrikakis, Manos.....	145
Arachchige, Indika.....	125	Maye, Mathew.....	45
Ashby, Paul.....	95	Miller, Dean.....	97
Balatsky, Alexander (Sasha).....	99	Miller, Michael.....	53
Borisevich, Albina.....	157	Minor, Andy.....	27
Caballero, Francisca.....	57	More, Karren.....	133
Caldwell, Marissa.....	123	Parish, Chad.....	161
Chabinyc, Michael.....	5	Paxton, Wally.....	89
Chan, Emory.....	115	Perea, Daniel.....	165
Chen, Jihua.....	81	Peteanu, Linda.....	75
Chi, Miaofang.....	11	Prendergast, David.....	79
Ciston, Jim.....	91	Proksch, Roger.....	33
Clavero, Cesar.....	131	Radmilovic, Velimir.....	47
Collier, Pat.....	93	Rajh, Tijana.....	63
Cotlet, Mircea.....	185	Ren, Gary.....	35
Dahmen, Ulrich.....	37	Robertson, Ian.....	41
Dal Negro, Luca.....	173	Sadowski, Jurek.....	149
Dattelbaum, Andrew.....	113	Sasaki, Kotaro.....	141
Fong, Dillon.....	155	Schmid, Andreas.....	15
Getty, Stephanie.....	49	Smith, Katherine.....	159
Gianola, Dan.....	25	Stach, Eric.....	111
Gibson, Murray.....	13	Starr, David.....	51
Goertz, Matt.....	65	Strauf, Stefan.....	105
Gray, Stephen.....	171	Su, Dong.....	39
Guisinger, Nathan.....	29, 117	Sutter, Peter.....	101
Gupta, Gautam.....	71	Svoboda, Vojtech.....	137
Hall, Ernest.....	1	Swan, Anna.....	83
Han, Weiqiang.....	135	Tanase, Mihaela.....	121
Huang, Jianyu.....	3	Tokarev, Ihor.....	167
Huber, Dale.....	119	Treacy, Mike.....	19
Idrobo, Juan Carlos.....	107	Unocic, Kinga.....	153
Jia, Quanxi.....	193	Valanoor, Nagarajan.....	61
Joy, David.....	43	Vazquez, Hector.....	181
Karavitaki, Domenica.....	73	Vertes, Akos.....	139
Kent, Paul.....	127	Wang, Debin.....	109
Kirk, Marquis.....	55	White, Michael.....	85
Kirkland, Angus.....	23	Whitelam, Stephen.....	87
Kisielowski, Christian.....	177	Wiederrecht, Gary.....	175
Li, An-Ping.....	183	Winarski, Robert.....	77
Liang, Chengdu.....	143	Wu, Qin.....	129
Liu, Xiaohua.....	147	Xiao, Kai.....	189
Liu, Yi.....	191	Yang, Judith.....	21
López, Daniel.....	163	Yun, Jonathan.....	69
Lukaszew, Ale.....	131	Zaluzec, Nestor.....	9
Lumpkin, Greg.....	151	Zettl, Alex.....	31
Ma, Biwu.....	187	Zhang, Yuegang.....	103
Marquis, Emmanuelle.....	59	Zhu, Yimei.....	7
Marrows, Christopher.....	17		



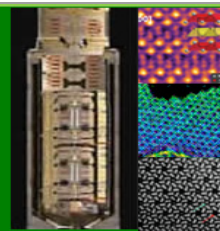
# Participant List



# E-Beam Microcharacterization Centers & Nanoscale Science Research Centers Contractors' Meeting

Sponsored by the U.S. Department of Energy, Office of Basic Energy Sciences

May 31 - June 2, 2011  
The Westin Hotel, Annapolis, Maryland

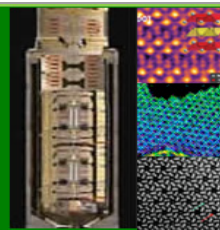


Name	Affiliation	Email
Caroline Ajo-Franklin	Lawrence Berkeley National Laboratory	<a href="mailto:cajo-franklin@lbl.gov">cajo-franklin@lbl.gov</a>
Shaul Aloni	Lawrence Berkeley National Laboratory	<a href="mailto:saloni@lbl.gov">saloni@lbl.gov</a>
Indika Arachchige	Los Alamos National Laboratory	<a href="mailto:indika@lanl.gov">indika@lanl.gov</a>
Paul Ashby	Lawrence Berkeley National Laboratory	<a href="mailto:pdashby@lbl.gov">pdashby@lbl.gov</a>
Alexander Balatsky	Los Alamos National Laboratory	<a href="mailto:balatsky@gmail.com">balatsky@gmail.com</a>
Albina Borisevich	Oak Ridge National Laboratory	<a href="mailto:albinab@ornl.gov">albinab@ornl.gov</a>
Francisca Caballero	National Center for Metallurgical Research	<a href="mailto:fgc@cenim.csic.es">fgc@cenim.csic.es</a>
Marissa Caldwell	Stanford University	<a href="mailto:macaldwe@stanford.edu">macaldwe@stanford.edu</a>
Altaf (Tof) Carim	Department of Energy	<a href="mailto:carim@science.doe.gov">carim@science.doe.gov</a>
Linda Cerrone	Department of Energy	<a href="mailto:Linda.Cerrone@science.doe.gov">Linda.Cerrone@science.doe.gov</a>
Michael Chabinyc	University of California, Santa Barbara	<a href="mailto:mchabinyc@engineering.ucsb.edu">mchabinyc@engineering.ucsb.edu</a>
Emory Chan	Lawrence Berkeley National Laboratory	<a href="mailto:EMChan@lbl.gov">EMChan@lbl.gov</a>
Jihua Chen	Oak Ridge National Laboratory	<a href="mailto:jihuac@gmail.com">jihuaac@gmail.com</a>
Miaofang Chi	Oak Ridge National Laboratory	<a href="mailto:chim@ornl.gov">chim@ornl.gov</a>
Jim Ciston	Lawrence Berkeley National Laboratory	<a href="mailto:JCiston@lbl.gov">JCiston@lbl.gov</a>
César Clavero	The College of William and Mary	<a href="mailto:cclavero@wm.edu">cclavero@wm.edu</a>
Pat Collier	Oak Ridge National Laboratory	<a href="mailto:colliercp@ornl.gov">colliercp@ornl.gov</a>
Mircea Cotlet	Brookhaven National Laboratory	<a href="mailto:cotlet@bnl.gov">cotlet@bnl.gov</a>
Ulrich Dahmen	Lawrence Berkeley National Laboratory	<a href="mailto:Udahmen@lbl.gov">Udahmen@lbl.gov</a>
Andrew Dattelbaum	Los Alamos National Laboratory	<a href="mailto:amdattel@lanl.gov">amdattel@lanl.gov</a>
Jim DeYoreo	Lawrence Berkeley National Laboratory	<a href="mailto:JJDeYoreo@lbl.gov">JJDeYoreo@lbl.gov</a>
Dillon Fong	Argonne National Laboratory	<a href="mailto:fong@anl.gov">fong@anl.gov</a>
Stephanie Getty	NASA Goddard Space Flight Center	<a href="mailto:Stephanie.A.Getty@nasa.gov">Stephanie.A.Getty@nasa.gov</a>
Dan Gianola	University of Pennsylvania	<a href="mailto:gianola@seas.upenn.edu">gianola@seas.upenn.edu</a>
J. Murray Gibson	Northeastern University	<a href="mailto:m.gibson@neu.edu">m.gibson@neu.edu</a>
Matthew Goertz	Sandia National Laboratories	<a href="mailto:mgoertz@sandia.gov">mgoertz@sandia.gov</a>
Stephen Gray	Argonne National Laboratory	<a href="mailto:gray@anl.gov">gray@anl.gov</a>
Katie Carrado Gregar	Argonne National Laboratory	<a href="mailto:kcarrado@anl.gov">kcarrado@anl.gov</a>
Mihal Gross	Department of Energy	<a href="mailto:Mihal.Gross@science.doe.gov">Mihal.Gross@science.doe.gov</a>
Nathan Guisinger	Argonne National Laboratory	<a href="mailto:nguisinger@anl.gov">nguisinger@anl.gov</a>
Gautam Gupta	Los Alamos National Laboratory	<a href="mailto:Gautam@lanl.gov">Gautam@lanl.gov</a>
Ernest Hall	GE Global Research	<a href="mailto:hallel@crd.ge.com">hallel@crd.ge.com</a>
Wei-Qiang Han	Brookhaven National Laboratory	<a href="mailto:whan@bnl.gov">whan@bnl.gov</a>
Tony Haynes	Oak Ridge National Laboratory	<a href="mailto:hayneste@ornl.gov">hayneste@ornl.gov</a>
Linda Horton	Department of Energy	<a href="mailto:Linda.Horton@science.doe.gov">Linda.Horton@science.doe.gov</a>
Jianyu Huang	Sandia National Laboratories	<a href="mailto:jhuang@sandia.gov">jhuang@sandia.gov</a>
Dale Huber	Sandia National Laboratories	<a href="mailto:dlhuber@sandia.gov">dlhuber@sandia.gov</a>
Juan C. Idrobo	Oak Ridge National Laboratory	<a href="mailto:jidrobo@gmail.com">jidrobo@gmail.com</a>
Quanxi Jia	Los Alamos National Laboratory	<a href="mailto:qxjia@lanl.gov">qxjia@lanl.gov</a>
David Joy	Oak Ridge National Laboratory	<a href="mailto:djoy@utk.edu">djoy@utk.edu</a>

# E-Beam Microcharacterization Centers & Nanoscale Science Research Centers Contractors' Meeting

Sponsored by the U.S. Department of Energy, Office of Basic Energy Sciences

May 31 - June 2, 2011  
The Westin Hotel, Annapolis, Maryland

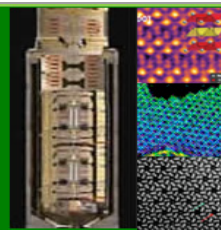


Name	Name	Name
Domenica Karavitaki	Harvard Medical School	<a href="mailto:domenica@alum.mit.edu">domenica@alum.mit.edu</a>
Paul Kent	Oak Ridge National Laboratory	<a href="mailto:kentpr@ornl.gov">kentpr@ornl.gov</a>
Helen Kerch	Department of Energy	<a href="mailto:Helen.Kerch@science.doe.gov">Helen.Kerch@science.doe.gov</a>
Marquis Kirk	Argonne National Laboratory	<a href="mailto:kirk@anl.gov">kirk@anl.gov</a>
Angus Kirkland	University of Oxford	<a href="mailto:angus.kirkland@materials.ox.ac.uk">angus.kirkland@materials.ox.ac.uk</a>
Christian Kisielowski	Lawrence Berkeley National Laboratory	<a href="mailto:cfkisielowski@lbl.gov">cfkisielowski@lbl.gov</a>
Harriet Kung	Department of Energy	<a href="mailto:Harriet.Kung@science.doe.gov">Harriet.Kung@science.doe.gov</a>
An-Ping Li	Oak Ridge National Laboratory	<a href="mailto:apli@ornl.gov">apli@ornl.gov</a>
Chengdu Liang	Oak Ridge National Laboratory	<a href="mailto:liangcn@ornl.gov">liangcn@ornl.gov</a>
Xiao Hua Liu	Sandia National Laboratories	<a href="mailto:xnliu@sandia.gov">xnliu@sandia.gov</a>
Yi Liu	Lawrence Berkeley National Laboratory	<a href="mailto:yliu@lbl.gov">yliu@lbl.gov</a>
Daniel Lopez	Argonne National Laboratory	<a href="mailto:dlopez@anl.gov">dlopez@anl.gov</a>
Alejandra (Ale) Lukaszew	The College of William and Mary	<a href="mailto:ralukaszew@wm.edu">ralukaszew@wm.edu</a>
Greg Lumpkin	ANSTO	<a href="mailto:grl@ansto.gov.au">grl@ansto.gov.au</a>
Biwu Ma	Lawrence Berkeley National Laboratory	<a href="mailto:BWMa@lbl.gov">BWMa@lbl.gov</a>
Emmanuelle Marquis	University of Michigan	<a href="mailto:emarq@umich.edu">emarq@umich.edu</a>
Christopher Marrows	University of Leeds	<a href="mailto:C.H.Marrows@leeds.ac.uk">C.H.Marrows@leeds.ac.uk</a>
Julio Martinez	Sandia National Laboratories	<a href="mailto:julmart@sandia.gov">julmart@sandia.gov</a>
Manos Mavrikakis	University of Wisconsin-Madison	<a href="mailto:manos_at_engr.wisc.edu">manos_at_engr.wisc.edu</a>
Mathew M. Maye	Syracuse University	<a href="mailto:mmmaye@syr.edu">mmmaye@syr.edu</a>
Emilio Mendez	Brookhaven National Laboratory	<a href="mailto:emendez@bnl.gov">emendez@bnl.gov</a>
Celia Merzbacher	Semiconductor Research Corporation	<a href="mailto:wright@src.org">wright@src.org</a>
Dean Miller	Argonne National Laboratory	<a href="mailto:miller@anl.gov">miller@anl.gov</a>
Michael Miller	Oak Ridge National Laboratory	<a href="mailto:millermk@ornl.gov">millermk@ornl.gov</a>
Andrew Minor	Lawrence Berkeley National Laboratory	<a href="mailto:aminor@lbl.gov">aminor@lbl.gov</a>
Karren More	Oak Ridge National Laboratory	<a href="mailto:morekl1@ornl.gov">morekl1@ornl.gov</a>
David Morris	Los Alamos National Laboratory	<a href="mailto:demorris@lanl.gov">demorris@lanl.gov</a>
Luca Dal Negro	Boston Universtiy	<a href="mailto:dalnegro@bu.edu">dalnegro@bu.edu</a>
Jeff Nelson	Sandia National Laboratories	<a href="mailto:snelso@sandia.gov">snelso@sandia.gov</a>
Chad Parish	Oak Ridge National Laboratory	<a href="mailto:parishcm@ornl.gov">parishcm@ornl.gov</a>
Wally Paxton	Sandia National Laboratories	<a href="mailto:wfpaxto@sandia.gov">wfpaxto@sandia.gov</a>
Daniel Perea	Los Alamos National Laboratory	<a href="mailto:d_perea@lanl.gov">d_perea@lanl.gov</a>
Linda Peteanu	Carnegie Mellon University	<a href="mailto:peteanu@andrew.cmu.edu">peteanu@andrew.cmu.edu</a>
Amanda Petford-Long	Argonne National Laboratory	<a href="mailto:petford.long@anl.gov">petford.long@anl.gov</a>
David Prendergast	Lawrence Berkeley National Laboratory	<a href="mailto:dgprendergast@lbl.gov">dgprendergast@lbl.gov</a>
Roger Proksch	Asylum Research	<a href="mailto:roger@asylumresearch.com">roger@asylumresearch.com</a>
Velimir Radmilovic	Lawrence Berkeley National Laboratory	<a href="mailto:VRRadmilovic@lbl.gov">VRRadmilovic@lbl.gov</a>
Tijana Rajh	Argonne National Laboratory	<a href="mailto:rajh@anl.gov">rajh@anl.gov</a>
Gang (Gary) Ren	Lawrence Berkeley National Laboratory	<a href="mailto:gren@lbl.gov">gren@lbl.gov</a>

# E-Beam Microcharacterization Centers & Nanoscale Science Research Centers Contractors' Meeting

Sponsored by the U.S. Department of Energy, Office of Basic Energy Sciences

May 31 - June 2, 2011  
The Westin Hotel, Annapolis, Maryland



Name	Name	Name
Ian Robertson	University of Illinois-Urbana	<a href="mailto:ianr@illinois.edu">ianr@illinois.edu</a>
Jeannie Robinson	Oak Ridge Institute for Science and Education	<a href="mailto:J.Robinson@orise.orau.gov">J.Robinson@orise.orau.gov</a>
Jurek Sadowski	Brookhaven National Laboratory	<a href="mailto:sadowski@bnl.gov">sadowski@bnl.gov</a>
Kotaro Sasaki	Brookhaven National Laboratory	<a href="mailto:ksasaki@bnl.gov">ksasaki@bnl.gov</a>
Andreas Schmid	Lawrence Berkeley National Laboratory	<a href="mailto:akschmid@lbl.gov">akschmid@lbl.gov</a>
Neal Shinn	Sandia National Laboratories	<a href="mailto:ndshinn@sandia.gov">ndshinn@sandia.gov</a>
Katherine Smith	Embassy of Australia	<a href="mailto:kath.smith@dfat.gov.au">kath.smith@dfat.gov.au</a>
Eric Stach	Brookhaven National Laboratory	<a href="mailto:estach@bnl.gov">estach@bnl.gov</a>
David Starr	Brookhaven National Laboratory	<a href="mailto:dstarr@bnl.gov">dstarr@bnl.gov</a>
Stefan Strauf	Stevens Institute of Technology	<a href="mailto:strauf@stevens.edu">strauf@stevens.edu</a>
Dong Su	Brookhaven National Laboratory	<a href="mailto:dsu@bnl.gov">dsu@bnl.gov</a>
Peter Sutter	Brookhaven National Laboratory	<a href="mailto:psutter@bnl.gov">psutter@bnl.gov</a>
Vojtech Svoboda	CFD Research Corporation	<a href="mailto:vxs@cfrc.com">vxs@cfrc.com</a>
Anna Swan	Boston University	<a href="mailto:swan@bu.edu">swan@bu.edu</a>
Mihaela Tanase	National Institute of Standards and Technology	<a href="mailto:mihaela.tanase@nist.gov">mihaela.tanase@nist.gov</a>
Ihor Tokarev	Clarkson University	<a href="mailto:itokarev@clarkson.edu">itokarev@clarkson.edu</a>
Michael Treacy	Arizona State University	<a href="mailto:treacy@asu.edu">treacy@asu.edu</a>
Kinga Unocic	Oak Ridge National Laboratory	<a href="mailto:unocicka@ornl.gov">unocicka@ornl.gov</a>
Nagarajan Valanoor	University of New South Wales	<a href="mailto:nagarajan@unsw.edu.au">nagarajan@unsw.edu.au</a>
Hector Vazquez	Columbia University	<a href="mailto:hv2138@columbia.edu">hv2138@columbia.edu</a>
Akos Vertes	George Washington University	<a href="mailto:vertes@gwu.edu">vertes@gwu.edu</a>
Debin Wang	Lawrence Berkeley National Laboratory	<a href="mailto:debinwang@lbl.gov">debinwang@lbl.gov</a>
Michael White	Brookhaven National Laboratory	<a href="mailto:mgwhite@bnl.gov">mgwhite@bnl.gov</a>
Stephen Whitelam	Lawrence Berkeley National Laboratory	<a href="mailto:swhitelam@lbl.gov">swhitelam@lbl.gov</a>
Gary Wiederrecht	Argonne National Laboratory	<a href="mailto:wiederrecht@anl.gov">wiederrecht@anl.gov</a>
Robert Winarski	Argonne National Laboratory	<a href="mailto:winarski@anl.gov">winarski@anl.gov</a>
Qin Wu	Brookhaven National Laboratory	<a href="mailto:qinwu@bnl.gov">qinwu@bnl.gov</a>
Kai Xiao	Oak Ridge National Laboratory	<a href="mailto:xiaok@ornl.gov">xiaok@ornl.gov</a>
Judith Yang	University of Pittsburgh	<a href="mailto:judyang@pitt.edu">judyang@pitt.edu</a>
Jonathan Yun	Columbia University	<a href="mailto:jpy2108@columbia.edu">jpy2108@columbia.edu</a>
Nestor Zaluzec	Argonne National Laboratory	<a href="mailto:Zaluzec@aaem.amc.anl.gov">Zaluzec@aaem.amc.anl.gov</a>
Alex Zetl	University of California, Berkeley	<a href="mailto:azetl@physics.berkeley.edu">azetl@physics.berkeley.edu</a>
Yuegang Zhang	Lawrence Berkeley National Laboratory	<a href="mailto:y Zhang5@lbl.gov">y Zhang5@lbl.gov</a>
Jane Zhu	Department of Energy	<a href="mailto:jane.zhu@science.doe.gov">jane.zhu@science.doe.gov</a>
Yimei Zhu	Brookhaven National Laboratory	<a href="mailto:zhu@bnl.gov">zhu@bnl.gov</a>